A STUDY OF THIN METALLIC FILMS PREPARED AT LOW TEMPERATURES.

Thesis submitted for the degree of
Doctor of Philosophy by R.Roden.

January 1975

Department of Metallurgy
and Materials Science,
Imperial College,
London S.W.7

ABSTRACT

Thin films of Ga,Fe,Cr,Co,Ni,In and Sn have been prepared and studied at $4^{O}K$ using a Scanning High Energy Electron Camera.All the films have been grown in a vacuum of better than 5.10^{-10}torr,and all,except In,exhibited a non-crystalline structure at very low temperatures.The electron diffraction data has been analysed using a set of computer programs to obtain their Radial Distribution Functions.A discussion on the methods of this analysis is given along with an alternative procedure for evaluating the film structure. The design of the liquid He substrate support stage used is described together with the other necessary apparatus modifications.

INTRODUCTION

The work described in this thesis was originally prompted by a report that films of Cd,Zn and Sn had been prepared in a non-crystalline form(Robertson and Unvala(1971)).In their work the films were prepared in a ultra high vacuum system and then transferred to a conventional electron diffraction camera for structural investigation.The equipment used in this research was a Scanning High Energy Electron Diffraction Camera.This enabled the "in situ" growth of films in a much cleaner environment.In addition to preparing and studying the metallic films mentioned,Fe,Cr,Co, In,Ni and Ga were prepared all at at low temperatures. A set of computer programs were written and developed in order to analyse the experimental data in terms of the Radial Distribution Function.

A general introductory discussion on non-crystalline thin films is given in Chapter 1.Chapter 2 describes the experimental apparatus and techniques,while Chapter 3 presents the method of analysis used.The results obtained and their analysis is in Chapter 4 and a summary of the work is given in Chapter 5.

CHAPTER 1

Non-Crystalline Materials

1.1 Non-Crystalline Solids

1.2 The Preparation and Properties of Non-Crystalline Films

CHAPTER 2

The Experimental Apparatus and Procedure

Chapter 3

Method of Analysis of the Experimental Data

Chapter 4

The Experimental Results and their Analysis

Chapter 5

Summary and Suggestions for Future Work

5.1 Summary and comparison of the results obtained

5.2 Discussion of the reliability of the data

5.3 Suggestions for future work

CHAPTER 1

Non-Crystalline Materials

1.1 Non-Crystalline Solids

In 1915 it was shown, by Debye, that short range order in liquids or non-crystalline solids would lead to a diffraction pattern of diffuse haloes. This was subsequently confirmed by Debye and Scherrer (1916), investigating a non-crystalline solid. Frost (1954) in a review paper on liquid metals mentions that liquid Ar, Benzene, N_2 and O_2 were also studied at about this time. It was found that the diffraction patterns of the liquids and the non-crystalline solids were very similar and led to the belief that the structures of the two phases were alike. Subsequently, however, further diffraction studies on a range of liquids and non-crystalline solids showed that their diffraction patterns were often quite different. Figure (1) shows electron diffraction curves for non-crystalline and molten Ge; the data being taken from Behrndt (1969). In these cases the solid is said to exhibit a lattice-like non-crystalline structure. That is they have the same basic structural element as the corresponding crystalline material. Breitling (1969)

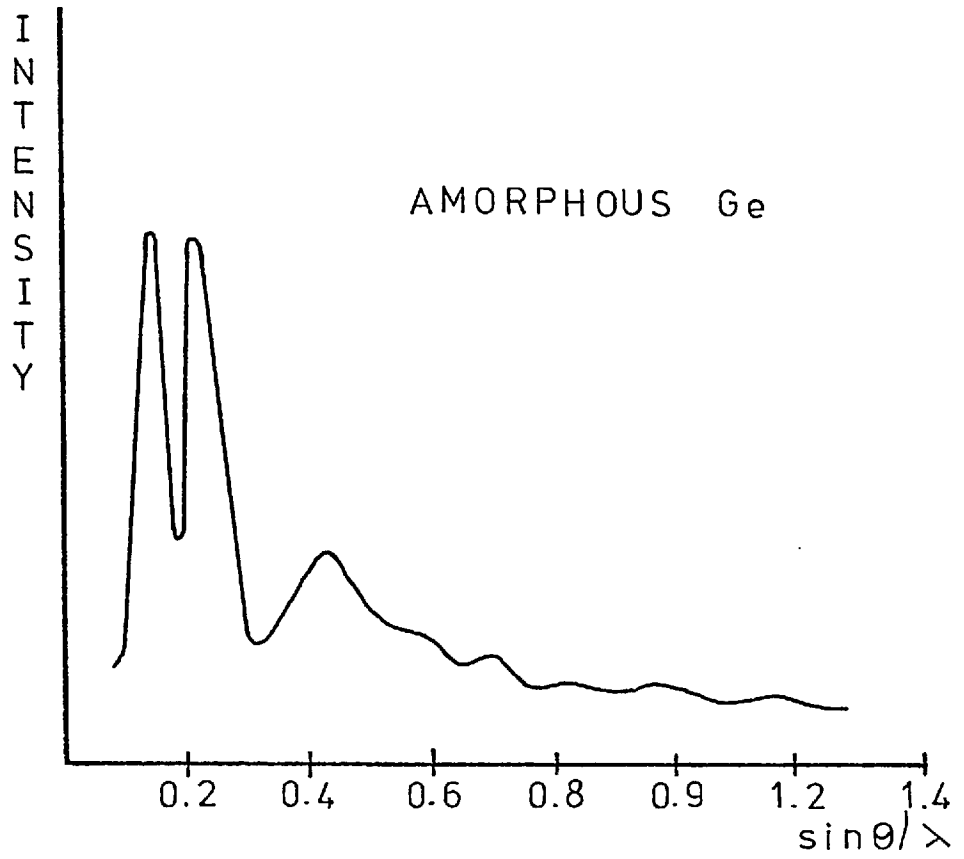
INTENSITY
AMORPHOUS Ge
0.2
0.4
0.6
0.8
0.9
1.2
1.4
sinθ/λ

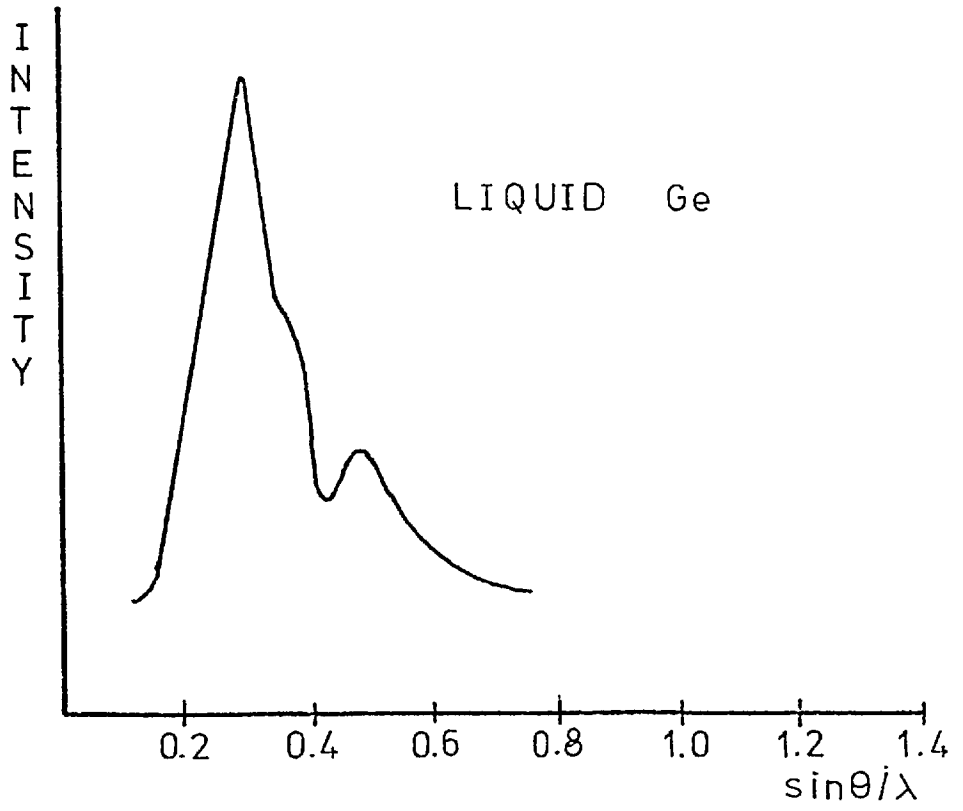
INTENSITY
LIQUID Ge
0.2
0.4
0.6
0.8
1.0
1.2
1.4
sinθ/λ

FIGURE (1)

indicates that Si, Ge, As, Sb and Se, as well as the vitreous substances B_2O_3 and SiO_2 are lattice-like when non-crystalline. Some materials, however, show similarities in the diffraction patterns produced by the two phases. Figure (2) which is from a paper by Leonhardt et al (1962) shows the diffraction curves for non-crystalline and molten Bi. Other materials which behave in this way are Ga, Fe and Cr, and they are called liquid-like, non-crystalline solids.

Although a number of non-crystalline solids have a structure similar to that of a liquid there are distinctions between the two states. In every case of the production of a non-crystalline state the transition to a polycrystalline state is irreversible. In contrast the solid-liquid transition takes place in thermal equilibrium and is hence reversible. Another difference is that the amplitudes of the maxima in the diffraction curves are larger in the non-crystalline case than in the liquid case (see figure (2)). This implies that the former possesses a greater degree of order. Similarly Wagner (1969) has studied the non-crystalline alloys Cu-Mg, Pd-Si, Fe-P-C, Ni-P and Ag-Cu and has established that they have a higher degree of order than that observed in liquid metals.

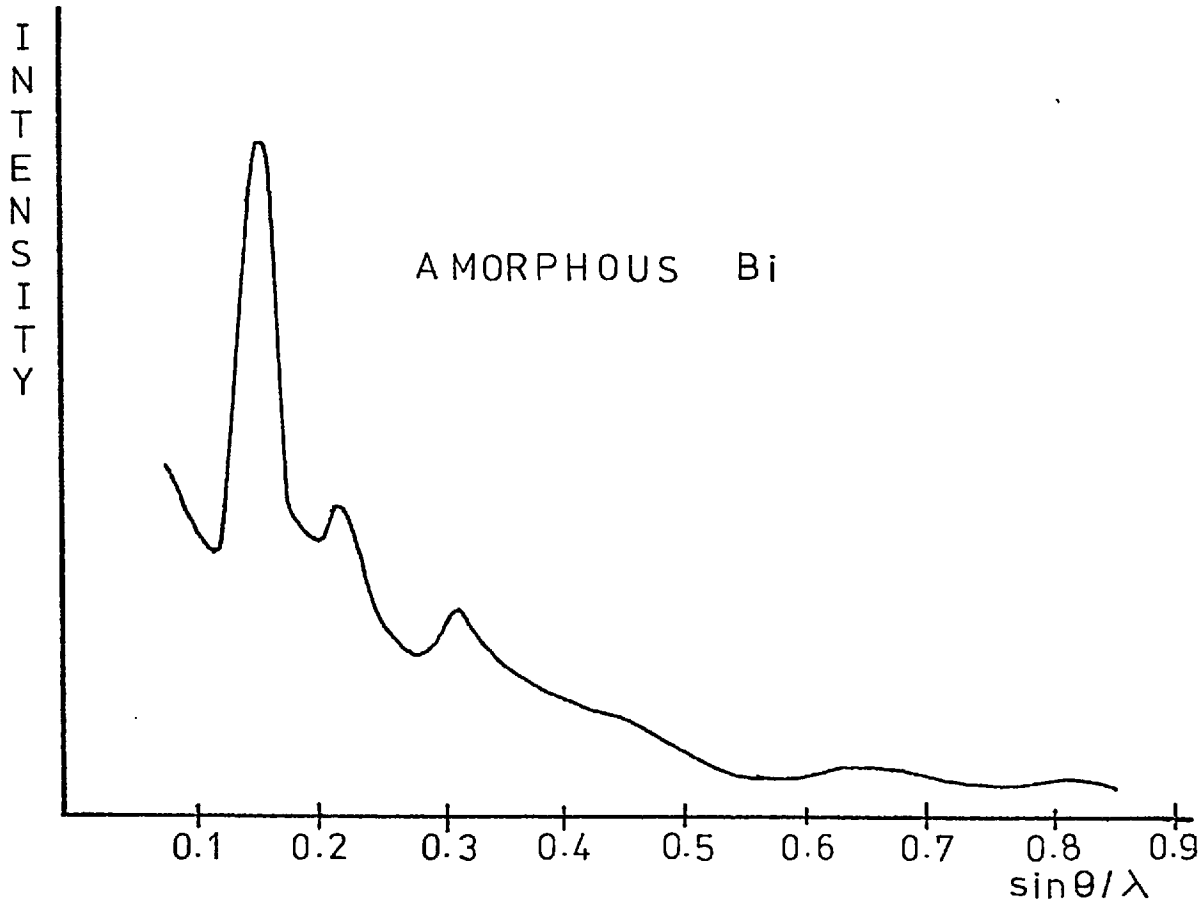
INTENSITY
AMORPHOUS Bi
0.1
0.2
0.3
0.4
0.5
0.6
0.7
0.8
0.9
sinθ/λ

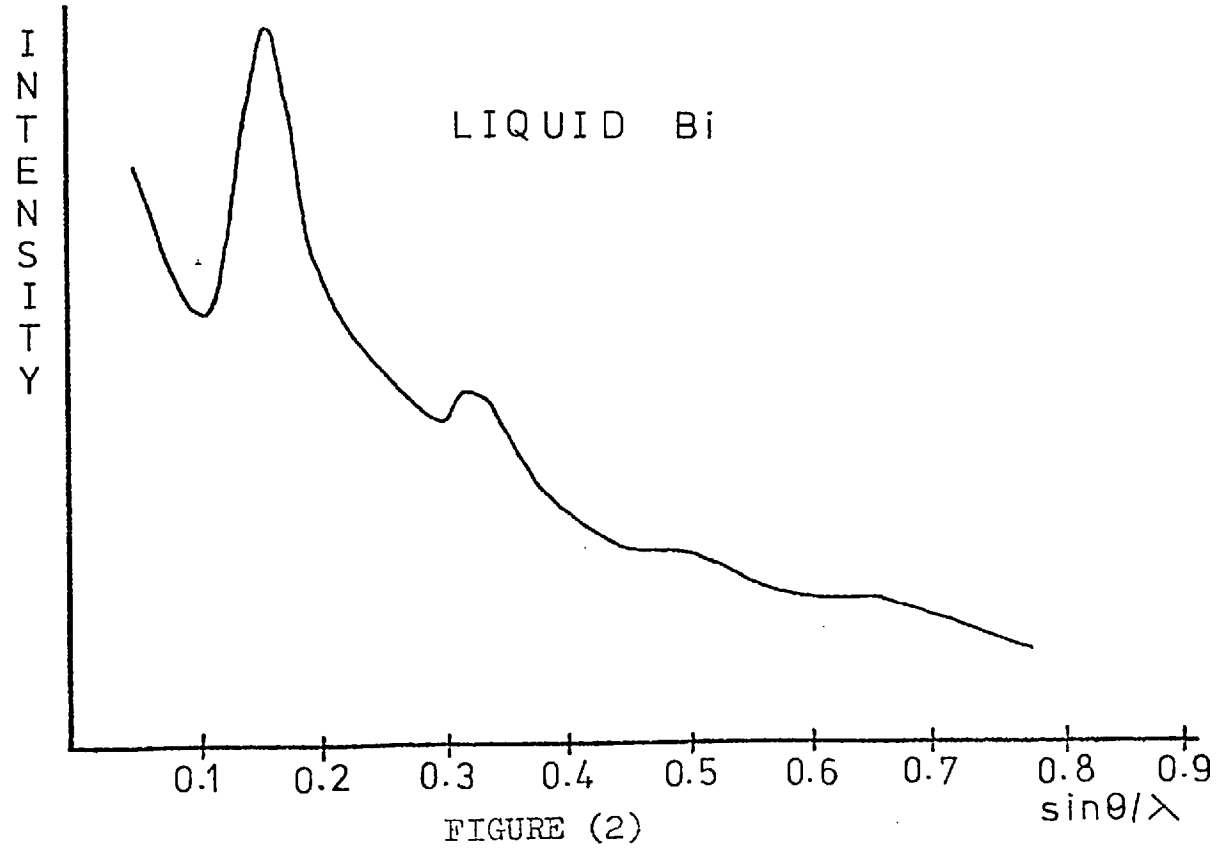
INTENSITY
LIQUID Bi
0.1
0.2
0.3
0.4
0.5
0.6
0.7
0.8
0.9
sinθ/λ

FIGURE (2)

Finally there is the much greater atomic mobility present in liquids. Longini and Pansino (1969) have studied the variation of electrical conduction of non-crystalline compounds on warming and have showed there is some re-ordering process. The atomic arrangement, however, does not change appreciably and does not affect the diffraction pattern.

There have been various models put forward to describe non-crystalline structures and these fall into two main types. There is the continuous model, originally suggested by Bernal (1964) to represent liquids, and the discontinuous arrangement postulated by Richter et al (1957). Bernal considered that a liquid was a homogeneous, coherent atomic assemblage and could be represented by randomly packed polyhedra. From experiments on models with a random arrangement of atoms he discovered that the co-ordination numbers in a closed packed model followed some definite curve and was certainly different from the regular case where every ball bearing had twelve contacts. From his close-packed, random model he calculated how the atomic density should vary and this agreed quite well with experimental results from liquid Ar. Scott (1962) produced a similar model and his results agree with those given by Bernal. This liquid model has since been used as a possible way of representing non-crystalline solids.

The discontinuous model proposed by Richter however consists of ordered agglomerates randomly arranged and surrounded by disordered atoms. The ordered agglomerates can take the form of spherical, close packed assemblies or segments of lattice planes.

Atomic density data evaluated from experiments on Ge and Si were interpreted as containing small randomly orientated crystallographic regions, while data from Ga and Bi led to the conclusion that both types of agglomerate were present. To explain the close packed spheres of atoms they used a model of statistically distributed spherical shells. The central atom is surrounded by atoms located approximately in the region of these shells. The atoms of the first shell will only be slightly displaced from it and will produce a pronounced maximum in the atomic density. The atoms of the further shells will show increasing positional variation and produce broad maxima in the atomic density curve. Such a model can explain the calculated atomic densities from non-crystalline films and in particular Richter (1969) obtains quite good agreement with data obtained from Cr by Fujime (1966).

Jonscher and Walley (1969) suggests that polymers and elements with homopolar bonding can best be explained

using a discontinuous model, while glasses are best thought of as having a continuous structure. Warren (1939) studied diffraction data from vitreous SiO_2 and concluded that it was non-crystalline. This was based on evaluating the possible crystallite size, by consideration of the diffraction line broadening, to be 7.7A. Warren argued that if these crystallites were present then they should produce low angle x-ray diffraction. On careful study for such effects he was unable to detect any peaks and hence concluded that SiO_2 could be represented by a continuous non-crystalline model. More recently, however, Bienenstock and Bagley (1966) have calculated the upper limits to such scattering. The calculated magnitude is extremely small compared to the independent atomic scattering and they regard it as extremely unlikely that it could be distinguished even if it were there.

This type of uncertainty in the interpretation of diffraction data is a major problem in investigating non-crystalline solids. A polycrystalline sample will give a diffraction pattern of rings and for small grain sizes these rings will become very diffuse. (Chapter 3 gives a method for calculating diffraction curves from polycrystalline solids). It then becomes very difficult to distinguish between this pattern and that produced by a non-crystalline solid. This of course,

is to be expected and leads on to the problem of deciding when a polycrystalline solid becomes non-crystalline. For example an arrangement of crystallites containing one or two unit cells possesses very little long range, crystallographic order. This problem has been briefly discussed by Behrndt (1969) and he points out one important difference between the two states. In general the polycrystalline sample is stable for all grain sizes while the non-crystalline state has always been found to be unstable. Consequently, the non-crystalline/polycrystalline transition should be accompanied by a change in atomic arrangement and this could possibly be detected by diffraction methods. However, Rudee and Howie (1972) have pointed out that great care should be taken in analysing such diffraction data. They assumed a hexagonal wurtzite structure for Ge and calculated the diffraction curve produced by such crystallites of size 14Å. The results were in good agreement with diffraction data which had previously been thought to have been produced by non-crystalline Ge. In addition they studied Ge with an electron microscope which confirmed that it was in fact comprised of small crystallites.

1.2 The Preparation and Properties of Non-Crystalline Films

The primary methods used to fabricate thin films are evaporation, sputtering, chemical vapour deposition and electrodeposition. A review paper on these methods, together with a discussion on structure-sensitive film properties, has been written by Behrndt (1969). The formation of non-crystalline films has been studied for many years and there are now a wide range of materials which have been prepared with such a structure. These can be conveniently classified into three groups: alloys, elements with covalent bonding and metals.

Buckel (19) attempted to prepare non-crystalline metallic films by condensation onto a liquid Helium surface. He reported that Ga and Bi could be produced in this form while metals such as Sn could not. However, as Behrndt (1970) indicates, the addition of a small amount of another element will often stabilise the non-crystalline structure. Similarly large numbers of alloys have been produced by quenching condensation (eg. Duwez and Willens (1963)). Mader et al (1967) studied the structure of Cu-Ag, Co-Au alloys formed at 77 K using electron diffraction and microscopy. They discovered that the formation of non-crystalline alloys was appreciably affected by the substrate. In particular they found it was important to

use a non-crystalline surface. Mader (1965) has suggested an explanation for the formation of non-crystalline alloys using the idea of the admixture retarding the long range order of the folvent. It was also established experimentally that such alloys transformed to the crystalline state at a temperature of approximately one third of its melting point. This idea of the impurity atoms helping in the formation of a non-crystalline state is also common with covalent elements and metals. Covalent elements such as As, Se, Sb, Si and Ge have all been prepared as non-crystalline films. As with alloys the crystallographic type of the substrate has an influence on non-crystalline film formation. The substrate temperature should also be below one third of the melting point of the element condensed. Adamsky et al (1969) reported that in an atmosphere with an oxygen partial pressure of 10^{-10} torr evaporated Ge films were non-crystalline on deposition, subsequently transforming at 50° C. Preparation of the films in an oxygen partial pressure of 5×10^{-8} torr resulted in a more stable non-crystallihe structure which transformed at 200°C. Similarly Bennet and Wright (1972) found that a number of transition elements could only be prepared as non-crystalline films by adding impurities.

Fe and Ni needed several per cent of impurity while pure films were always microcrystalline. Non-crystalline

films of pure Co however, could be prepared. They investigated the structural changes by monitoring the electrical resistivity. The behaviour of these films on annealing, and in particular their transition temperatures depended on the amount of impurity present. Bulow and Buckel (1956) studied the behaviour of thin films on annealing using electron diffraction while concurrently monitoring their resistivity. They showed that a non-crystalline/polycrystalline transition is accompanied by an abrupt resistance change, while grain growth is indicated by a gradual decrease of resistance. Kato and Horikoshi (1965) also measured the resistance of Fe films prepared in a vacuum of 5×10^{-6} torr by condensation onto a liquid nitrogen cooled glass substrate. They observed an irreversible change on warming of the film at a temperature which varied with the thickness of the film. This transition temperature had an approximate value of $150^{\circ}K$ with a variation of about $40^{\circ}K$. Suits (1963) has studied the effect of residual gases on the non-crystalline/crystalline transition in Fe films. The films were prepared, at $4^{\circ}K$ with a residual gas pressure of 10^{-14} torr, and their resistance monitored during deposition. The films underwent a sharp change in resistance at a certain thickness and this was interpreted as being caused by a transition. He then deposited a thicker film in an oxygen partial pressure of 10^{-8} torr. No thickness

dependent transition was observed but a sharp resistance drop did occur on annealing to 75°K. This would seem to indicate how the oxygen impurity has stabilised the non-crystalline phase and increased the transition temperature by 70°K. Further work on Fe has been done by Grigson et al (1964) who also report a thickness dependent transition, although not at liquid Helium temperature. Fujime (1966) obtains a different transition temperature again, whilst not finding a thickness dependent change. The variation in these results is a good illustration of the effect on film properties caused by the growth conditions and the impurities present. The effect of oxygen on evaporated films has also been studied by Preece and Wilman (1967) and Caswell and Budo (1964). Paulson and Friedberg (1970) studied the structure if evaporated Au films in different atmospheres. The presence of N_2 and H_2 had only a slight effect whilst O_2 caused the film to form with a small island structure. This was attributed to the oxygen reducing the atomic mobility of the Au atoms. Similar work was performed by Moss and Thompson (1964), who showed that evaporating Ag films in an improved vacuum resulted in small crystallites being formed. They also found that deposition onto a previously outgassed surface resulted in a smaller crystallite size.

Quite a lot of work has been done on investigating the phase of condensed atoms over a range of temperatures. Palatnik et al (1962) deposited various metals in an effort to discover if the condensate became crystalline immediately (v→c) or if there was an intermediate liquid phase (v→l→c). They found the mechanism depended on the substrate temperature such that:

$$\tfrac{2}{3}\ \mathrm{Tmp} < T < \tfrac{1}{3}\ \mathrm{Tmp} \qquad v \rightarrow l \rightarrow c$$

$$\tfrac{1}{3}\ \mathrm{Tmp} < T < \tfrac{2}{3}\ \mathrm{Tmp} \qquad v \rightarrow c$$

where Tmp = melting point.

Krikorian and Sneed (1963) evaporated Ge films and concluded that the phase during deposition depended on the substrate used and the growth rate. Figure (3) shows how the phase depends on the substrate temperature and the growth rate.

Behrndt (1966) quotes some interesting results obtained from evaporated Ag films which were deposited over a range of temperatures and thicknesses. The films were poly-crystalline on deposition but would melt on warming at some temperature Tmf. The ratio Tmf/Tmp varied with thickness and only approached unity for films thicker than 500A°. It was also found that somewhat different behaviour occurred for films prepared at temperatures

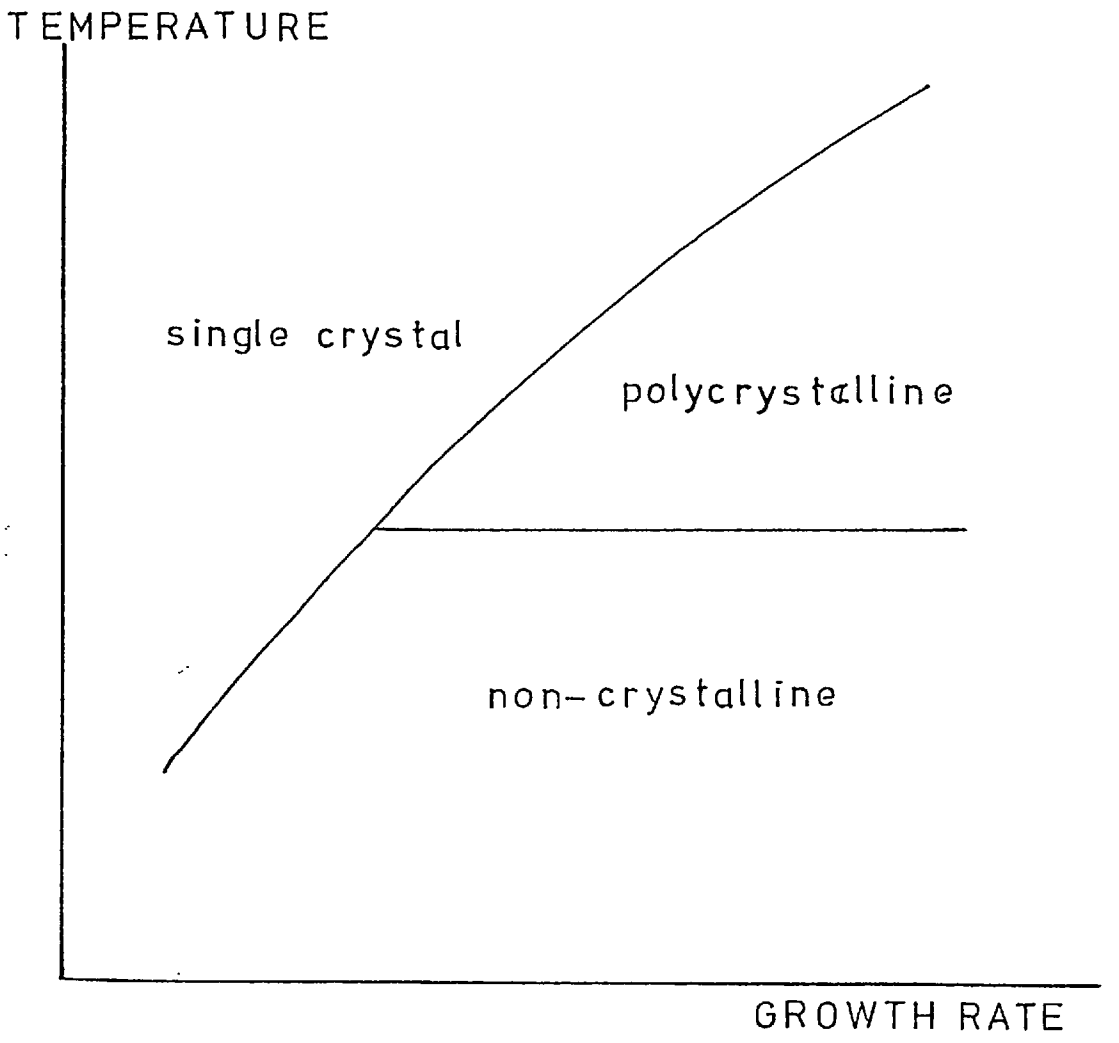
TEMPERATURE
single crystal
polycrystalline
non-crystalline
GROWTH RATE

FIGURE (3)

below $\frac{1}{5}$ Tmp.

Whilst much of the work carried out with thin films has produced inconclusive, or even contradictory results, genuine discoveries have been made. Probably the most interesting property of non-crystalline films is that many elements although not normally superconductors become so in such a form. Hilsh (1951) first discovered this phenomena with Bi films. Since then a great deal of research has been carried out and more recently Glover (1969) has shown that some superconductivity related contribution to the electrical conductance is present at temperatures of twice that of the critical temperature.

CHAPTER 2

The Experimental Apparatus and Procedure

The basic S.H.E.E.D. apparatus was supplied by Vacuum Generators Ltd., and is shown in figure (1). The system is decribed in section (2.1). Details of the modifications to the equipment are given in section (2.2), while section (2.3) indicates the experimental procedure.

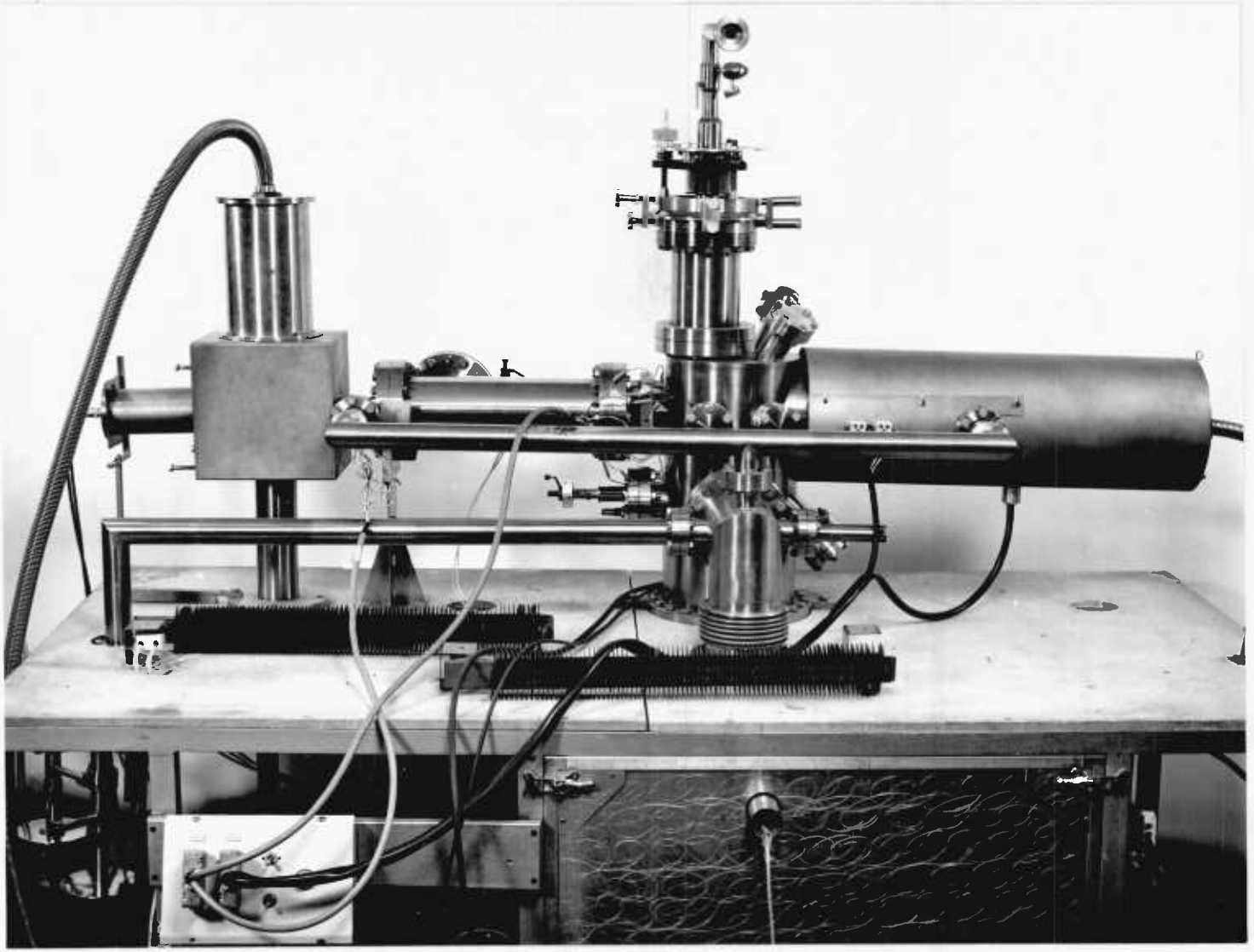

2.1 Description of the basic Scanning High Energy Electron Diffraction Camera

2.1.1 Vacuum Details

The vacuum system had been constructed entirely from stainless steel except for two glass view ports. All the flanges were sealed using O.H.F.C. copper gaskets. It was pumped by two sorption pumps, a triode ion pump and a titanium sublimation pump. These pumps enabled a hydrocarbon free, ultra high vacuum (conventionally less than 10^{-7}torr) to be attained. The pressure was measured down to 10^{-2} torr by two Pirani gauges and below this by a nude ionisation gauge. Bake out heaters, shrouds and a control unit enabled the apparatus to be baked for extended periods.

2.1.2 The Electron Optics Details

A schematic diagram of the electron optics arrangement is shown in figure (2).

The H.E.G.4 gun produces a collimated beam of electrons with energy up to 50Kev ; the high tension voltage being supplied by a stabilised power supply. A variable cathode bias can be applied to vary the intensity of the beam while its direction is controlled using the electrostatic alignment plates. The beam is focussed using the magnetic lens and can be tilted in the vertical plane by the electrostatic deflector plates. Using these controls a suitable electron beam can be directed into the experimental chamber enabling either reflection or transmission diffraction to be undertaken. The resulting diffraction pattern is formed on the first phosphor screen ; this phosphor containing a small central aperture. The pattern is viewed, by means of a mirror, again with a central aperture, positioned at an angle of 45^{o} to the screen and immediately behind it, through a suitable viewing port.

A little way behind the substrate and outside of the chamber are two orthogonal pairs of scanning coils.

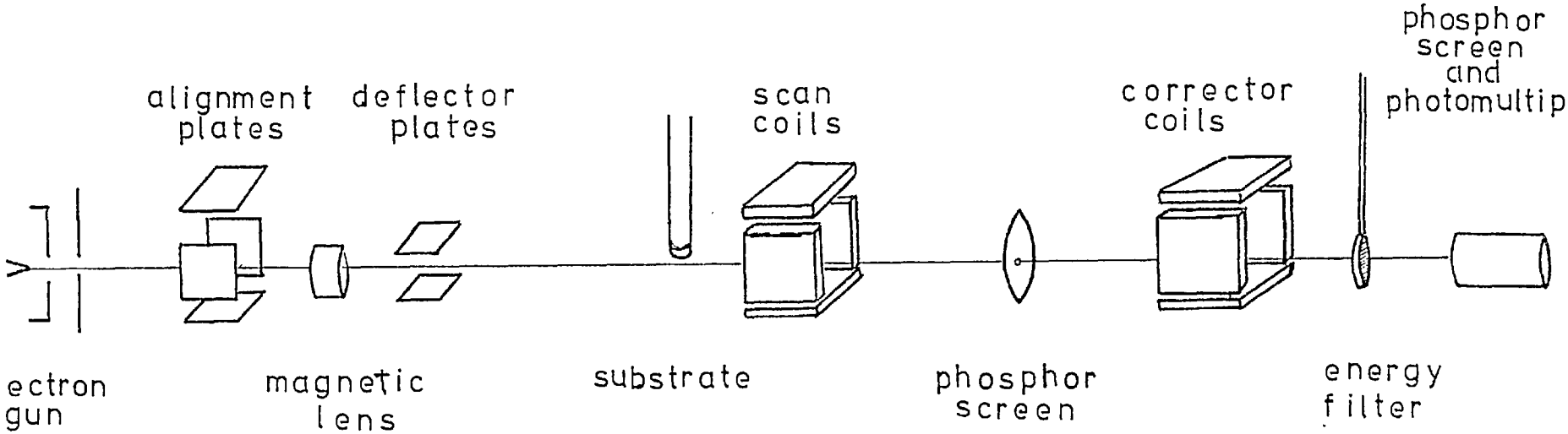
alignment plates
deflector plates
scan coils
corrector coils
phosphor screen and photomultiplier
electron gun
magnetic lens
substrate
phosphor screen
energy filter

FIGURE (2)

By applying a ramp voltage to the vertical pair of coils the entire diffraction pattern can be scanned vertically across the screen aperture. Those electrons which pass through this aperture fall onto a second phosphor screen. The light so produced is picked up by a photomultiplier and the resulting signal fed into an X-Y recorder as the ordinate. The ramp voltage itself provides the abscissa. An additional feature of the equipment is the provision of an energy filter. This is a very fine copper mesh held normally to the electron axis which is biased positively with respect to the electron gun. The biasing voltage can be varied between 0 and 45 volts or set at 250 volts. Since the high tension supply to the filter is common to that to the electron gun the effects of any voltage fluctuations are eliminated. The filter prevents those electrons which have lost more than the corresponding energy from reaching the second phosphor screen and hence contributing to the recorded intensity. It is important for the correct operation of the filter that the electrons should strike it normally. However, because the scan coils deflect the electrons from some way behind the specimen, it is necessary to deflect them back onto the electron axis and this is achieved by the two pairs of orthogonal corrector coils. To enable the energy filter to be aligned perpendicularly

to this axis it is enclosed in a small chamber which can be tilted in both the horizontal and vertical planes.

In addition to making a single vertical scan it is possible to produce a three dimensional representation of the pattern. This is accomplished by taking a series of vertical scans and applying a step voltage to the horizontal coils after each one. Alternatively, the pattern can be scanned horizontally by applying the ramp voltage to the horizontal coils.

2.1.3 The Specimen Chamber

The specimen chamber is eight inches in diameter and contains one eight inch, one six inch, two four inch and eight two and three quarter inch ports.

The six inch port on the top of the chamber is used for attachment of the substrate supporting device, including the substrate cooling tube. This is called a Universal Motion Drive (U.M.D.). It permits all the necessary degrees of freedom that are required for obtaining a diffraction pattern. The six inch flange on which it is mounted also contains six electrical lead throughs. The flexible, stainless steel, cooling tube is mounted in another six inch flange.

The evaporation boats used were made from either Tungsten, Molybdenum or Tantulum sheet depending on the material to be evaporated. It was supported by copper strips attached to high current electrical lead throughs in one of the small flanges. A shutter attached to a stainless steel bellows, itself argon are welded into a small flange, was used to shield the substrate when required.

The other ports were used at various times to support A.E.I. M.S.10 mass spectrometer and an Edwards Quartz Crystal thickness monitor.

2.2 Modications to the basic equipment

2.2.1 A Double Substrate Arrangement

To improve efficiency the substrate and associated shielding arrangement was modified in order to be able to perform two depositions for each pump down.

Two substrates projecting from a copper block and parallel to each other were used in conjunction with a stationary shield. When the substrates had been inserted into the system the Universal Motion Drive was used to rotate the substrates so that they were parallel to the electron axis. When necessary the two substrates could then be moved horizontally so that both were covered by the shield from the boat. To deposit on one substrate the U.M.D. was again used to expose it to the boat. To deposit onto the other substrate they were rotated through 180^{o}. The substrates are shown in figure (3), along with their mode of operation.

DOUBLE SUBSTRATE

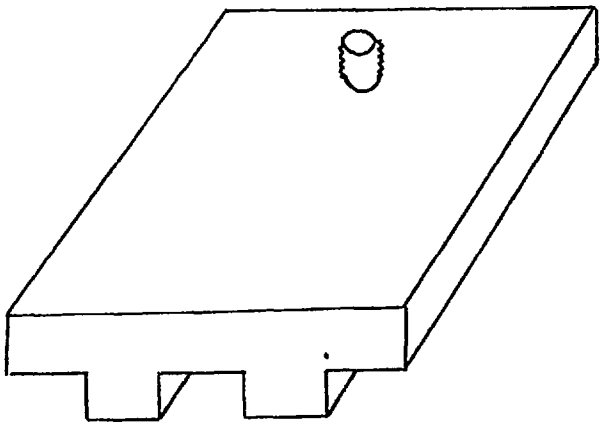

SHIELD

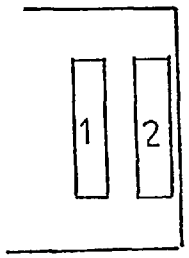

outgassing position

lateral motion gives:

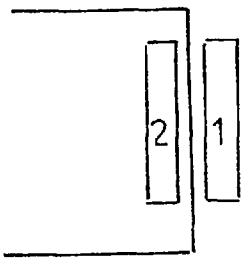

deposition onto 1

rotation gives:

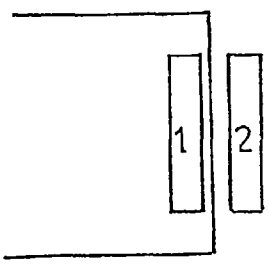

deposition onto 2

FIGURE (3)

2.2.2 The Liquid Helium Stage

The two main problems involved in designing a suitable Helium stage were:

1. to reduce all heat inputs to the cooled surface to the lowest possible level

2. to provide all the necessary degrees of freedom.

In addition the provision of a multiple substrate, enabling more than one run per pump down to be carried out, would be a great advantage. To provide some control of warming rate of the substrate it was decided to use a continuous flow method. This also has the advantage of easier transfer of the Helium.

In order to reduce the heat input from radiation a shield, which could be filled with liquid nitrogen, was designed to surround the substrate. This radiation shield would then perform two further functions:

a. it would reduce the amount of condensation onto the liquid Helium cooled surface

b. it would allow more than one substrate to be used if it contained a suitable defining aperture for the evaporant.

The shield was constructed from stainless steel with the joints formed by argon are welding and is shown in figure (4). It consists basically of two in inter-connected nitrogen resevoirs which are aligned above and below the substrate, the lower one containing an evaporation aperture. The resevoirs are filled by means of a standard V.G. liquid feed-through attached to the top tank via a length of flexible tubing. Attached to the two resevoirs is a cylindrical shell which is aligned to be on the electron axis. This has electron entry and exit apertures as well as baffled pumping holes. The shield is supported by three rods which can be screwed into the bottom tank. These rods are then attached to an annulus itself supported by two rods fixed to a four inch flange. The height of the shield above this annulus can be varied, to align the electron apertures, by the nuts attaching the rods to the annulus. The horizontal position can be adjusted by sliding the annulus along the horizontal support rods.

On the same four inch flange are two high current electrical lead throughs to which are attached the copper supports for the evaporation boat. The flange also holds the bellows and associated winding arrangement

for supporting and moving the shutter. A schematic diagram of this flange is shown in figure (5).

In order to provide a method of manipulating the substrate it was decided to retain part of the Univeral Motion Drive. A similar bellows was used welded into a six inch flange. Attached to the top end of the bellows and passing through it are the vertical Helium inlet and tubes. Using the U.M.D. manipulating framework this bellows can then be moved as before. The only movement now not possible is rotation of the substrate which for non-crystalline or polycrystalline films is in any case not necessary. A diagram of the stage is shown in figure (6). To minimise the heat input the inlet/outlet tubes were concentric and a further concentric tube provided an interspace which could be evacuated. Since the outlet tube was outside the inlet, the cold escaping gas would cool the inlet tube. Furthermore all the tubes used were thin walled cryotubing. The tubes were kept in position by P.T.F.E. spacers. To minimise heat conduction through these spacers they were made triangular in shape with suitable holes. Further reduction in heat input through conduction was made by making the support tubes as long as possible. This necessitated using a spacer between the Helium stage and the system's six inch port.

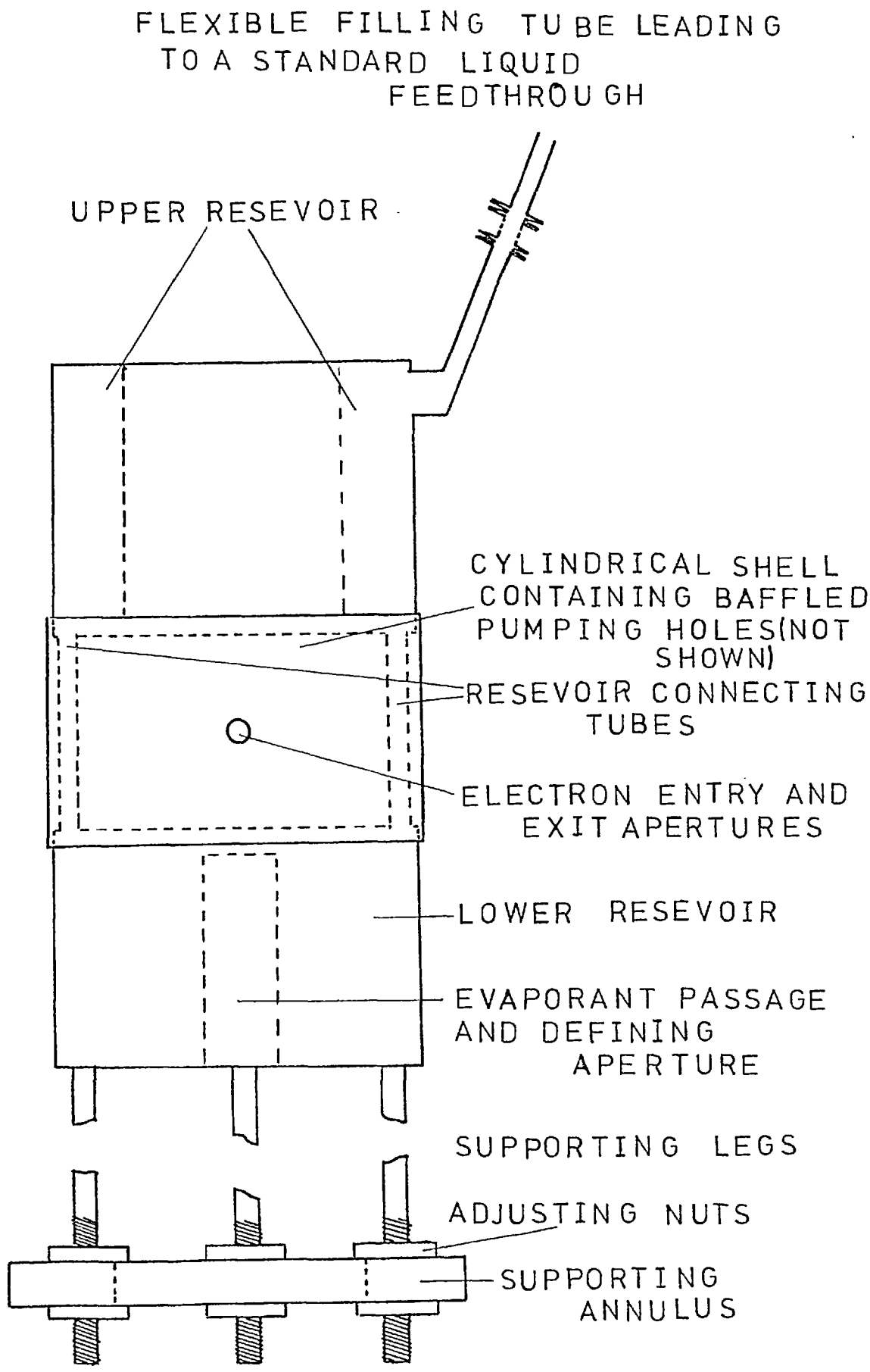
FLEXIBLE FILLING TUBE LEADING TO A STANDARD LIQUID FEEDTHROUGH
UPPER RESEVOIR
CYLINDRICAL SHELL CONTAINING BAFFLED PUMPING HOLES(NOT SHOWN)
RESEVOIR CONNECTING TUBES
ELECTRON ENTRY AND EXIT APERTURES
LOWER RESEVOIR
EVAPORANT PASSAGE AND DEFINING APERTURE
SUPPORTING LEGS
ADJUSTING NUTS
SUPPORTING ANNULUS

FIGURE (4)

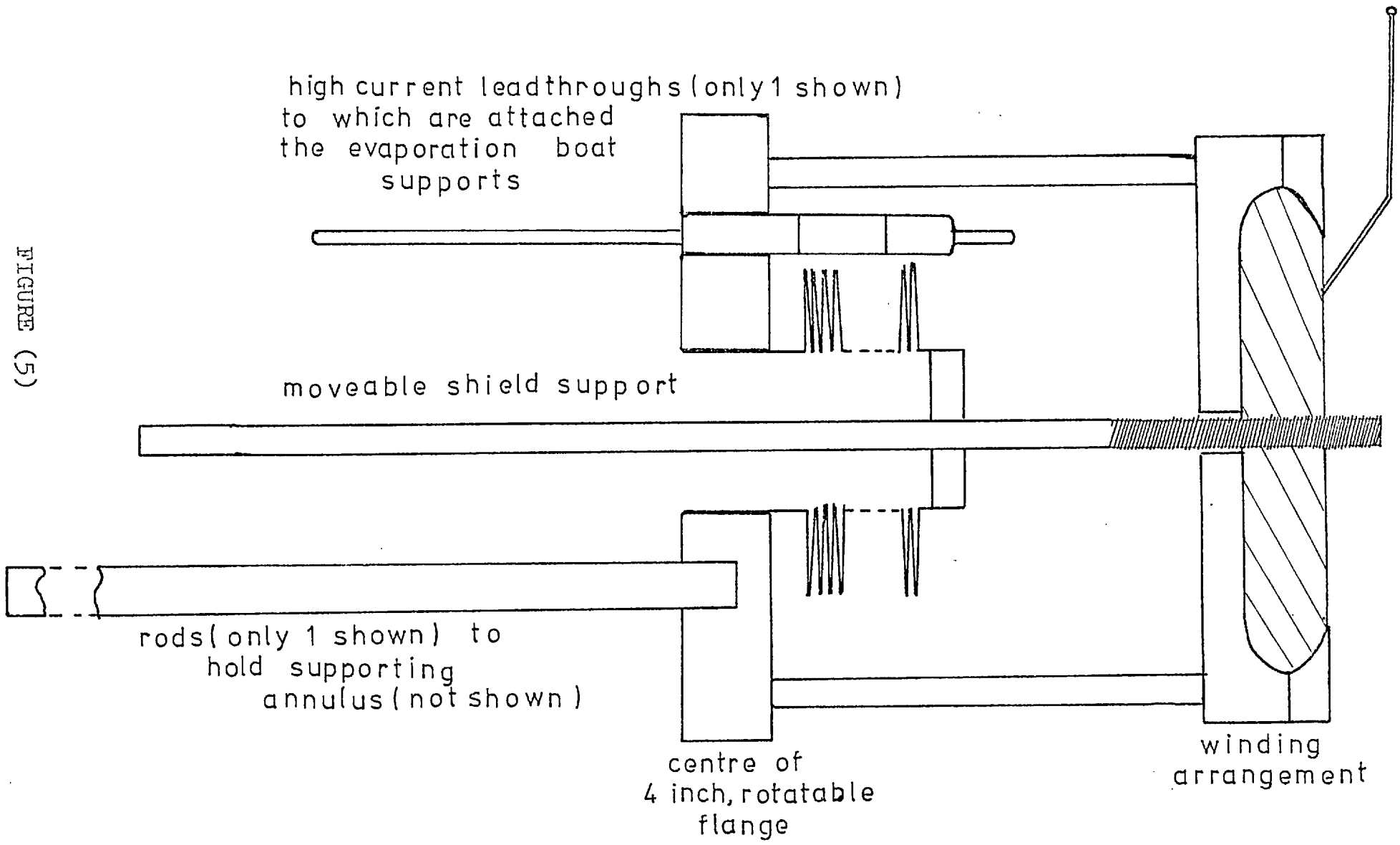
high current leadthroughs (only 1 shown)
to which are attached
the evaporation boat
supports
moveable shield support
rods (only 1 shown) to
hold supporting
annulus (not shown)
centre of
4 inch, rotatable
flange
winding
arrangement

FIGURE (5)

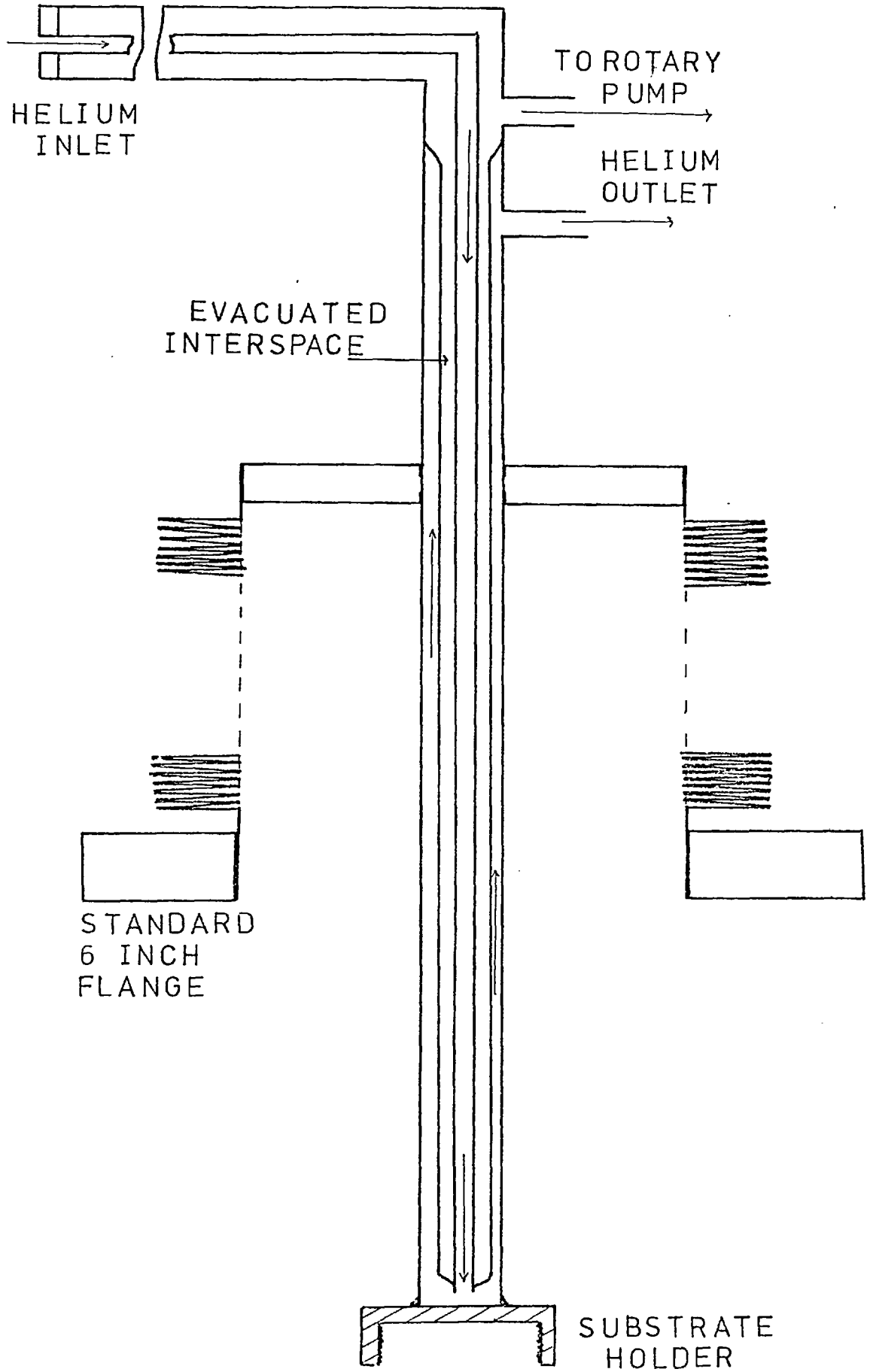
HELIUM
INLET
TO ROTARY
PUMP
HELIUM
OUTLET
EVACUATED
INTERSPACE
STANDARD
6 INCH
FLANGE
SUBSTRATE
HOLDER

FIGURE (6)

A copper substrate was designed, to screw into the support, with three individual projecting surfaces. Suitable use of the U.H.D. manipulator enable any one of the three substrates to be positioned over the evaporating aperture. The increase in length from the bellows to the substrate mentioned above also resulted in an increased amount of horizontal movement. This is because the substrate is no longer the pivot and so by tilting, the substrate can also be moved horizontally.

Limitations on space made it necessary to have the filling tube horizontal. As a result the top plate of the U.H.D. attachment had to have a slot cut in it so that it could be passed over the right angle bend.

Eight lead throughs were welded into the six inch flange. Two of these were used for attaching the thermocouple, the other end of which was clamped to the copper substrate. In the temperature range used ($4^{o}K$ - $300^{o}K$) the thermocouple used was gold-iron/chromel supplied by Johnson-Mathey.

2.3 Experimental Procedure

2.3.1 Calibration of the System

To obtain the experimental data in a form suitable for analysis it is first necessary to calibrate the system so that the scattering angles are known. In the analysis discussed in chapter (3), the diffracted intensity is defined in terms of a function s defined by

$$s = \frac{4\pi \sin\theta}{\lambda}$$

where θ = scattering angle

λ = wavelength of incident radiation

One result of using this expression is that the intensity at a given s value is independent of the incident radiation. Considering elastic scattering, Bragg's Law states:

$$n\lambda = 2d \sin\theta$$

where n = order of diffracted beam

d = inter-planar spacing

So for the first order scattering,

$$\frac{\sin\theta}{\lambda} = 1/2d$$

which indicated that $s = 4\pi \sin\theta/\lambda$ is directrly proportional to $1/d$

In the case of the S.H.E.E.D. apparatus the actual amount of pattern scanned is controlled by the Scan Generator. In this calibration and in all subsequent experiments, this was set such that the entire pattern was just scanned. The diffracted intensity is displayed on the (Y axis of an) X-Y recorder while the displacing voltage produced by the Scan Generator is applied to the X-axis. The sensitivity of the X-axis was set so that a full scan caused a displacement of 25cms exactly. In order to fix the position of the main beam on the trace, it is scanned through at a greatly reduced sensitivity.

To provide a known diffraction pattern a Au film was formed which gave a pattern of sharp rings. Using an accelerating voltage of 30 Kv several intensity traces were taken and one of them is shown in figure (7). Two traces were taken for the reading of peak positions and the values obtained are shown in table (1).

Using this data it is possible to calculate the camera constant which is defined by

$$2\lambda . L = D . d$$

where $2\lambda L$ = camera constant

D = displacement of peak from main beam in cms

d = inter planar distance corresponding to peak at D

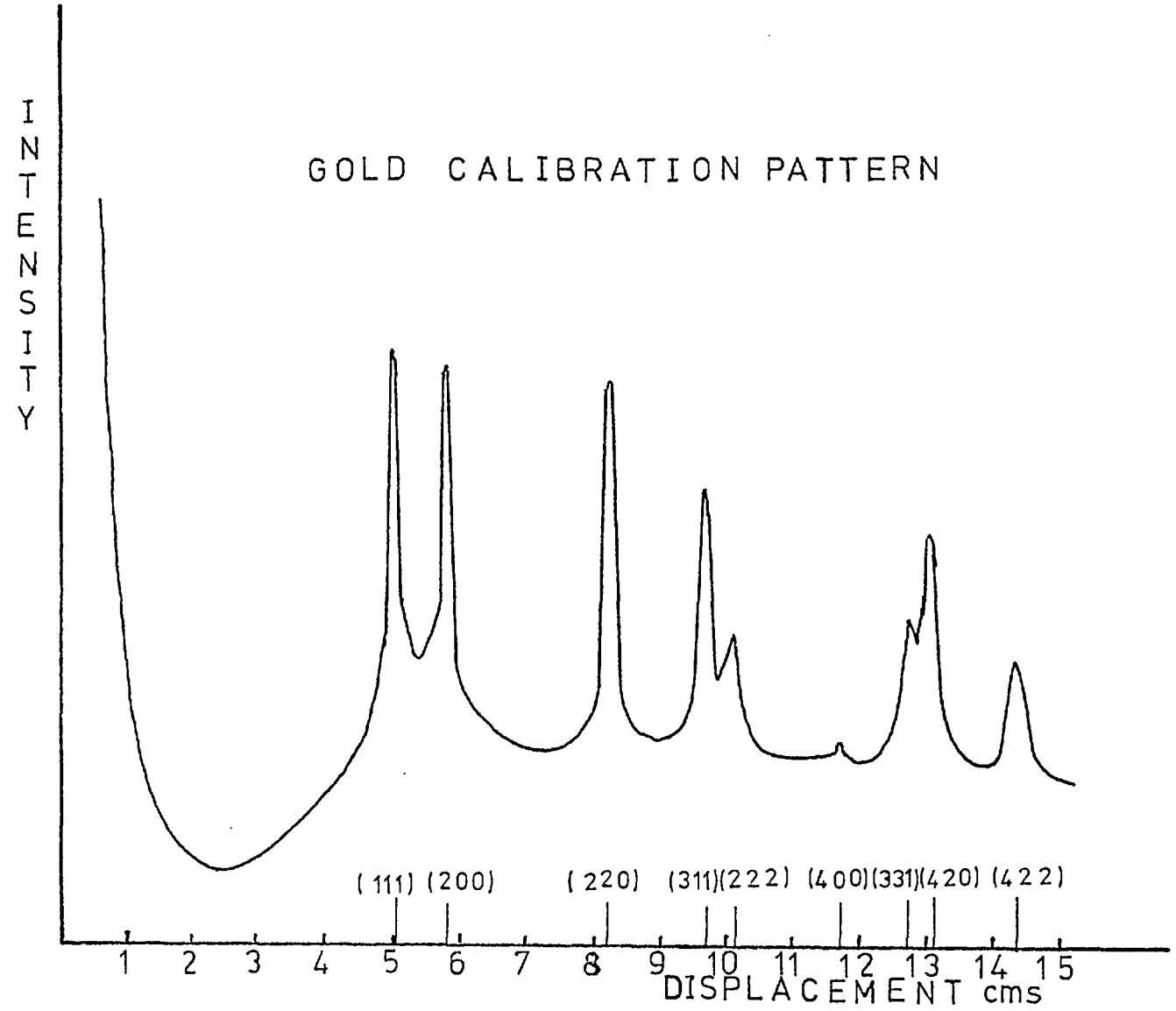
GOLD CALIBRATION PATTERN
INTENSITY
(111) (200) (220) (311)(222) (400)(331)(420) (422)
1 2 3 4 5 6 7 8 9 10 11 12 13 14 15
DISPLACEMENT cms

FIGURE (7)

PEAK	DISPLACEMENT FROM MAIN BEAM	
	TRACE1 (CMS)	TRACE2 (CMS)
1	5.05	5.05
2	5.85	5.85
3	8.30	8.30
4	9.75	9.75
5	10.15	10.15
6	11.75	11.85
7	1285	1285
8	13.10	13.15
9	1440	14.45

TABLE (1)

PEAK	CAMERA CONSTANT
1	11.92
2	11.93
3	11.95
4	12.00
5	11.98
6	12.04
7	12.08
8	11.92
9	11.95

TABLE (2)

The calculated camera constants for each of the peaks is shown in table (2) using the values of d given by. ASTM card 4-0784.

From Bragg's Law:

$$d = \lambda / 2\sin\theta$$

$$\therefore \quad s = 4\pi \sin\theta/\lambda = 2\pi/d = 2\pi D/2\lambda L$$

Hence using an averaged camera constant we have $s = 0.53D$.

This, then, is a general expression relating the X-axis displacement to the scattering angle and can bw u æd to convert the measured displacement into the corresponding s-value.

2.3.2 Using the basic S.H.E.E.D. system

2.3.2.1 Preparation of the Substrate

In order to obtain a suitable surface on which to deposit the films, the copper was carefully polished to form a non-crystalline layer, known as the Beiby layer.

Initially this was carried out using wet and dry abrasive papers followed by polishing wheels. This was followed by Alumina polishing powder and distilled water. Once the layer had been formed subsequent polishing between experimental runs was restricted to the last stage. Finally the substrate was thoroughly cleaned using distilled water and iso-propyl alcohol. This procedure was found to produce a surface which gave a diffraction pattern of two very diffuse rings indicating a non-crystalline layer was indeed formed. Figure (8) shows an intensity trace taken from such a diffraction pattern.

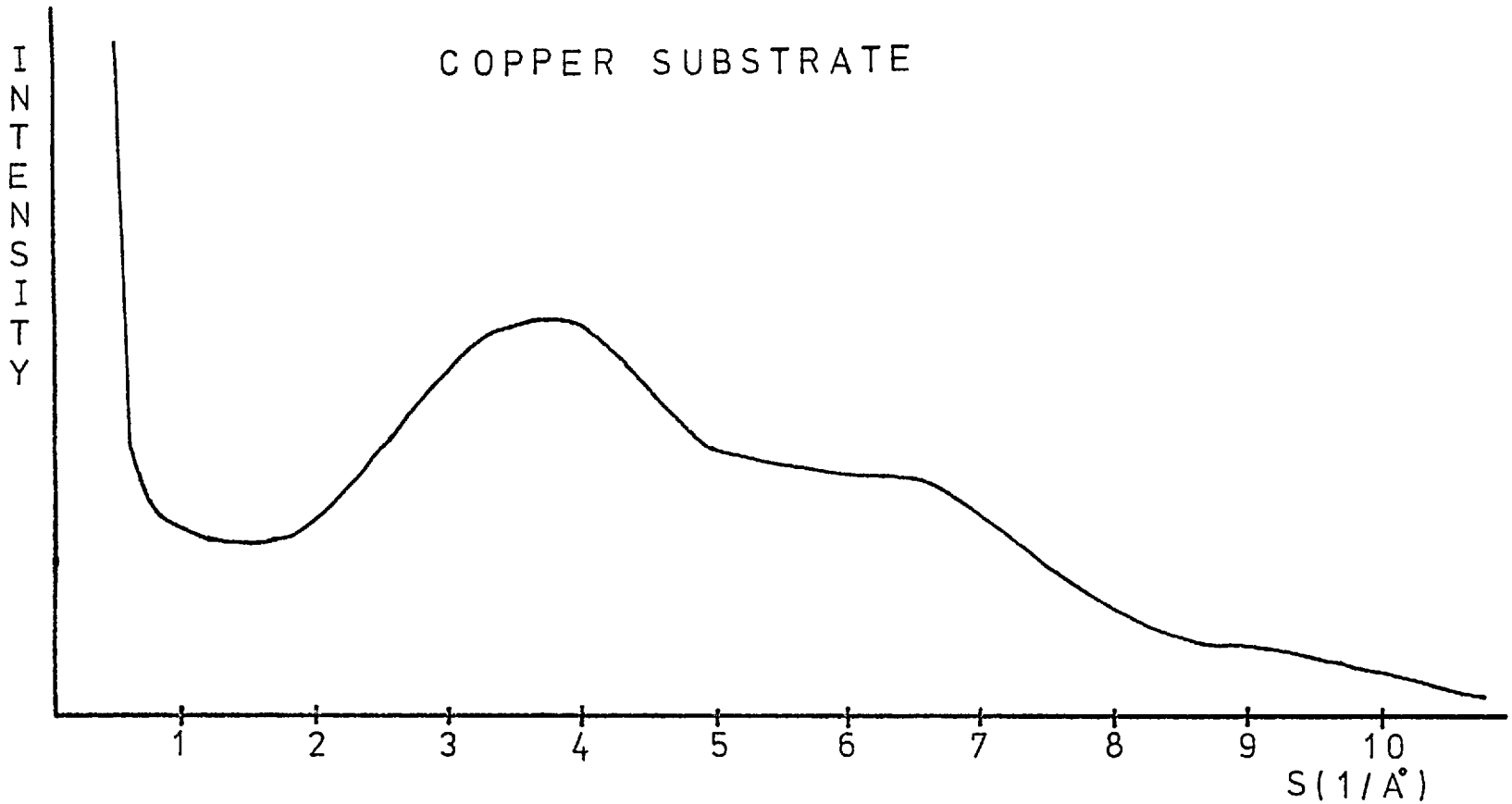

FIGURE (8)

2.3.2.2 Obtaining an Ultra High Vacuum

The sorption pumps were used, in succession, to rough pump the system to a pressure of 10^{-2} torr at which point the ion pump could be started. The titanium pump was used in on /off cycles ; the on time being one and a half minutes, while the off time was varied depending on the system pressure. Typically this would be ten minutes soon after starting the ion pump and would vary to several hours at pressures below 10^{-9} torr. Using the pumps a s indicated the base pressure of 10^{-7} torr could be reached from atmosphere in about two hours.

To improve on this pressure it was necessary to bake the apparatus. The bake-out could be controlled using the supplied control unit which caused the heaters to switch on and off at pre-determined values of the ion pump current. It is important to take care in selecting the cut-out pressure levels or thermal run away will occur. This is where the system become s hot too quickly and, although the heaters are switched off as the pressure rises, so much gas is evolved that the ion pump is switched off using its protection circuit. In practice it wa s normally possible to bake the system for 24 hours in the temperature range of

150°C - 200°C quite satisfactorily. After this treatment the pressure could be reduced to approximately 1×10^{-9} torr. Subsequent use of the titanium sublimation pump enabled this to be reducted further and the ultimate pressure reached was 2×10^{-10} torr. Using this procedure the total pump down time from atmosphereic was about 36 hours.

2.3.2.3 Evaporation and Study of the Thin Films

Immediately after obtaining a suitable vacuum the ion gauge, electron gun filament and the evaporation boat are outgassed. The latter was carried out, with the substrate shielded, by heating the boat to near the evaporation temperature of the material being investigated for about half an hour.

Following this the electron beam is obtained with typically an accelerating voltage of 30 kilovolts and an emission of 100 microamps. Adjustments are then made to set the energy filter normal to the electron axis. Denbigh and Grigson (1965) indicate that if the electrons are inclined at an angle γ to the filter normal then the cut-off will occur when

$$\frac{V - V_f}{V} = \mathrm{Sin}^2\gamma$$

where V = electron gun potential
V_f = energy filter potential

$$\frac{E_f}{V} = \mathrm{Sin}^2\gamma$$

where $E_f = V - V_f$ = energy filter biasing

In practice the beam will have a small angular divergence and so even if the filter is set exactly normal to the

electron axis the cut-off will occur at some value of E_f not equal to zero. However if the energy filter is arbitrarily set up the cut-off value of E_f will increase because of the larger angle δ . Hence the procedure is to adjust the setting until the value of E_f at which the electron beam is cut-off becomes a minimum. A plot of beam intensity against E_f for an arbitrary filter position is shown in figure (9) along with the plot obtained with the best possible energy filter position. It can be seen that in this case the beam cut-offs when E_f = 7 volts and so this is the optimum resolution possible.

After setting up the energy filter the diffraction pattern from the copper substrate is obtained. Liquid nitrogen is then sucked through the capillary cooling tube by means of a small pump. The thermocouple output is monitored using a digital volt meter and deposition is carried out when the lowest steady temperature is reached. The time taken to cool the substrate to $77^{o}K$ was usually about ten minutes. The warming of the film could be varied to a certain extent by sucking air through the capillary tube and the time taken to reach room temperature ranged from about one to two hours.

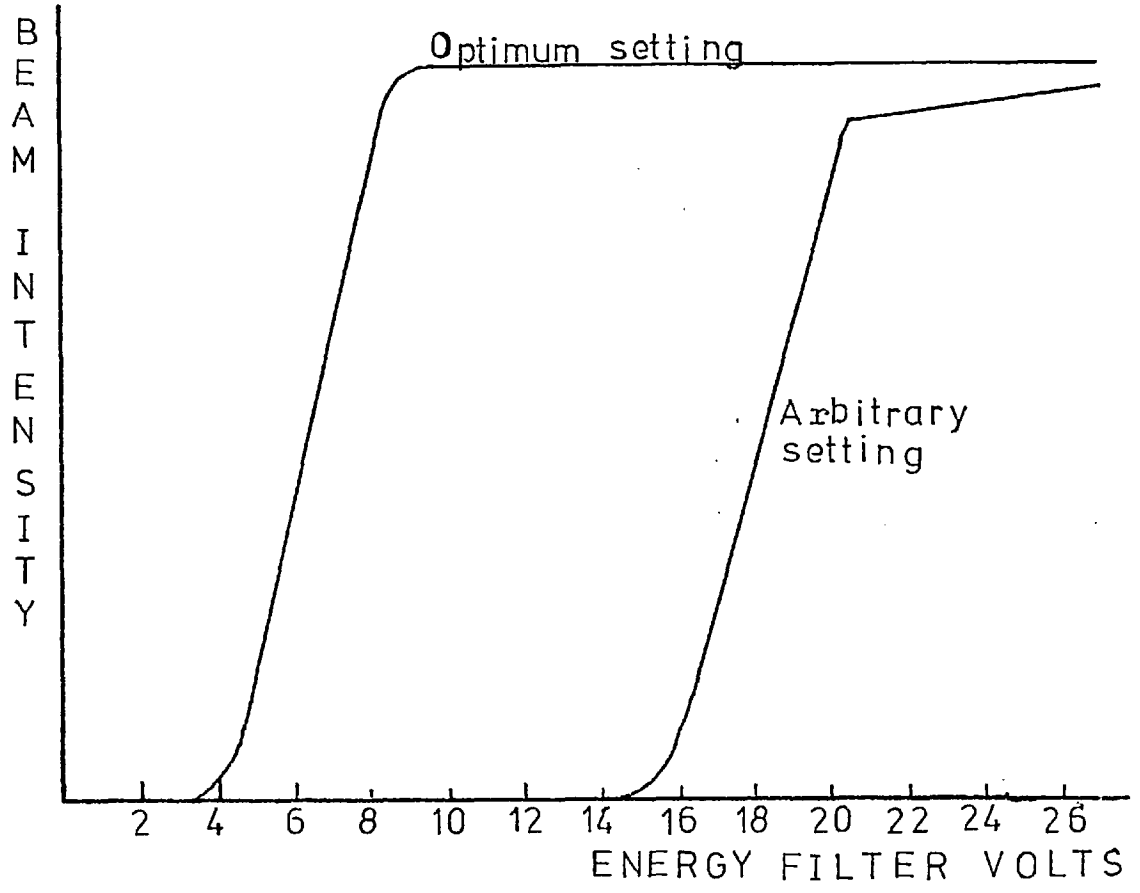
BEAM INTENSITY
Optimum setting
Arbitrary setting
2 4 6 8 10 12 14 16 18 20 22 24 26
ENERGY FILTER VOLTS

FIGURE (9)

2.3.3 Using the Liquid Helium Stage

It is essential when using liquid Helium to attain the best possible vacuum in the system. Several hours before the Helium transfer the radiation shield was filled with liquid nitrogen. It also became standard practice to evacuate the interspace in the Helium stage immediately before each run.

One of the three substrates was manipulated into position to give a diffraction pattern. Since the radiation shield was aligned such that the evaporant aperture was along the electron axis this substrate was then exposed to the evaporation boat.

When the diffraction pattern of the substrate was set up satisfactorily the Helium transfer was started. The syphon used was a standard L-shaped one with a flexible arm supplied by Oxford Instruments. The method which was found to work best was to suck the Helium through the stage by means of a rotary pump connected to the exit tube. The actual thermocouple used was not calibrated individually and this means that there is probably an error of up to 10% on the output. However, its output was measured at liquid Helium and liquid

Nitrogen temperatures and the former reading showed that the copper substrate did reach very nearly $4^{o}K$. Typically the time taken to reach this temperature was ten minutes and the amount of Helium used was about two litres. The time taken to warm to room temperature could be varied, by sucking through air, between two and six hours.

Some of the experiments, owing to a leak developing in the radiation shield, were carried out using the Helium stage on its own. This had the disadvantage of allowing only one run for every pump down but did not affect the performance significantly. The temperatures reached were the same as before although it did use about half a litre extra of Helium. It is likely that it also resulted in increased condensation onto the cold copper substrate.

2.3.4. Resistance Measurements

When the radiation shield was not used it was possible to modify the substrate so that the resistance of the deposited films could be monitored. In this way electrical resistance measurements could be performed concurrently with diffraction studies.

2.3.4.1 Preparation of the Substrate

The basic substrate arrangement used with the Helium stage is three individual substrates projecting from the flat copper surface. To obtain resistance measurements one of these triple copper substrates was modified by the removal of the three projections to give a flat surface. This flat copper surface was polished to produce a non-crystalline surface as described in section (2.3.2.1).

Using an auxillary, diffusion pumped, vacuum system silicon monoxide was evaporated from a tungsten boat onto the copper surface. This resulted in the formation of a suitable non-crystalline, non-conducting surface layer which was probably a mixture of silicon monoxide and dioxide. It was found by experience that an adhesive, good quality film could be produced providing that:

1. the copper surface was not allowed to become too hot
2. the deposited film was not too thick
3. the film was not exposed to the atmosphere for more than a few hours
4. the copper surface was very clean

The first condition was satisfied by simply placing the copper block at least six inches away from the evaporation boat. Thick deposited films were found to peel after several hours and a suitable thickness was when the film became light brown whilst still remaining just transparent. To minimise the effects of atmospheric contamination the practice followed was to leave the evaporated film inside the coating unit until it was to be inserted into S.H.E.E.D. The cleanliness of the copper surface was very important and in particular the slightest amount of finger grease would cause the film to flake. Consequently great care was taken in the preparation of the copper surface and particularly with its final cleaning with iso-propyl alcohol.

2.3.4.2. Attachment of the Leads

Several methods were tried. The easiest and most reliable was found to be the use of Silver Dag. The auxillary vacuum system was used to evaporate two gold contacts onto the film using an aluminium mask. Thin, flexible copper wires were then placed on these contacts and secured by the silver dag. The use of this colloidal paint had no effect on the performance of the ultra high vacuum system.

Having fitted the substrate into the Helium stage and attached the wires and the thermocouple, the system was pumped down and baked as before.

2.3.4.3 Monitoring the Film Resistance

A constant current power supply capable of supplying currents between 1μA and 10mA was built. This was used to obtain a voltage from the film directly proportional to its resistance. In conjunction with the thermocouple output, and using an X-Y recorder, a graph of resistance change against thermocouple output could be obtained.

CHAPTER 3

Methodof Analysis of the Experimental Data

3.1 The method of approach

There are two main ways in which information about structure can be obtained from diffraction data from a liquid or non-crystalline solid.The more usual approach is to evaluate the Radial Distribution Function. This is related to the atomic density and can in principle be determined from the experimental data. This method is discussed inthe first part of this chapter. The alternative procedure is to postulate a structural model and then attempt to predict the scattering produced from this structure.This calculated scattering can then be compared with that obtained by experiment.This latter approach is considered at the end of this chapter.As might be expected both methods have their advantages and disadvantages and these will be fully discussed.

3.2 The Radial Distribution Function (R.D.F.)

3.2.1 Non-crystalline solids

As mentioned in Chapter 1 there have been various models suggested for the structure of non-crystalline solids. Common to all of them is that they possess short range order of some kind while long range crystalline order is absent.This short range order occurs because the atoms in the solid have a finite 'size'-that is two atoms have a distance of nearest approach.Inthis way the atoms cannot be arranged completely randomly in the sense that some positions are forbidden by the presence of other atoms.This short range order results in the formation of a diffraction pattern generally consisting of diffuse rings.

3.2.2 Scattering from liquids and non-crystalline solids

Consider incident radiation represented by the unit vector $\underline{s}_0$ impinging on two scattering atoms A_1, A_2 separated by $\underline{r}$.Let the scattered radiation be represented by the unit vectot $\underline{s}_c$.

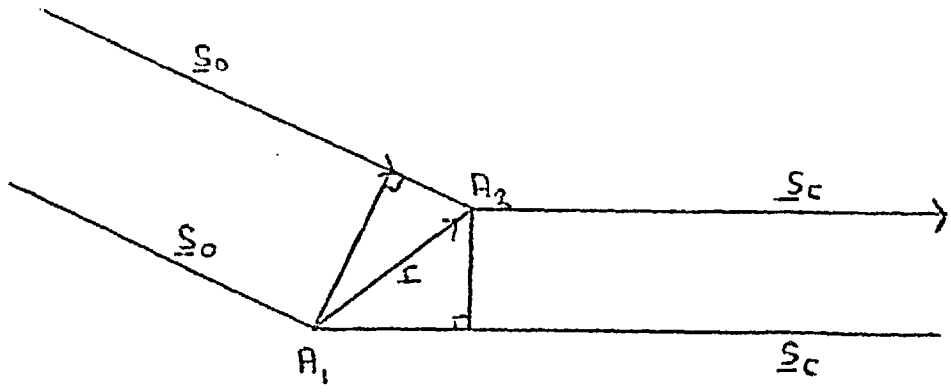

Figure (1)

The path difference between the waves is given by

$$\underline{r}.(\underline{s}_c - \underline{s}_0) = \underline{r}.\underline{s} \quad \text{where } \underline{s} = (\underline{s}_c - \underline{s}_0)$$

The phase difference $pd = k.\underline{r}.\underline{s}$ where $k = 2\pi/\lambda$

λ = wavelength of incident radiation

Now consider the amplitude of the scattered wave at a point P far from the scattering centres

$$\text{Amplitude } A = A_0/R.(\exp(iwt - ik\underline{r}.\underline{s}) \quad \text{————(1)}$$

where:

R = distance from P to the scattering centres (which can be considered at the same point since $R \gg |\underline{r}|$)

A_0 = amplitude of the scattered wave at unit distance away along $\underline{s}_c$

By considering the mechanism of atomic scattering we can replace A_0 with $-(e^2/mc^2)f$ where e, m and c have their standard notation and f is the atomic scattering factor for the particular atom under consideration. Hence the intensity from the whole scattering region, comprising N scattering centres, is

$$A^2 = (1/R^2)(e^2/mc^2)\sum_P^N \sum_q f_p f_q^* \exp(-ik(\underline{r}_p - \underline{r}_q).\underline{s} \quad \text{—(2)}$$

where f^* represents the complex conjugate of f and in general can be put equal to f. Considering the sums over p and q, there will be N terms for which p=q (where $r_p = r_q$). In these terms the exponential term will

be unity.Hence we have

$$I = |A|^2/C = \sum_p f^2 + \sum_p \sum_{q \neq p} f_p f_q \exp(-ik\underline{s}.(\underline{r}_p - \underline{r}_q) \quad \text{——(3)}$$

where $C = (e^2/mc^2)^2/R^2$

In the case of scattering from a single element $f_p = f_q$

Then $I = |f|^2(N + \sum_p \sum_{q \neq p} \exp(-ik\underline{s}.(\underline{r}_p - \underline{r}_q)))$ ————(4)

Now apply this expression to a monatomic liquid or non-crystalline solid.The expression has to be averaged over all possible arrangements and this is done by first considering just two atoms p and q.The average contribution to the intensity from these two atoms is found and this is then integrated over the whole scattering volume. The probability that atom p lies in the volume dv_p at the same time that atom q lies within dv_q is given by

$$W(\underline{r}_{pq})(dv_p/V)(dv_q/V)$$

where V = volume of the scattering region

$W(\underline{r}_{pq})$ = spherically symmetric probability function that p and q will be separated by $|\underline{r}|$. It is taken to be unity when all distances are equally probable as in a completely random arrangement.It will be the same for all atoms and so will be replaced by $W(\underline{r})$.

The average contribution from atoms p and q is the product of this probability and the term due to p and q in equation (4).The double summation over p and q has N(N-1) terms and the average value will be the same for each.Hence we have for the average intensity from all N scattering atoms

$$\bar{I} = |f|^2(N+N(N-1)\iint W\exp(-ik\underline{s}.(\underline{r}_p-\underline{r}_q)dv_p dv_q/V^2 \quad \text{—(5)}$$

In the ideal case of point atoms which is approached by a gas W =1. In this case we have

$$\bar{I} = |f|^2(N+N(N-1)\iint \exp(-ik\underline{s}.(\underline{r}_p-\underline{r}_q)dv_p dv_q/ V^2) \quad \text{—(6)}$$

In this ideal case the positions of p and q are completely independant of each other, so that the double integral can be written as the product of two single integrals. These single integrals have the form

$$X_p = \int \exp(-ik\underline{s}.\underline{r})dv/V$$

To evaluate this integral take the scattering volume to be a sphere with radius R and its centre at the origin. Let $\underline{s}$ and $\underline{r}$ make an angle α, so that

$$k\underline{s}.\underline{r} = 4\pi r\cos\alpha(\sin\theta)/\lambda = sr\cos\alpha$$

where $s = 4\pi(\sin\theta)/\lambda$

(N.B. s is conventionally used to express this term and should not be confused with $\underline{s}$.)

Let the volume element dv be the volume between the spheres of radii r and r+dr and the cones having $\underline{s}$ as axis and the semi-vertical angles α and $\alpha+d\alpha$.

Then

$$X_p = 2\pi/V \int_0^{\pi}\int_0^{R} r^2\exp(-isr\cos\alpha)\sin\alpha\, dr d\alpha$$
$$= 4\pi/V \int_0^{R} r^2\sin(rs)/rs\, dr$$
$$= 4\pi/V \quad R^3/3 \quad Z(Rs)$$

where $Z(Rs) = 3(\sin(Rs) - Rs\cos(Rs))/(Rs)^3$

The other integral X_q will have the same value as X_p, so that

$$I(s) = |f|^2(N+N(N-1)(Z(Rs))^2) \quad \text{——————} \quad (7)$$

The form of Z(Rs) is such that it can be neglected in equation (7) when

$$Rs > 1.430$$

Typically then for a scattering sphere of radius 10$\mathring{A}$, $I(s) = N|f|^2$ for values of s greater than about $0.5\mathring{A}^{-1}$. This result is entirely reasonable as a completely random arrangement would be expected to give just the sum of the intensities scattered by the individual atoms.

Now return to the real case where W is not unity. The integral to be evaluated is

$$Y = \int\int W\exp(-ik\underline{s}.(\underline{r}_p-\underline{r}_q))dv_p/V\ dv_q/V$$

and this is done by replacing W with 1-(1-W). So we have

$$Y = Y_1 - Y_2$$

where Y_1 is the integral X_p discussed before and can be neglected except near s=0

$$Y_2 = \int\int (1-W)\exp(ik\underline{s}.\underline{r}_{pq})dv_p/V\ dv_q/V$$

To evaluate Y_2, first suppose the atom p to lie anywhere within the volume V with equal probability (as indeed the first atom can).Integrating with respect to dv_p then gives the factor unity.Take the position of p as the origin and let r be the radial distance from q to p.Let α be the angle between $\underline{r}$ and $\underline{s}$ then as before we have

$$Y_2 = 1/V \int\int 2\pi(1-W)\, r^2 \exp(isr\cos\alpha)\sin\alpha \, d\alpha \, dr$$

The limits of integration are from 0 to π for α and we can put 0 to ∞ for r since W becomes unity,and the integrand zero, for large r.Therefore

$$Y_2 = 4\pi/V \int_0^\infty (1-W)r^2 \, \sin Sr \, /Sr \, dr$$

and

$$I(s) = |f|^2 \, (N-4\pi N(N-1)/V \int_0^\infty (1-W)r^2 \sin(rs)/rs \, dr \,) \qquad \text{——(8)}$$

It is now convenient to replace the probability function W with the atomic density function $\rho(\underline{r})$.This atomic density function is defined such that $4\pi\rho(r)r^2dr$ is the average number number of atoms lying,at any instant,between r and r+dr from the centre of some specified atom p.Both W(r) and $\rho(r)$ are spherically symmetric and have the same dependance on r.To determine the numerical factor relating the two consider a

completely random distribution of atoms.In this case $\rho(r)$ is the average number of atoms per unit volume and hence equals ρ_o,the average atomic density.However W(r) is unity and so for N scattering centres in a volume V we have

$$\rho(r) = \rho_o W(r) = (N/V)\ W(r)$$

So replacing W(r) with $\rho(r)/\rho_o$ in equation (8) gives

$$I(s) = |f|^2 N\ (1-4\pi \int_o^\infty (\rho_o - \rho(r))r^2\ \sin(rs)/rs\ dr)$$

having put N-1 = N

Now defining the normalised intensity $I_N(s)$ as

$I_N(s) = I(s)/N$ and the R.D.F. as

$G(r) = 4\pi r(\rho(r)-\rho_o)$ we have

$$s(I_N(s)/\ |f|^2\ -1) = \int_o^\infty G(r)\sin(rs)dr \quad \text{——— (9)}$$

Now put $i(s) = s(I_N(s)\ /\ |f|^2\ -1)$ in equation (9)

$$\underline{i(s) = \int_o^\infty G(r)\sin(rs)dr} \quad \text{——————— (10)}$$

By Fourier's Integral theorem then

$$\underline{G(r) = 2/\pi \int_o^\infty i(s)\sin(rs)ds} \quad \text{——— (11)}$$

3.2.3 The Radial Distribution Function, Density Function and the information obtainable.

The equations (10) and (11), which shows that i(s) (called the interference function) and G(r) form a Fourier pair, are the basic starting point for the analysis of diffraction data from liquids and non-crystalline solids. In addition, the Radial Density function D(r) is of use with

$$D(r) = 4\pi \rho(r) r^2$$

The basic information to be obtained from D(r) and G(r) are interatomic distances and co-ordination numbers. From the defination of $\rho(r)$ $\int_{r_1}^{r_2} D(r)dr$ represents the number of atoms betweem the spheres of radii r_1 and r_2. Hence by evaluating the area under the peaks in D(r) one can arrive at a estimate for the co-ordination numbers. This process is complicated by the overlapping of the various peaks and Mrafko, Duhai (1974) give three methods of measuring the areas. Consider the typical peak shown in figure (2). The co-ordination number is given approximately by the three following expressions:

$$N = 2\int_{r_{min}}^{r_{max}} 4\pi\rho(r)r^2 dr \qquad \text{method 1}$$

$$N = \int_{r_{min}}^{r'_{min}} 4\pi\rho(r)r^2 dr \qquad \text{method 2}$$

$$N = \int_{r_{min}}^{r_s} 4\pi\rho(r)r^2 \, dr \qquad \text{method 3}$$

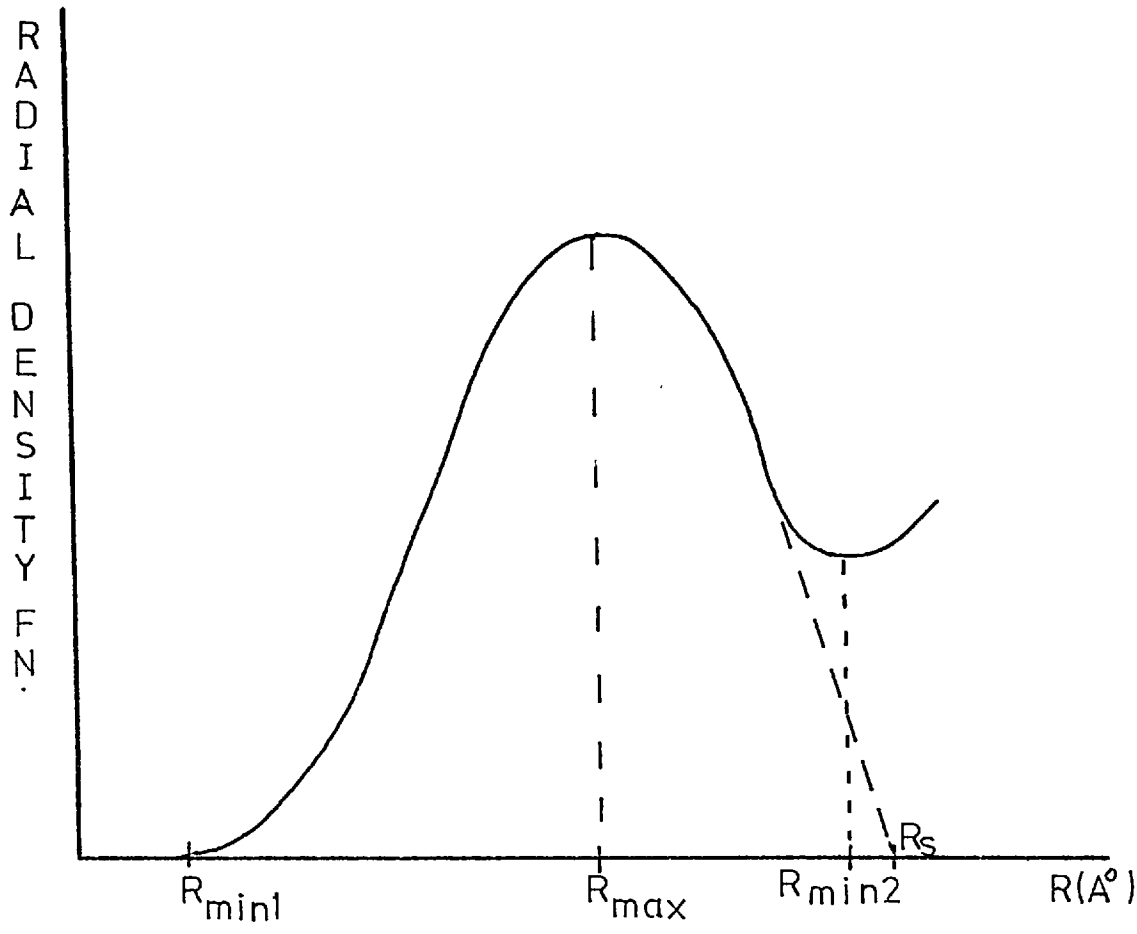

Figure (2)

The three integrals are calculated and the results obtained are said to agree to within two percent.An alternative method,suggested by Karle and Karle(1949) is to approximate the peaks in D(r) with Gaussians of the form

$$D(r) = (N_i/\sqrt{4\pi A_i})\exp((r - r_i)^2/4A_i)$$

where r_i = position of i^{th} peak

$2A_i$ = mean square deviation of r_i

N_i = co-ordination number

Hence by fitting the best Gaussian to D(r) peaks the values for N_i and A_i can be deduced.

In addition to the evaluation of these basic quantities, Gokularathnam(1974) has pointed out a further use to which the R.D.F. can be put.This is in the case of where the specimen is suspected of containing micro-crystalline regions and gives an estimate of their maximum possible size.A size factor V(r) is introduced such that

$V(r) = 1$ inside the diffracting region

$V(r) = 0$ outside the diffracting domain

Suppose G(r) is calculated from equation (11) using diffraction data from a micro-crystalline specimen.This will lead to a $D(r) = 4\pi\rho^*(r)r^2$ given by

$$4\pi\rho^{*}(r)r^{2} = 4\pi\rho_{o}r^{2} + rG(r)$$

The apparent density $\rho^{*}(r)$ being evaluated without considering the size factor appropiate for the micro crystals. Let the true atomic density be $\rho(r)$ and define

$$g(r) = \rho(r)/\rho_{o}$$
$$g^{*}(r) = \rho^{*}(r)/\rho_{o}$$

Then taking the size factor into acoount

$$4\pi r^{2}\rho^{*}(r) = 4\pi r^{2}\rho_{o}(1-V(r)) + 4\pi r^{2}\rho_{o}\, g(r)V(r)$$

Hence $g^{*}(r) = 1-V(r) + g(r).V(r)$

Therefore $g^{*}(r) \longrightarrow 1$ when $V(r) \longrightarrow 0$ or $g(r) \longrightarrow 1$. Now for a non-crystalline material, $g(r)$ approaches unity before $V(r)$ becomes zero, while in the micro-crystalline case $V(r)$ becomes zero before $g(r)$ becomes unity. Hence by inspecting the calculated $G(r)$ to see when it becomes zero (i.e. $\rho^{*}(r) = \rho_{o}$) it is possible to estimate the size of any micro-crystalline regions.

3.3 Computation of the Radial Distribution Function

3.3.1 The errors involved in obtaining the R.D.F. and their treatment.

In principle the R.D.F. can be evaluated exactly from the interference function by the use of equation(11). However in practice serious errors can be introduced into the resultant R.D.F. due to two main causes.These are:

(1) errors in the interference function caused by improper normalisation of the experimental intensity

(2) collection of the data over an incomplete range. This results in a termination error and is mainly because the data is only known to some maximum value of s.

In addition equation (11) refers only to the coherent scattering.This necessitates the removal of the inelastic scattering from the total intensity diffracted.In the case of X-rays this Compton scattering is usually calculated and then used to correct the experimental data.In electron diffraction it is possible,as in this project,to eliminate the inelastic contribution experimentally.

The usual method chosen to normalise the data is to fit the experimental intensity (I(s)) to the independant a tomic scattering (i.e. $|f|^2$) at large scattering angles.This is utilising the fact that at such scattering angles the intensity approaches that from a completely random arrangement of atoms.This procedure of course

then relies on accurate measurement of a small intensity. A modification of this method is to fit s.I(s) to s.$|f|^2$ over the whole range of experimental data.An alternative procedure due to Krogh-Moe is obtained by again considering equation (11).

$$4\pi r\rho(r) - 4\pi r\rho_o = 2/\pi \int_o^\infty i(s)\sin(rs)\, ds$$

so $$2\pi^2 r\rho(r) - 2\pi^2 r\rho_o = \int_o^\infty i(s)\sin(rs)ds$$

Differentiating with respect to r gives

$$2\pi^2\rho(r) + 2\pi^2 r\rho'(r) - 2\pi^2\rho_o = \int_o^\infty si(s)\cos(rs)ds$$

Since the atoms have a distance of closest approach, $\rho(0) = 0$.Then at $r = 0$

$$\int_o^\infty s.i(s)\, ds = -2\pi^2\rho_o \qquad \text{——————(12)}$$

Let $I_N(s) = A.I(s)$

where $I(s)$ = experimental intensity measured in arbitrary units

$I_N(s)$ = normalised intensity

A = normalisation factor

Hence $i(s) = s.(A.I(s)/|f|^2 - 1)$

So substituting for i(s) in equation (12)

$$A = \left(\int_0^\infty s^2 ds - 2\pi^2\rho_o\right) / \int_0^\infty s^2 . I(s) / f^2 ds \quad \text{——— (13)}$$

Equation (13) indicates that if the average atomic density is known then the normalisation factor can be calculated. Furthermore it can be seen that the integral in the numerator can be evaluated analytically. If the data is known out to say $s = 12\ \text{Å}^{-1}$ then the integral has a value of about 550. (Its exact value depends on the minimum value of s, which is generally not zero). This means that in most cases the second term in the numerator can be neglected without affecting the resulting normalisation factor.

The form of the error introduced into the R.D.F. by faulty normalisation has beendiscussed by Krogh-Moe (1956), Wagner(1972) and Kaplow et Al(1965). Following the approa ch of kaplow et Al let the fractional error in the normalisation constant be $\Delta A/A$. The interference function is:

$$i(s) = s(A.I(s)/f^2 - 1)$$

so the corresponding error function is:

$$\Delta i(s) = s.\Delta A.I(s)/|f|^2 = s.\Delta A/A.I_N(s)/|f|^2$$

Hence $\Delta i(s) = (\Delta A/A).s.(I_N/|f|^2 - 1) + (\Delta A/A).s$

This error function is shown in figure (3) for a one

per cent error, while figure (4) illustrates the resulting error in the R.D.F. Kaplow et Al also considered the effect of errors in the atomic scattering factors. They point out that it is impossible to be sure of the exact form of the error but it is likely that it will be of the form $\Delta (I_N / |f|^2) = I_N / |f|^2 .E$ where E is a slowly varying function of s. The resultant error in i(s) is given by:

$$\Delta i(s) = E.s.(I_N / |f|^2 - 1) + E.s$$

and it will combine with the normalisation error to give

$$\Delta i(s) = (E + \Delta A/A).s.(I_N / |f|^2 - 1) = (E + \Delta A/A).s \qquad (14)$$

The error in the R.D.F. from the first term in equation (14) will consist of the convolution of $(E + \Delta A/A)$ with the true R.D.F. Since $(E + \Delta A/A)$ is a slowly varying function of s this will result mainly in a scale change. The second term will cause an error most significant below the first peak and so it the more important term.

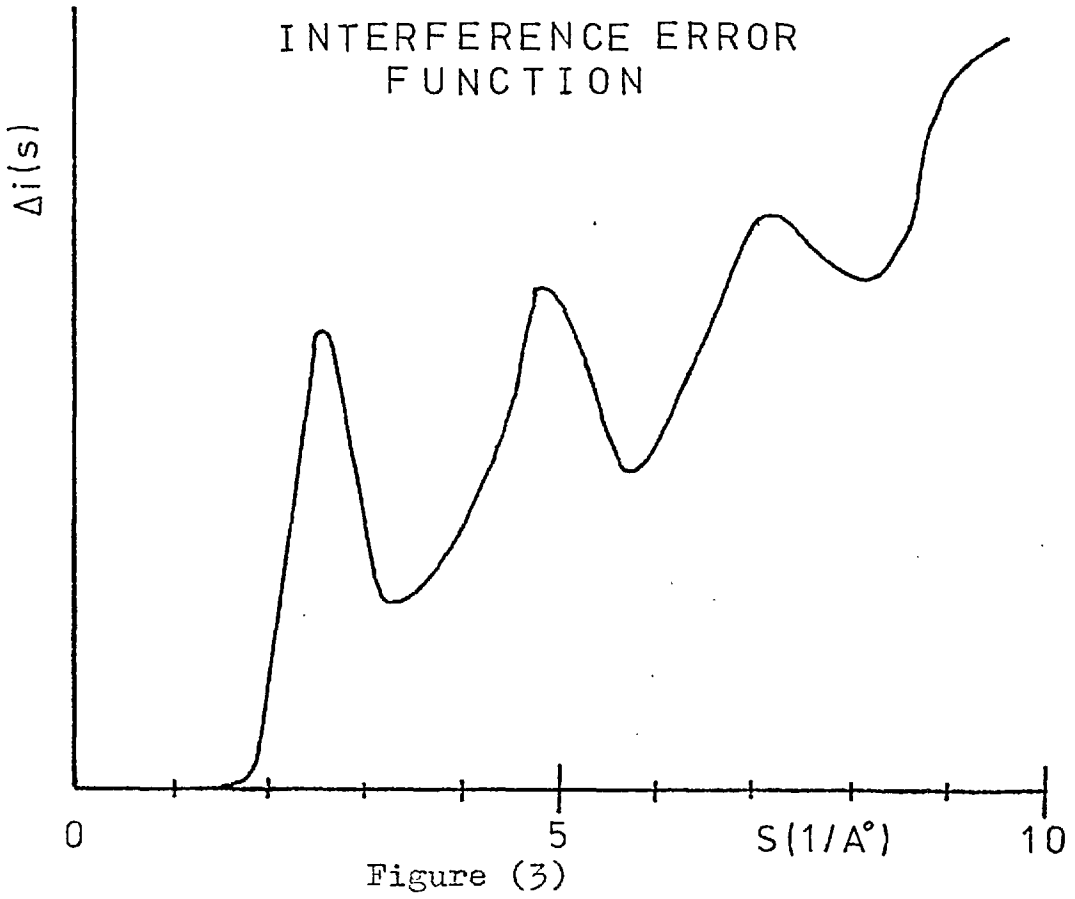

Figure (3)

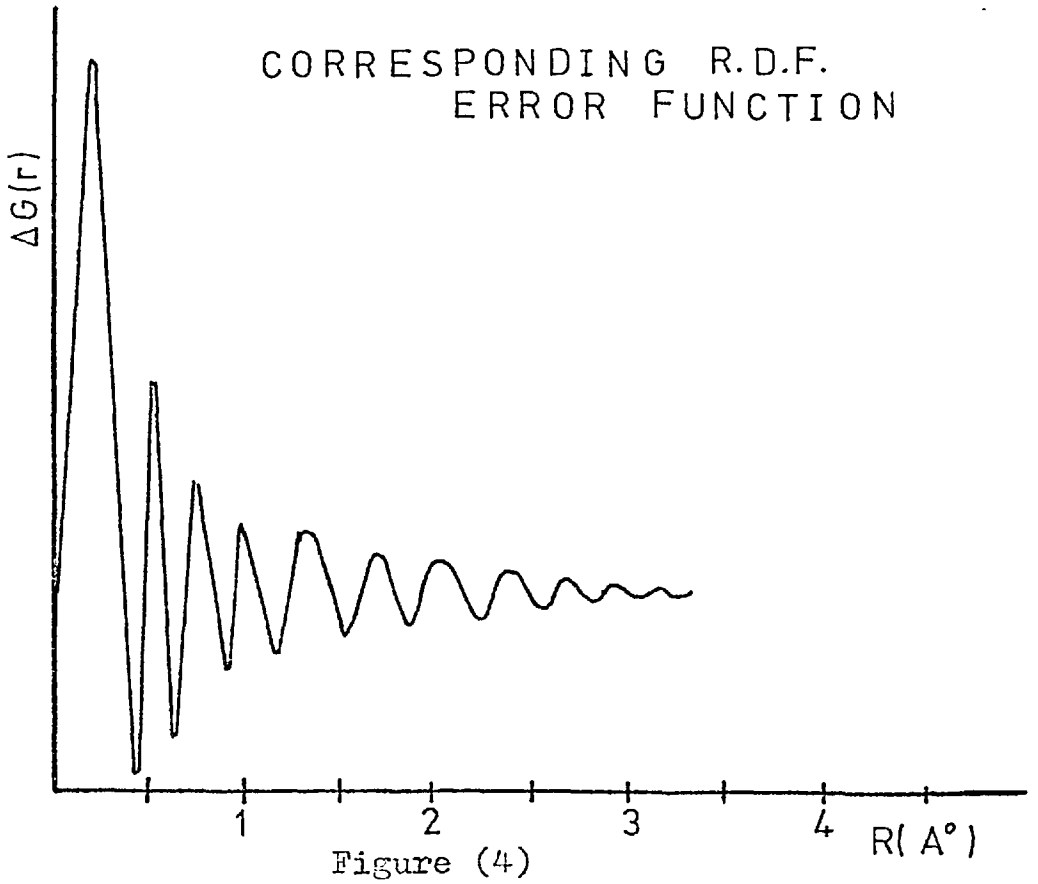

Figure (4)

Kaplow et al also considered the problem that in general the data is only known from some minimum s to some maximum value (S_{max}). The absence of data at small s values is not too important because the intensity is very small in this region. The upper limit, however, affects the resultant R.D.F. quite considerably by causing spurious oscillations.

Mathematically it can be treated by modifying the true interference function i(s) with a function c(s) where

$$c(s) = 1 \qquad s < S_{max}$$

$$c(s) = 0 \qquad s > S_{max}$$

Consequently instead of evaluating the Fourier transform of i(s) the transform of i(s) . c(s) is performed instead. The Convolution theorem then indicates that the true R.D.F. is modified by a function of the form:

$$G'(r) = 2S_{max} \frac{\text{Sin } 2\pi S_{max} \cdot r}{2\pi S_{max} \cdot r} \qquad \text{(15)}$$

This results in subsidiary maxima and minima appearing around the true R.D.F. peaks at distances of:

$$r = \pm 5/4S_{max}, \pm 9/4S_{max}, \quad \text{(maxima)}$$

$$r = \pm 3/4S_{max}, \pm 7/4S_{max}, \quad \text{(minima)}$$

Kaplow et al undertook a computational study of the effect of the termination error. They concluded that the main error in the R.D.F. was in the vicinity of the first peak, as would be expected from equation (16). Since the R.D.F. is altered by the normalisation/scattering factor error and the termination error at different positions, they devised a method of treating them separately.

This is outlined below:

In a real R.D.F. the value of $\rho(r)$ would be zero before the first peak leading to a R.D.F. of $-4\pi\rho_c.r$. The normalisation and scattering factor errors will be apparent by oscillations about this straight line. In this small r region a straight line of gradient $-4\pi\rho_o$ is calculated and the difference between this and the experimental R.D.F. is defined as Δ G(r). As discussed before, the transform of this error function will appoximately equal $S(E + \Delta A/A)$. Then, as can be seen from equation (14), the corresponding interference error function Δ i(s) can be obtained by multiplying this by $I_N(s)/|f|^2$. This calculated error function is then used to modify the original interference function.

Rahman (1965) has derived a reliability criterion with which the accuracy of the interference function can be tested. Since the atomic density ρ (r) is zero at values of r less than the hard-core diameter of the atoms he has shown that the following equation should hold:

$$S(U, d) = S_{exp}(U, d)$$

where

$$S(U, d) = 4\pi \rho_o r^3 J_1 (Ud)/ Ud$$

$$S_{exp}(U, d) = (d/\pi U) \int_0^\infty i(s) \cdot \left(J_0((S+U)d) - J_0((S-U)d) \right) ds$$

J_0 and J_1 are spherical Bessel functions

ie. $J_0(x) = (\sin x)/ x$

$J_1(x) = (\sin x/x^2) - (\cos x/x)$

U is any arbitrary value and d may have any value less than the hard core radius.

It can be seen, then, that the reliability criterion S(U,d) depends only on the average atomic density and should be compared with S_{exp} (U, d) calculated from the experimental data.

In an attempt to reduce the termination error Kaplow et al suggested imposing two, or more, additional cut-offs on the data. Transforming with the three values of S_{max} leads to three different R.D.F.s. By inspection of these curves the underlying trend is observed and by following these trends a fourth R.D.F is constructed. This fourth R.D.F. should then be transformed to give an interference function which will hopefully extend meaningfully behong S_{max} to S'_{max} say. In general this new function ($i'(s)$) will not agree with $i(s)$ below S_{max}. In this case $i'(s)$ should again be transformed, using the two cut-off points S_{max} and S'_{max}, to obtain two further R.D.F.s. The difference between these two curves is defined as $\Delta G_{term}(r)$ and represents the error induced in the true R.D.F. by the termination error. This error function is then used to modify the original R.D.F. This process can be repeated until a satisfactory R.D.F. is obtained. This final R.D.F. should satisfy two basic criteria: (1) The R.D.F. should be linear below the first peak; (2) When transformed the interference function produced should agree with the original function out to S_{max} and extend beyond it.

Finally it should be noted that by far the most common way of treating the termination error is to damp the interference function before transorming it. This is done by including a factor of the form:

$$\exp\ (-\ Bs^2)$$

where B is a constant (see for example Fujime (1966), Ichikawa (1970), Karle and Karle (1949), Maitrepierre (1969). This leads to equation (11) becoming:

$$G\ (r)\ =\ \frac{2}{\pi} \int_0^{S_{max}} i(s)\ \exp\ (-Bs^2)\ \sin rs\ ds \qquad \text{(16)}$$

The extra factor is called the artifical temperature factor and Fujime (1966) has suggested that a reasonable value for B is given by:

$$\exp\ (-\ BS^2_{max})\ =\ 0.1$$

A radial density function obtained using a damping factor can still have Gaussian functions fitted to its peaks. They should now be of the form:

$$D(r)\ = \left(N_i / \sqrt{4\pi(A_i+B)}\right) \exp\left((r-r_i)^2 / 4\pi(A_i+B)\right)$$

3.3.2 The Implementation of Suitable Computer Programs

A set of computer programs were developed to analyse the experimental data. The use of the energy filter made it unnecessary to consider the inelastically scattered electrons and the intensity was read, in arbitrary units, directly from the x-y recorder. This method of collection of the data is not entirely satisfacotyr especially at the larger values of s. In this region the intensity has fallen to a small value and the associated error is of the order of 5-10%. Furthermore the resultant interference function contains the factor of s, which with this equipment extends to about 12.0 $A^{o\ -1}$. Hence all the errors that occur in the reading of the data at such s values are multiplied by this factor.

The interference function is defined as:

$$i(s) = s\,(A.I(s)/|f(s)|^2 - 1)$$

with the same notation as before.
Hence an error of Δ I(s) in I(s) leads to a corresponding error in i(s) of

$$\Delta i(s) = S\left(\frac{A}{|f(s)|}\right)^2 . \Delta\ I(s) \qquad (17)$$

If we substitute typical values for the quantities in equation (17) of:

$$s = 10A^{o\,-1}, \qquad A \sim 0.5$$
$$|f(10)|^2 \sim 0.5, \qquad \Delta I(s) = 0.05$$

then

$$\Delta i(10) \sim 10 \cdot \frac{0.5}{0.5} \cdot 0.05 \sim 0.5$$

This is a rather large error because at $s = 10A^{o\,-1}$ the interference function should probably be approaching zero. With the present experimental set up the only answer appears to be extreme care in the collection of the data. It is often possible, however, to improve the collected data by inspection of the calculated interference function. Any sharp fluctuations in this function at large s can be traced back to the original data and corrected if necessary. In addition the use of a small damping factor, as in equation (16), could now be possibly justified.

The main programs used are listed in appendix A. The collected experimental intensity is normalised and a corresponding interference function calculated using program NORMAL. The two methods of normalisation described in section (3.2.1) are used. The presence of the main beam results in a minimum value of s, not equal to zero, from which the data can be read. The intensity

at low values of s, however, is negligible compared with the value of $|f|^2$. It follows then from the definition of the interference function as:

$$i(s) = s \left(I_N(s)/|f|^2 - 1 \right)$$

that for small values of s

$$i(s) = -s$$

The usual next stage in the analysis was to obtain the corresponding R.D.F. This would contain a great deal of spurious detail arising from the errors mentioned previously, but would be inspected to determine the position of the first real minimum which was then used in the main program. This is called RDFGEN and basically follows the method outlined in section (3.3.1). This program is fully documented and so will not be described in detail here. The main addition to the method already described is the removal of obvious irregularities below the first peak that still remain after the normalisation error routine.In paticular it was often found to be necessary to discard a very deep minimum just below the first peak.The justification for this was that the R.D.F. should be linear at small values of r.Furthermore the position of this minimum is that predicted by equation (15) and so would appear to be due to the termination error. In addition a routine using the Rahman criterion is used.

Having obtained Radial Distribution and Density Functions an attempt to estimate the co-ordination numbers was made by program GAUSS.This program estimates the area under the peaks in D(r) using methods (1) and (2) described in section (3.2.3).It also approximates the first peak by a Gaussian function to derive another estimate.

Finally consideration is given to the actual process of transforming the data.The Fourier pair G(r) and i(s) are related by:

$$G(r) = 2/\pi \int_0^\infty i(s)\sin(rs)ds$$

$$i(s) = \int_0^\infty G(r)\sin(rs)dr$$

The simplest way to evaluate these integrals is to replace them with summations such that

$$G(r) = 2/\pi \, \Delta s \sum_{n=0}^{\infty} i(n\Delta s)\sin(rn\Delta s)$$

$$i(s) = \Delta r \sum_{m=0}^{\infty} G(m\Delta r)\sin(sm\Delta r)$$

where $\Delta s, \Delta r$ are the respective sampling increments.

Hence

$$G(r+2\pi/\Delta s) = 2/\pi.\Delta s \sum i(n\Delta s)\sin(rn\Delta s+2\pi n)$$
$$= G(r)$$

and $i(s+2\pi/\Delta r) = i(s)$

G(r) and i(s),therefore,calculated in this way will be periodic with half periods of $\pi/\Delta s$ and $\pi/\Delta r$ respectively.This means that Δs and Δr should be chosen such that the corresponding half periods $\pi/\Delta s$ and $\pi/\Delta r$ are significantly greater than the values at which G(r) and i(s) approach zero.In the analysis carried out here it was assumed that both i(s) and G(r) would be zero at values of s = 25 A^{o-1} and r = 25 A^{o} respectively.This then leads to the conditions

$$\Delta s \lesssim 0.125\ A^{o-1}$$
$$\Delta r \lesssim 0.125\ A^{o}$$

In implementing the actual transform,in order to improve effiency,especially in view of the large number of transforms undertaken the so-called fast fourier transform was used.This is a method of performing the summation without the large number of redundant calculations that are normally done.The basic routine was written by D.Monroe of the Electrical Engineering Department

of Imperial College and was modified to be applicable in this case.The concepts used in the transform,together with the mathematics required to manipulate equation (11) into a suitable form,are given in Appendix B. Its introduction resulted in the transform being executed in a quarter of the time taken by the usual summation method.It should be pointed out that the F.F.T. is not an approximation.In fact it is slightly more accurate than the conventional summation because of the fewer number of rounding off errors.

3.4 Computer Predictions of Scattering Intensity

3.4.1 General scope and advantages of the method

This method of utilizing the experimental data entails calculating scattering intensities for a postulated model and comparing with experiment.The one big advantage this indirect method has over the method just described is that there is no termination error involved.In principle if the given model is well defined then a complete range of intensities can be predicted.The major disadvantage is the multitude of models which can be put forward.A model aimed at representing a non-crystalline structure can be produced using the Monte-Carlo method with which various degrees of packing can be obtained(Alder et Al(1955)).Similarly various polycrystalline models can be adopted and the resulting diffraction intensity calculated.It would then be possible to compare this with that obtained experimentally in an effort to decide if the sample was indeed non-crystalline.

3.4.2 Computation of scattering intensities for a polycrystalline sample

Morozumi anr Ritter (1953),and Grigson and Barton(1966) have both calculated diffracted intensities from randomly orientated cubic lattices.By considering the scattering from such a sample it can be shown (James(1948)) that the diffracted intensity is given by:

$$\bar{I}_0(s) = |f|^2 \left(\sum_{-(N-1)}^{N-1} \sum \sum (N_1-|p|)(N_2-|q|)(N_3-|1|) \right.$$
$$\left. \sin(2\pi s l_{pql} / 2\pi s l_{pql}) \right)$$

where

$\bar{I}_0(s)$ = intensity at the point s

f = atomic scattering factor

N_1, N_2, N_3 = number of atoms along crystal sides

l_{pql} = distance from the origin to the point p,q,1 of the crystal lattice

In the case of small crystallites $\bar{I}_0(s)$ becomes slowly varying with s so that the contribution from the structure factor has to be considered.This has to be calculated for the particular lattice being considered and then averaged over all possible orientations.In this work the effects caused by interference between scattered waves from different crystallites has not benn considered. It is assumed that for all but the very smallest crystallites the path difference between the crystals would be too long to support significant interference.

The programs written to evaluate this scattering are listed in Appendix A, along with full documentation. The actual intensities predicted will be illustrated and compared with experimental data in Chapter 5.

CHAPTER 4

The Experimental Results and their Analysis

4.1 Preliminary Study of Tin, Zinc and Cadmium Films Prepared at 77°K

This initial work was performed in an attempt to confirm that these films could be formed with a non-crystalline structure. It was carried out in an un-baked system with a pressure of 1×10^{-7} torr. This procedure enabled a great deal of time to be saved while still having vacuum conditions comparable with Kato and Horikoshi (1965), Fujime (1966) and Belevtsev and Kommik (1971) whose work was mentioned in Chapter 1.

The first metal to be investigated was Tin. A set of intensity traces taken over a range of temperatures, as the deposited film was warming, are shown in figure (1). On deposition the pattern consisted of diffuse rings which sharpened on warming of the film. At 160°K an abrupt change occurs in the pattern which becomes one of sharp, textured rings. At 175°K the pattern again suddenly changes to one similar to that observed just below 160°K. No further change in the pattern takes place on warming of the film to room temperature.

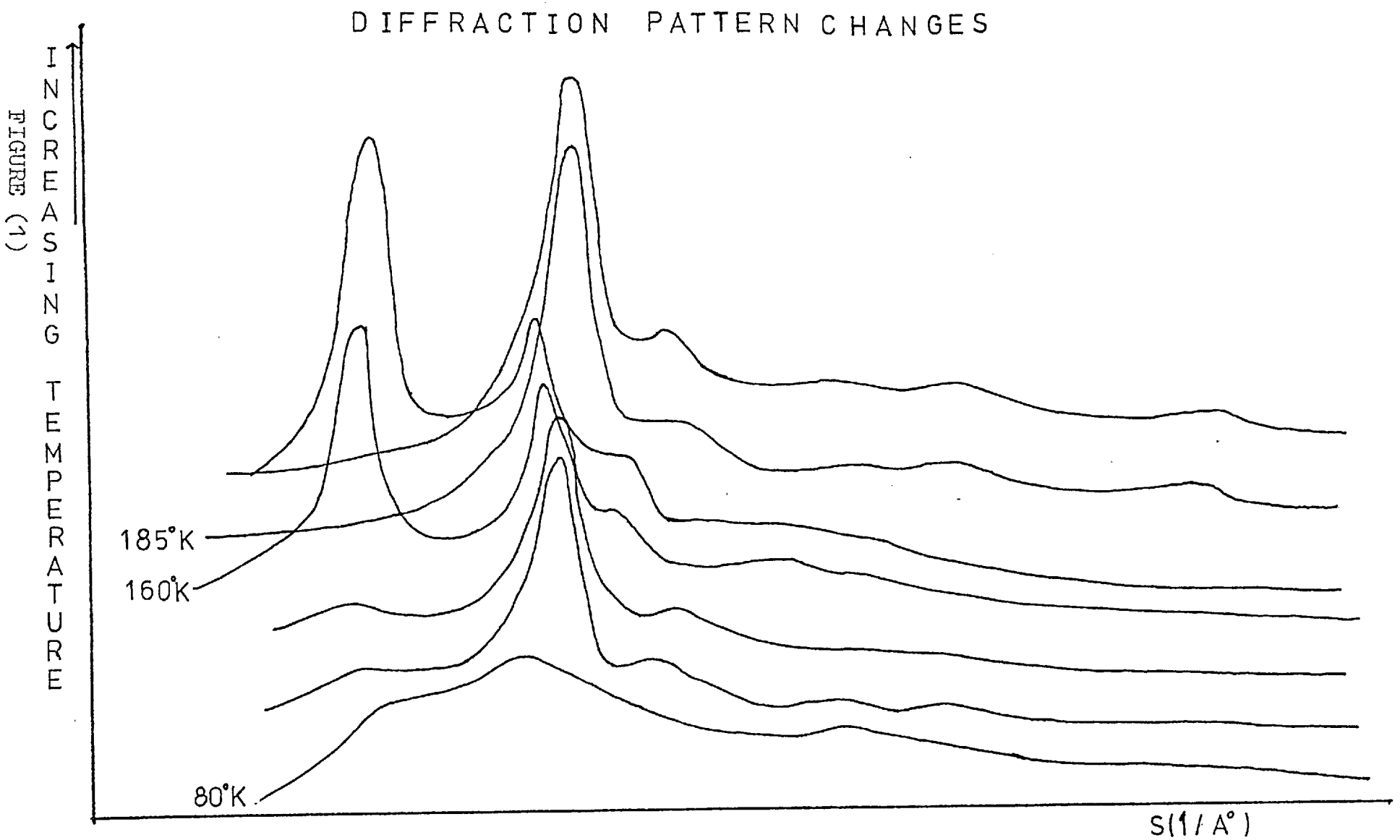
DIFFRACTION PATTERN CHANGES
INCREASING TEMPERATURE
185°K
160°K
80°K
S(1/A°)

FIGURE (1)

Similar results were obtained when Tin was deposited onto a Carbon layer which had previously been evaporated onto the Copper. Furthermore the observed effects did not depend on the rate of deposition or the thickness of the film. On thermally recycling a Tin film no significant change took place while cooling but similar changes were apparent on warming. Further experiments were performed entailing the preparation of Zinc and Cadmium films with the same results.

At this point a M.S.10 mass spectrometer was attached to the system and this indicated that water vapour was the main residual gas with a partial pressure of 4×10^{-8} torr. A final experiment was performed where the Copper substrate alone was thermally cycled while concurrently monitoring the partial pressure of water vapour. The variation with temperature, along with that of the total pressure, is shown in figure (2).

On cooling of the substrate the water vapour partial pressure decreases. When warming begins it increases and the rate of increase is very rapid within the temperature range $140^{o}K$ to $180^{o}K$. Soon after $180^{o}K$ the partial pressure levels off and remains steady on warming to room temperature. The total pressure follows

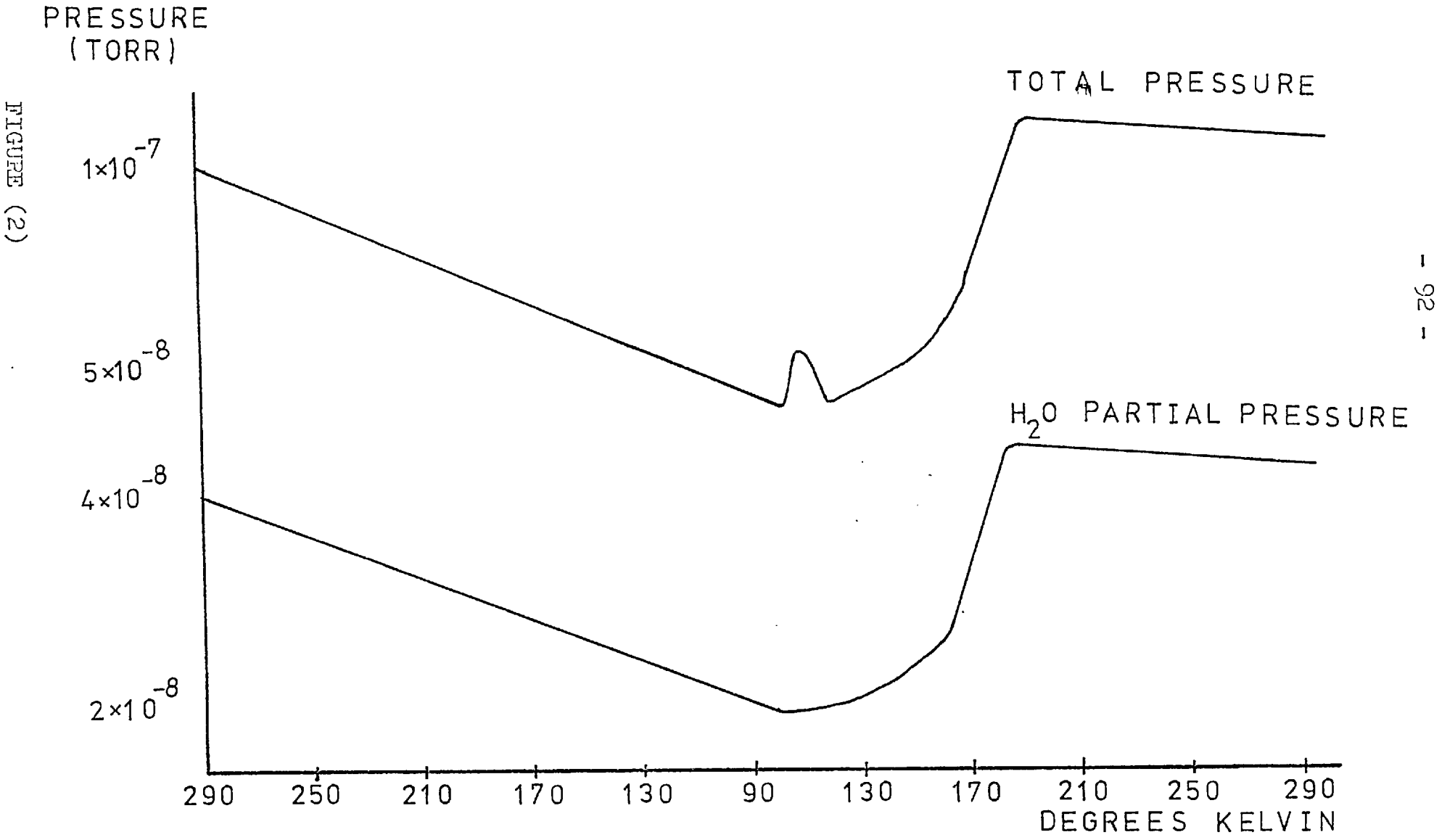
PRESSURE
(TORR)
TOTAL PRESSURE
1×10^{-7}
5×10^{-8}
H_2O PARTIAL PRESSURE
4×10^{-8}
2×10^{-8}
290
250
210
170
130
90
130
170
210
250
290
DEGREES KELVIN

FIGURE (2)

this general behaviour although there is an additional small peak, the beginning of which coincides with the start of the substrate warming.

The results strongly suggest that the observed diffraction pattern changes are caused directly by the condensation of water vapour onto the substrate and its subsequent evaporation. To support this, figure (3) shows the diffraction pattern produced during the temperature range 150°K - 180°K. Marked on this diagram are the calculated peak positions due to a tetragonal ice structure (ASTM card number 16-598).

As confirmation the experiments were performed in a baked system where the water vapour had a partial pressure of 5×10^{-9} torr. Under these conditions the effects described above were not observed.

The results described emphasise the importance of attaining the best possible vacuum especially when preparing films at low temperatures. In particular it would appear essential to bake the apparatus before each experiment. This condition made it impossible to prepare Zinc and Cadmium films since both elements possess a very high vapour pressure (e.g. 10^{-3} torr at 230°C for Cadmium).

FIGURE (3)

4.2 The Preparation of Films at 77°K

All the work described in this section was performed in a vacuum of between 1×10^{-8} torr and 2×10^{-10} torr, using a Copper substrate.

4.2.1 Gallium

It had been hoped that these films would exhibit a non-crystalline structure but it was found that all but the thinnest produced a diffraction pattern of sharp, polycrystalline type, rings. On examining the growth of these films it was seen that they passed through stages during which they showed a fibre texture. Oshima and Nakamure (1969) have reported that evaporated Silver and Copper films when condensed at 77°K also display fibre texture and it was decided to study the growth of these Gallium films.

The evaporation rate and the thickness of the films were determined using an Edwards Thickness Monitor. This was calibrated using a half-covered glass slide mounted next to the substrate. This produced a film step from which the film thickness could be estimated using the Tolansky interferrometric method. The calibration graph obtained using Sodium wavelength of 5890 Å is shown in figure (4).

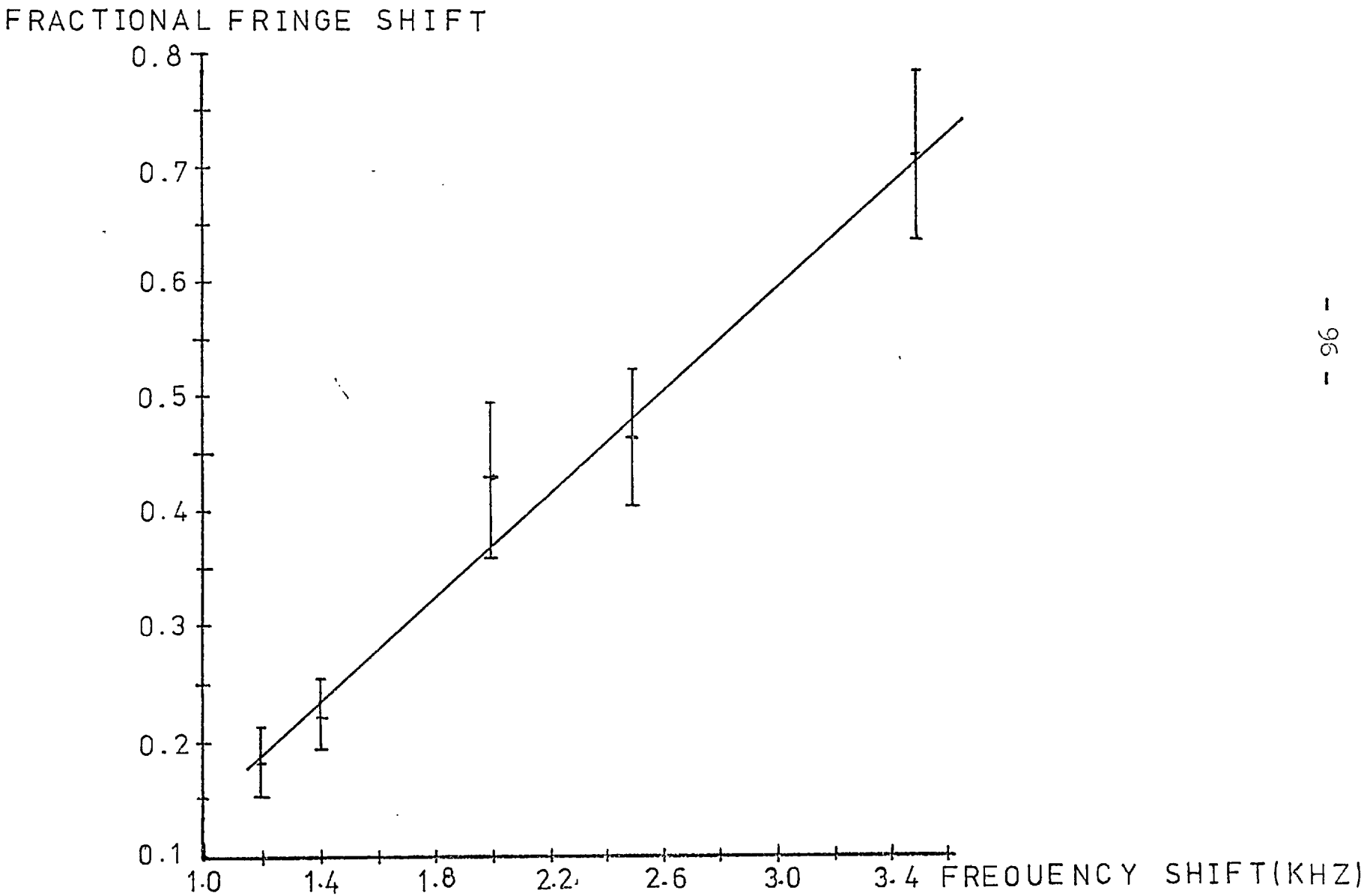
FRACTIONAL FRINGE SHIFT
0.8
0.7
0.6
0.5
0.4
0.3
0.2
0.1
1.0
1.4
1.8
2.2
2.6
3.0
3.4
FREQUENCY SHIFT(KHZ)

FIGURE (4)

A typical growth sequence is shown in figure (5). The diffraction pattern changes shown occurred on polycrystalline, as well as non-crystalline, substrates and for a range of deposition rates. At deposition rates of below 2 A^{o} per second the two intermediate stages showing the fibre texture did not appear. On condensing the films at temperatures above 80°K the Gallium gave first a diffraction pattern of diffuse rings which gradually sharpened on further deposition. Furthermore it was found that both forms of texture disappeared on warming of the film to room temperature.

Figure (6) shows a schematic diagram of the position of diffraction spots when the $\langle 11\bar{1} \rangle$ axes of the Gallium crystallites are perpendicular to the film surface normal. Comparing this with figure (5 (d)) it can be seen that the spots are in similar positions to the arcs. It is therefore concluded that the pattern in question possesses a $\langle 111 \rangle$ fibre axis.

Oshima and Nakamura in discussing their results suggest a likely hypothesis to explain the observed effects. They show, by considering the mechanism of nucleation, that those planes with the higher atomic density are most likely to nucleate. At very low evaporation rates the impinging atoms condense exactly where they land and have no energy to cause crystal growth. This results in the

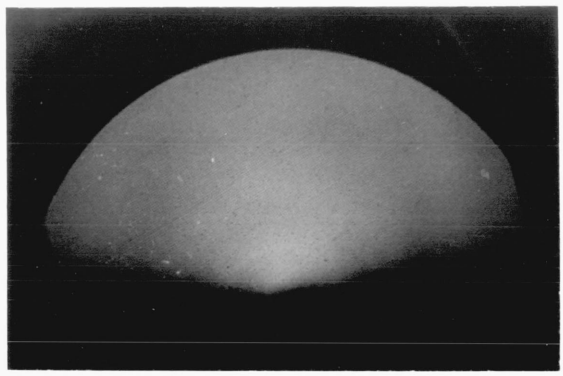

a

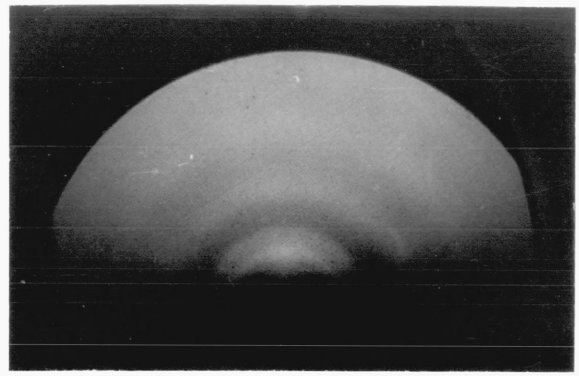

b

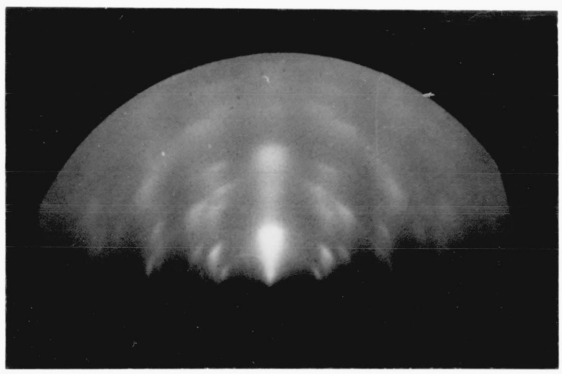

c

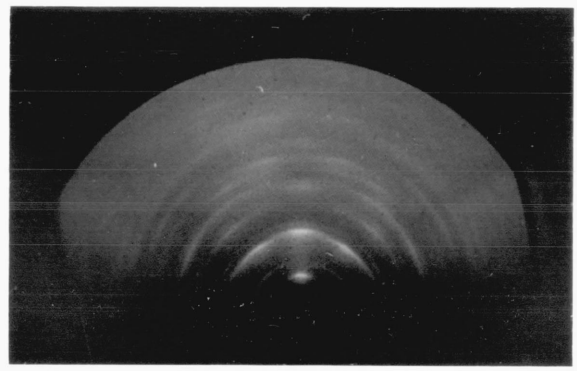

d

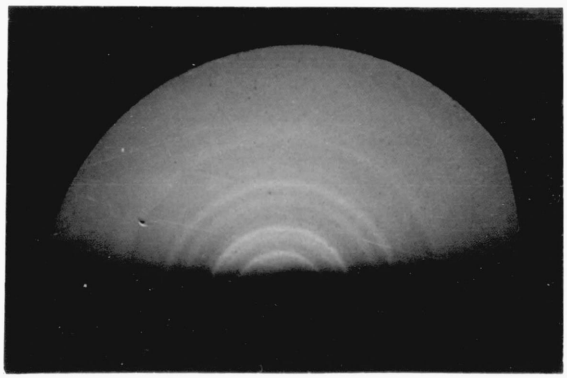

e

FIGURE (5)

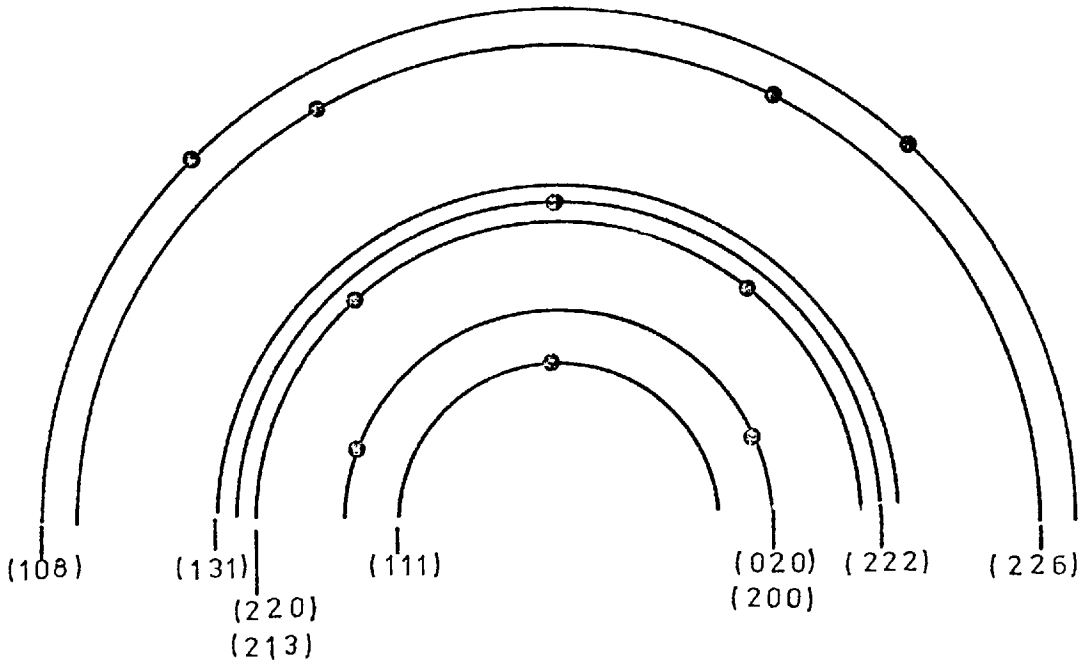

FIGURE (6)

formation of very small grains with completely random orientation. At higher rates of evaporation surface diffusion may be possible and this would result in more ordering of the atoms leading to preferred nucleation on those planes with the highest atomic density. Deposition at higher temperatures results in extra atomic migration being possible allowing the formation of larger crystallites without fibre axes. This extra surface migration at higher temperatures could also explain why the texture vanishes on warming.

4.2.3. Chromium

Chromium films deposited onto a non-crystalline Copper substrate held at 77°K were found to undergo structural changes during growth. A typical growth sequence is shown in figures (7-10). The first three stages all appear to show that Chromium is in a non-crystalline phase while the fourth stage indicates a polycrystalline form. It should be added that the growth is continuous and it has been split into stages only for presentation. One noticeable effect is that the first peak moves outward during growth until it assumes the position due to the <211>planes. Figure (11) shows the indexed pattern produced by the film after warming to room temperature.

The estimated thickness at which the film becomes definitely polycrystalline is approximately 300° although it should be stressed that no abrupt transition was observed.

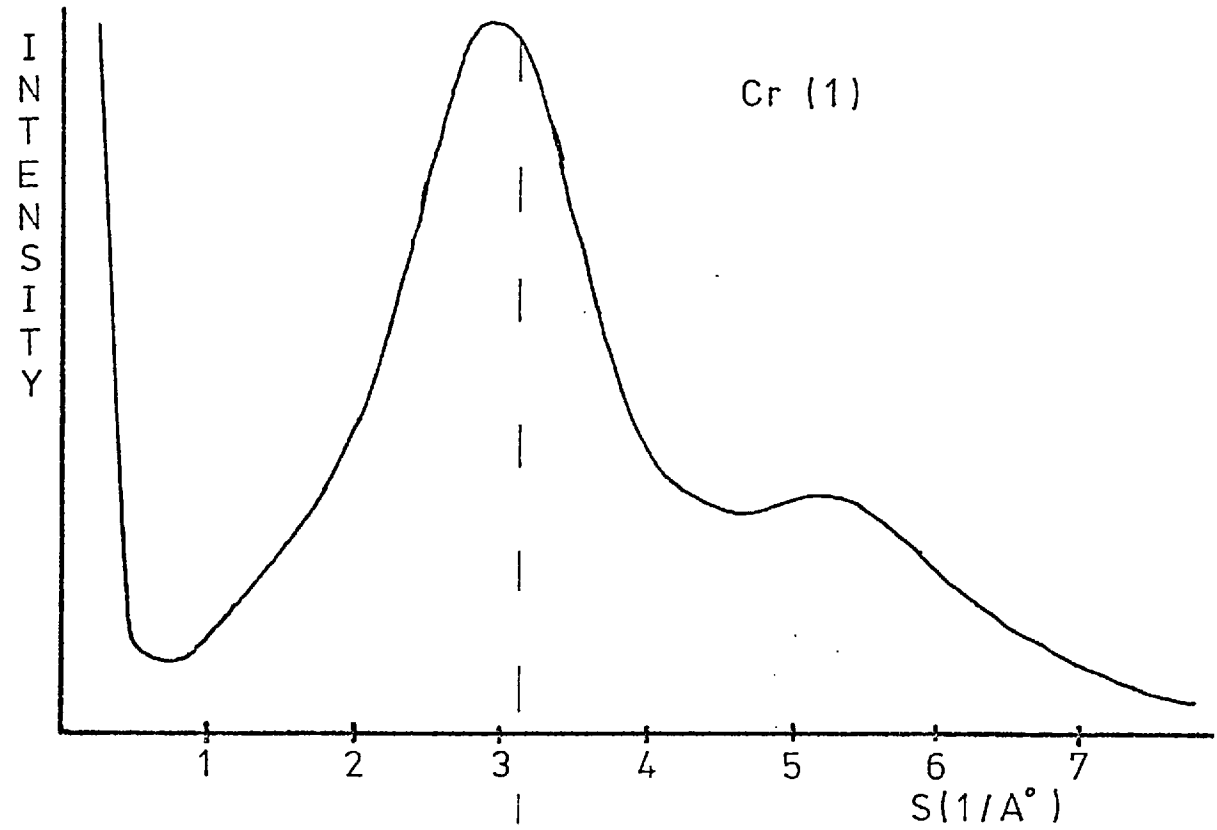

FIGURE (7)

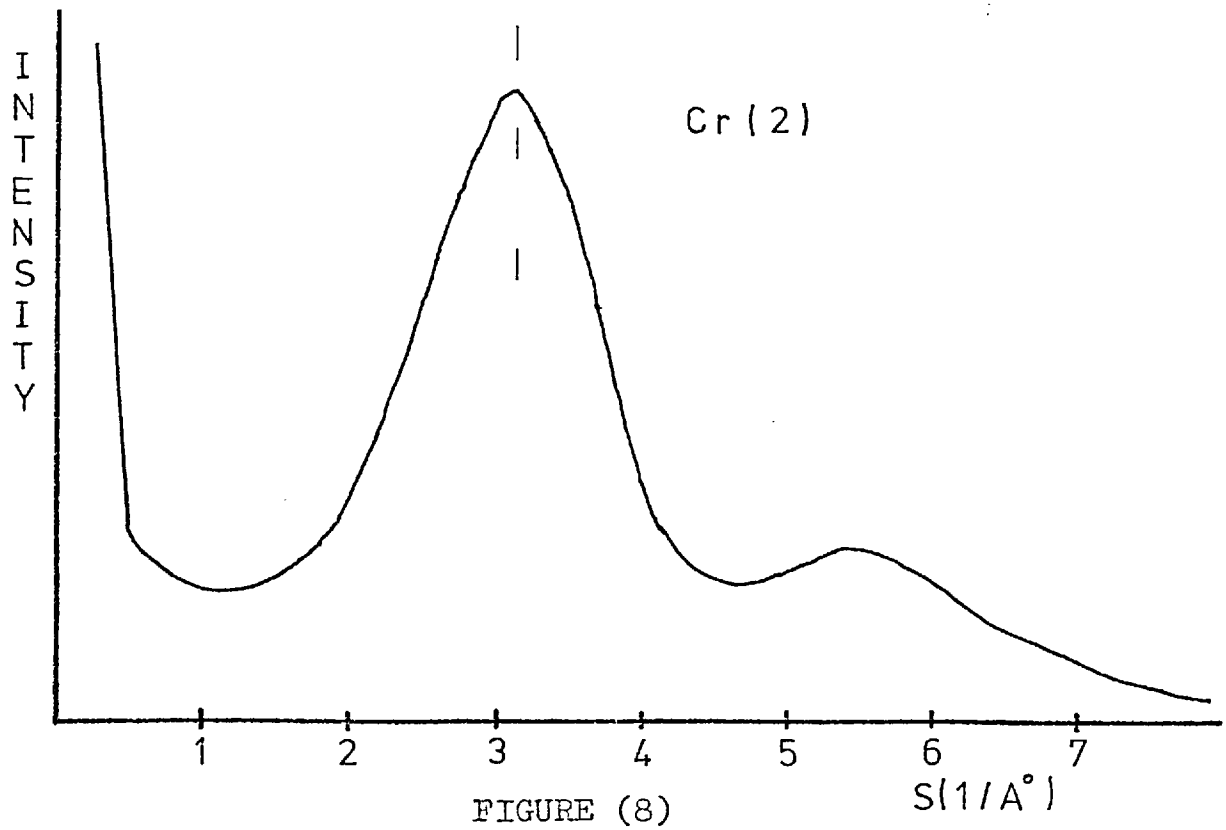

FIGURE (8)

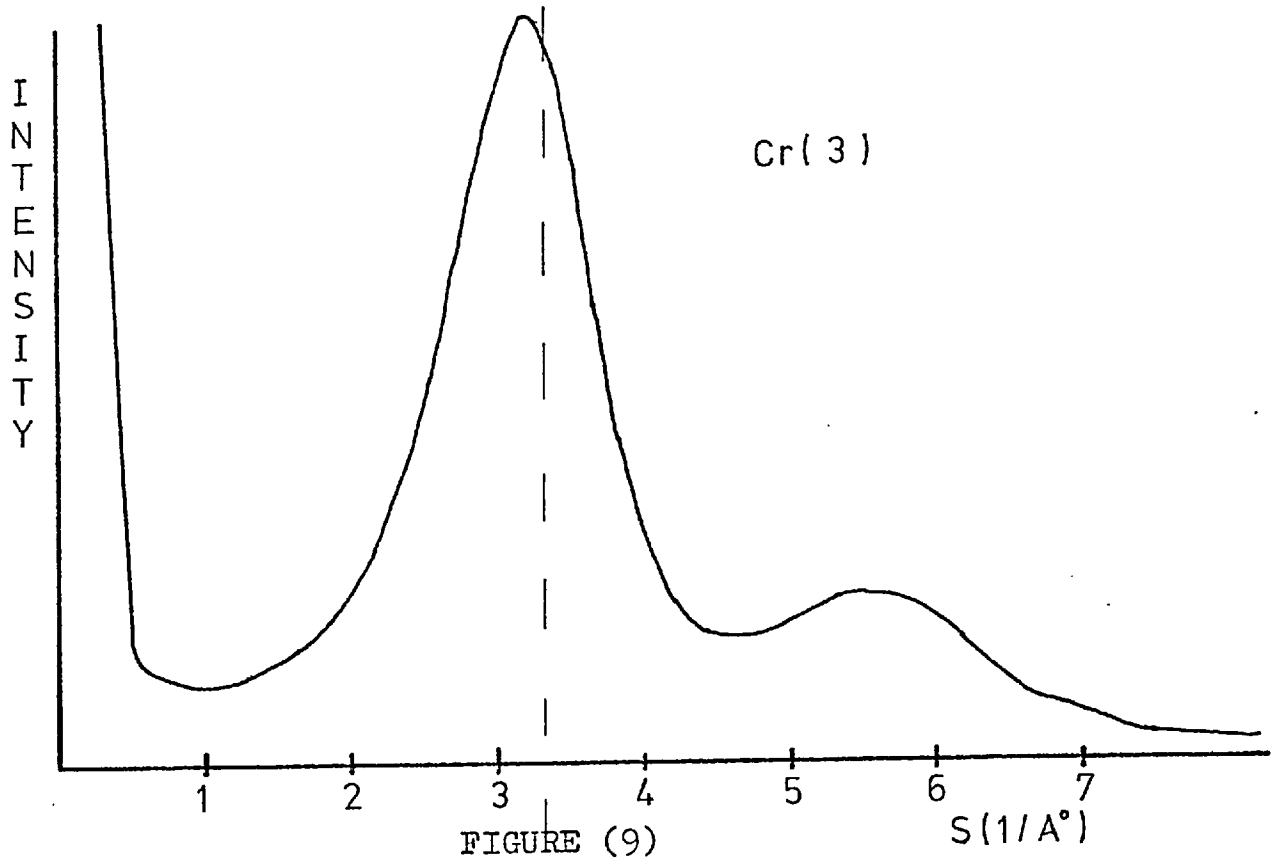

FIGURE (9)

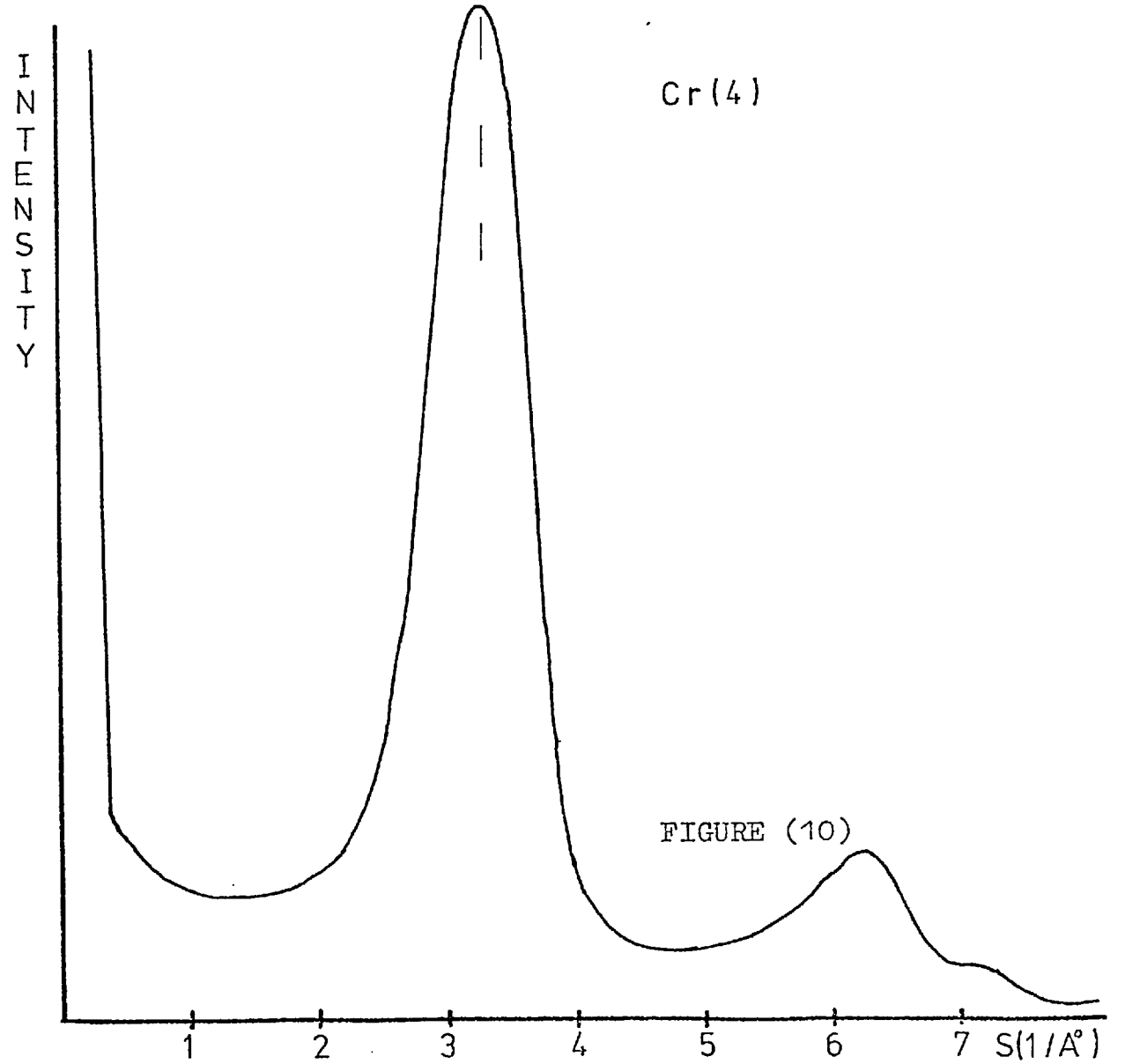

FIGURE (10)

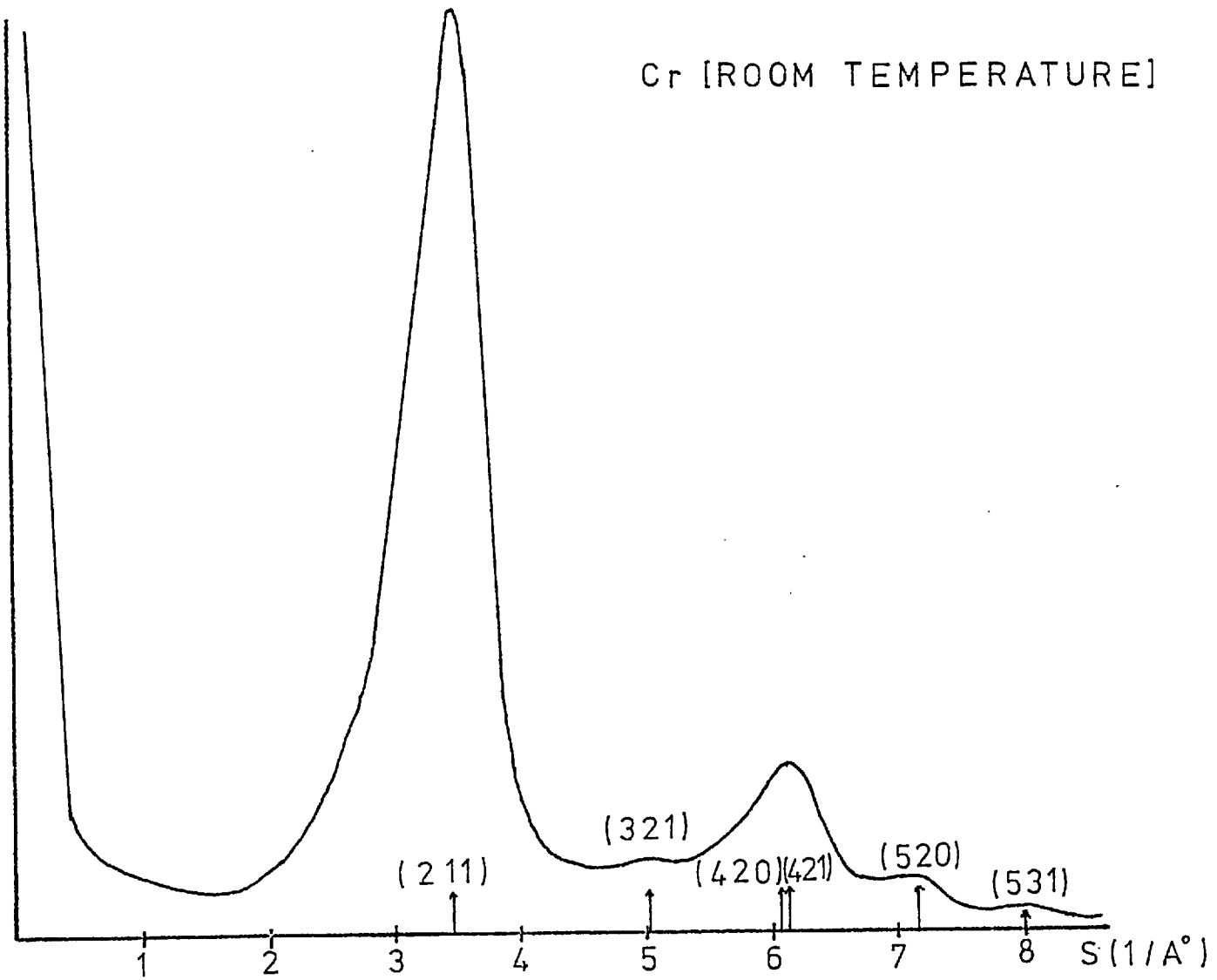
Cr [ROOM TEMPERATURE]
INTENSITY
(211)
(321)
(420)(421)
(520)
(531)
1
2
3
4
5
6
7
8
S(1/A°)

FIGURE (11)

4.2.3 Iron

Iron films grown under similar conditions as Chromium films exhibited a very similar growth pattern. A series of traces showing the observed effects are given in figures (12-15). Again the first two stages indicate a non-crystalline structure while by stage 4 a poly-crystalline pattern is apparent. The movement of the first peak was, as with Chromium, a gradual process and it was difficult to estimate at what thickness a crystalline structure was observed. Such a structure however had always appeared before the film had become about 300 A^{o} thick.

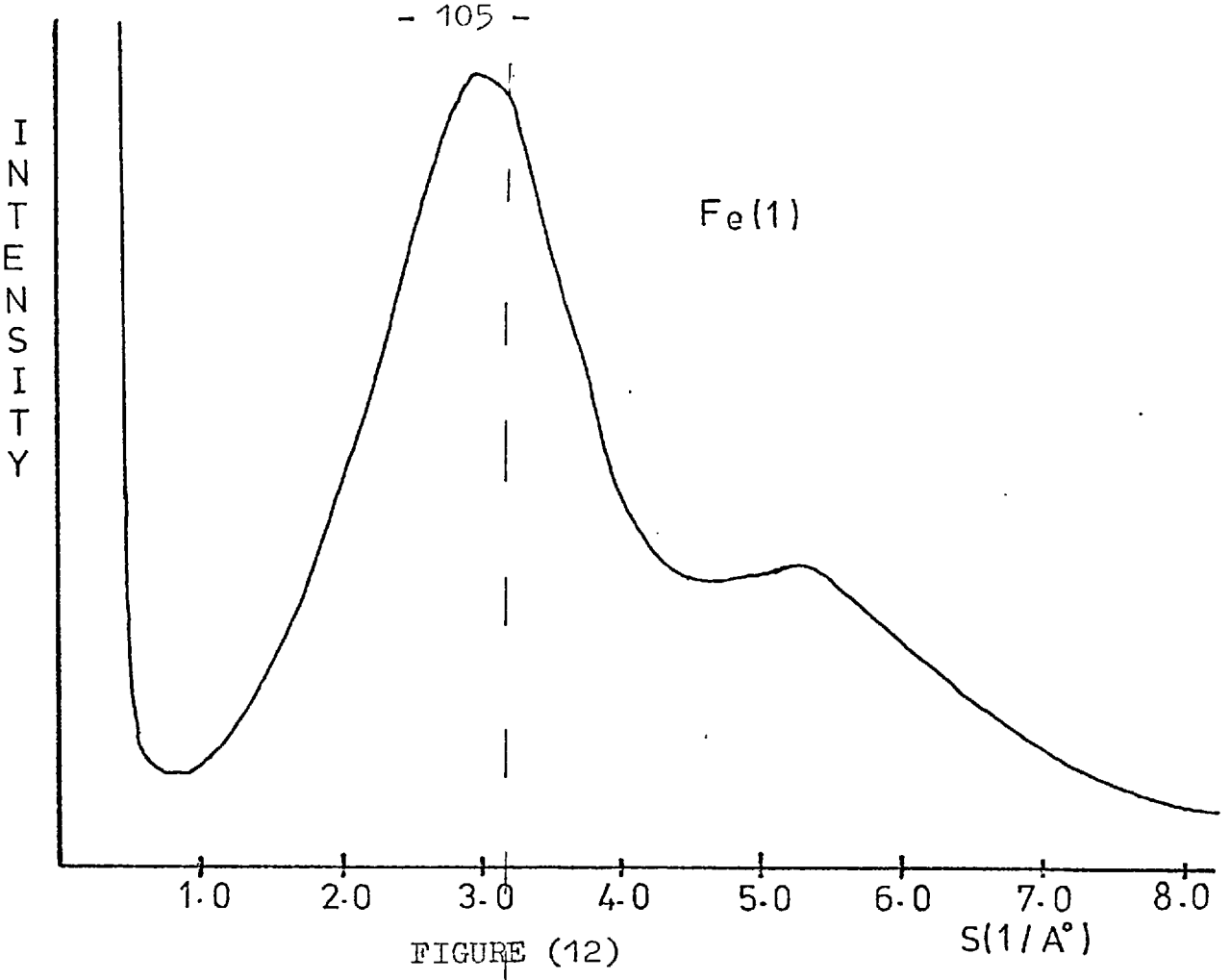

FIGURE (12)

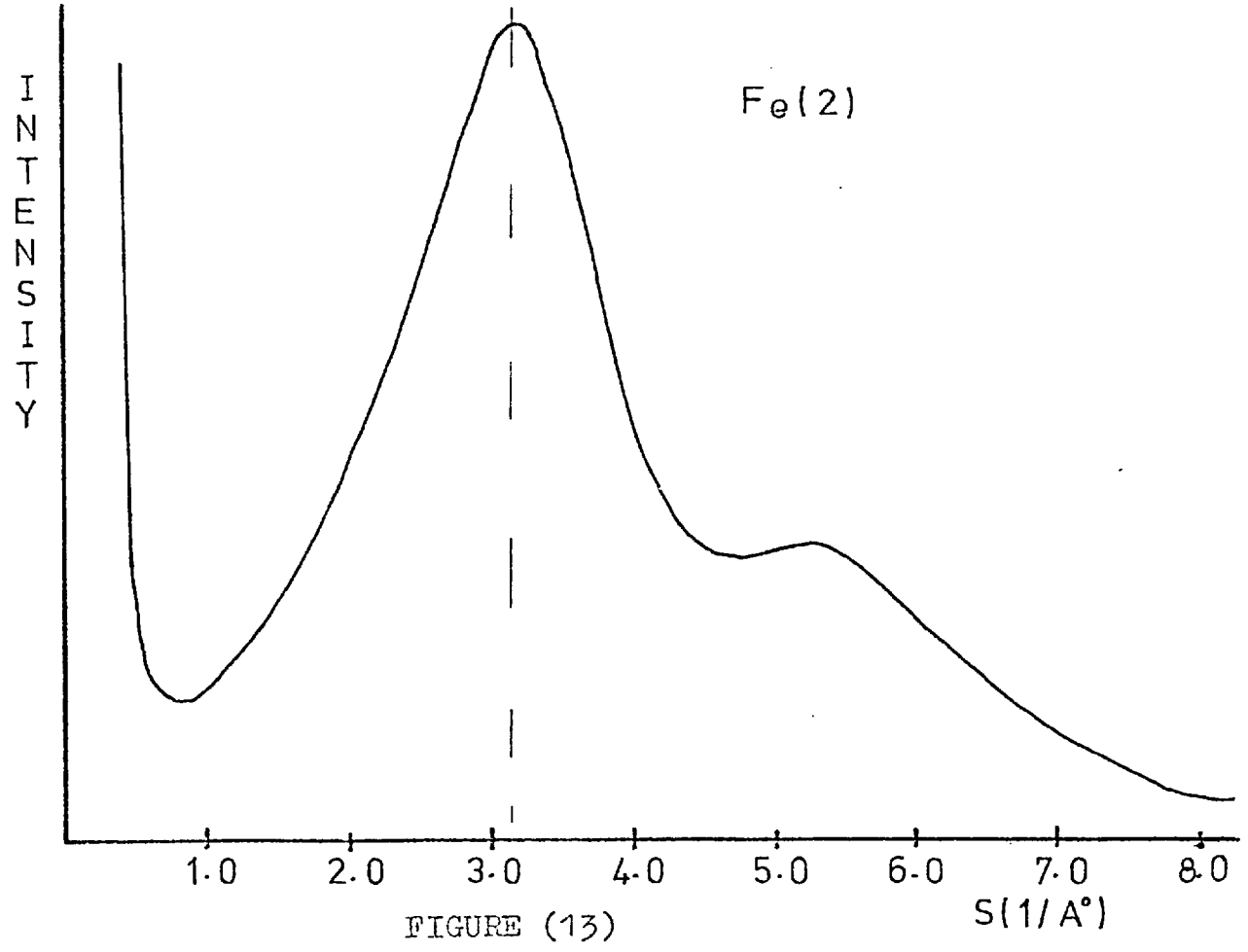

FIGURE (13)

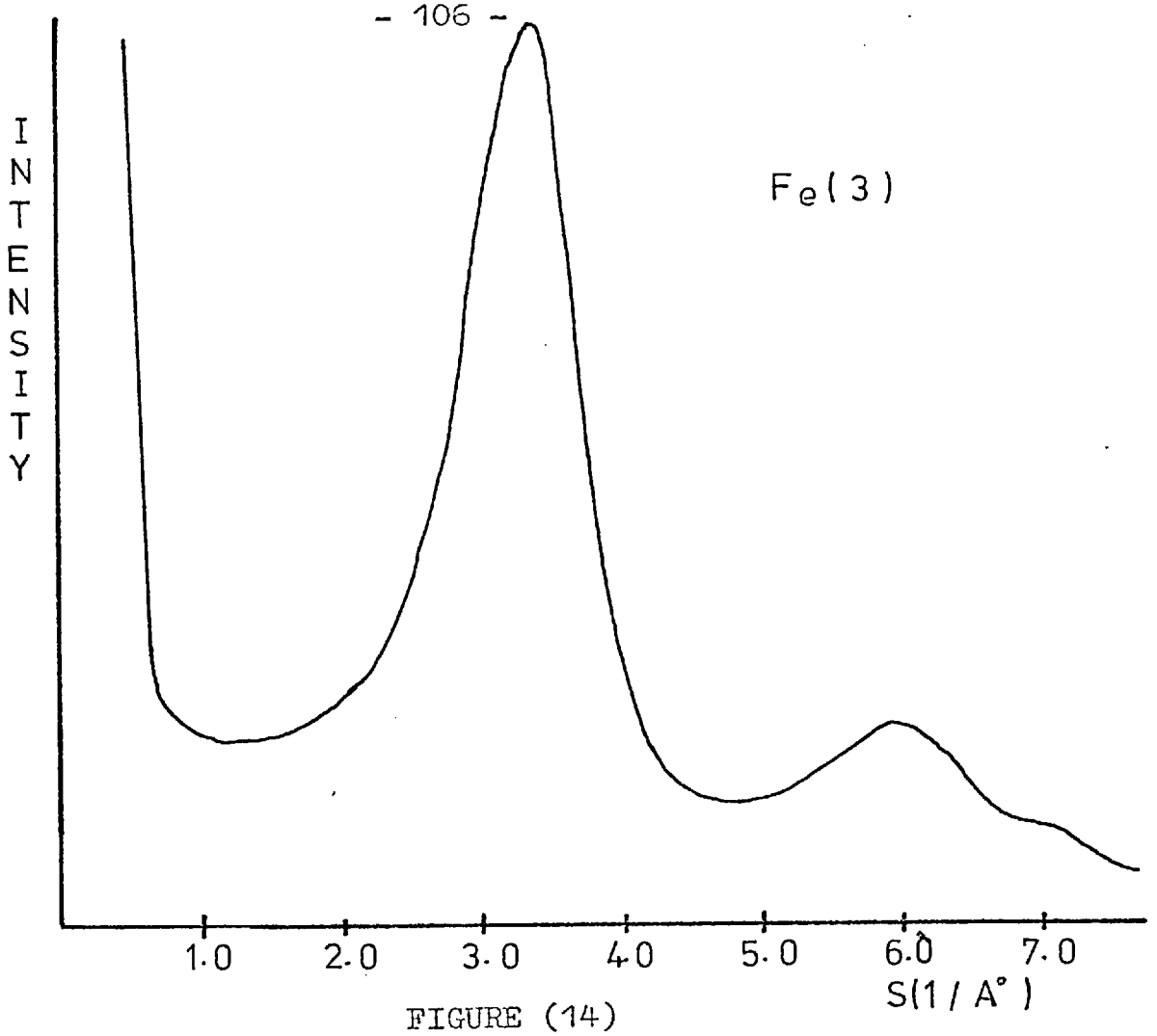

FIGURE (14)

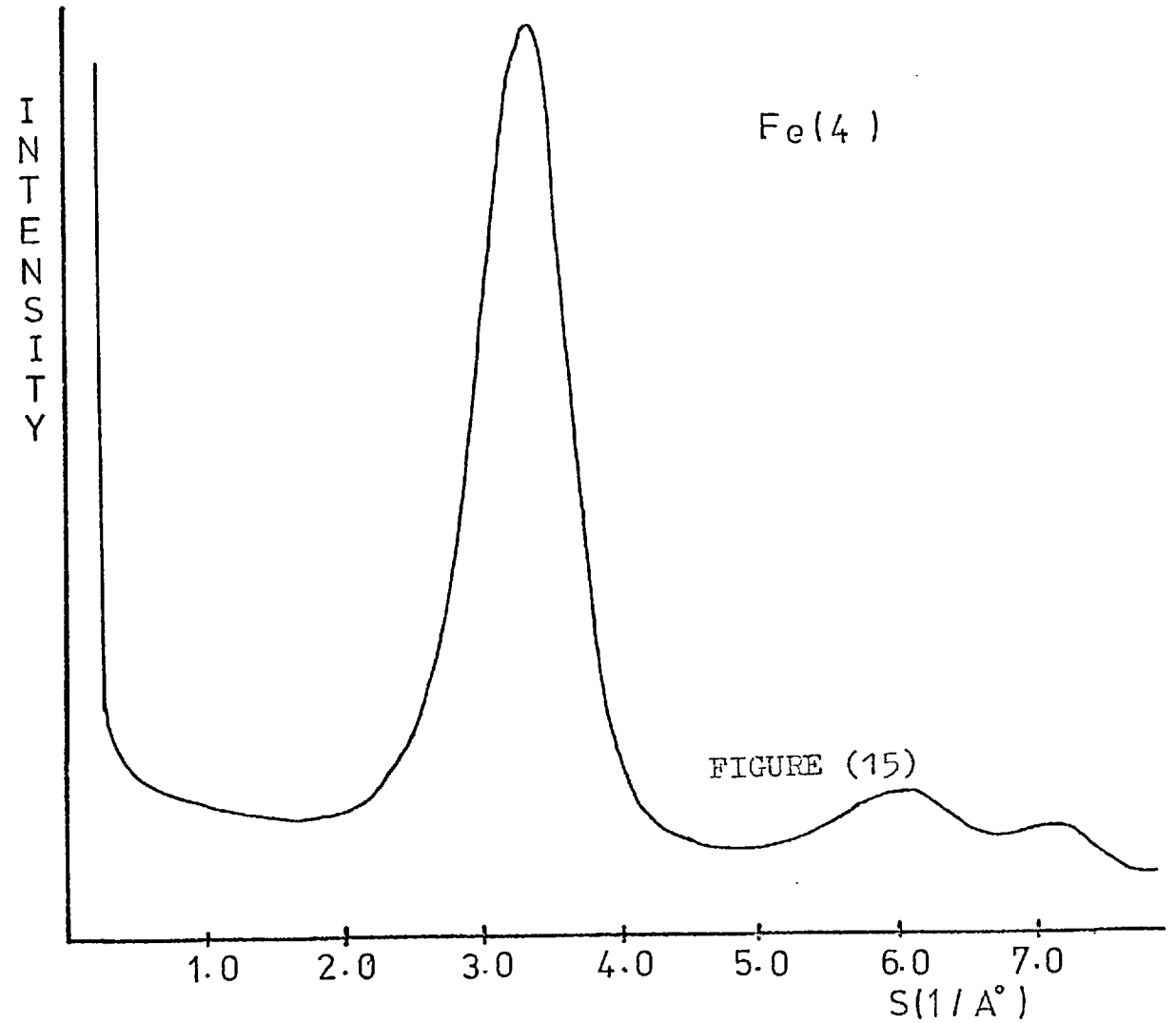

FIGURE (15)

4.3 The Study and Analysis of Films Prepared at Approximately 4°K

All the results described in this section are from experiments performed in a vacuum of better than 5×10^{-10} torr. In all the cases, except Indium, non-crystalline films appeared to be formed and in these cases the computed R.D.F.'s are shown. In section 4.3.1, using the results obtained with Gallium, a number of intermediate functions are shown in order to illustrate the working of the computer programs.

4.3.1.1 Gallium

Numerous Gallium films were prepared with thicknesses ranging approximately from 50A° to 500A°. Similar results were obtained from all the films and the description given here is felt to be entirely representative.

Immediately after deposition the Gallium produced a diffraction pattern typical of a non-crystalline solid. On warming of the film, fairly sharp polycrystalline rings were observed to have appeared by 100°K although an abrupt transition was not observed. Further warming caused the diffuse rings to re-appear at a temperature

of approximately 250°K presumably as a result of the film melting. This structure then remained stable at room temperature. A graph showing the variation of resistance of the film during warming is shown in figure 16. A sharp decrease in resistance occurs immediately after deposition followed by a levelling off which continues to about 200°K. After this point the resistance begins to increase and by 280°K the film has become discontinuous.

On re-cooling of the liquid Gallium film crystallisation occurs in the temperature range 250°K - 170°K. By 170°K the film has reverted to the polycrystalline structure it possessed on warming. This crystallisation process is shown in figures (17 and 18). Figure (18) shows the intermediate pattern observed on cooling in the region 250°K to 190°K, while figure (17) shows the final pattern obtained.

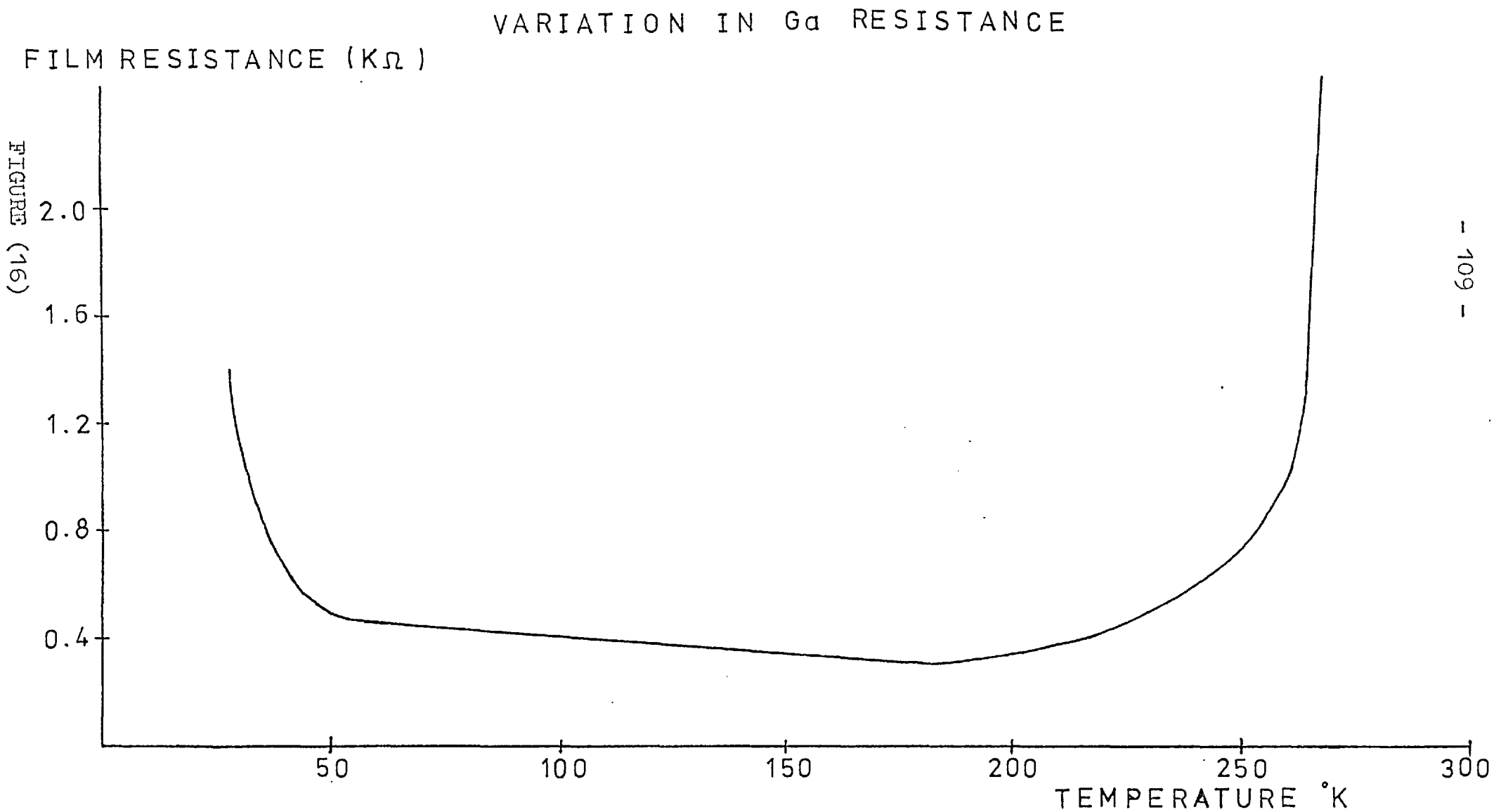
VARIATION IN Ga RESISTANCE
FILM RESISTANCE (KΩ)
2.0
1.6
1.2
0.8
0.4
50
100
150
200
250
300
TEMPERATURE °K

FIGURE (16)

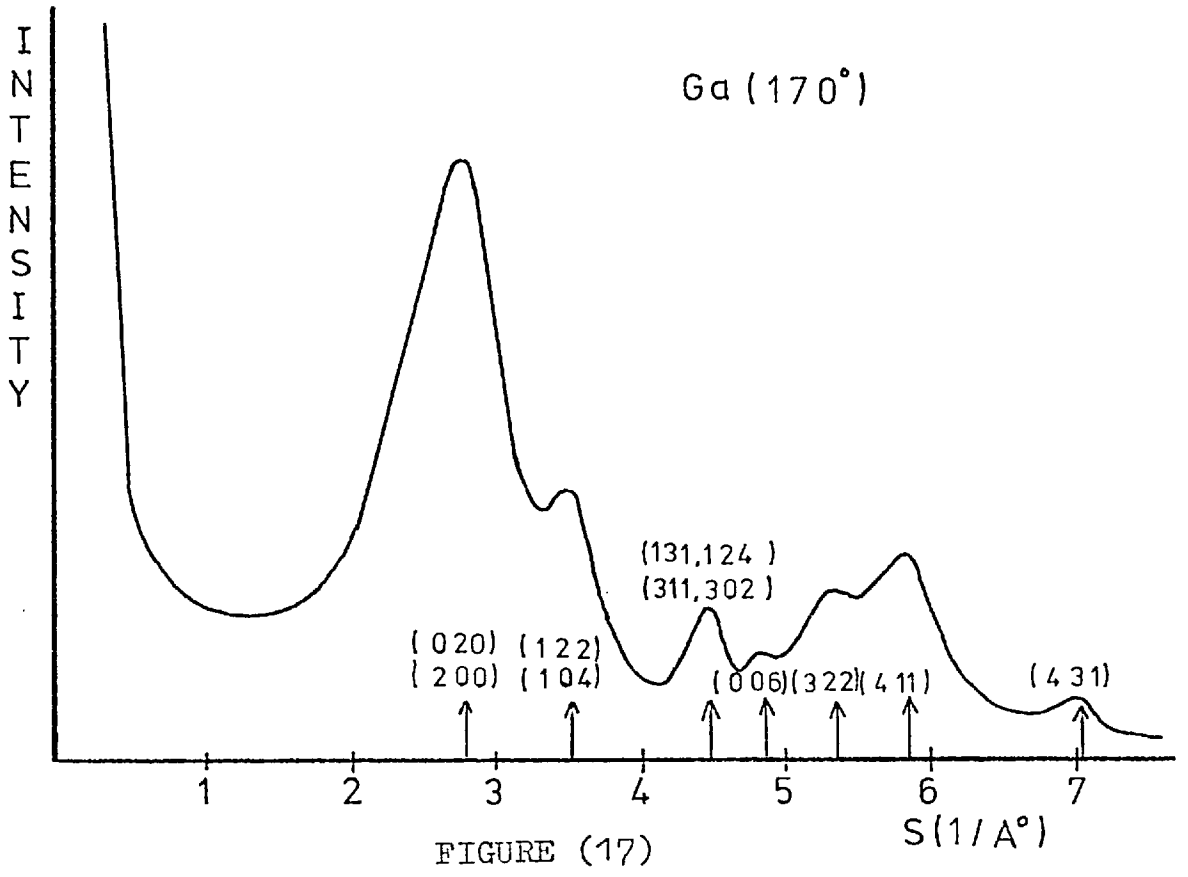

FIGURE (17)

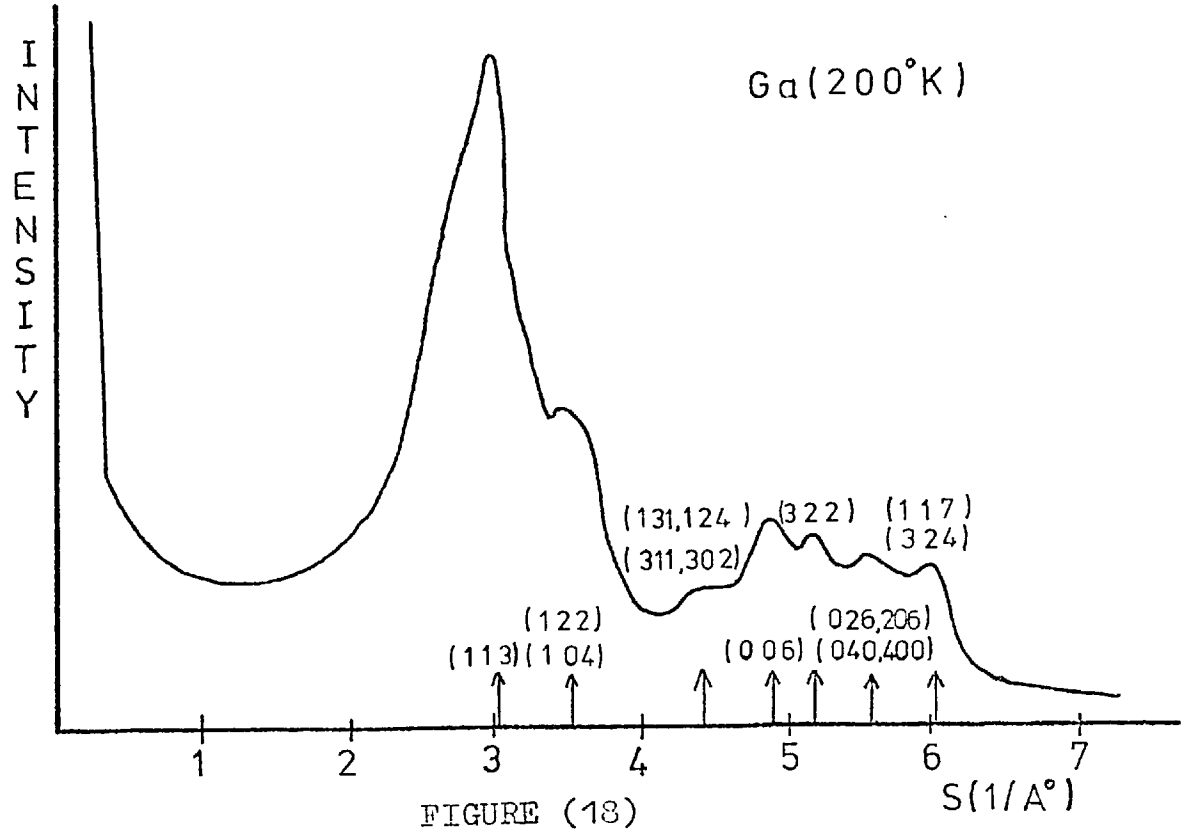

FIGURE (18)

4.3.1.2 Detailed Analysis of Liquid Gallium Data

Using the atomic scattering factor calculated by the Self Consistent Field method, the experimental data was normalised and the interference function calculated. This is shown in figure (19) while the corresponding R.D.F. is in figure (20). The effect of damping the interference function, as described in Chapter 3, is shown by the two R.D.F.s shown in figures 21 and 22. The damping factors used are 0.005 and 0.05 respectively.

The interference function is now treated for a normalisation error by the routine ERNORM. Figures 23 and 24 give the normalised intensities before and after this error minimisation routine respectively. Similarly figure (25) gives the interference function and figure (26) the corresponding R.D.F. after treatment by this routine. The extrapolated interference function is shown in figure (27) while the final treated R.D.F. is given in figure (28). The corresponding Radial Density Function is shown in figure (29).

It is interesting to consider what happens if the atomic scattering factor calculated using Thomas-Fermi-Dirac statistics is used instead. It would be expected that

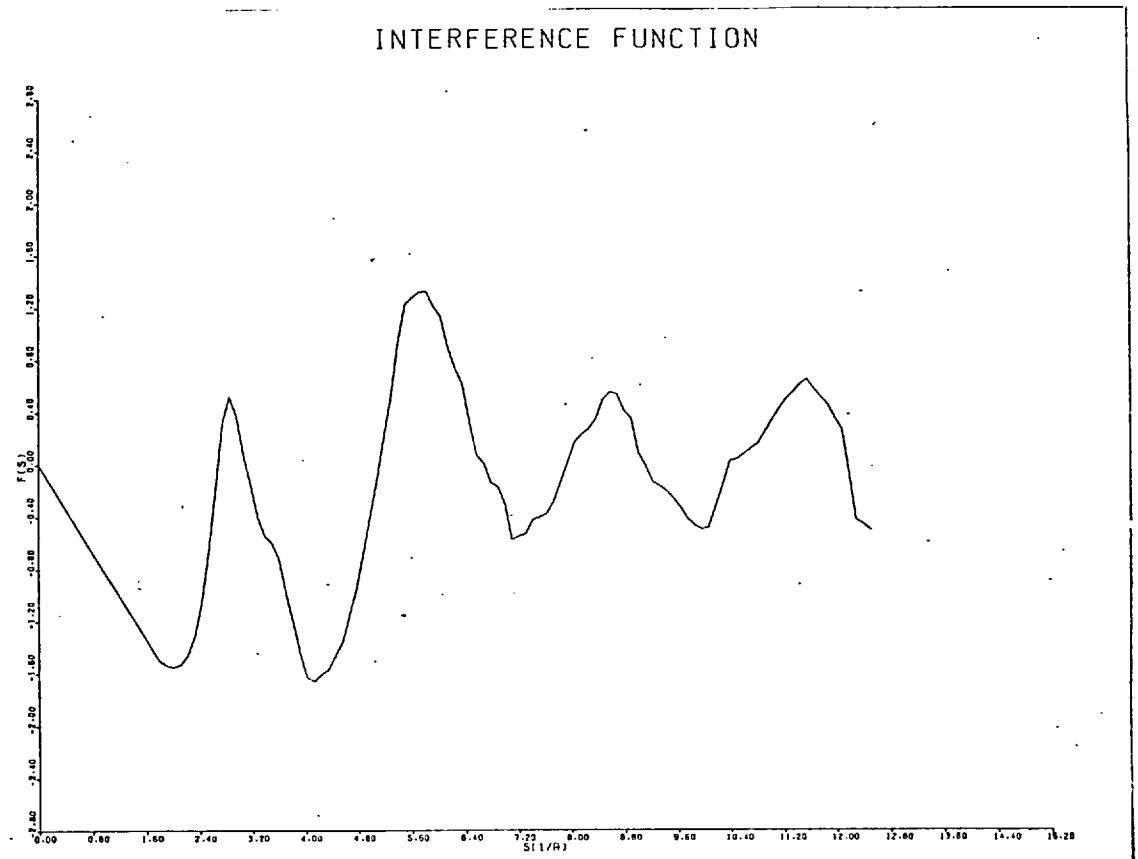

FIGURE (19)

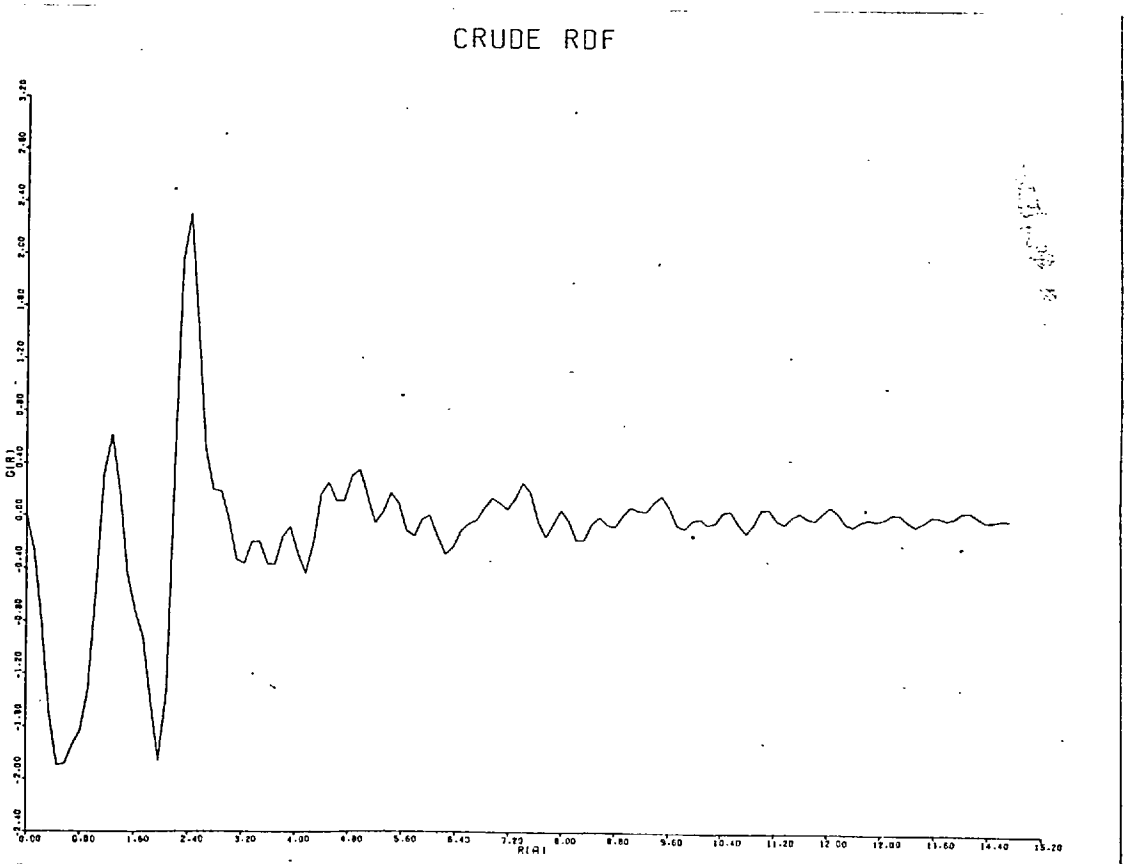

FIGURE (20)

RDF FOR DAMPED INTERFERENCE FUNCTION

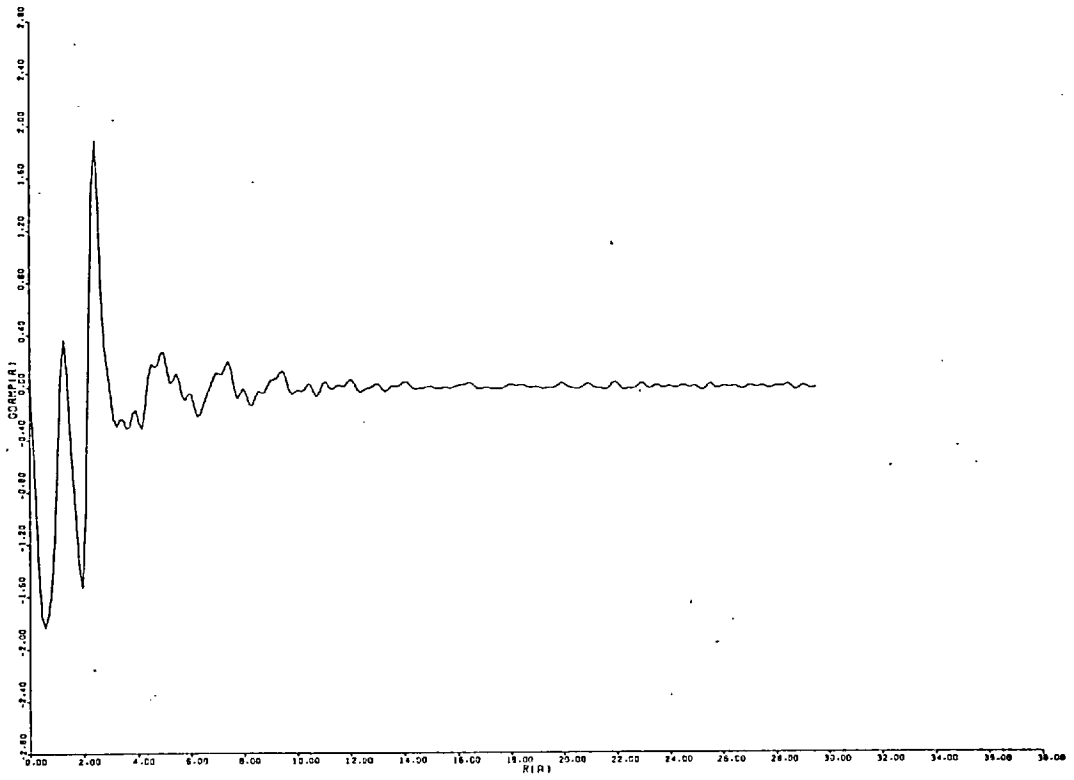

FIGURE (21)

RDF FOR DAMPED INTERFERENCE FUNCTION

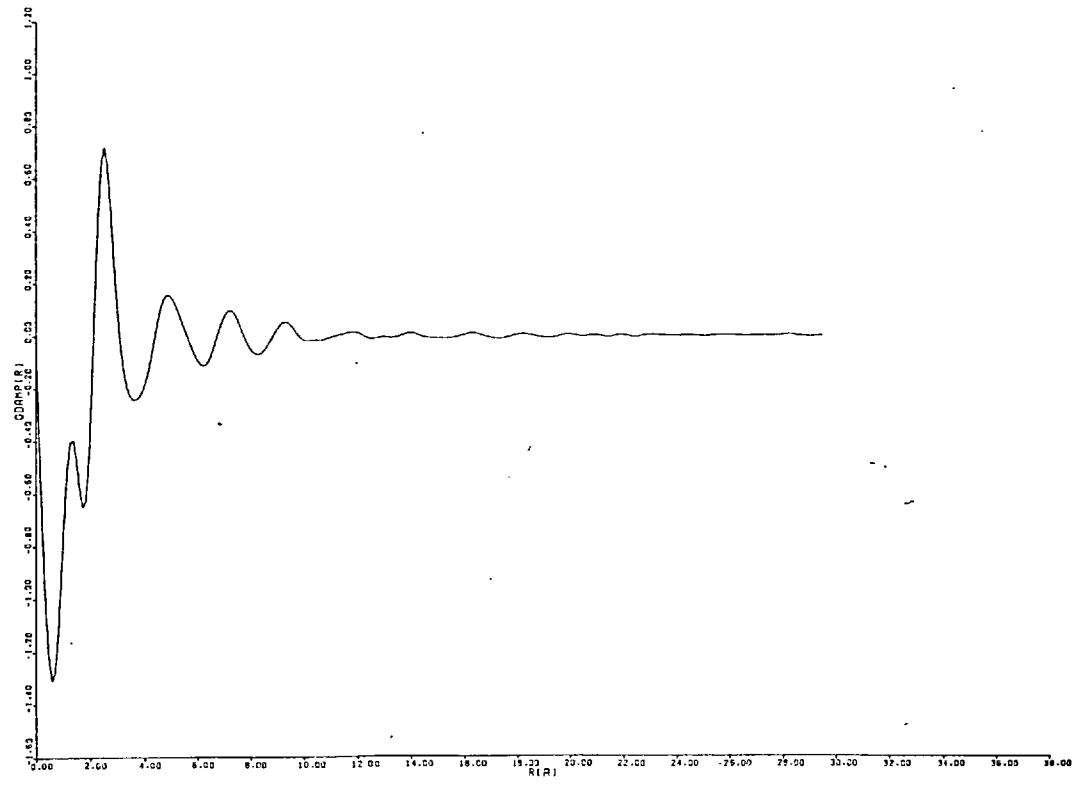

FIGURE (22)

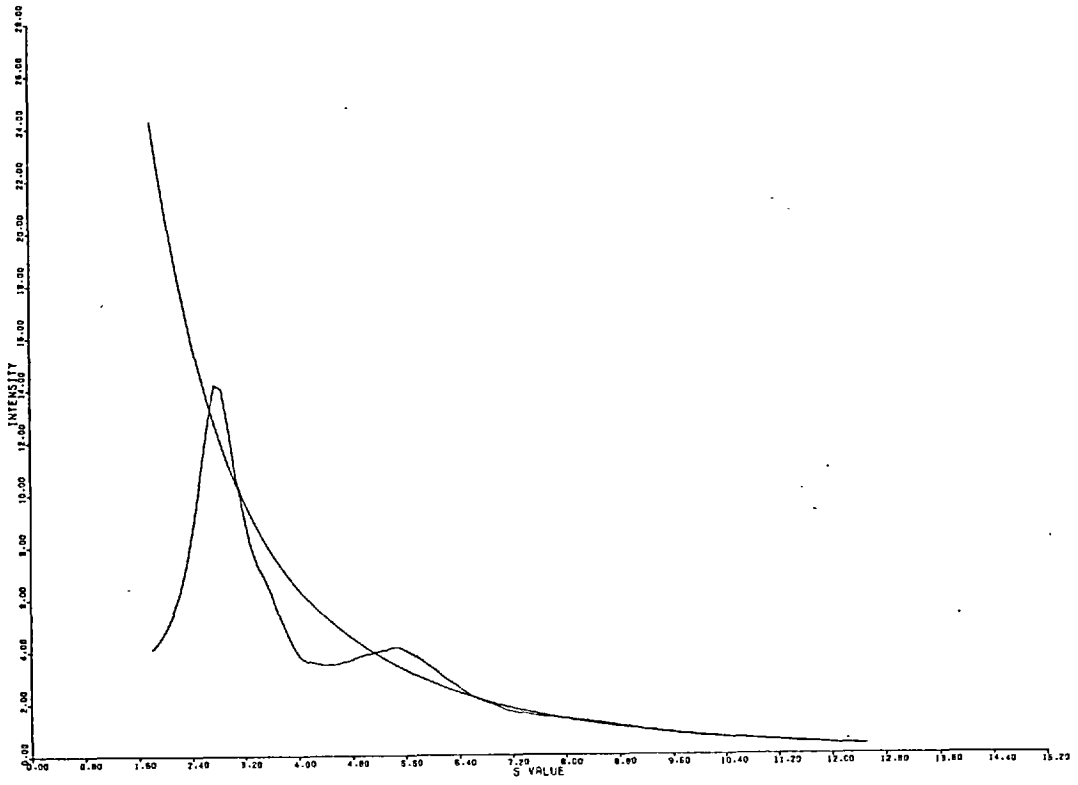

FIGURE (23)

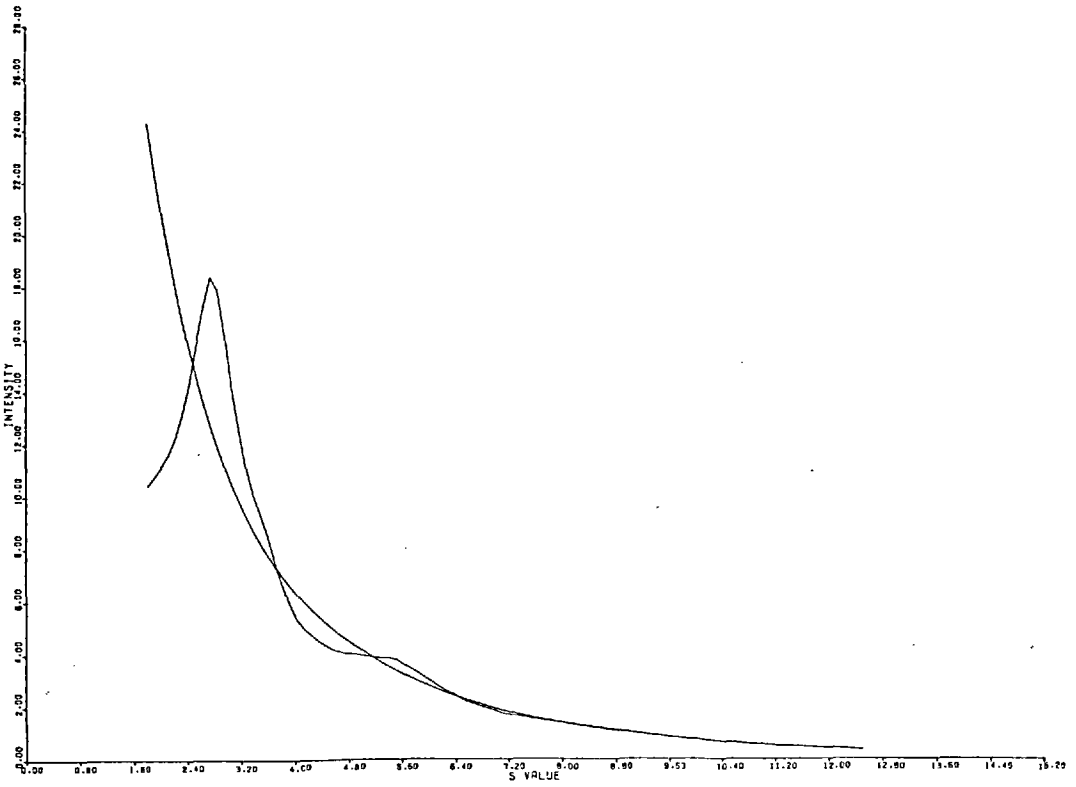

FIGURE (24)

RDF CORRESPONDING TO FNORM

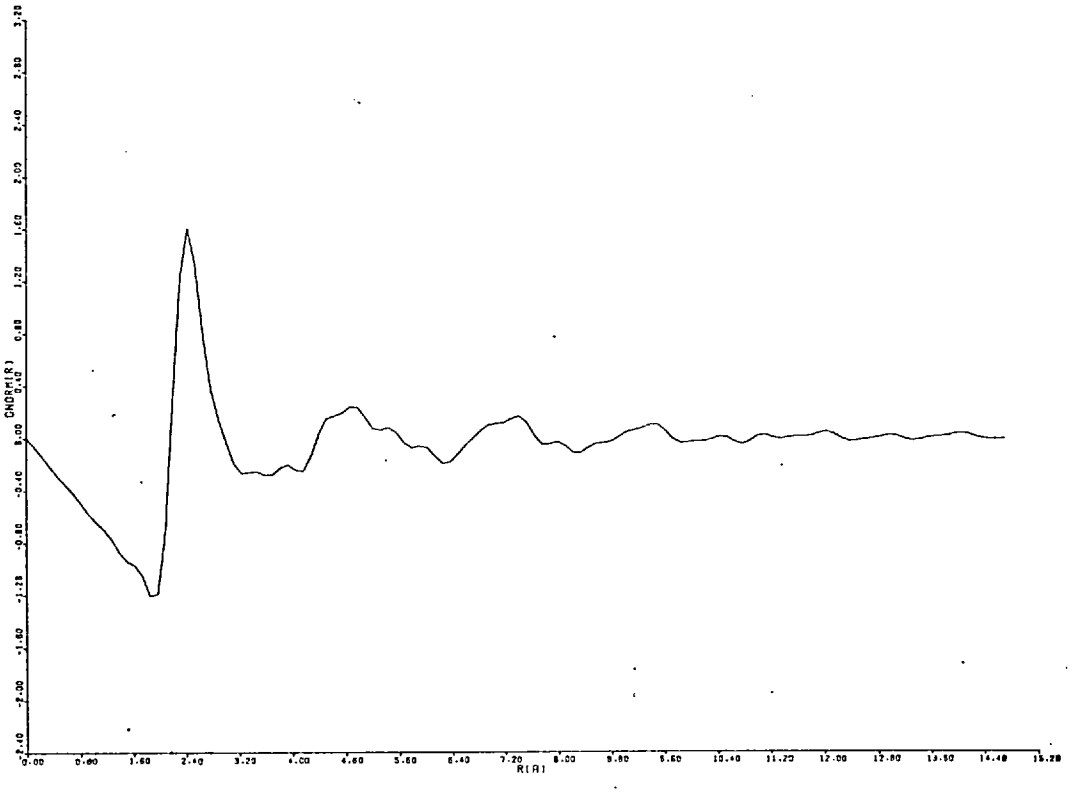

FIGURE (26)

INTERFERENCE FUNCTION WITH IMPROVED NORMALISATION

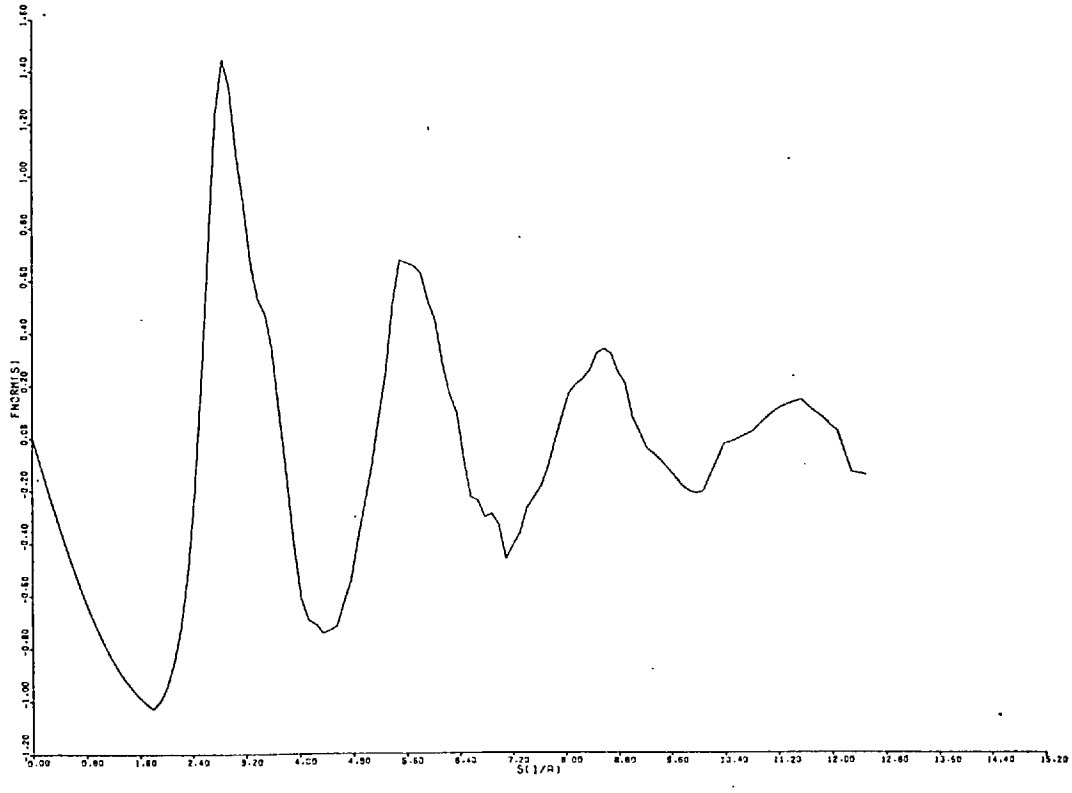

FIGURE (25)

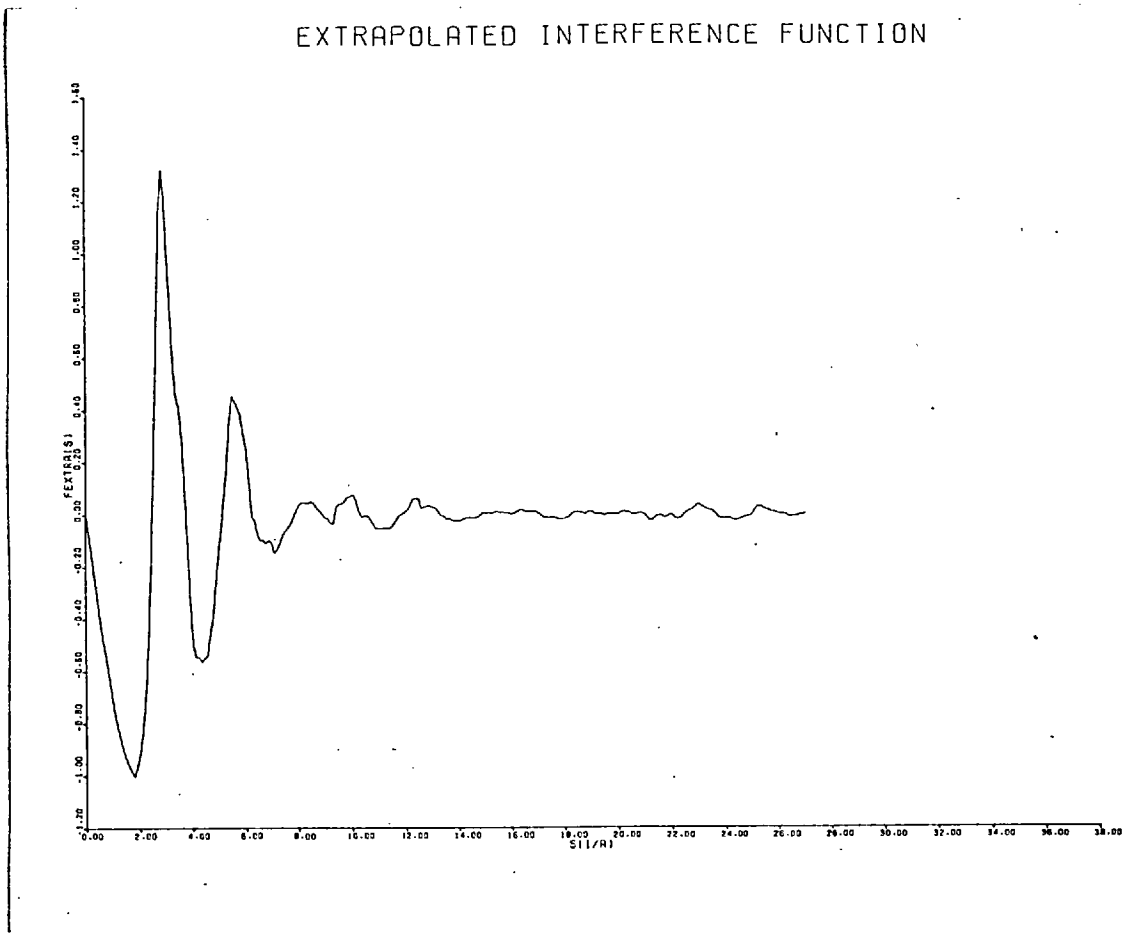

FIGURE (27)

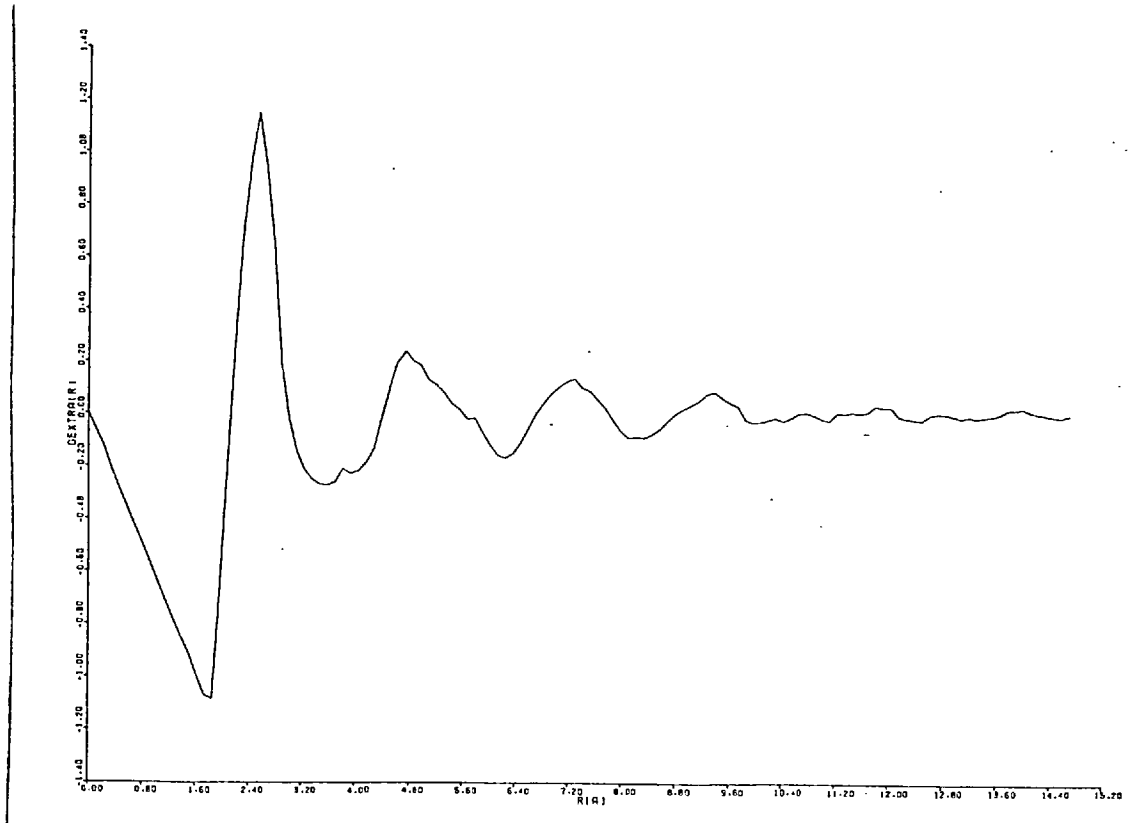

FIGURE (28)

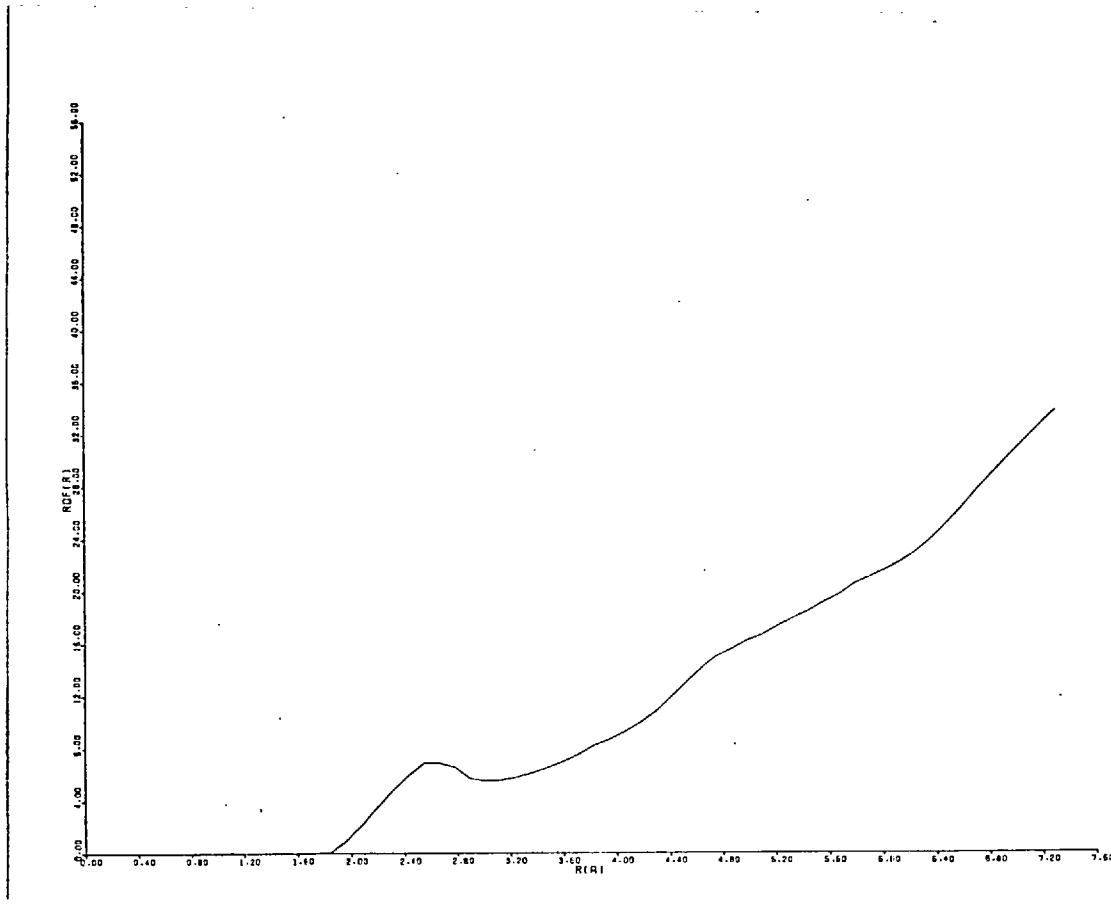

FIGURE (29)

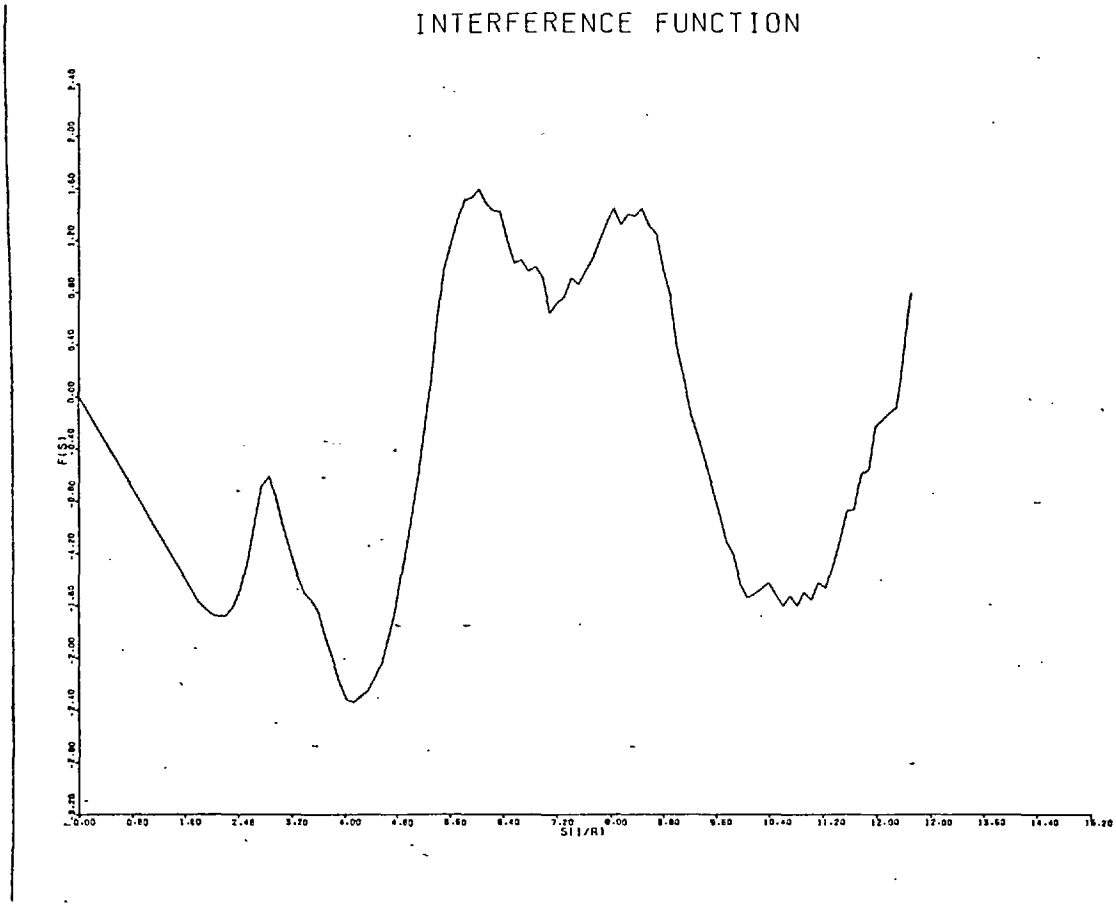

FIGURE (30)

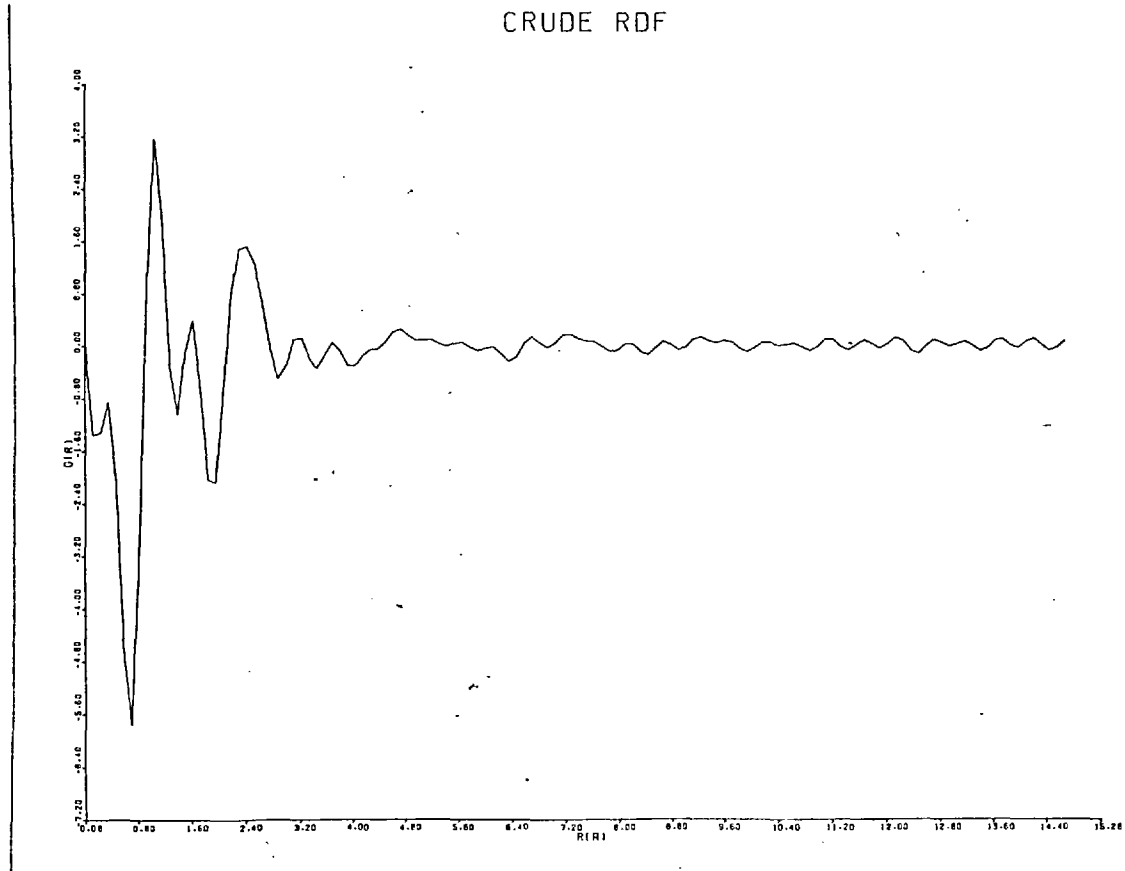

FIGURE (31)

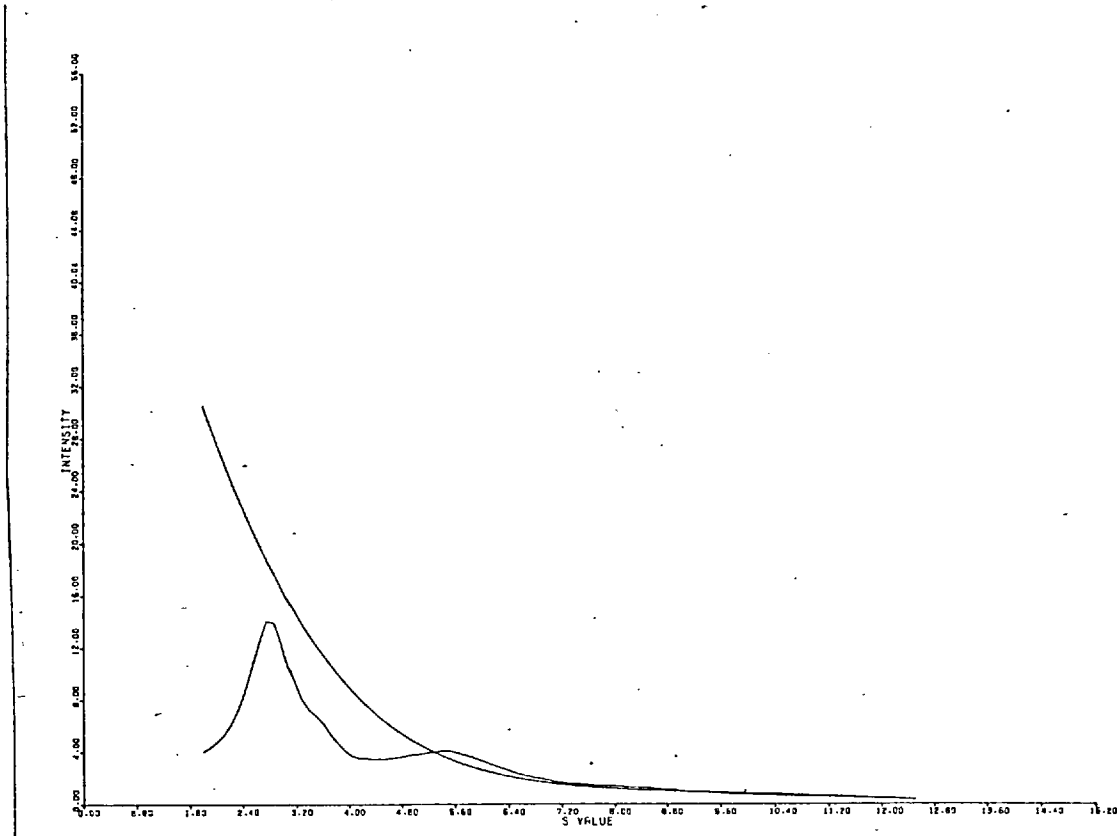

FIGURE (32)

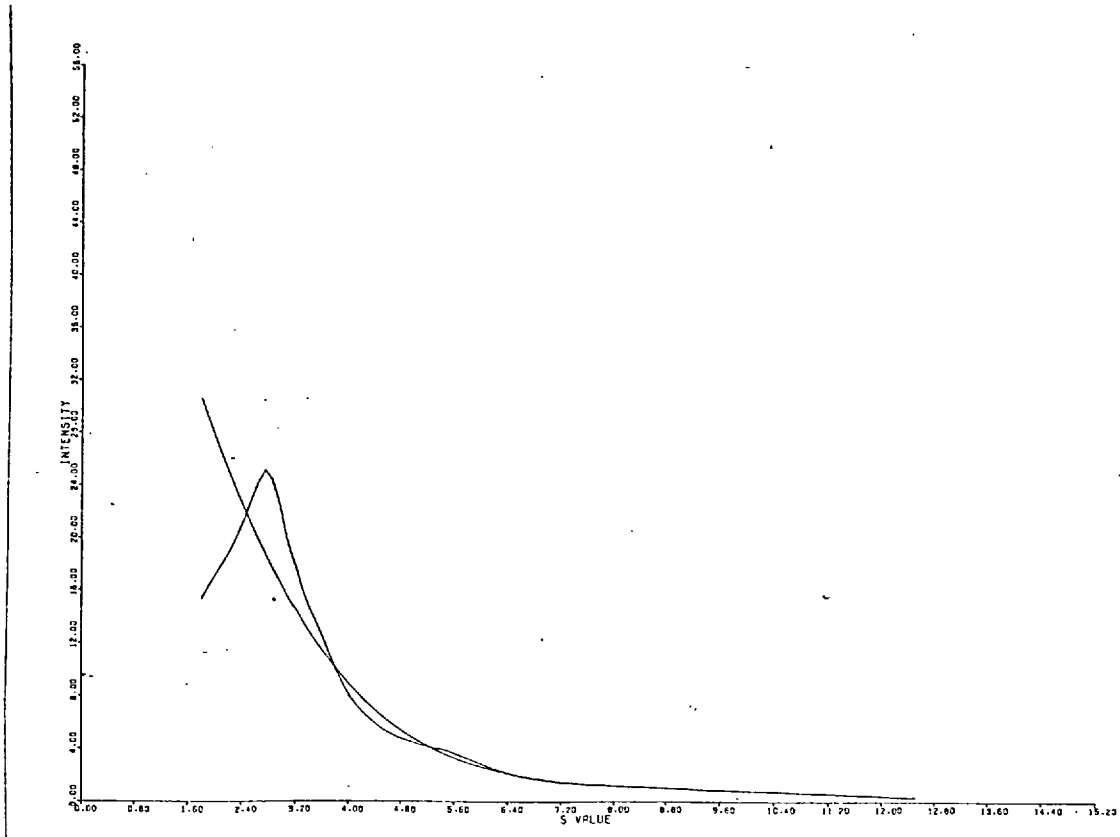

FIGURE (33)

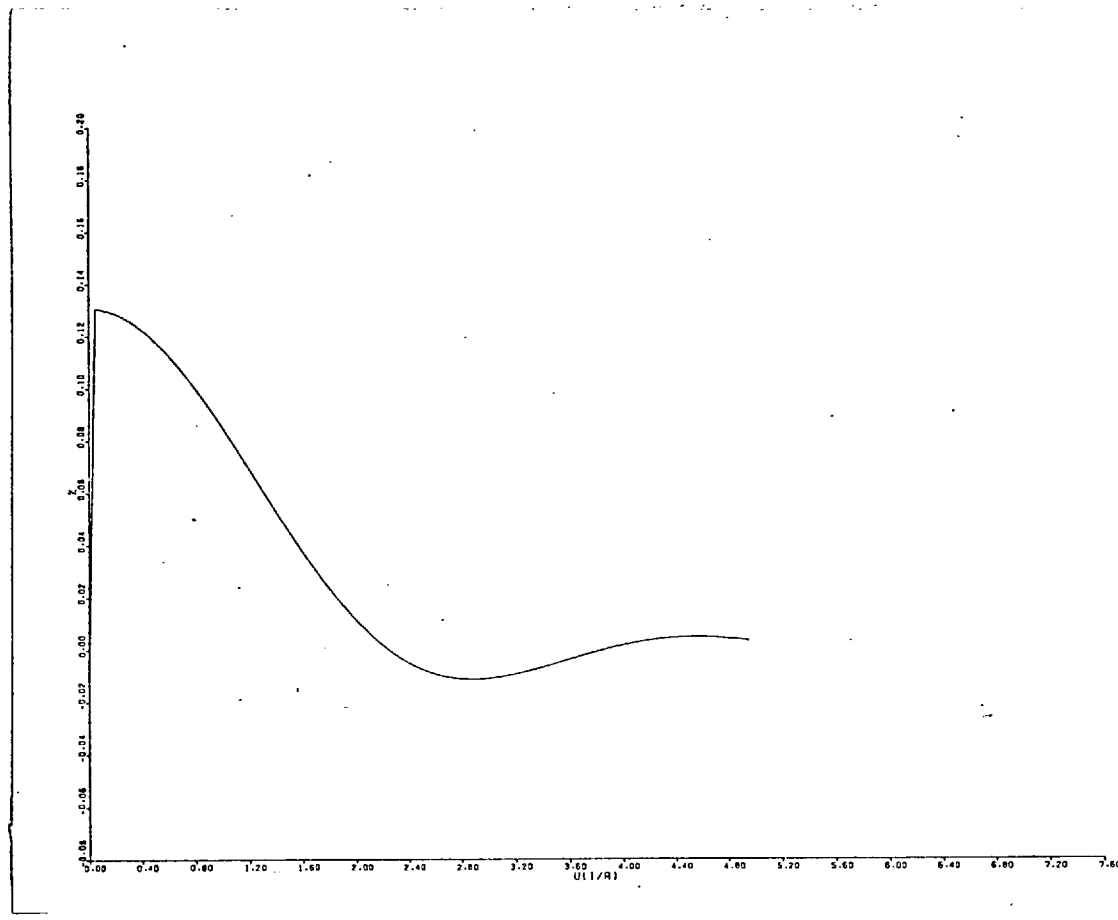
0.20
0.18
0.16
0.14
0.12
0.10
0.08
0.06
0.04
0.02
0.00
-0.02
-0.04
-0.06
-0.08
0.00
0.40
0.80
1.20
1.60
2.00
2.40
2.80
3.20
3.60
4.00
4.40
4.80
5.20
5.60
6.00
6.40
6.80
7.20
7.60
U(I/A)

FIGURE (34)

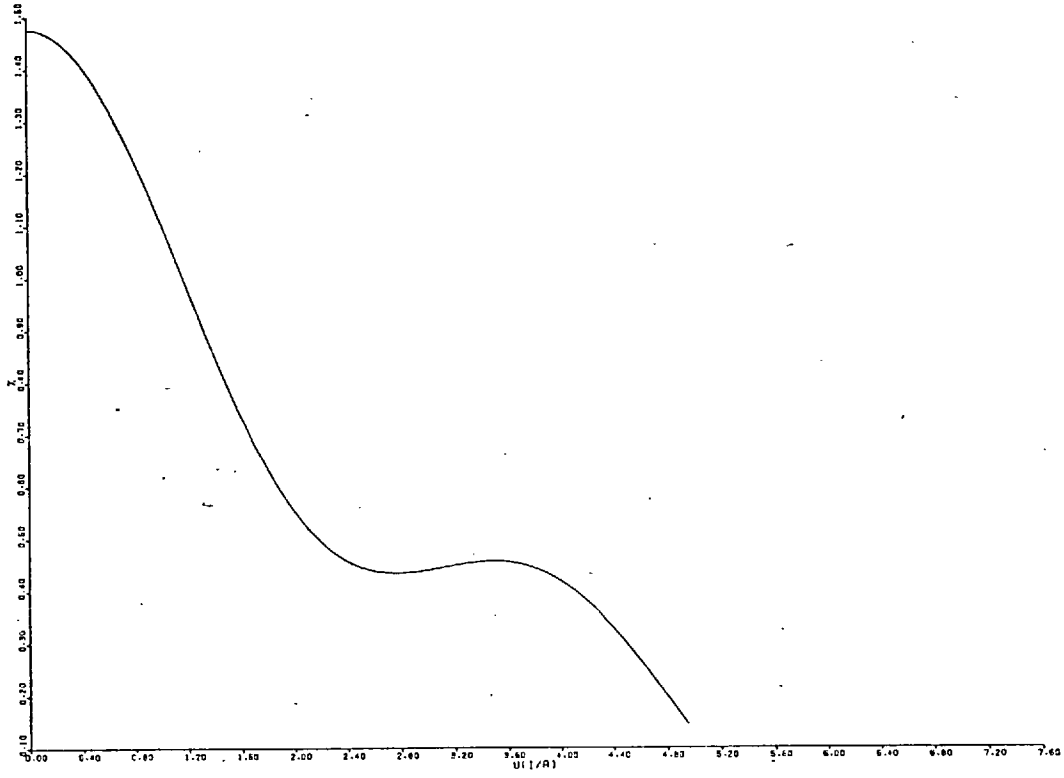

FIGURE (35)

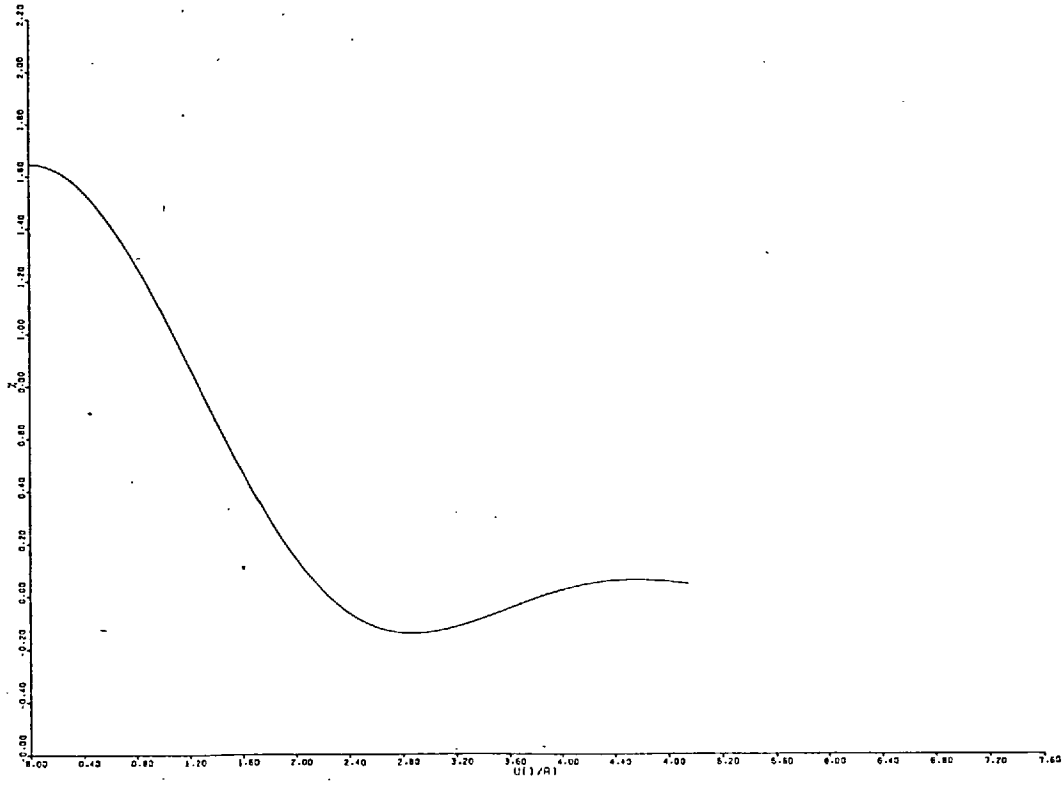

FIGURE (36)

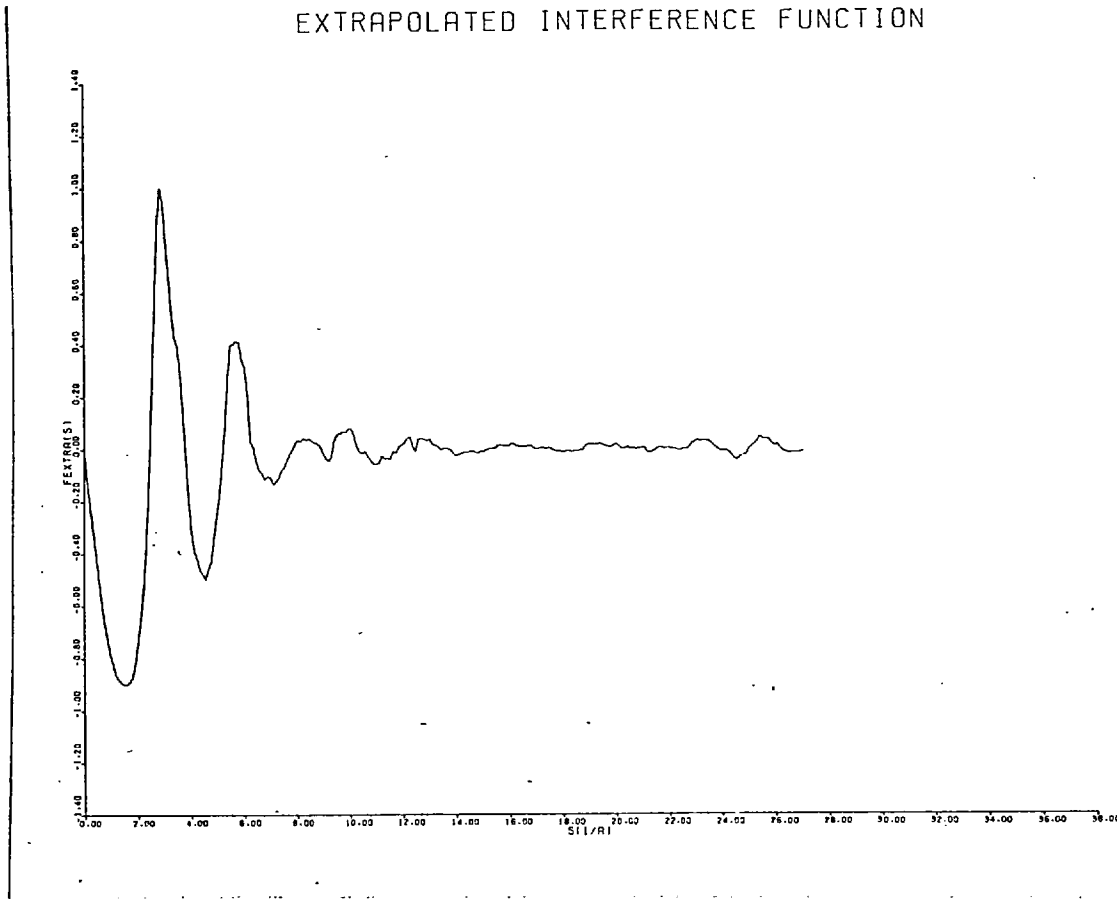

FIGURE (37)

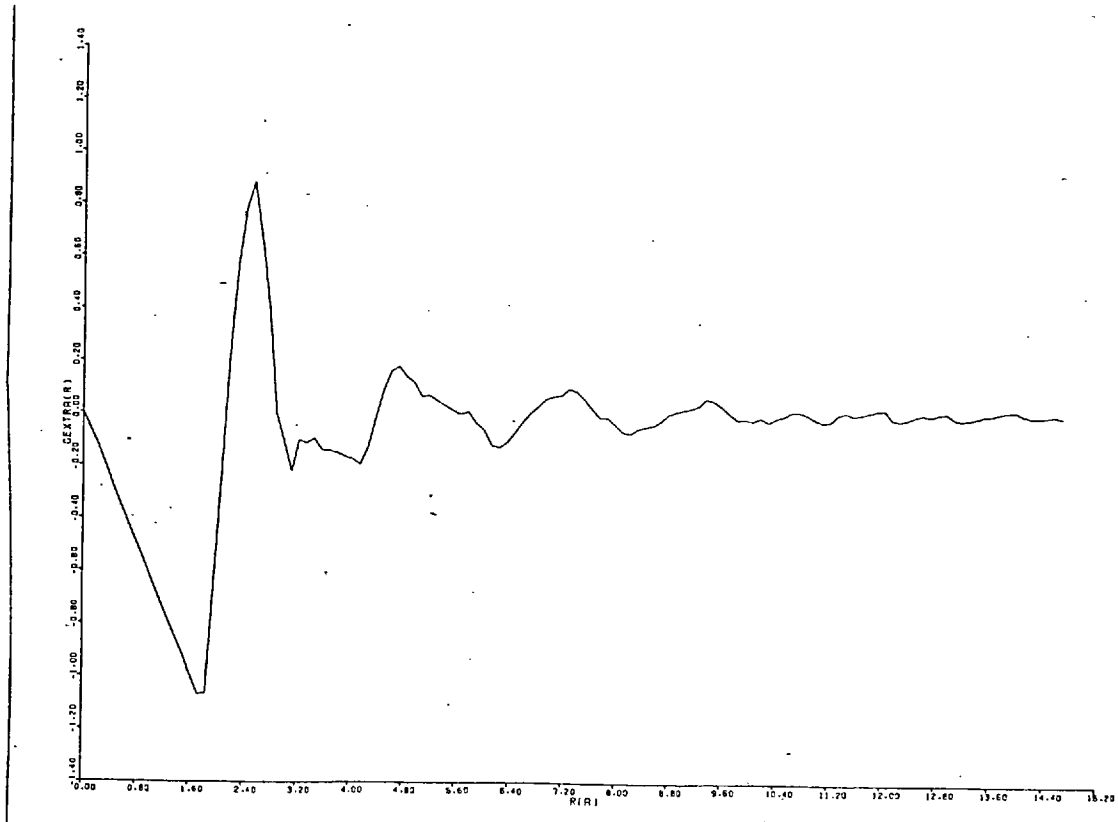

FIGURE (38)

LIQUID Ga
GAUSSIAN FIT TO FIRST PEAK OF RDF
GAUSSIAN FIT:
RDF:
RADIAL DENSITY FUNCTION
0.00
4.00
8.00
12.00
16.00
0.00
0.80
1.60
2.40
3.20
4.00
4.80
5.60
R(A)

FIGURE (39)

a worse result would be obtained in this case because of the approximate nature of the scattering calculation. Using the same Gallium data figure 30 and 31 show the calculated interference function and R.D.F. respectively. Figures 32 and 33 are the normalised intensities before and after being treated for normalisation error. In conjunction with this the Rahman normalisation criterion can be applied. Figure 34 is the function SUD calculated from the averafe atomic density of Gallium. Figures 35 and 36 are the functions SUDEX calculated from the experimental data before and after being treated for the error respectively. The Rahman criterion says that SUD and SUDEX should agree if the normalisation is correct.

Finally figures 37 and 38 are the extropolated interference function and the treated final R.D.F. respectively. These can be compared with corresponding functions obtained using the self consistent field scattering factor.

The final stage in the analysis, having obtained a reasonable R.D.F., is to estimate the first co-ordination number. Figure 39 shows the Gaussian function fitted to the first Radial Density Function peak. Program Gauss having fitted this function estimates the co-ordination number using the three methods indicated in Chapter 3. These are:

symmetrical method	minimum to minimum method	Gaussian method
5.0	6.4	6.6

4.3.1.3. Analysis of the Non-Crystalline Data

This data is taken immediately after deposition of the film. In the analysis and for all other materials the self consistent field scattering factor is used.

The final interference function is shown in figure 40 while the corresponding Radial Distribution Function is in figure 41.

The Gaussian function fitted to the first peak in the density function is shown in figure 42. The three methods of estimating the co-ordination number give an average value of 6.

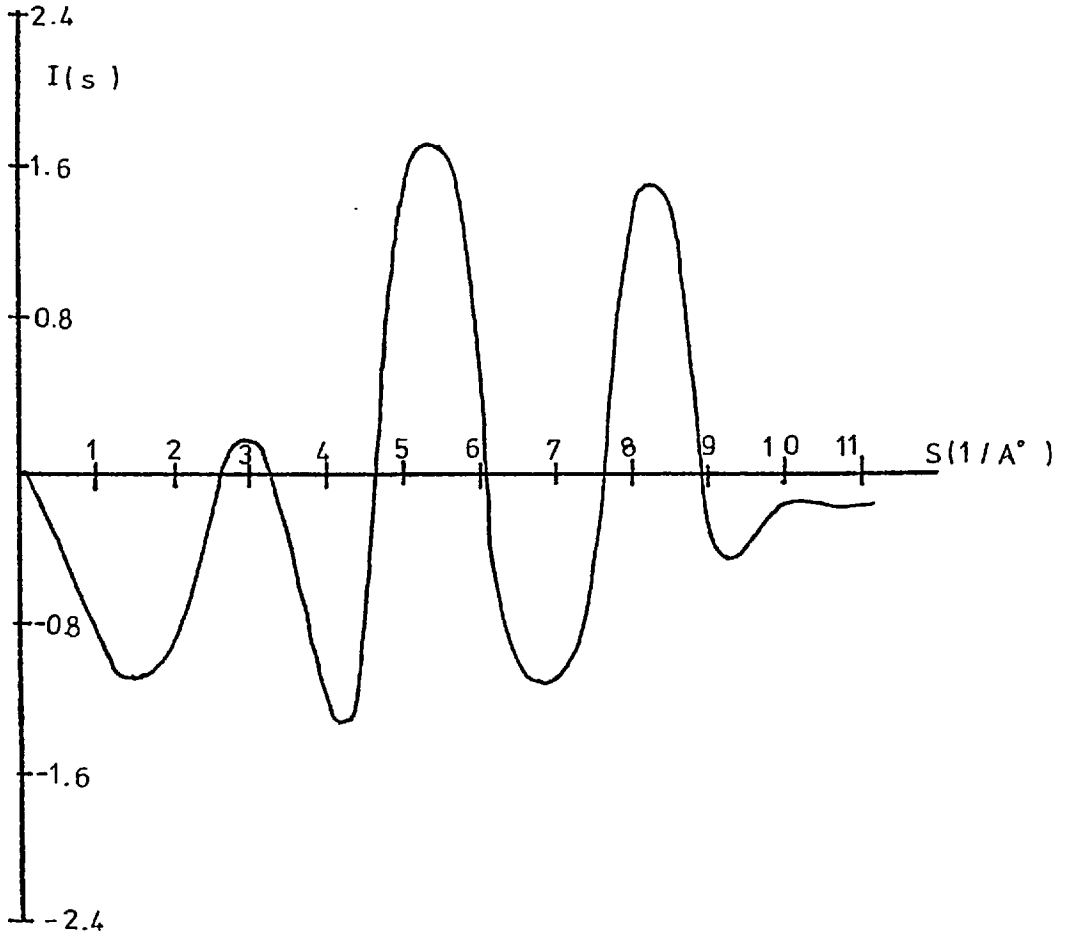

FIGURE (40)

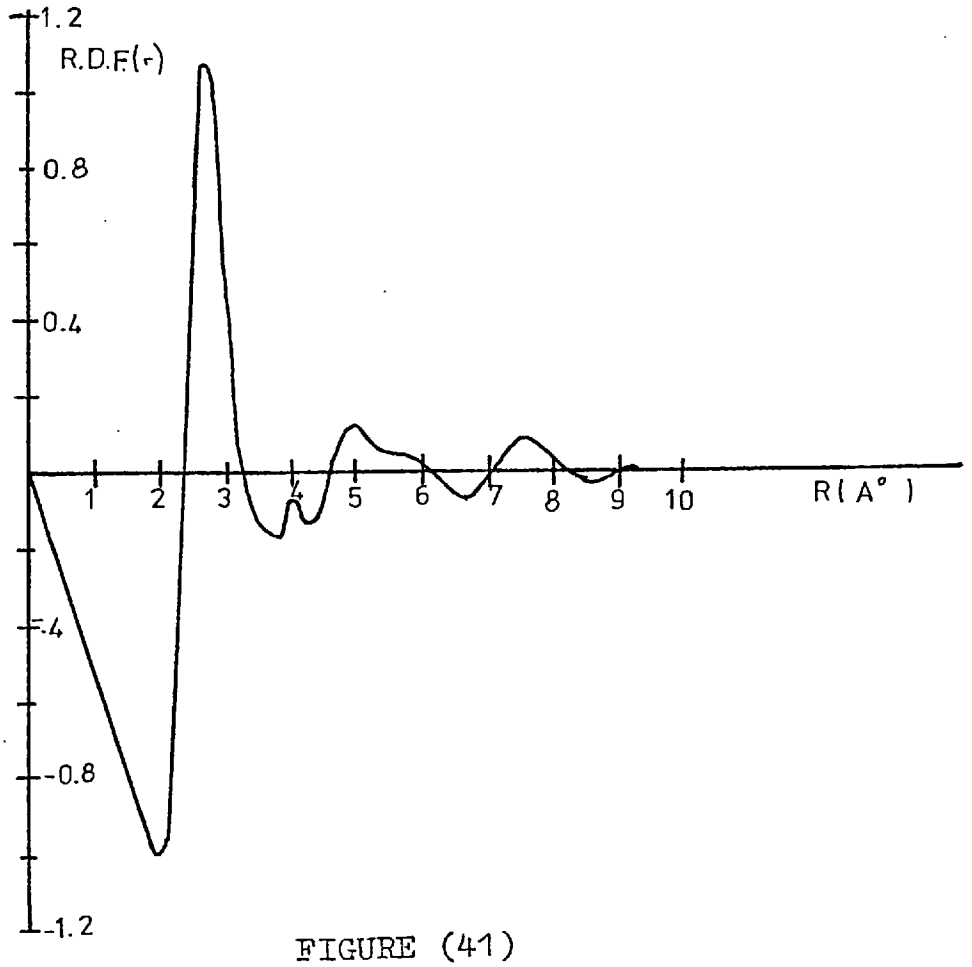

FIGURE (41)

NON-CRYSTALLINE Ga
GAUSSIAN FIT TO FIRST PEAK OF RDF
GAUSSIAN FIT:
RDF:
RADIAL DENSITY FUNCTION
0.00
4.00
8.00
12.00
16.00
0.00
0.80
1.60
2.40
3.20
4.00
4.80
5.60
R(A)

FIGURE (42)

4.3.2. Nickel

On deposition onto the liquid Helium cooled substrate, the Nickel films produced a diffraction pattern of diffuse rings. This pattern did not appear to change significantely with increasing thickness. During the process of warming the film to room temperature polycrystalline rings were observed to appear. However as with the Gallium films no particular temperature could be assigned to this change.

The calculated interference function is shown in figure 43 while the corresponding R.D.F. is given in figure 44 The normalised intensity is figure 45. The extrapolated interference function is illustrated in figure 46 while figure 47 shows the final, treated R.D.F. Figure 48 is the Radial density function and figure 49 is the Gaussian fit to the first peak in this function. The average co-ordination number is 7.

INTERFERENCE FUNCTION

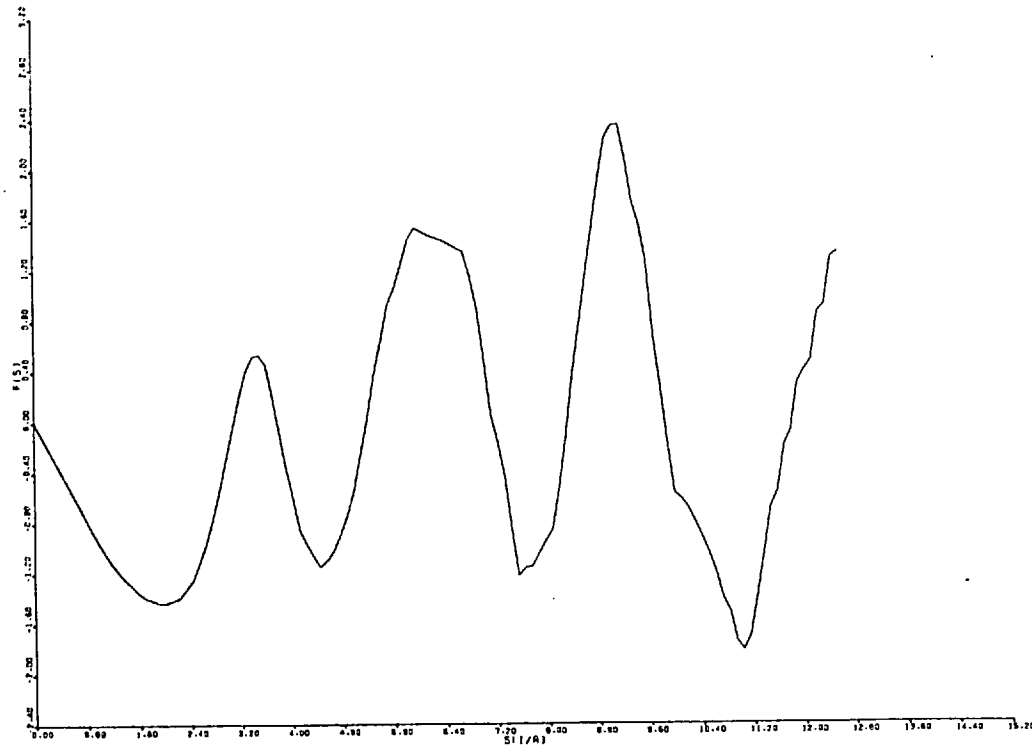

FIGURE 43

CRUDE RDF

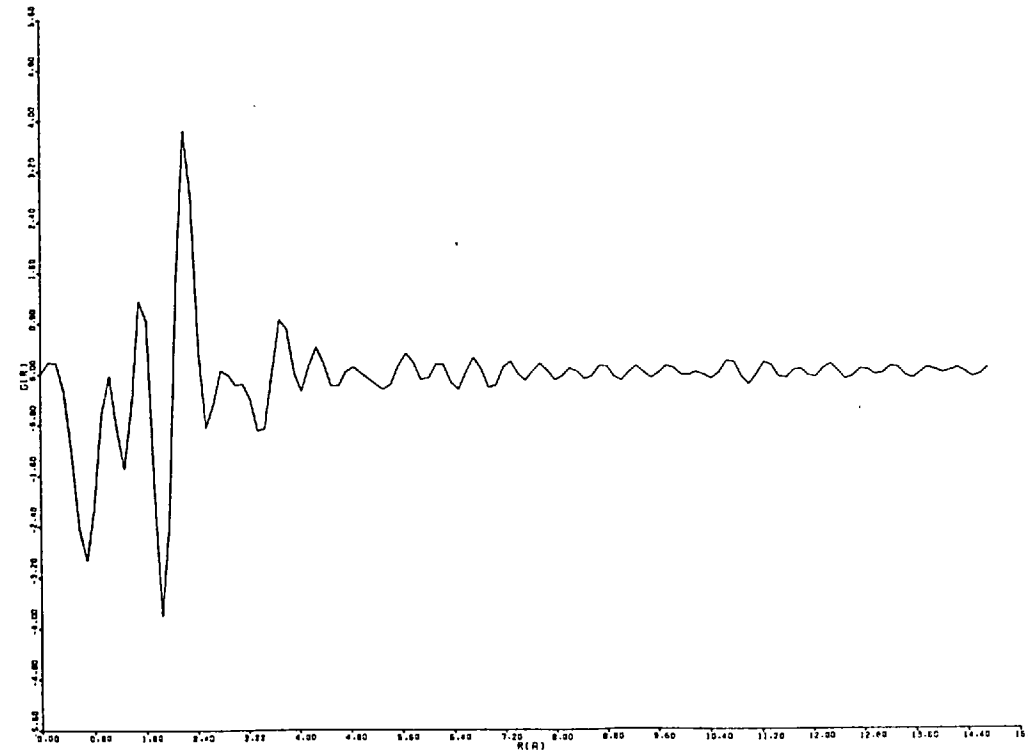

FIGURE 44

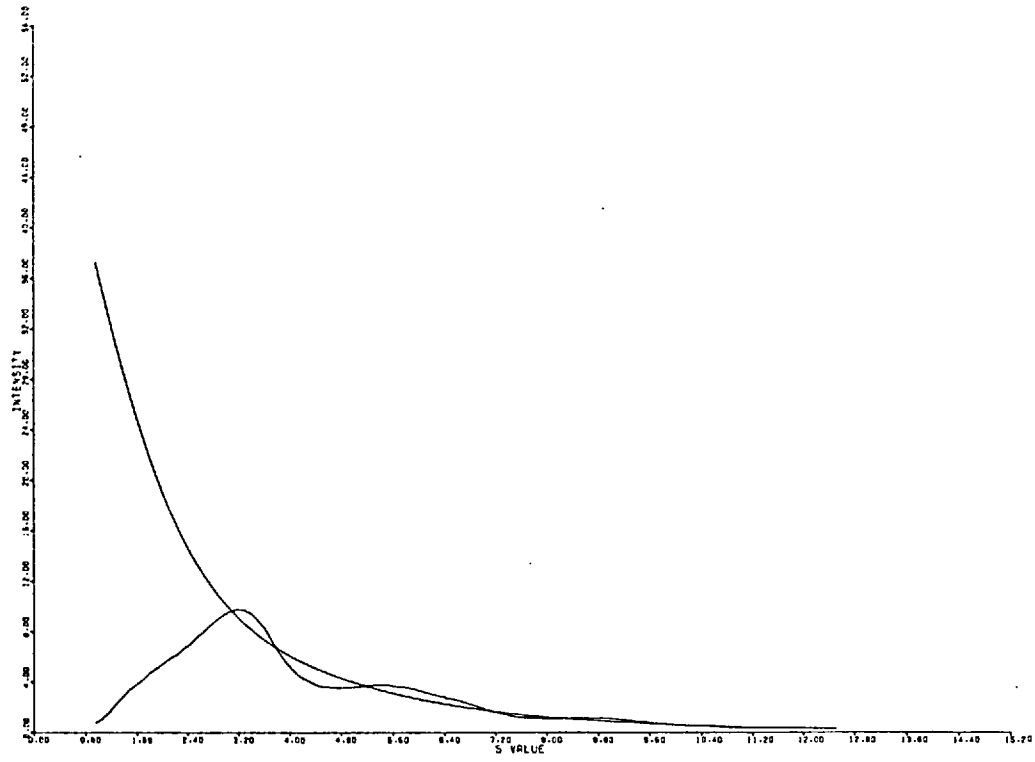

FIGURE 45

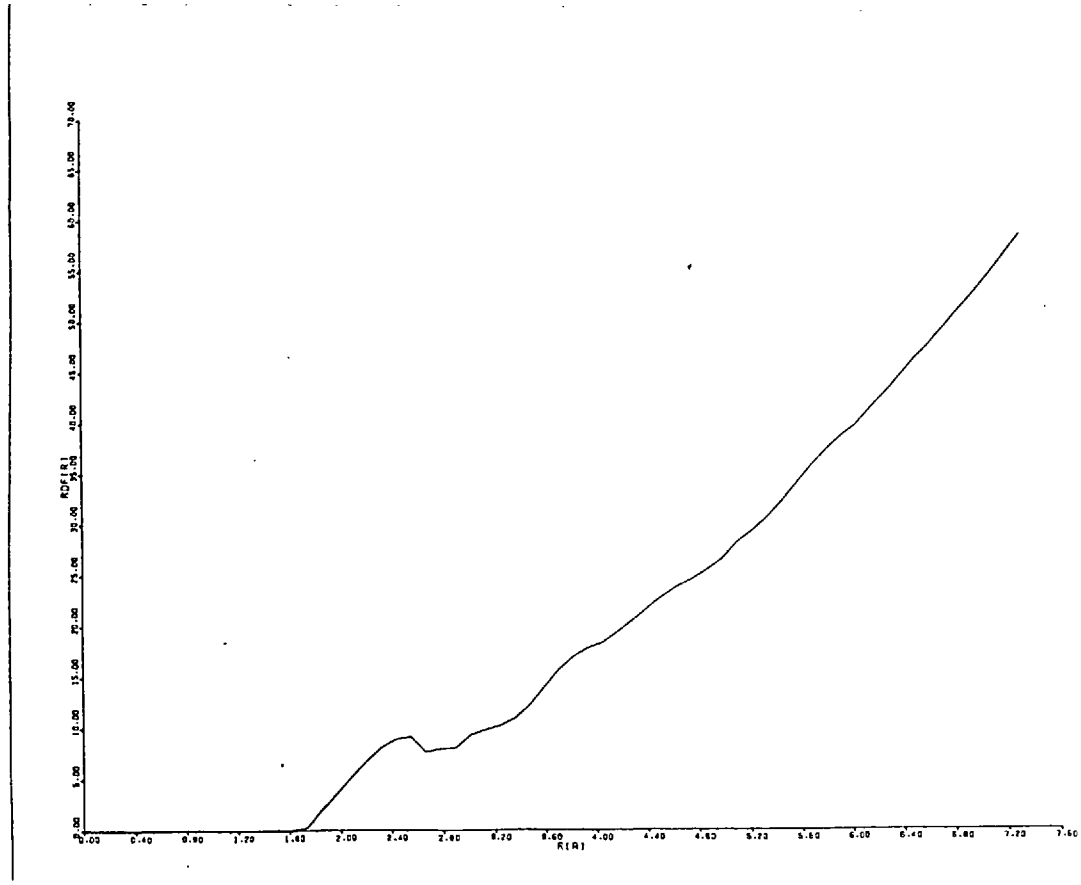

FIGURE 48

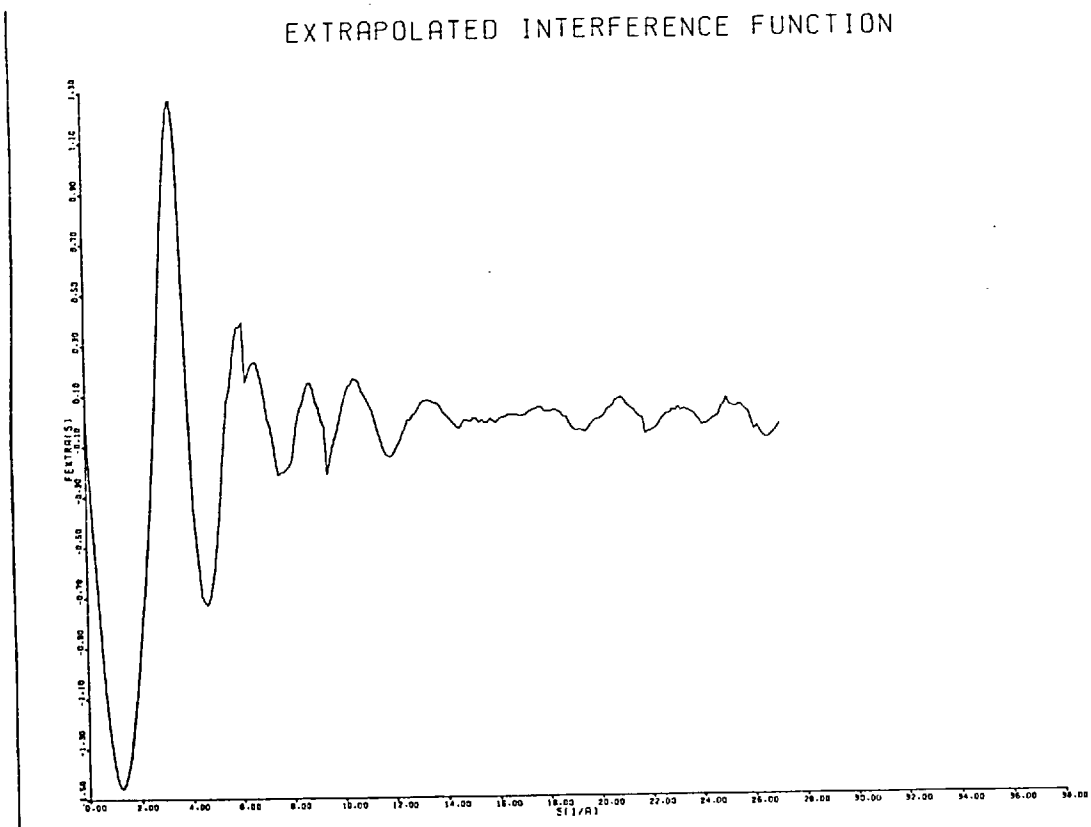

FIGURE 46

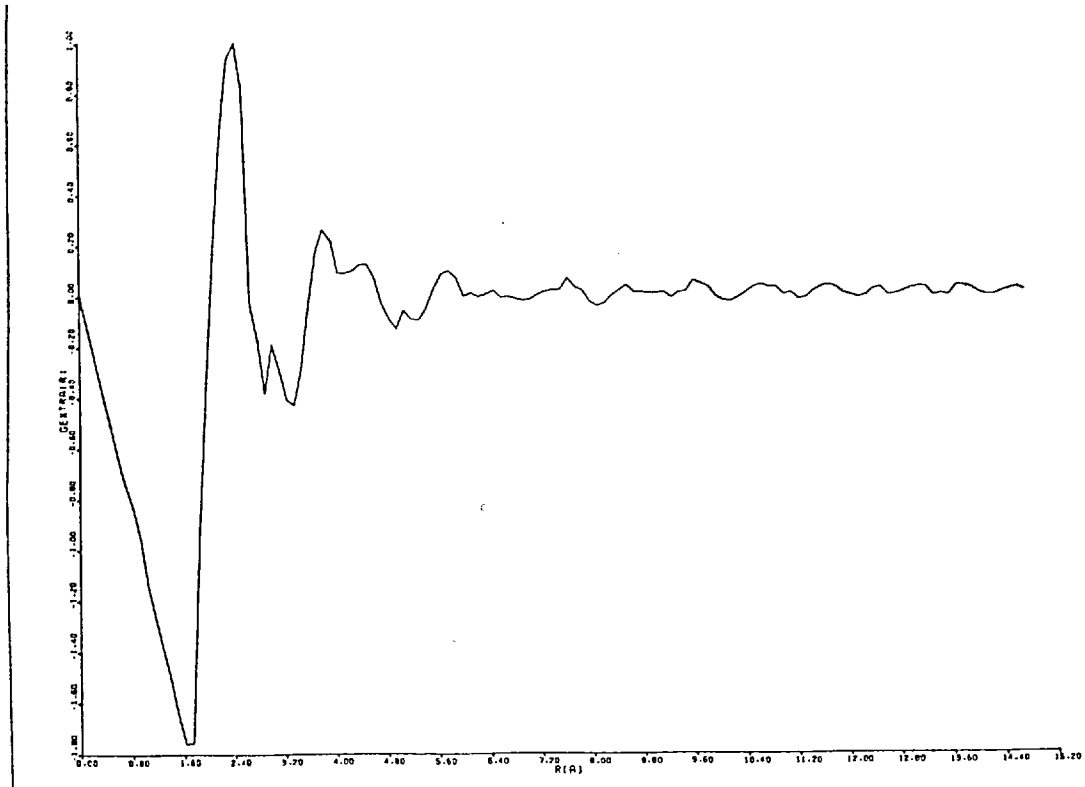

FIGURE 47

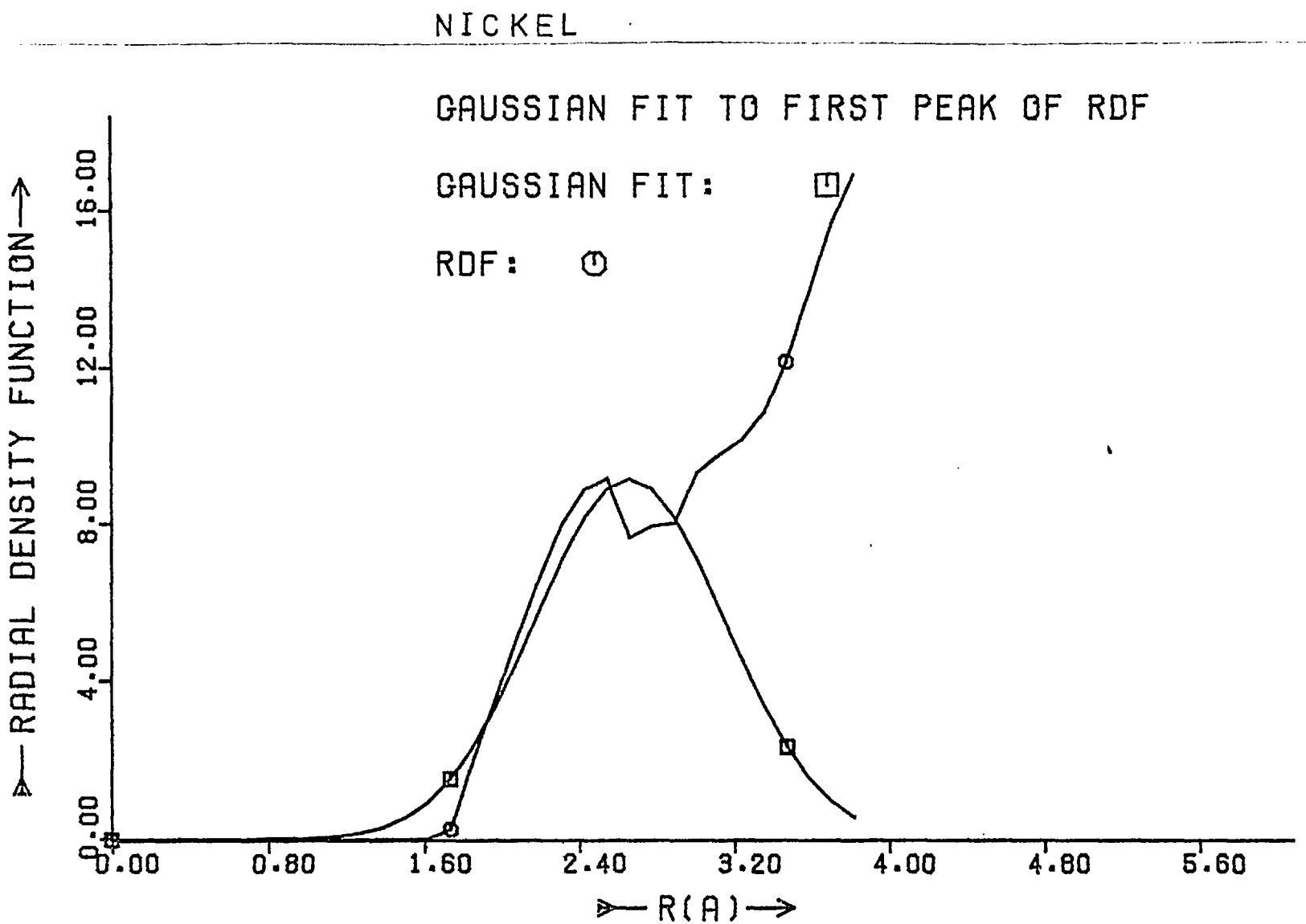
NICKEL
GAUSSIAN FIT TO FIRST PEAK OF RDF
GAUSSIAN FIT:
RDF:
RADIAL DENSITY FUNCTION
0.00
4.00
8.00
12.00
16.00
0.00
0.80
1.60
2.40
3.20
4.00
4.80
5.60
R(A)

FIGURE (49)

4.3.3. Cobalt

Thin films of Cobalt prepared at approximately 5°K appeared to have a non-crystalline structure (see figure 50). Further deposition, however, caused the film to transform into a polycrystalline form illustrated in figure 51. This structural change had occurred by the time the film was about 300A°.

The data shown in figure 50 was analysed and figure 52 shows the calculated interference function. Figure 53 is the corresponding R.D.F. The normalised intensity is shown in figure 54. Figures 56 and 57 are the extrapolated interference function and the final R.D.F. respectively. Figure 55 is the Radial Density function and the fitted Gaussian is in figure 58. The average calculated co-ordination number for Cobalt is 8.

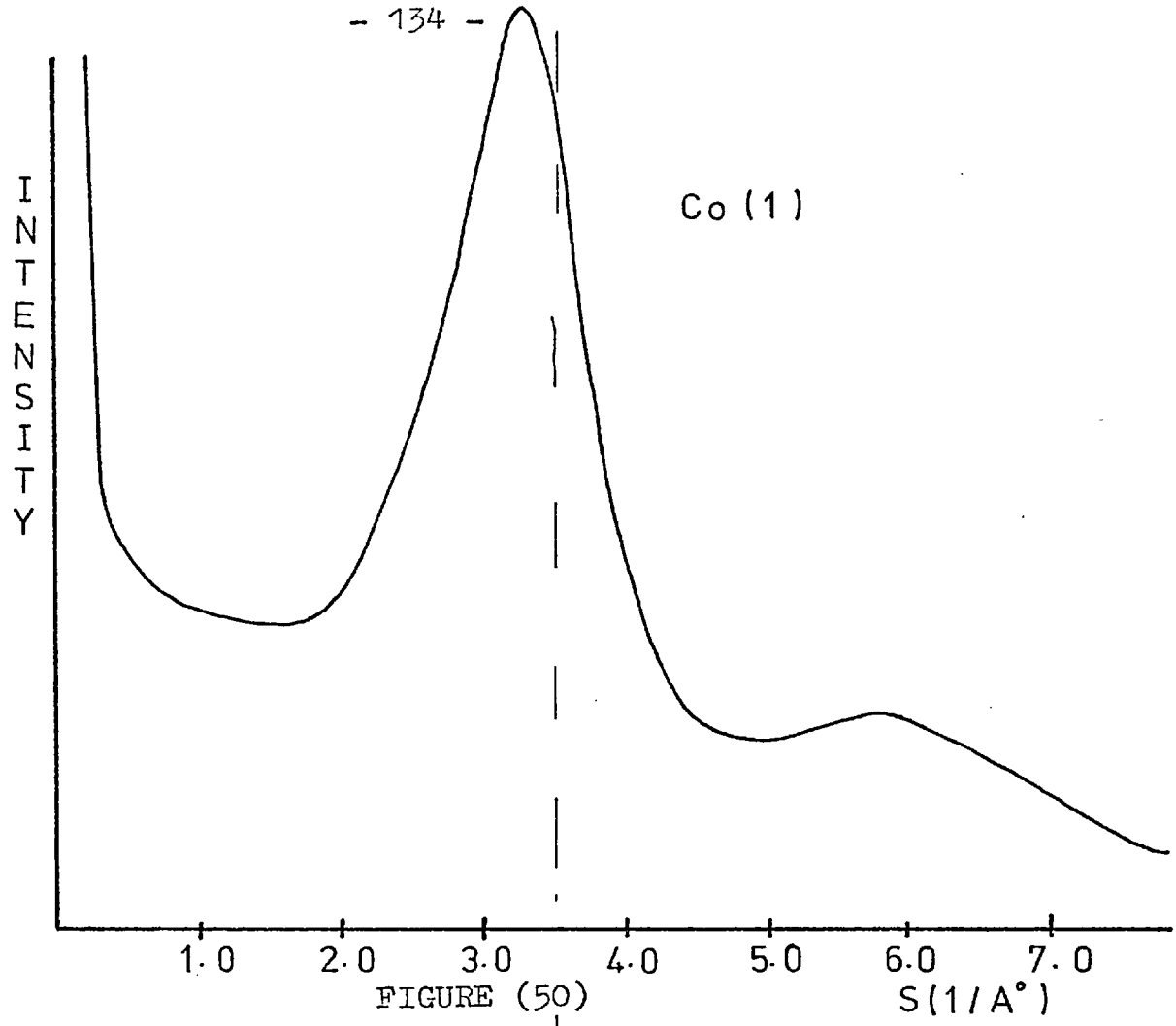

FIGURE (50)

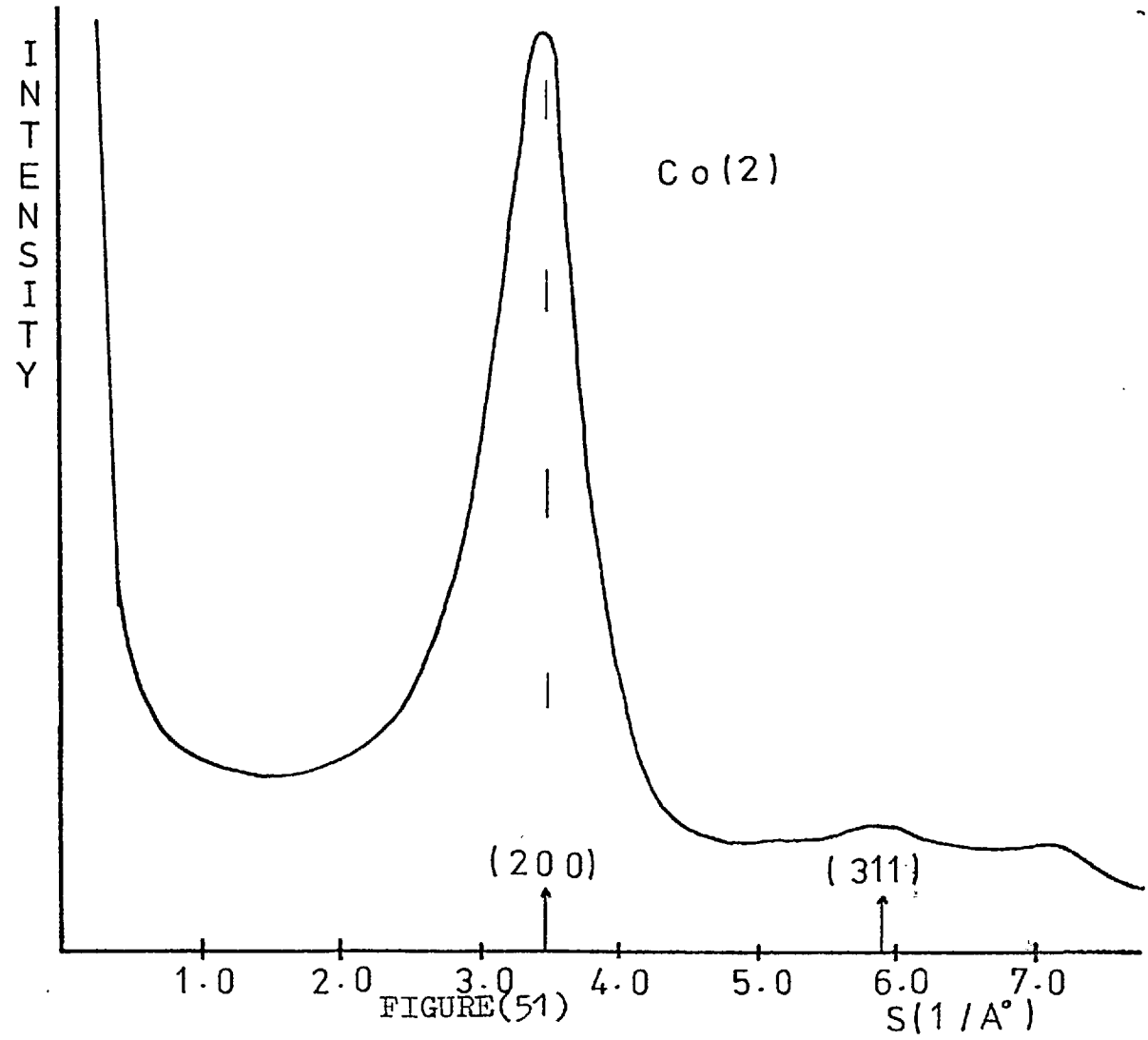

FIGURE(51)

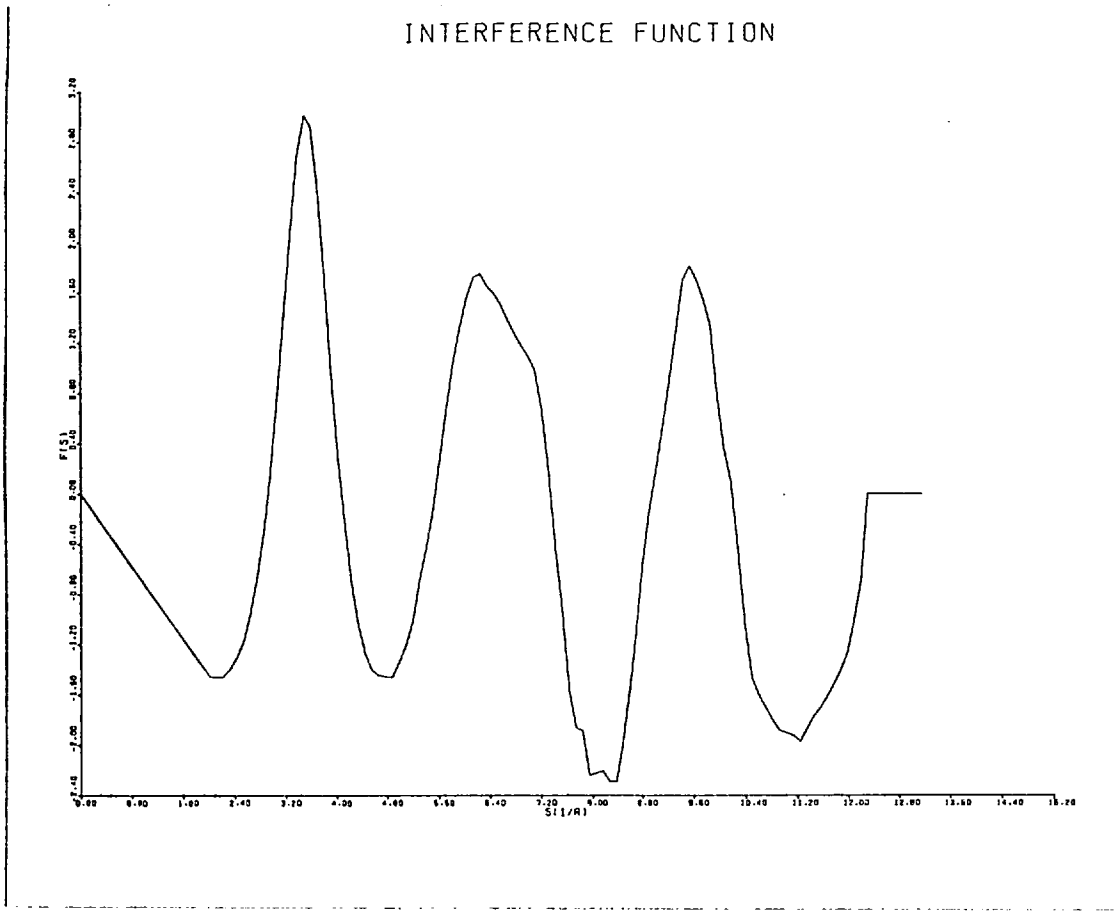

FIGURE (52)

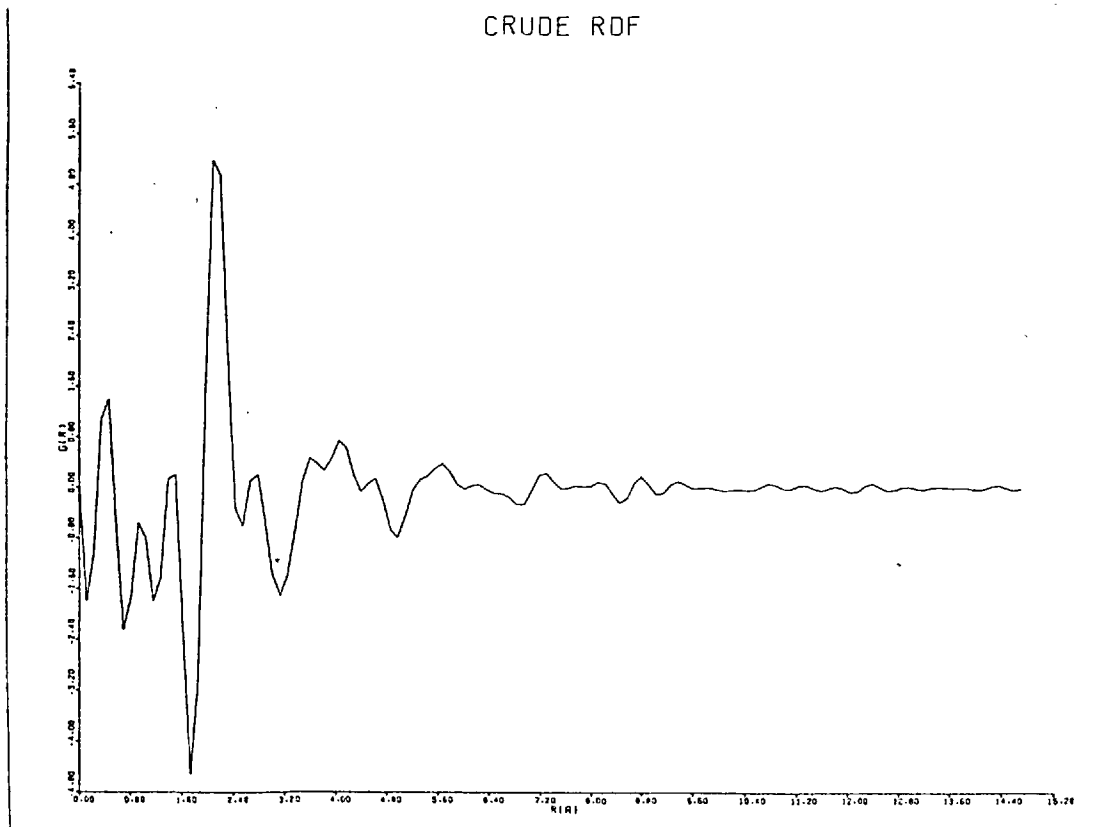

FIGURE (53)

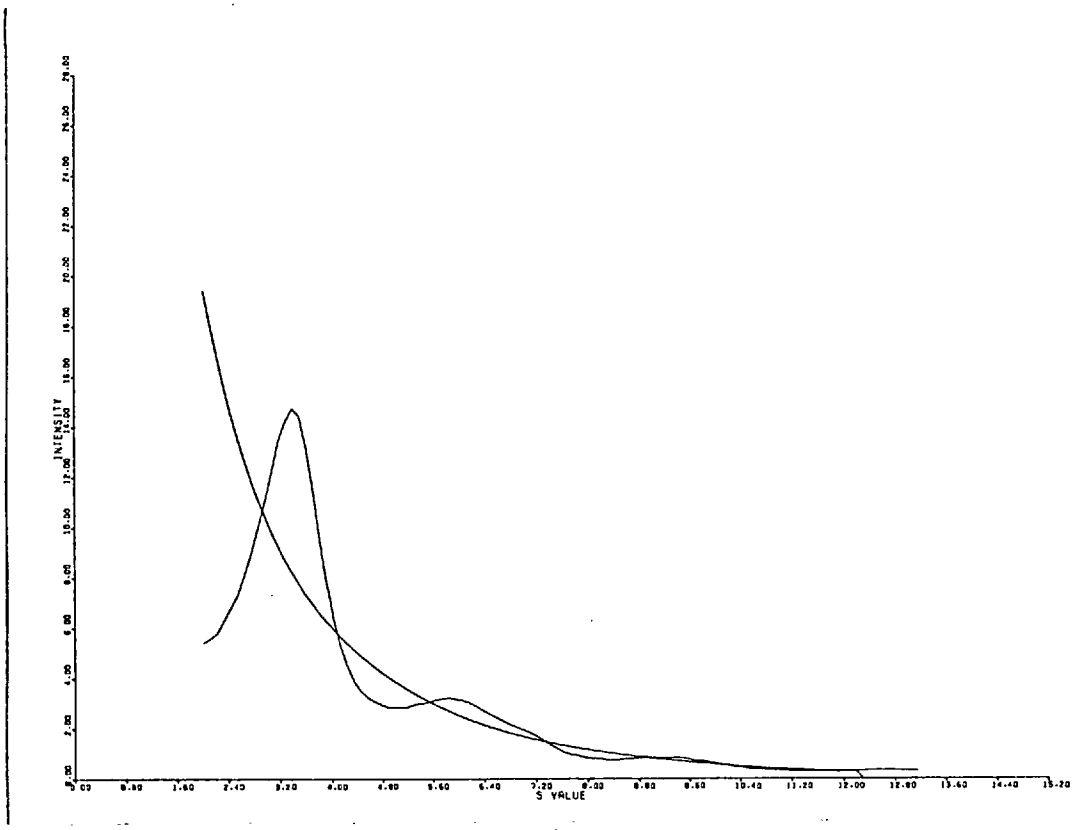

FIGURE (54)

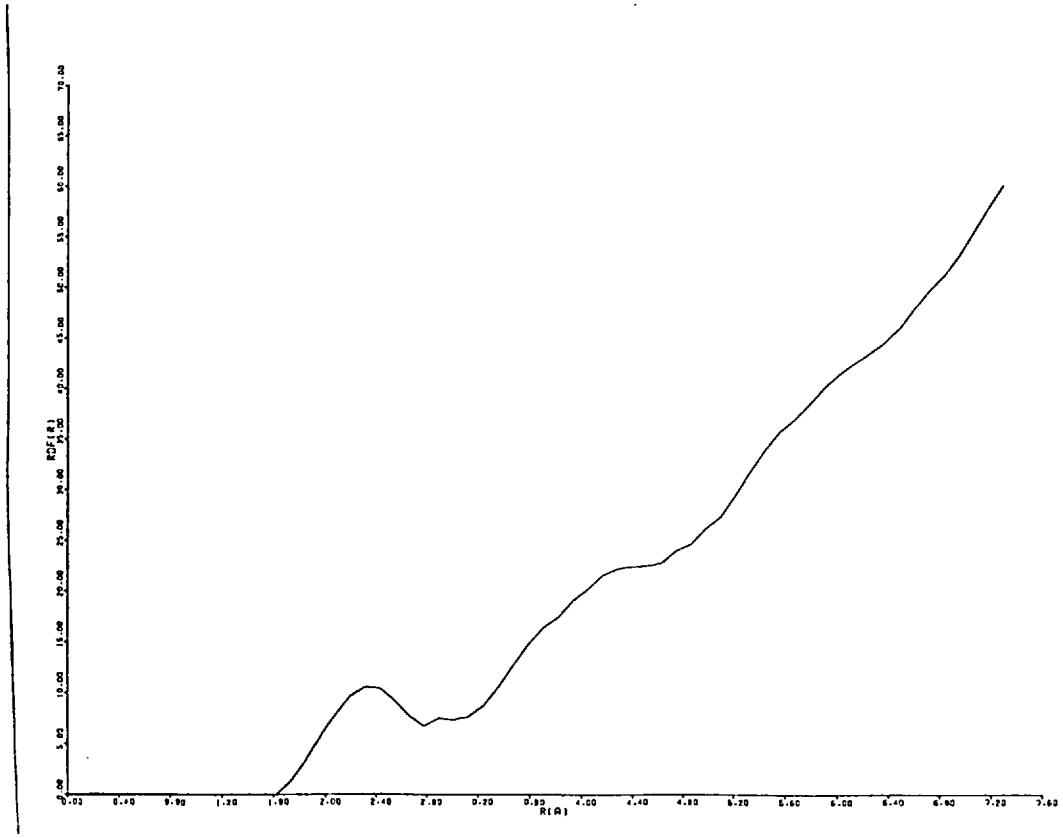

FIGURE (55)

EXTRAPOLATED INTERFERENCE FUNCTION

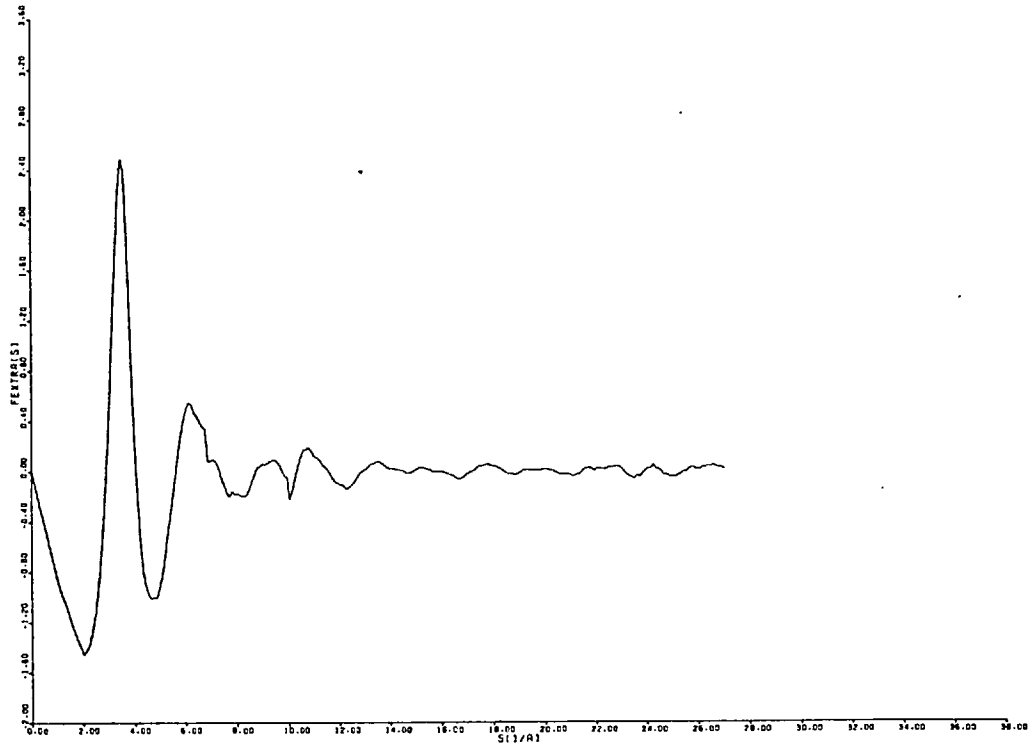

FIGURE (56)

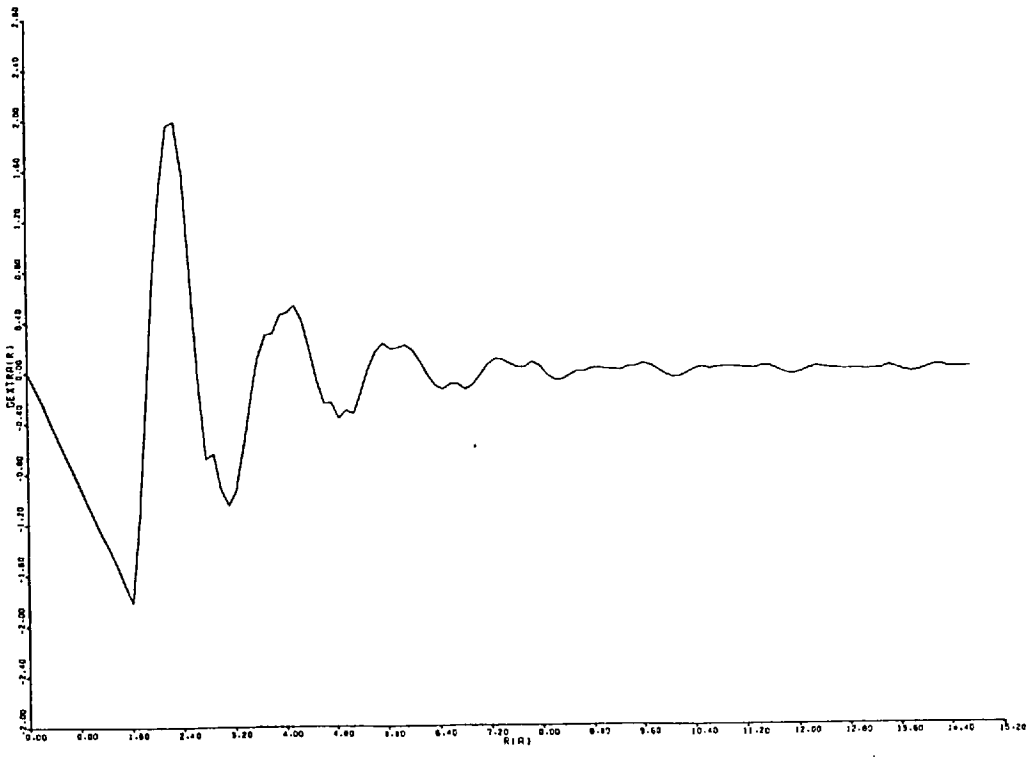

FIGURE (57)

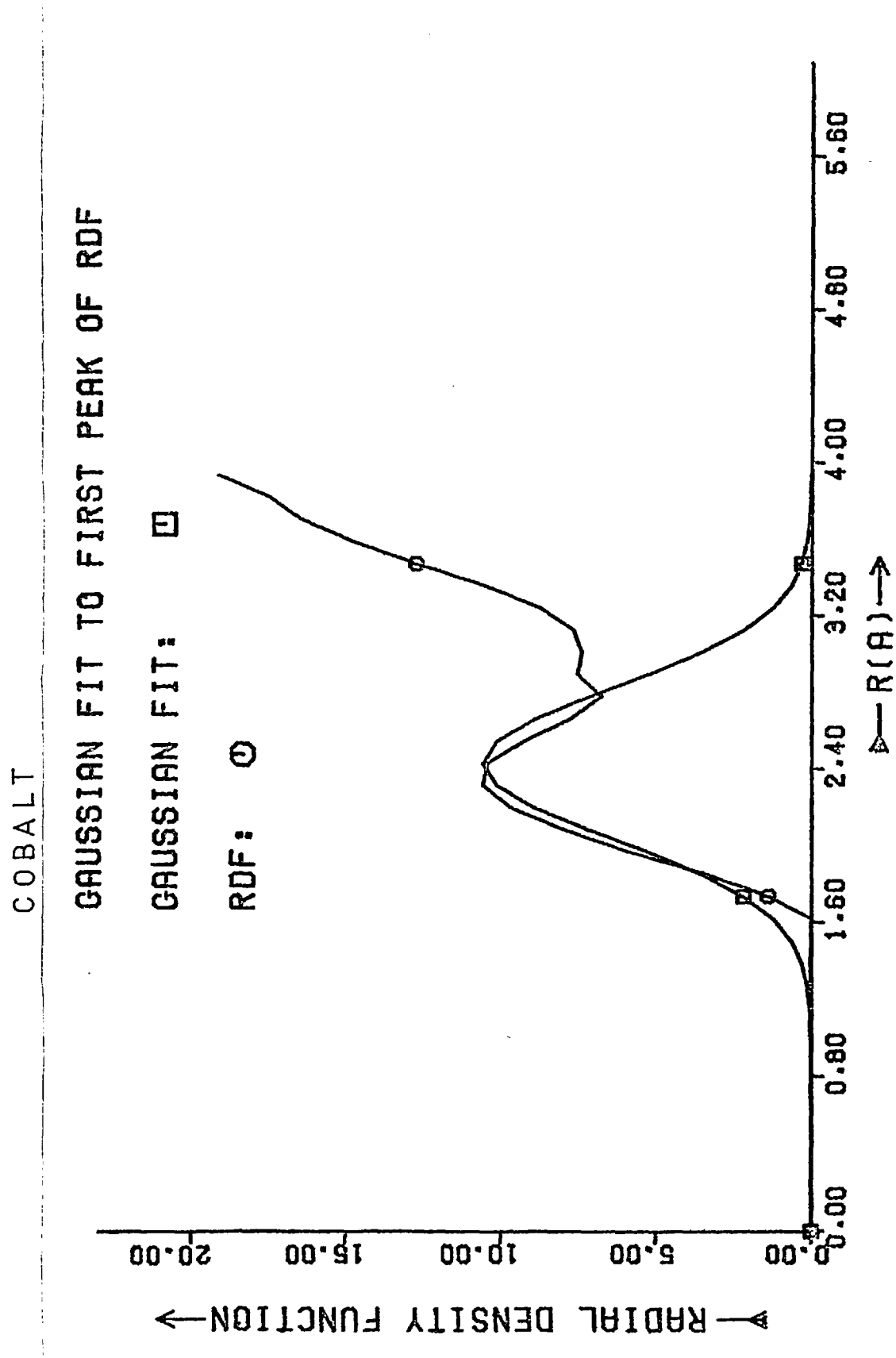
COBALT
GAUSSIAN FIT TO FIRST PEAK OF RDF
GAUSSIAN FIT: □
RDF: ○
RADIAL DENSITY FUNCTION
0.00
5.00
10.00
15.00
20.00
0.00
0.80
1.60
2.40
3.20
4.00
4.80
5.60
R(A)

FIGURE (58)

4.3.4. Chromium

The films of Chromium prepared at 5°K exhibited a diffraction pattern typical of a non-crystalline solid. Increasing the thickness of the films appeared to have no appreciable effect on the observed pattern although no films thicker than about 500A° were produced. During warming of the films polycrystalline rings appeared and were certainly present at a temperature of 150°K. The transition, however, may have occurred at a lower temperature.

An intensity trace taken at approximately 5°K is shown in figure 59, while figure 60 is the polycrystalline pattern observed at 150°K. These traces can be compared with figures 9 and 11 respectively which were obtained from Chromium deposited at 77°K.

The data from figure 59 was analysed and figure 61 shows the calculated interference function.

Figures 62 and 63 are the corresponding R.D.F. and the normalised intensity respectively. The extrapolated interference function and the final R.D.F. are given in figures 65 and 66. The Radial Density Function and the fitted Gaussian function are illustrated in figures 64 and 67. Using these last two functions the average co-ordination number for Chromium is 6.

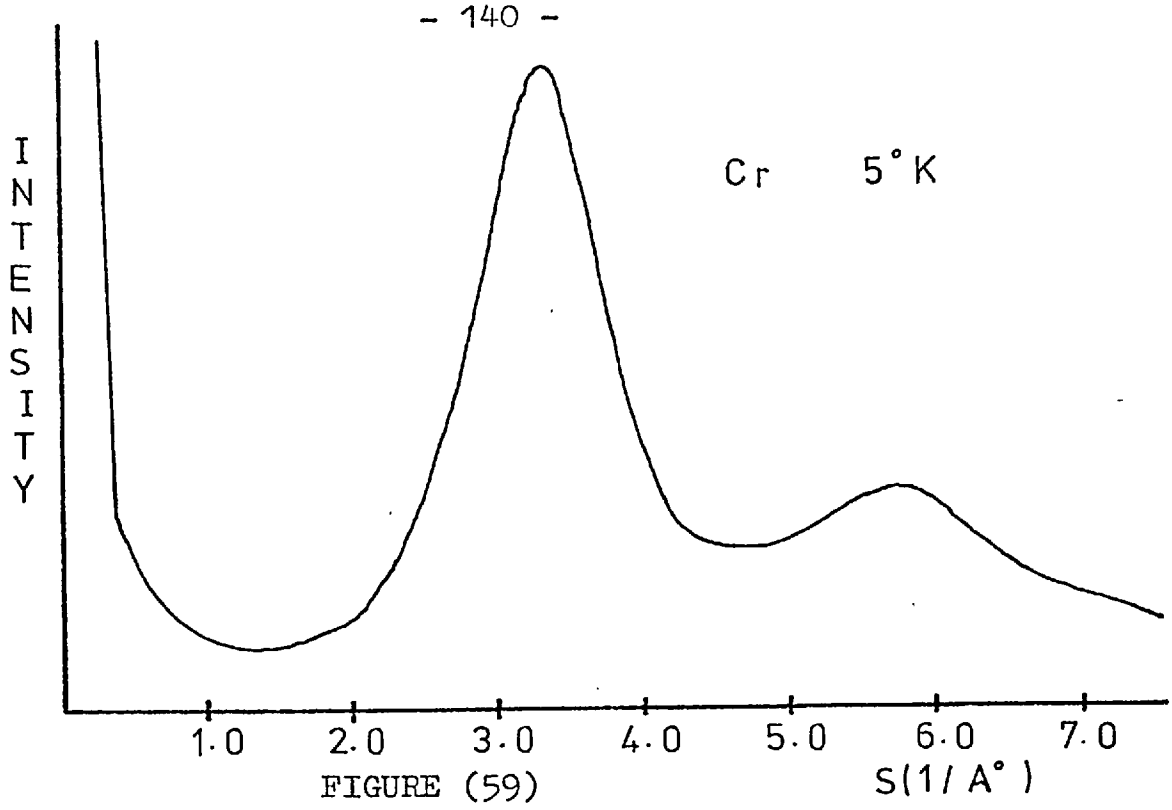

FIGURE (59)

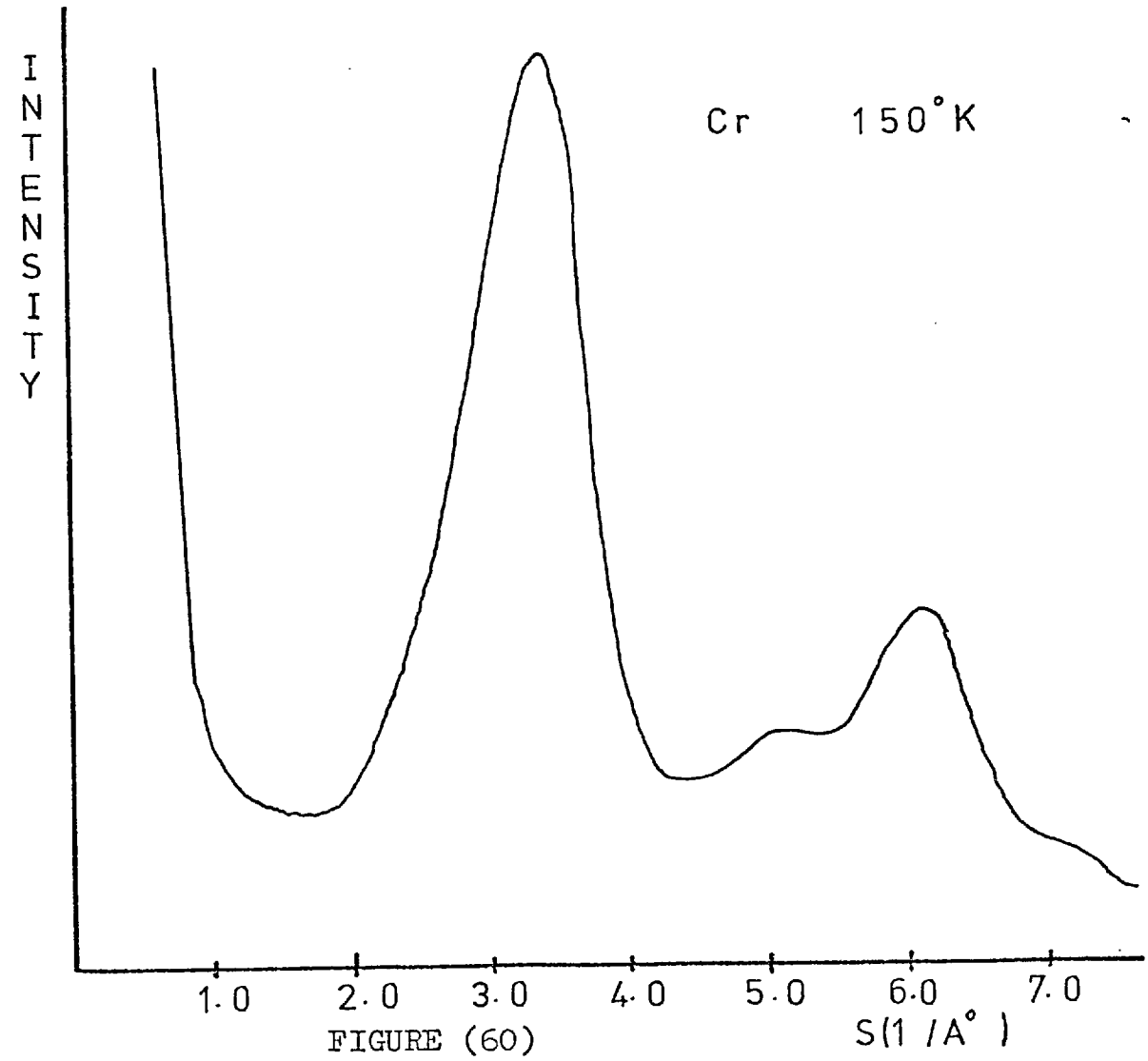

FIGURE (60)

INTERFERENCE FUNCTION

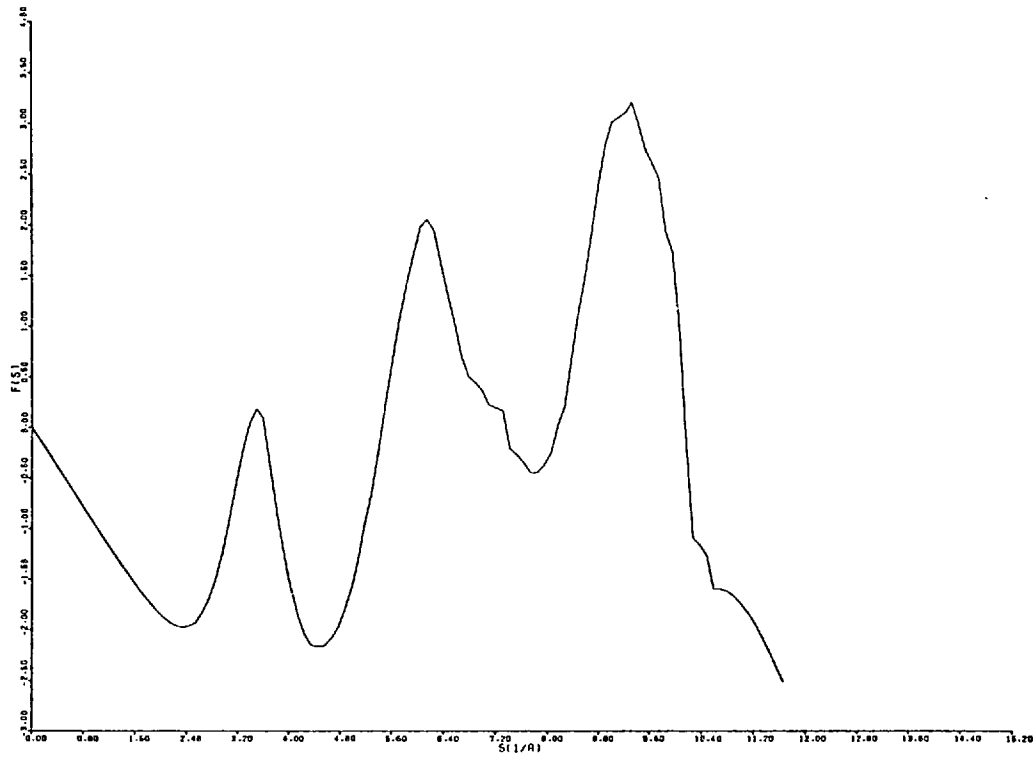

FIGURE (61)

CRUDE RDF

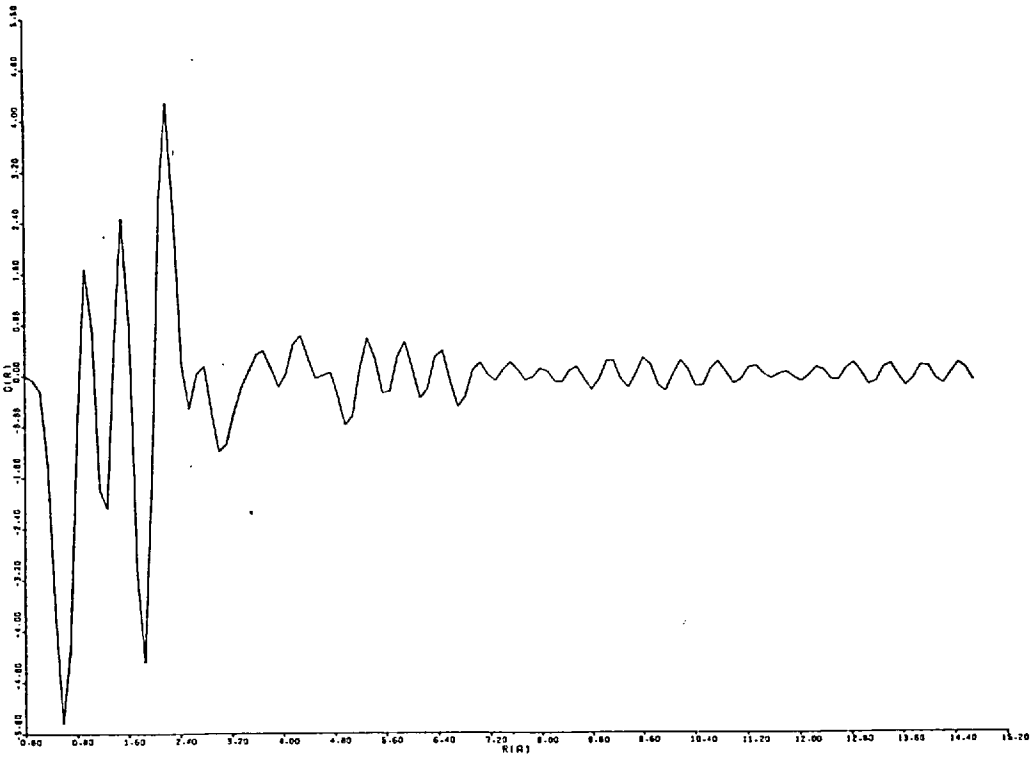

FIGURE (62)

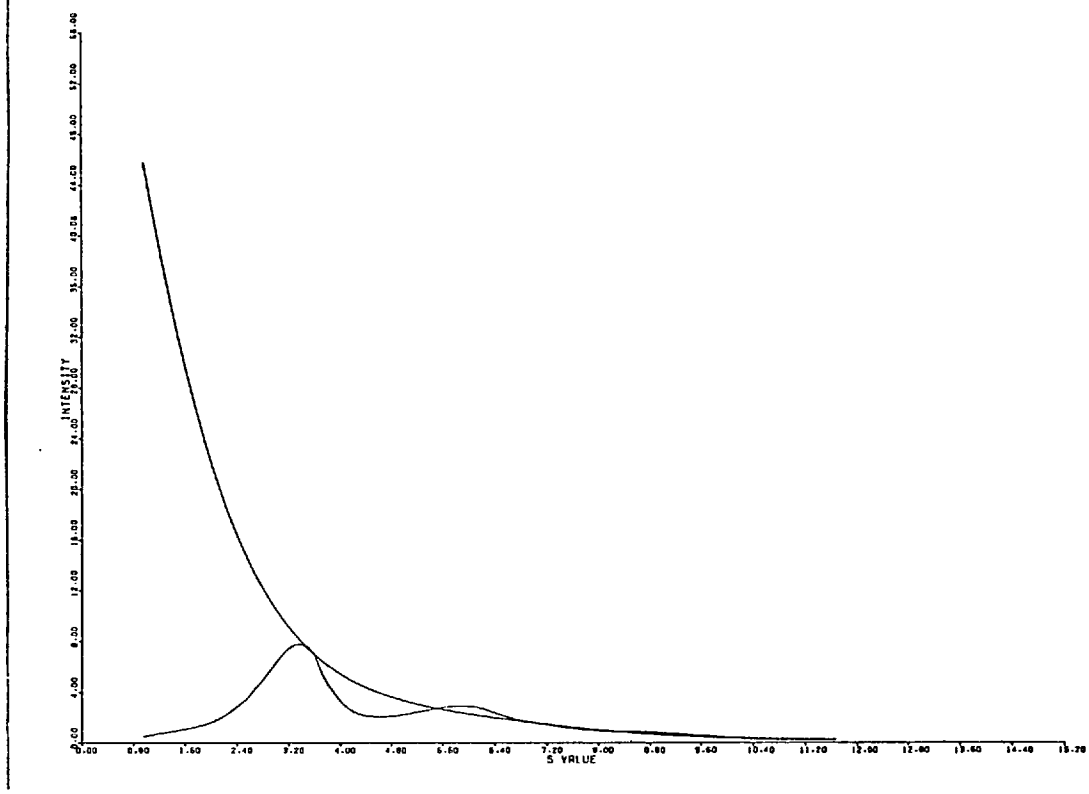

FIGURE (63)

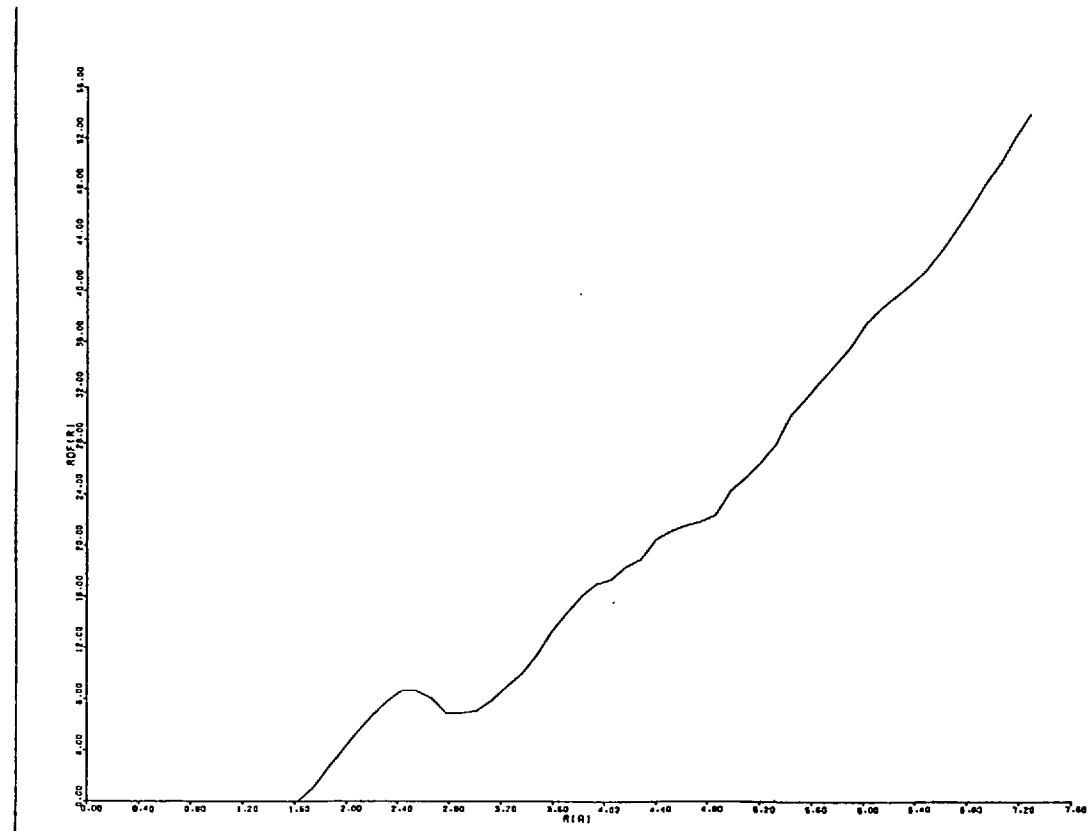

FIGURE (64)

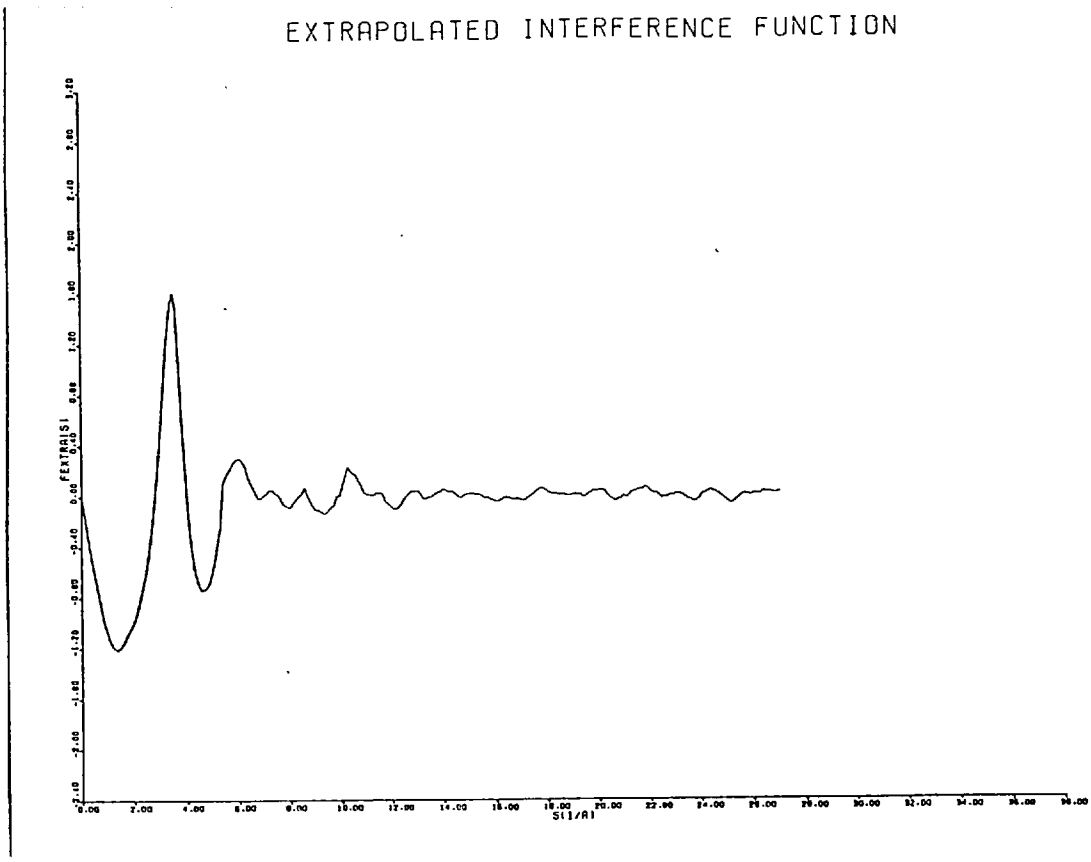

FIGURE 165)

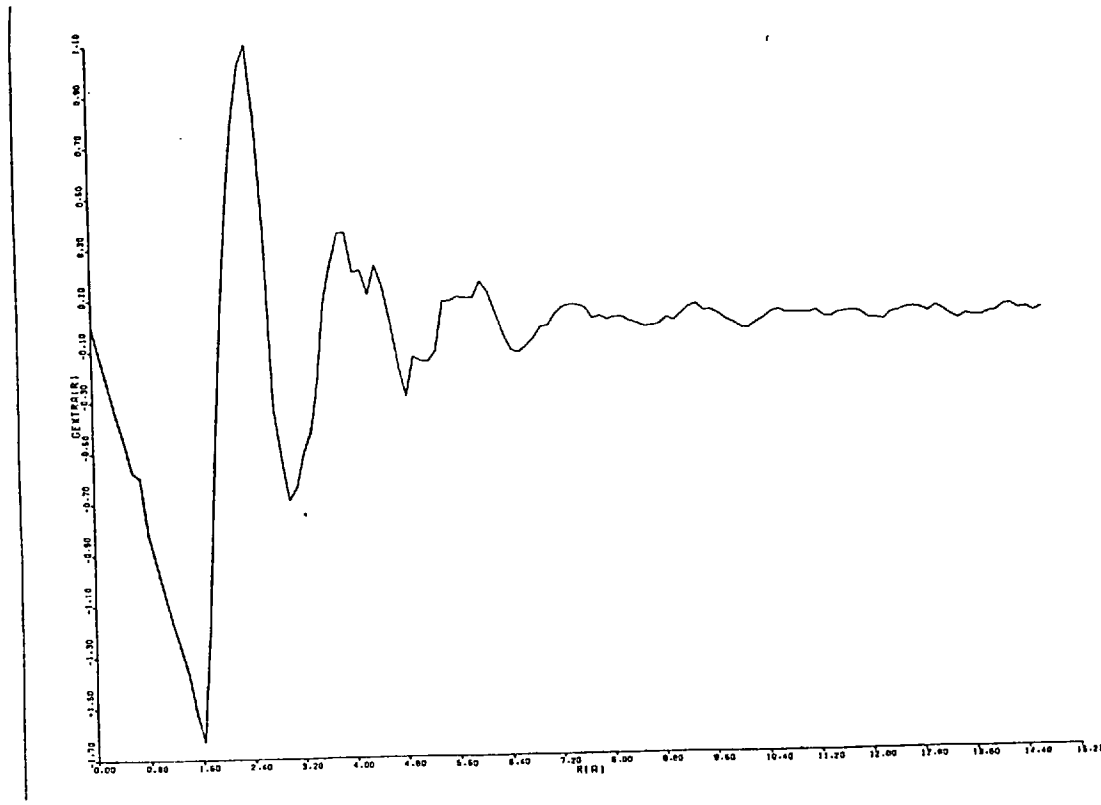

FIGURE 166)

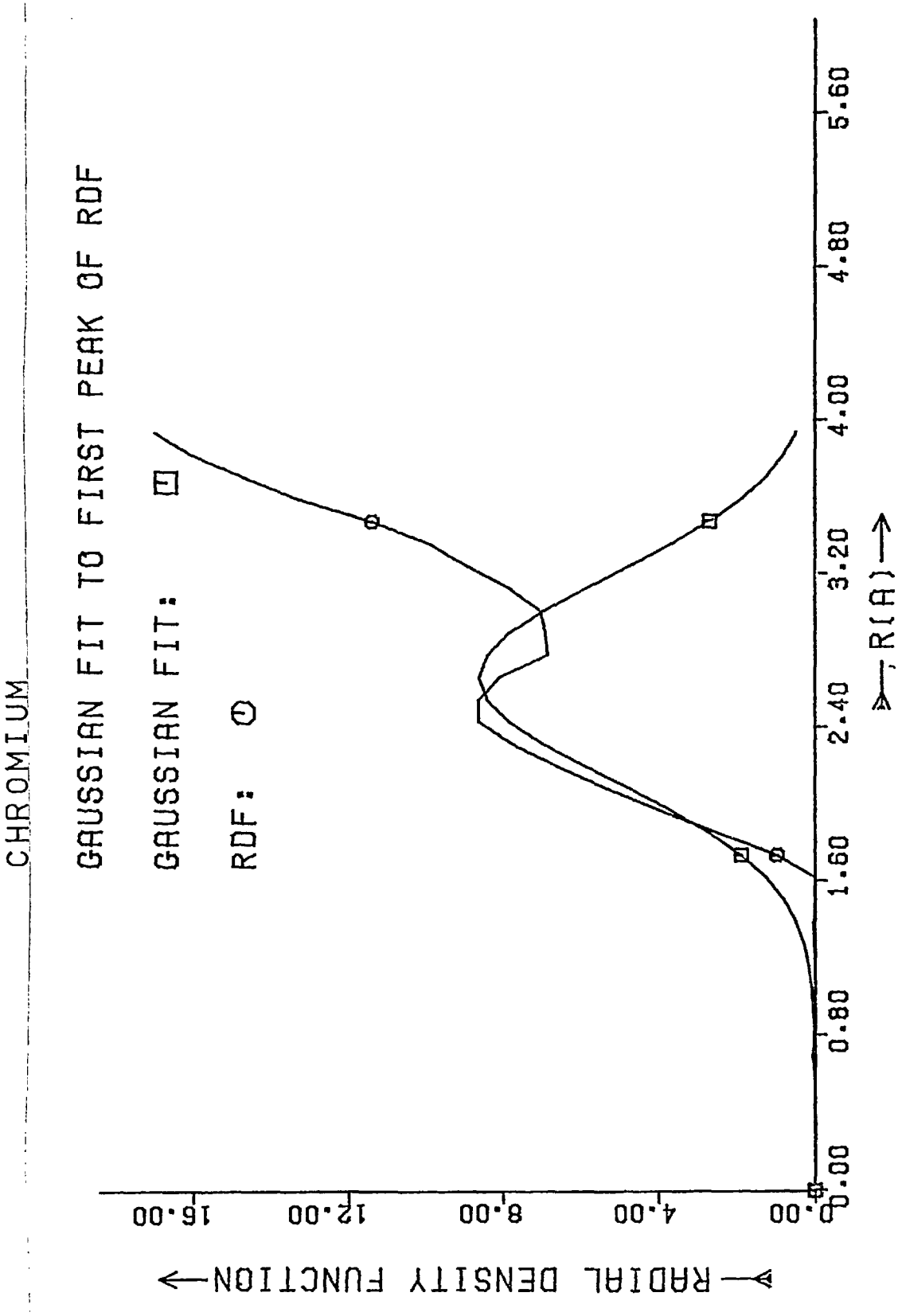
CHROMIUM
GAUSSIAN FIT TO FIRST PEAK OF RDF
GAUSSIAN FIT:
RDF:
RADIAL DENSITY FUNCTION
R(A)
0.00
4.00
8.00
12.00
16.00
0.00
0.80
1.60
2.40
3.20
4.00
4.80
5.60

FIGURE (67)

4.8.5. Iron

Iron films prepared at 5°K appeared to have a non-crystalline structure over a range of thicknesses up to about 500A°. On warming of the films polycrystalline rings were apparent by a temperature of 100°K. The non-crystalline type pattern observed at 5°K is shown in figure 68, while figure 69 gives the polycrystalline pattern seen at 100°K.

The experimental data of figure 68 was analysed and gave the final interference function shown in figure 70. The corresponding R.D.F. is given in figure 71. Figure 72 is the fitted Gaussian to the first peak in the Radial Density Function from which an average value of 8 is obtained for the co-ordination number.

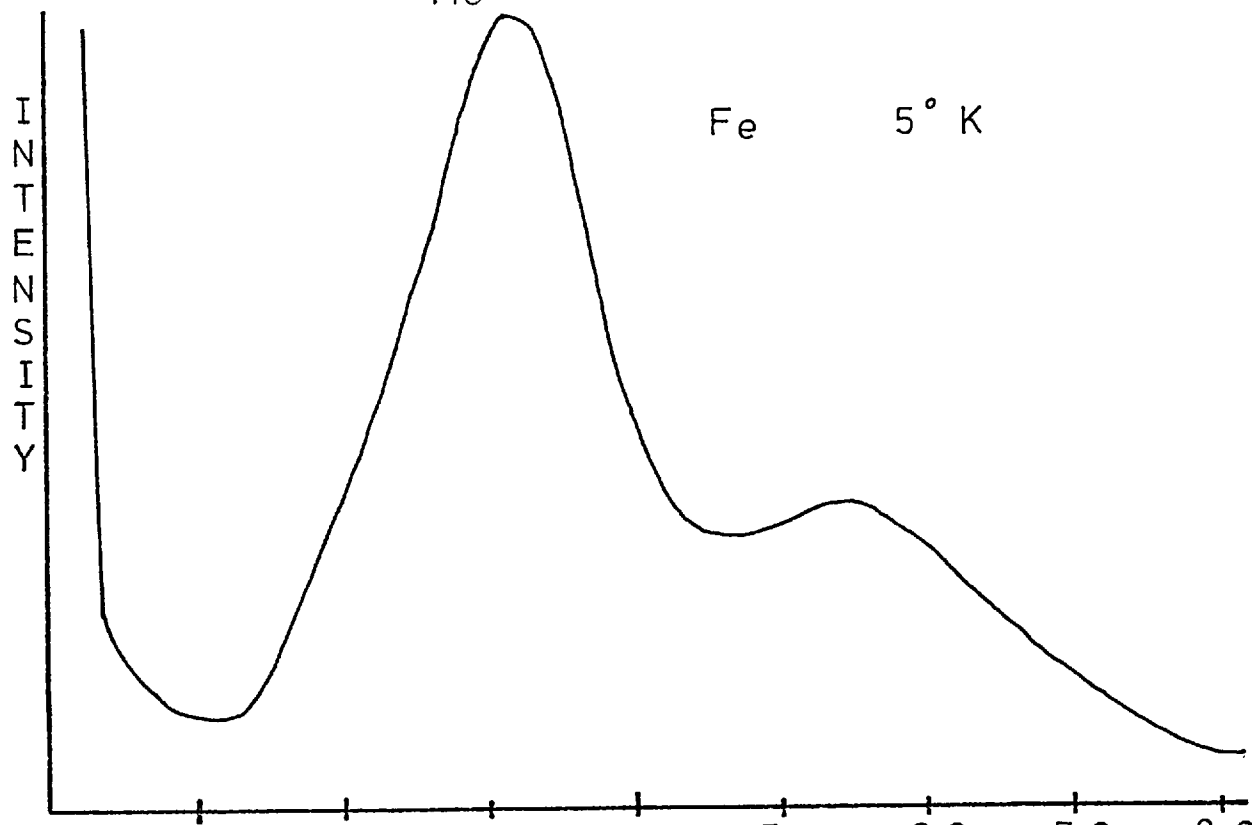

FIGURE (68)

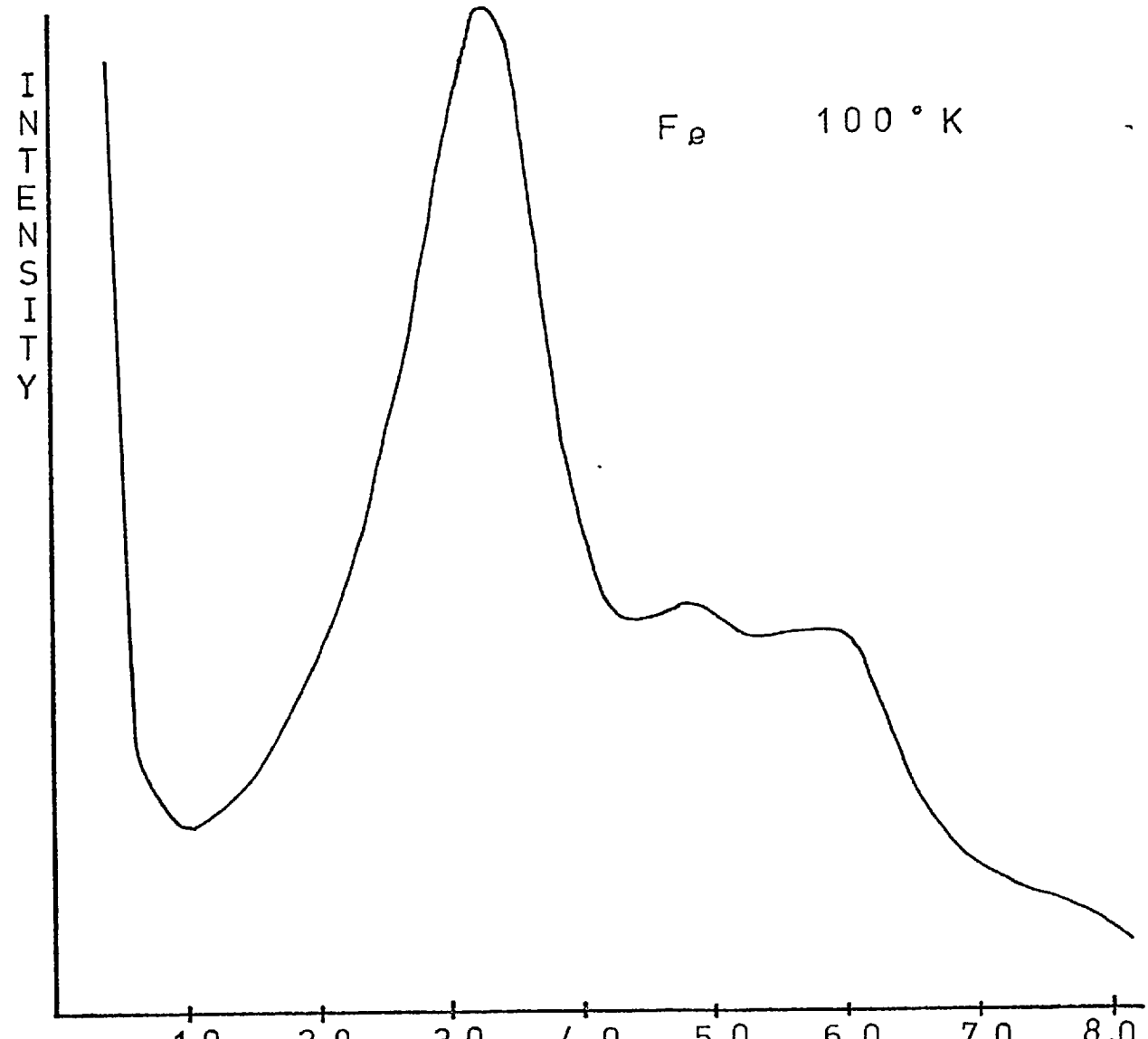

FIGURE (69)

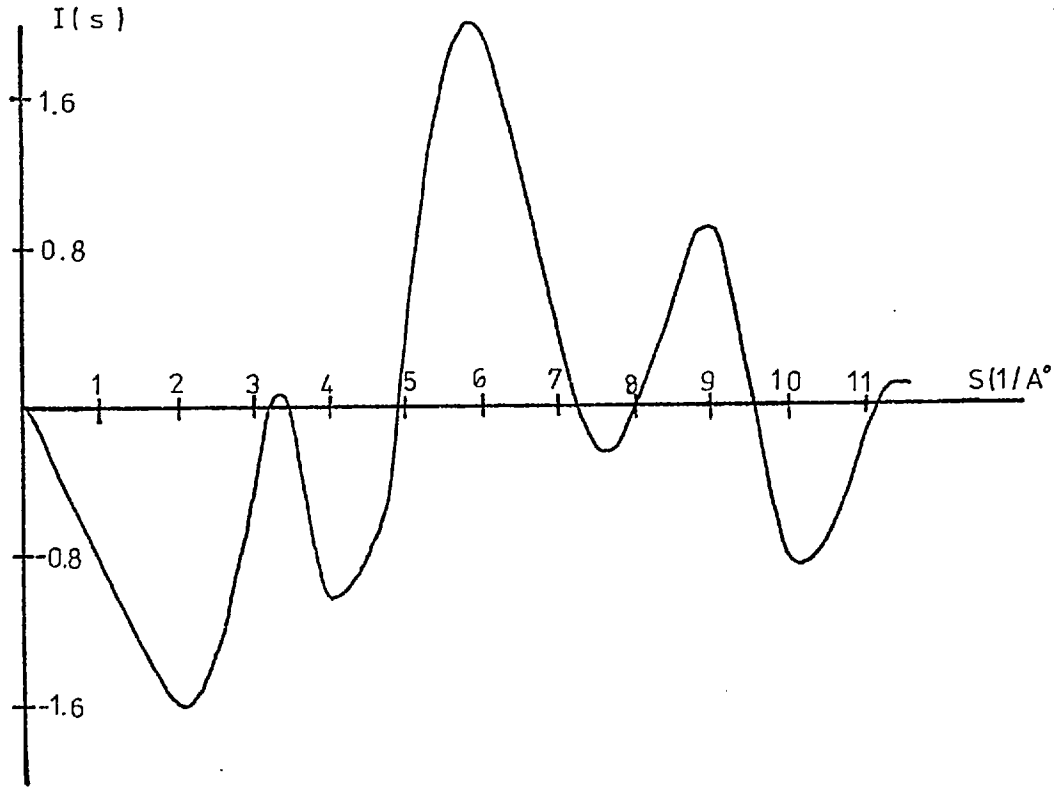

FIGURE (70)

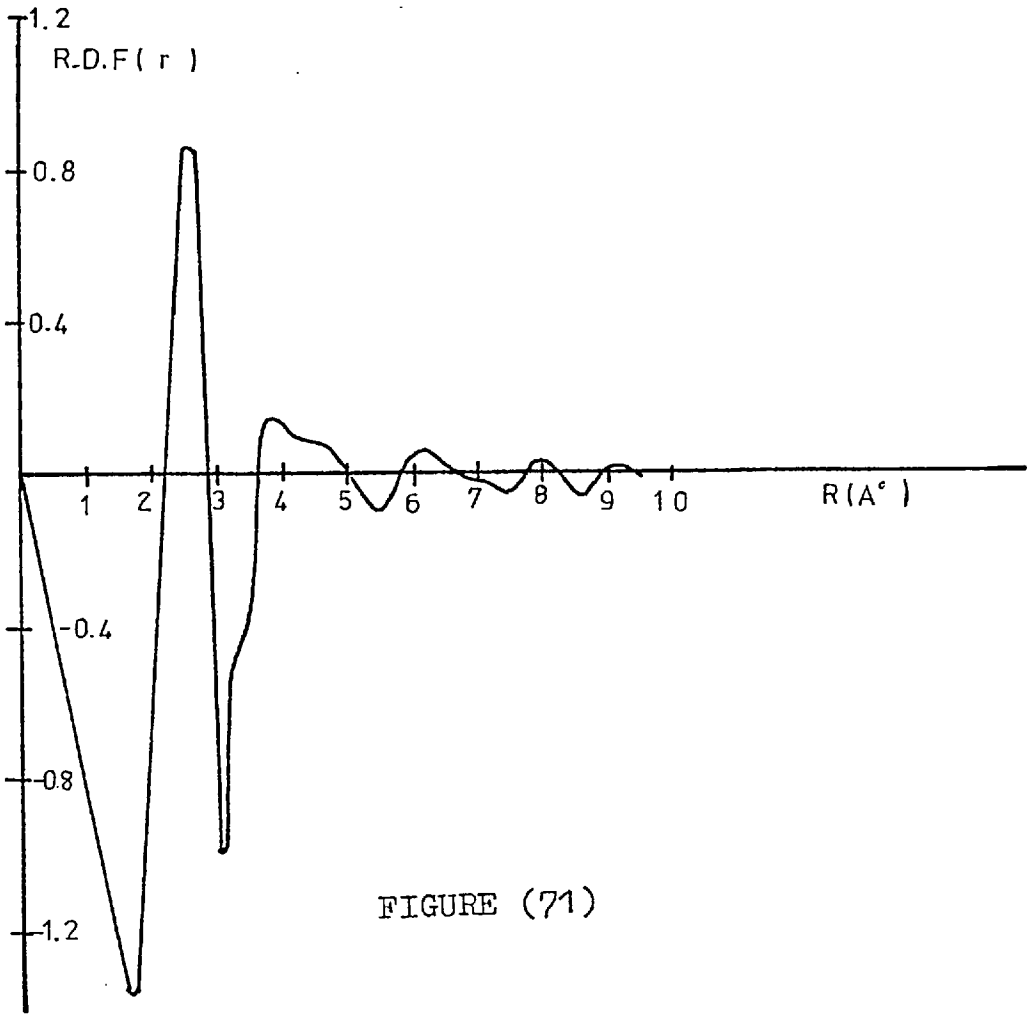

FIGURE (71)

IRON

FIGURE (72)

4.3.6. Tin

Tin films prepared on the liquid Helium cooled substrate produced a non-crystalline type pattern. As previously no films thicker than about 400A° were formed. Polycrystalline rings had appeared when the film had been warmed to 89°K. A non-crystalline and an indexed polycrystalline trace are shown in figures 73 and 74 respectively.

The experimental data when analysed produced the final interference function shown in figure 75. The corresponding R.D.F. is shown in figure 76.In this case because of the high atomic number of Sn the atomic scattering factor used was one calculated using Thomas-Fermi-dirac statistics.The Gaussian fit to the first Radial Density Function peak is given in figure77. The average co-ordination number is 6.

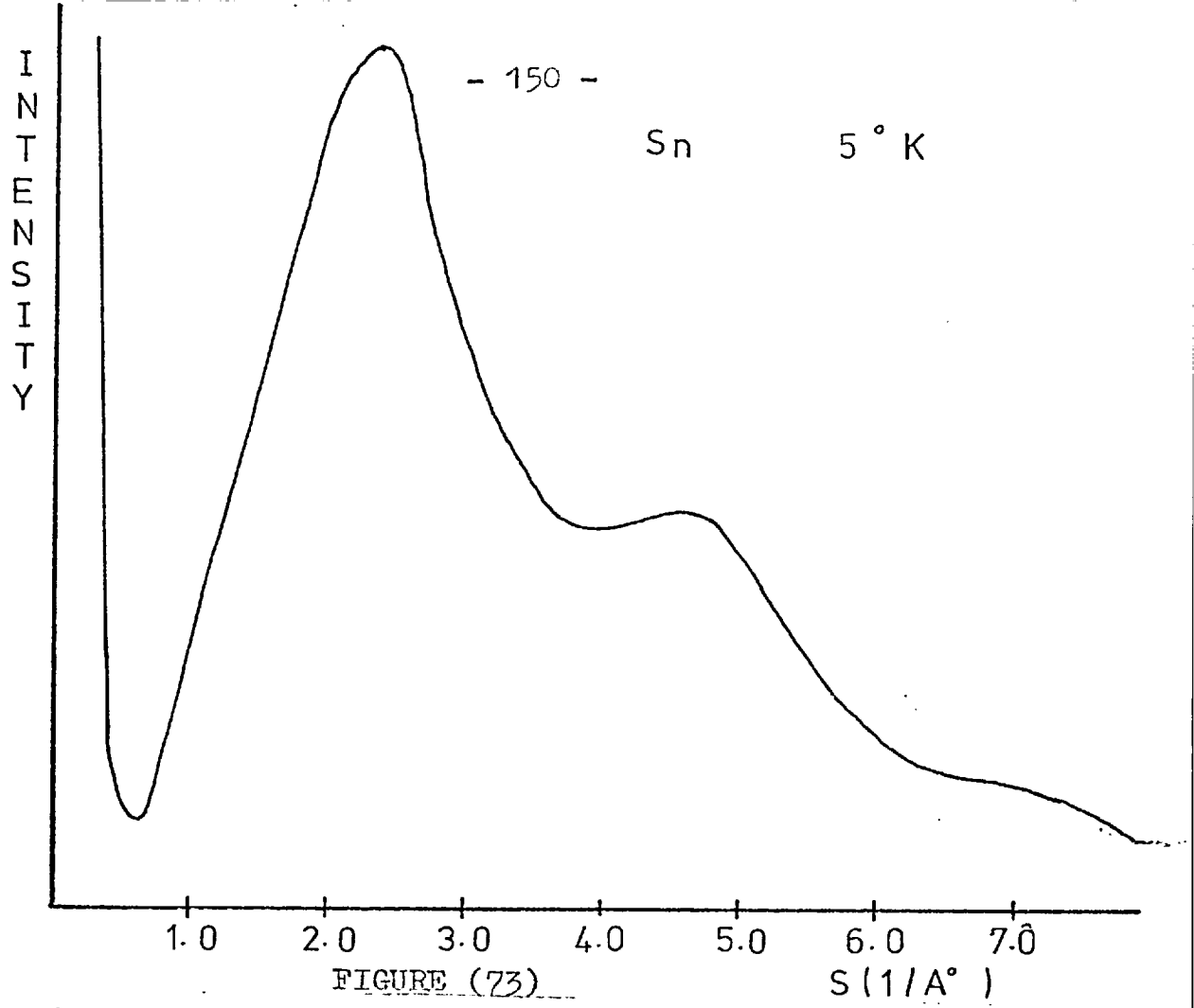

FIGURE (73)

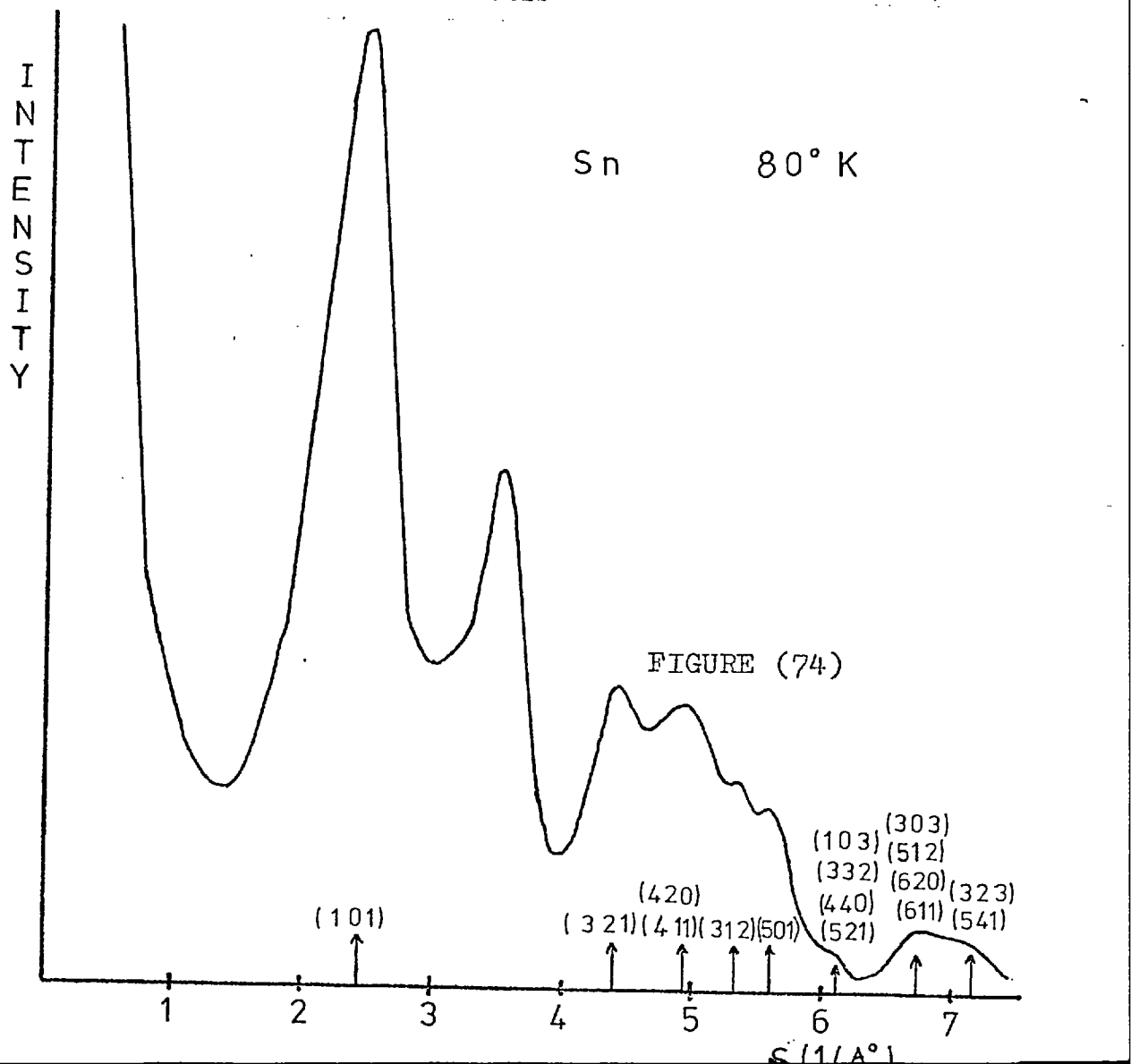

FIGURE (74)

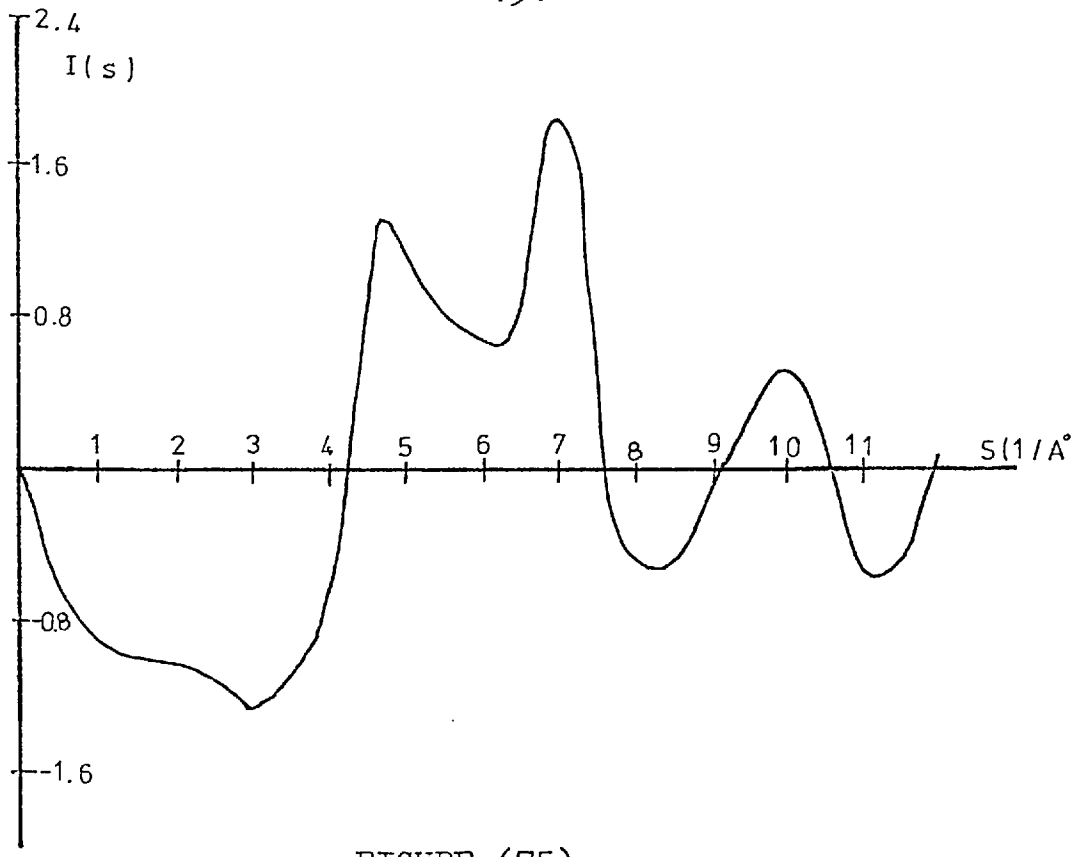

FIGURE (75)

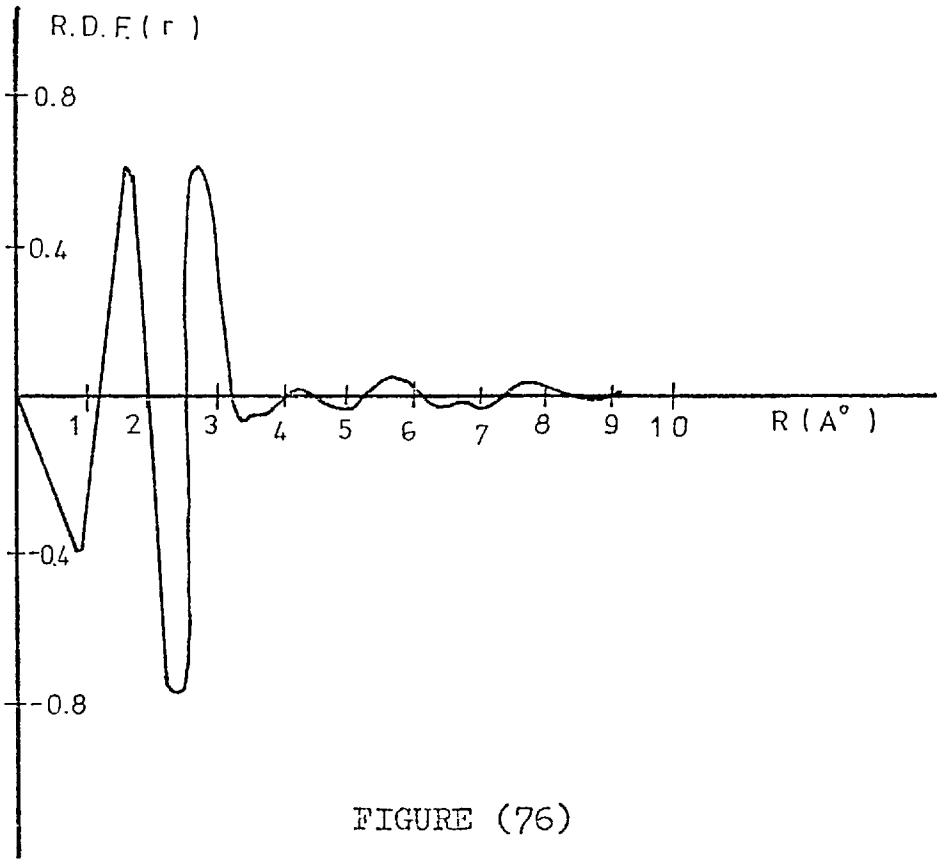

FIGURE (76)

TIN

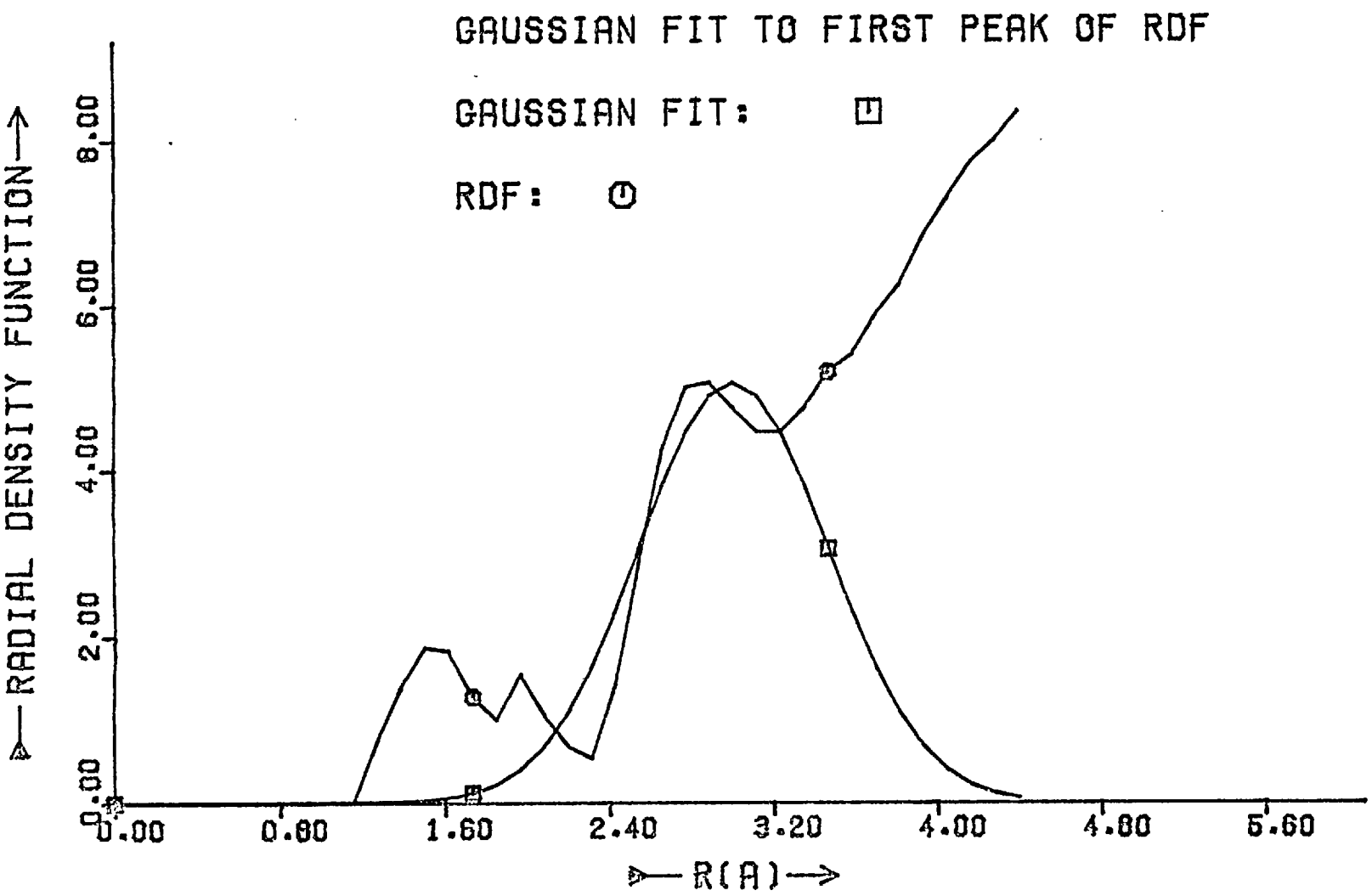

FIGURE (77)

4.3.7. Indium

Indium, of the seven metals studied, was the only element to apparently have a polycrystalline structure on deposition at 5°K. Figure 78 shows a trace of the diffraction produced by the film immediately after deposition. This is quite different to those produced by the other metals but very similar to the pattern at room temperature (see figure 79).

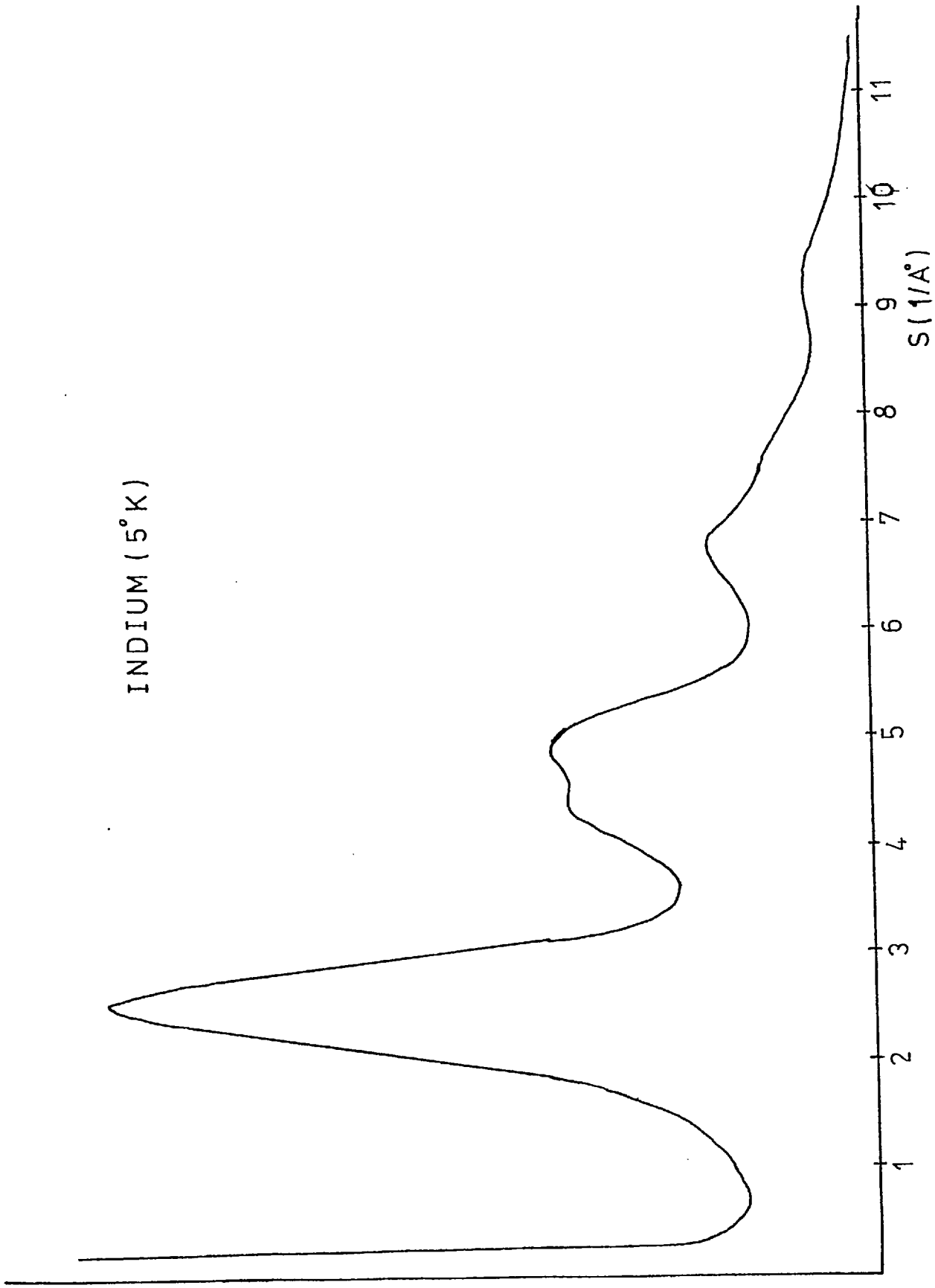

FIGURE (78)

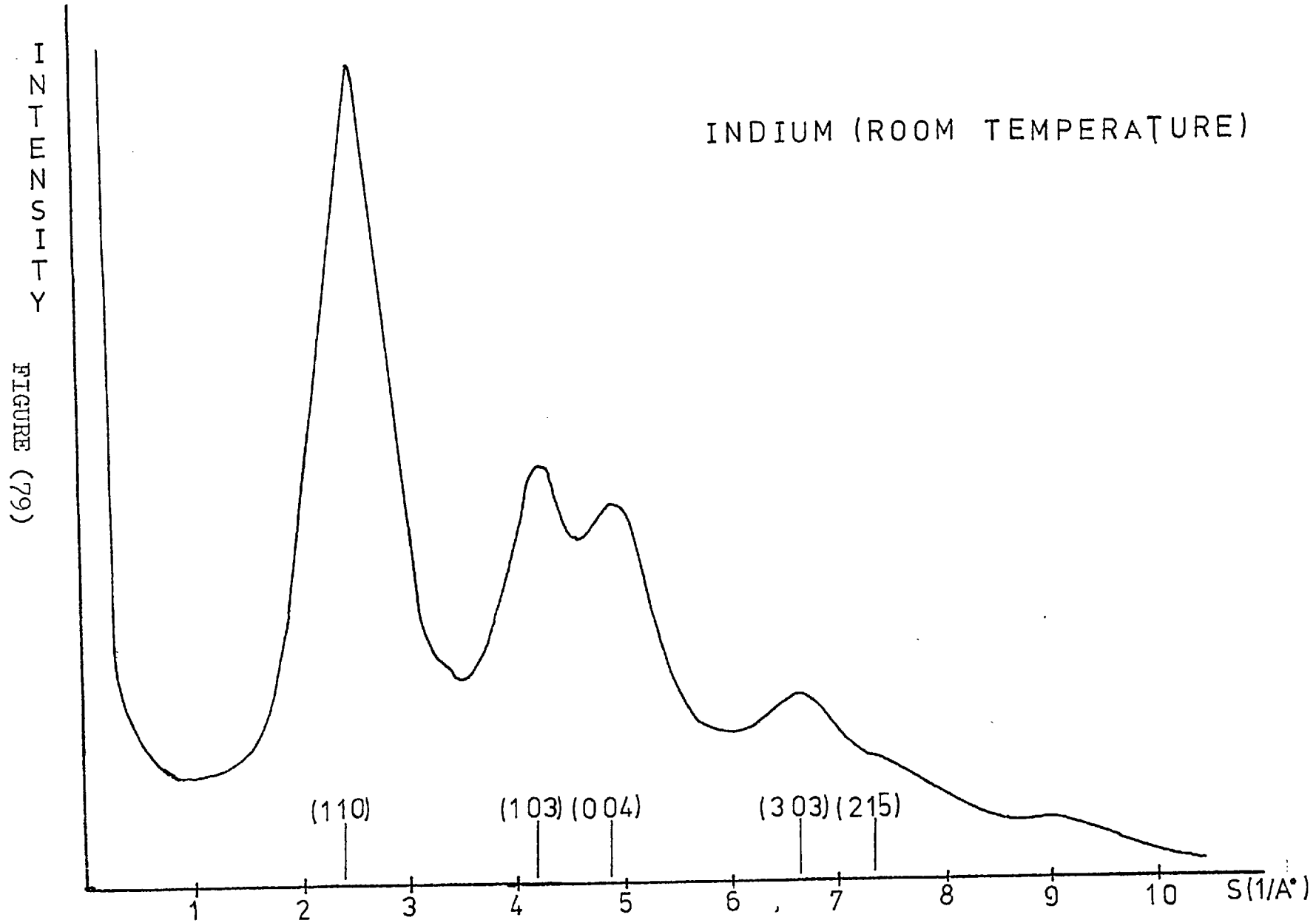
INDIUM (ROOM TEMPERATURE)
INTENSITY
(110)
(103) (004)
(303) (215)
1
2
3
4
5
6
7
8
9
10
S(1/A°)

FIGURE (79)

4.4. Computer Predicted Diffraction Intensities from Randomly Orientated Cubic Crystallites

Diffraction intensities were calculated for Nickel, Cobalt, Chromium and Iron. In addition the spherically integrated structure factors derived from the face-centred and body-centred lattices were calculated. These are shown in figures 80 and 81 respectively.

It was found that for a crystallite with more than two atoms along each edge the calculated intensity distribution was appreciably more detailed than the non-crystalline type patterns observed experimentally. Consequently the size of the crystals were set such that:

$$N_a = 2 \qquad N_b = 2 \qquad N_c = 2$$

or

$$N_a = 1 \qquad N_b = 2 \qquad N_c = 3$$

where N_a, N_b, N_c = number of atoms along the three edges

One example of a calculated intensity function is shown in figure 82. To obtain the total diffracted intensity this should be multiplied by the product of the relevant scattering factor and structure factor. A number of such intensities are shown in figures 83-88.

These can be compared with the experimentally obtained results. It would appear that even such small crystallites produce a diffraction pattern of three or four disinct peaks. These do not agree very well with those patterns considered to represent a non-crystalline structure which in general contain only two or possibly three peaks.

FACE—CENTRED CUBIC LATTICE
STRUCTURE FACTOR
30.00
28.00
26.00
24.00
22.00
20.00
18.00
0.00
2.00
4.00
6.00
8.00
10.00
12.00
14.00
16.00
18.00
S VALUE

FIGURE (80)

BODY—CENTRED CUBIC LATTICE
STRUCTURE FACTOR
15.30
15.70
16.10
16.50
16.90
17.30
17.70
0.00
2.00
4.00
6.00
8.00
10.00
12.00
14.00
16.00
18.00
S VALUE

FIGURE (81)

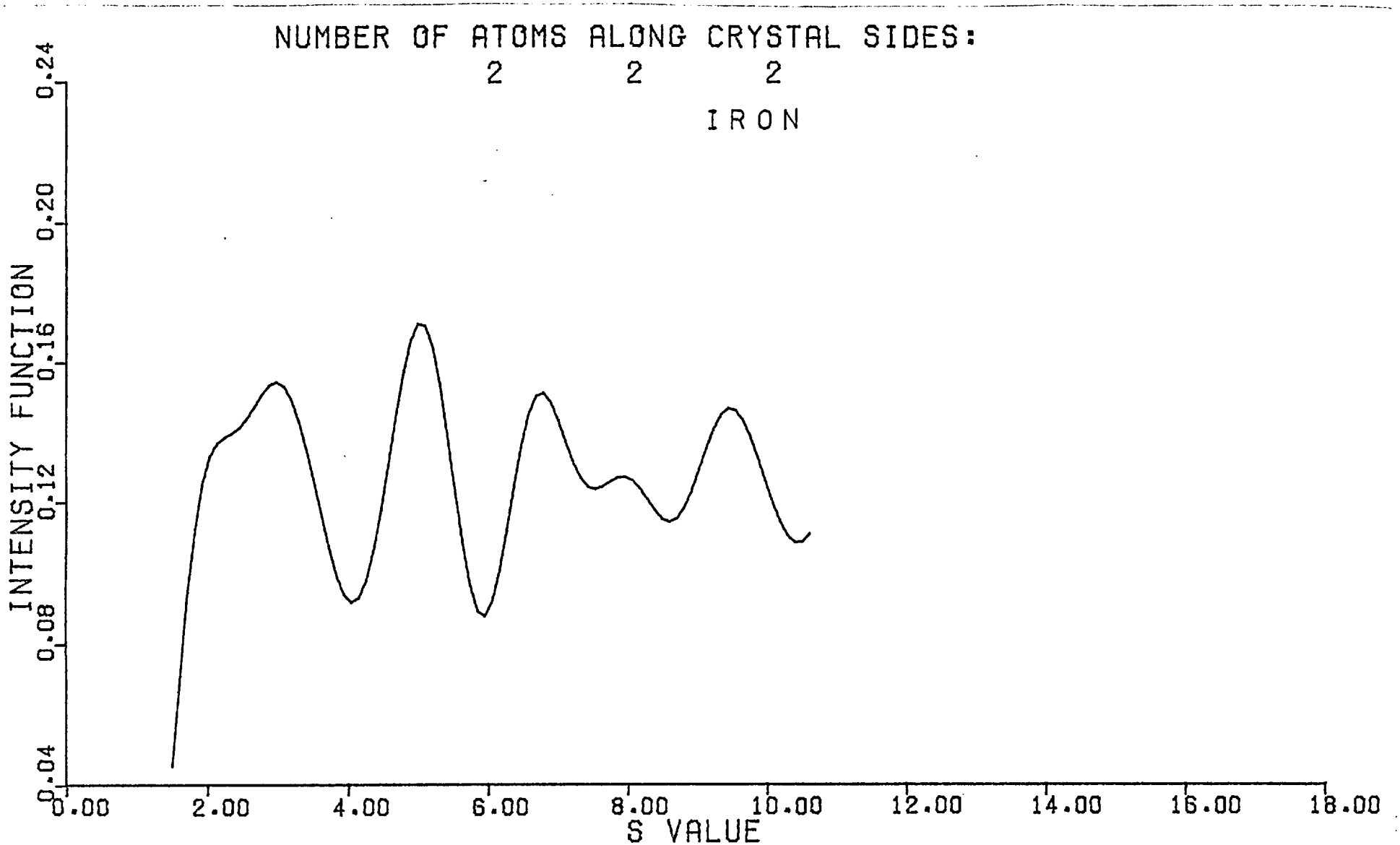
NUMBER OF ATOMS ALONG CRYSTAL SIDES:
2 2 2
IRON
INTENSITY FUNCTION
0.04
0.08
0.12
0.16
0.20
0.24
0.00
2.00
4.00
6.00
8.00
10.00
12.00
14.00
16.00
18.00
S VALUE

FIGURE (82)

Ni
Na=1
Nb=2
Nc=2
TOTAL INTENSITY
0.00
40.00
80.00
120.00
160.00
200.00
0.00
2.00
4.00
6.00
8.00
10.00
12.00
14.00
16.00
18.00
S VALUE

FIGURE (83)

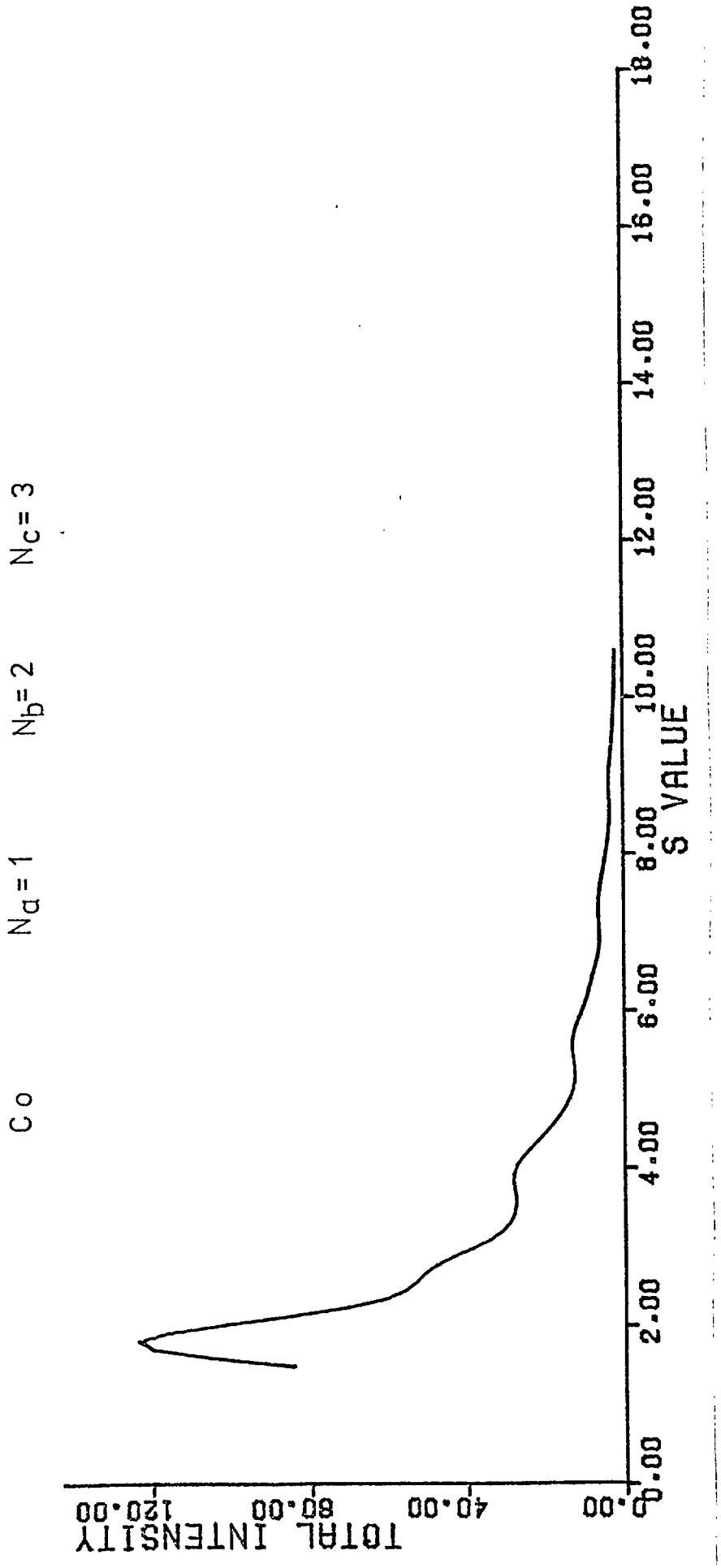
Co
Na= 1
Nb= 2
Nc= 3
TOTAL INTENSITY
0.00
40.00
80.00
120.00
0.00
2.00
4.00
6.00
8.00
10.00
12.00
14.00
16.00
18.00
S VALUE

FIGURE (84)

Cr Na = 1 Nb = 2 Nc = 3
TOTAL INTENSITY
0.00
20.00
40.00
60.00
80.00
100.
0.00
2.00
4.00
6.00
8.00
10.00
12.00
14.00
16.00
18.00
S VALUE

FIGURE (85)

Fe
$N_a = 1$
$N_b = 2$
$N_c = 3$
TOTAL INTENSITY
0.00
20.00
40.00
60.00
80.00
100.00
0.00
2.00
4.00
6.00
8.00
10.00
12.00
14.00
16.00
18.00
S VALUE

FIGURE (86)

Fe
$N_a = 2$
$N_b = 2$
$N_c = 2$
TOTAL INTENSITY
0.00
10.00
20.00
30.00
40.00
50.00
0.00
2.00
4.00
6.00
8.00
10.00
12.00
14.00
16.00
18.00
S VALUE

FIGURE (88)

CHAPTER 5

5.1 Summary and comparison of the results obtained

Of the seven metals investigated Ga,Co,Fe,Sn,Cr and Ni are all concluded to possess a non-crystalline structure when prepared at 4^{0}K.Their co-ordination numbers along with their first and second R.D.F. peak positions are tabulated in table (5.1).Also included are their respective crystalline interatomic distances ta ken from the standard tables.

As was pointed out in Chapter 1 the results obtained from the study of thin films can vary quite widely. The results given here do not in fact agree terribly well with other published data.Almost certainly a major contribution to these differences is provided by the method of calculation as well as the difference in experimental conditions mentioned previously.

Table (5.2) gives data obtained from Fe and Cr prepared at 4^{0}K by Fujime(1966).From his results he also concluded that these metals were exbiting a non-crystalline structure.In table (5.3) data for liquid Sn,Ga and Ni is listed.In comparing this with the results found here two things should be noted.First of all a liquid structure is not necessarily the same as a non-crystalline solid and secondly the work on Sn and Ni was done at 280^{0}C and 1500^{0}C respectively.

TABLE (5.1)

material	co-ordination number	r_1 A	r_2 A	r_{cryst} A
Ga(liquid)	6	2.55	4.70	2.5
Ga(non-cryst.)	6	2.70	4.90	2.5
Co	8	2.30	4.20	2.5
Fe	7-8	2.45	3.80	2.5
Sn	6	1.50	2.90	3.0
Cr	5-6	2.45	4.00	2.5
Ni	7-8	2.40	3.80	2.50

TABLE (5.2)

material	r_1	r_2	co-ordination number
Fe	2.60	4.50	7
Cr	2.64	4.50	

TABLE (5.3)

material	r_1	co-ordination number	temperature C
Sn	3.20	10	280
Ga	2.77	11	20
Ni	2.52	10-11	1500

5.2 Discussion of the reliability of the data

The study of non-crystalline solids is fraught with difficulties and these have been discussed in the preceeding chapters.Probably the most important in the work described here are:

(1) collection of the data
i.e. reading the results from the graphs

(2) the analysis of the experimental data

It is quite clear that errors introduced by (1) and (2) above can seriously affect the resulting R.D.F. However it is also true that certain information can be quite accurately found.In particular the effect of (1) will little effect on the actual diffracted peak positions.Similarly (2) will not effect significantly the peak positions in the R.D.F. Consequently it is possible to regard the calculated nearest neighbour distances as quite reliable.

The errors in (1) and (2) will however effect the shape of the R.D.F. and hence the co-ordination number obtained.In addition there is quite a lot of room for error in evaluating the area under irregular,overlapping peaks.It is therefore quite likely that the co-ordination numbers quoted contain some,possibly large,error.

5.3 Suggestions for future work

Before further work on non-crystalline thin films is undertaken it would be desirable to modify the existing equipment.

Firstly, when preparing films at $4^{O}K$ it would be a great advantage to use a cryopump. Initial designs have been drawn up for this and it is contemplated that it will involve the fabrication of an additional eight inch port on S.H.E.E.D. In view of the already complicated procedure during an experimental run it would seem to be a good idea to make the cryopump such that the resvoir need only be filled once for each run. Preliminary calculations indicate that for a two hour run the resevoir should be approximately two litres in volume and of course surrounded by a liquid Ni cooled baffle.

The second modification necessary is the introduction of some form of data-logging system to collect the experimental data. This would eliminate one major source of error and make the analysis much less tedious. It might even be worthwhile to go one step further and use an on-line mini computer. Alternatively, and certainly much cheaper, it would be possible to input the paper tape produced immediately into an Imperial College Computing Centre terminal. If suitable arrangements

were made this could be virtually on-line.
Once these modifications have been carried out a great deal of useful work on non-crystalline films could be carried out.In particular it would be possible to produce much more accurate and reliable results.
One aspect of the research done which would be interesting to pursue is the relationship between liquid and non-crystalline structures.This would of course involve further equipment modifications in order to be able to melt the films.

APPENDIX A

Computer Programs

The programs used in this thesis were run on the Imperial College CDC 6400 ma chine.The main program RDFGEN was run as a batch job and is in standard Fortran IV. The other smaller programs were designed to run interactively and hence have some non-standard features (mainly in input/output).

```
      PROGRAM RDFGEN(INPUT,OUTPUT,TAPE1,TAPE2,TAPE3,TAPE4,
     1TAPE5,TAPE6=OUTPUT,TAPE13,TAPE14,TAPE17,TAPE62)
C
C     THE MAIN PROGRAM CALLS A SERIES OF ROUTINES IN ORDER TO
C    CALCULATE A R·D·F· EACH ROUTINE IS DOCUMENTED,WHILE THE
C    BASIC IDEAS ARE DESCRIBED IN THE TEXT·
C
C CCCCCCCCCCCCCCCCCCCCCCCCCCCCCCCCCCCCCCCCCCCCCCCCCCCCCCCCCCCCCCC
C
C      INPUT:
C              F=INTERFERENCE FUNCTION
C             ATOM=ATOMIC SCATTERING FACTOR
C          EXNORM=NORMALISED INTENSITY
C          RHO=AVERAGE ATOMIC DENSITY
C          RMIN=R VALUE OF FIRST MINIMUM IN THE R·D·F·
C           BETA=DAMPING CONSTANT(PUT=Ø·Ø IF NONE REQUIRED)
C          IFILM(SEE ROUTINE RAHMAN)
C
C     OUTPUT:
C           ROF=RADIAL DENSITY FUNCTION
C           G=INITIAL CALCULATED R·D·F·
C          FNORM=INTERFERENCE WITH IMPROVED NORMALISATION
C          GNORM=R·D·F· CORRESPONDING TO FNORM
C           GEXTRA=EXTRAPOLATED R·D·F·
C          FEXTRA=INTERFERENCE FUNCTION CORRESPONDING TO
C                       GEXTRA
C          GMOD=R·D·F· MODIFIED BY TERMINATION ERROR
C           FMOD=INTERFERENCE FUNCTION CORRESPONDING TO GMOD
C          GDAMP=CALCULATED R·D·F· USING A DAMPING FACTOR
        PROGRAM ROFGEN(INPUT,OUTPUT,TAPE1,TAPE2,TAPE3,TAPE4,TAPE5,
     +          TAPE6=OUTPUT,TAPE13,TAPE14,TAPE17,TAPE62)
C
C CCCCCCCCCCCCCCCCCCCCCCCCCCCCCCCCCCCCCCCCCCCCCCCCCCCCCCCCCCCCCCC
C
      COMMON PI,DELR,DELS
      DIMENSION F(512),G(512),FNORM(512),GNORM(512)
       DIMENSION SINES(512),FEXTRA(512),GEXTRA(512)
       DIMENSION ITITLE(1Ø),COOROT(1Ø,2),COORDN(1Ø,2),INUMB(1Ø)
      DIMENSION GDAMP(512),FMOD(512),GMOD(512)
       DIMENSION EXNORM(2ØØ),ATOM(2ØØ),S(2ØØ),ROF(512)
      DATA PIE/172162Ø773252Ø42Ø551Ø/
      EQUIVALENCE(GDAMP,GEXTRA,GMOD),(F,FEXTRA,FMOD)
       N=512
      INCS=3Ø
C  N IS THE NUMBER OF POINTS TO BE USED FOR THE
C   F·F·T· ROUTINE
C
C    INCS IS DEFINED IN THE ROUTINE EXTRAP WHERE IT IS USED
C
C    SET THE MICROFILM COUNTER
C
       NFRAME=4
      NPLO=N/4
      CALL START(2)
      CALL FRAME1
      CALL FRAME2
      PI=PIE
      N2=N/2
      READ(1,1Ø)NUMS,DELS,(F(I),I=1,NUMS)
       READ(2,1Ø)NUMS,DELS,(ATOM(J),J=1,NUMS)
       READ(5,372)IFILM,RHO,RMIN,BETA
      READ(13,11)NUMS,NMIN,DELS,(EXNORM(J),J=NMIN,NUMS)
```

```
372   FORMAT(I3,3F7.4)
11    FORMAT(2I4,F10.4/(6(2X,F8.4)))
10    FORMAT(I4,F10.4/(6(2X,F8.4)))
      DELR=2.*PI/(FLOAT(N)*DELS)
      WRITE(6,400)
400   FORMAT(1H1,21HINTERFERENCE FUNCTION)
       WRITE(6,71)
71    FORMAT(37H    NUMBER OF POINTS    INCREMENT     )
      WRITE(6,18)NUMS,DELS
18    FORMAT(10X,I4,7X,F10.4)
      WRITE(6,20)(F(I),I=1,NUMS)
20    FORMAT(8(2X,F9.4))
C
C   CALL THE PLOTTING ROUTINE FILM TO PLOT THE INTERFERENCE
C                  FUNCTION
C
      CALL FILM(DELS,NUMS,F,2,4,1,ITITLE,COORDT,0,INUMB,COORDN,
     +          NFRAME)
C
C       CALL THE F.F.T. ROUTINE TO TRANSFORM THE INTERFERENCE
C                  FUNCTION
C
      CALL FASTFT(F,G,SINES,N,1,1,NUMS)
       WRITE(6,401)
401   FORMAT(1H1,12HCRUDE R.D.F.)
      WRITE(6,71)
      WRITE(6,18)N2,DELR
      WRITE(6,20)(G(I),I=1,N2)
C
C     CALL FILM TO PLOT THE R.D.F.
C
      CALL FILM(DELR,NPLO,G,1,14,1,ITITLE,COORDT,0,INUMB,
     +          COORDN,NFRAME)
C
C   CALL THE ROUTINE WHICH CALCULATES RADIAL DISTRIBUTION
C     FUNCTIONS USING SUPPLIED DAMPING FACTORS
 C
      CALL DAMP(F,N,N2,NUMS,SINES,GDAMP,NFRAME)
 C
C    IF REQUIRED THE ORIGINAL INTERFERENCE FUNCTION CAN BE DAMPED
C
      IF(BETA.EQ.0.0) GO TO 999
      DO 998 J=1,NUMS
998   F(J)=F(J)*EXP(-BETA*(FLOAT(J-1)*DELS)**2)
       WRITE(6,408)
408   FORMAT(1H1,28HDAMPED INTERFERENCE FUNCTION)
       WRITE(6,71)
      WRITE(6,18)NUMS,DELS
      WRITE(6,20)(F(J),J=1,NUMS)
C
C   CALL FILM TO PLOT THE DAMPED INTERFERENCE FUNCTION
C
      CALL FILM(DELS,NUMS,F,2,5,1,ITITLE,COORDT,0,INUMB,CODRDN
     +          ,NFRAME)
C
C   CALL THE F.F.T. ROUTINE TO CALCULATE A R.D.F. USING
 C  THE DAMPED DATA
C
      CALL FASTFT(F,G,SINES,N,0,1,NUMS)
       WRITE(6,409)
```

```
409   FORMAT(1H1,13HDAMPED R·D·F·)
      WRITE(6,996)BETA
996   FORMAT(20H DAMPING CONSTANT = ,F7·4)
      WRITE(6,71)
      WRITE(6,18)N2,DELR
      WRITE(6,20)(G(I),I=1,N2)
C
C   CALL FILM TO PLOT THE CALCULATED R·D·F·
C
      CALL FILM(DELR,NPLO,G,1,15,1,ITITLE,COORDT,0,INUMB,COORDN
     +          ,NFRAME)
999   KCHECK=0
C
C    ARRANGE THE NORMALISED INTENSITY AND THE SCATTERING
C  FACTOR INTO A SUITABLE FORM FOR PLOTTING TOGETHER
C
      DO 471 J=NMIN,NUMS
      K=J-NMIN+1
      S(K)=FLOAT(J-1)*DELS
471   ATOM(K)=ATOM(J)
      KI=NUMS+1-NMIN
      KL=KI+1
      KJ=KI+2
      CALL SCALE(ATOM,14·0,KI,1)
      CALL SCALE(S,19·0,KI,1)
      DELTAV=0·0
      IF(ATOM(KJ)·GT·DELTAV)DELTAV=ATOM(KJ)
      DO 472 J=NMIN,NUMS
      K=J-NMIN+1
472   EXNORM(K)=EXNORM(J)
672   CALL SCALE(EXNORM,14·0,KI,1)
      IF(EXNORM(KJ)·GT·DELTAV)DELTAV=EXNORM(KJ)
      ATOM(KL)=0·0
      ATOM(KJ)=DELTAV
      EXNORM(KL)=0·0
      EXNORM(KJ)=DELTAV
C
C   CALL THE KINGMATIC PLOTTING ROUTINES
C
      CALL AXIS(0·0,0·0,9HINTENSITY,+9,14·0,90·0,0·0,DELTAV)
      CALL AXIS(0·0,0·0,7HS VALUE,-7,19·0,0·0,S(KI+1),S(KI+2))
      CALL LINE(S,ATOM,KI,1,0,INTEQ)
      CALL LINE(S,EXNORM,KI,1,0,INTEQ)
      CALL NEWPAGE
      KCHECK=KCHECK+1
      IF(KCHECK·EQ·2)GO TO 675
C
C   CALL THE ROUTINE WHICH IMPROVES THE NORMALISATION OF THE
C  DATA· THE NEWLY NORMALISED INTENSITY TOGETHER WITH THE
C  SCATTERING FACTOR ARE THEN PLOTTED·
C
      CALL ERNORM(F,G,NUMS,N,SINES,FNORM,GNORM,
     +          EXNORM,ATOM,RHO,RMIN,N2,NMIN)
      GO TO 672
675   NFRAME=NFRAME+2
      WRITE(6,46)
46    FORMAT(1H1,41H      CORRECT          R VALUE OF THE FIRST)
      WRITE(6,47)
47    FORMAT(39H MATERIAL DENSITY    MINIMUM IN THE RDF)
      WRITE(6,48)RHO,RMIN
```

```
48     FORMAT(4X,F10.4,12X,F10.4)
       WRITE(6,402)
402    FORMAT(1H1,
      +     45HINTERFERENCE FUNCTION(IMPROVED NORMALISATION))
       WRITE(6,71)
       WRITE(6,18)NUMS,DELS
       WRITE(6,20)(FNORM(I),I=1,NUMS)
       WRITE(6,403)
403    FORMAT(1H1,35HR.D.F. AFTER IMPROVED NORMALISATION)
       WRITE(6,71)
       WRITE(6,18)N2,DELR
       WRITE(6,20)(GNORM(I),I=1,N2)
C
C    CALL FILM TO PLOT THE IMPROVED INTERFERENCE FUNCTION
C
       CALL FILM(DELS,NUMS,FNORM,2,6,1,ITITLE,COORDT,
      +          0,INUMB,COORDN,NFRAME)
 C
C    CALL FILM TO PLOT THE CORRESPONDING R.D.F.
 C
       CALL FILM(DELR,NPLO,GNORM,1,16,1,ITITLE,COORDT,0<INUMB,COORDN
      +          ,NFRAME)
C
C    CALL THE ROUTINE CONTAINING A NORMALISATION RELIABILITY
C    CRITERION TO ANALYSE THE DATA BEFORE AND AFTER CALLING
C            ERNORM
C
       CALL RAHMAN(F,NUMS,RHO,N2,IFILM,NFRAME)
        CALL RAHMAN(FNORM,NUMS,RHO,N2,IFILM,NFRAME)
 C
C    CALL THE ROUTINE WHICH,BY IMPOSING TWO EXTRA CUT-OFFS,
C    PRODUCES A NEW R.D.F.
C
       CALL EXTRAP(FNORM,NUMS,N,SINES,INCS,BETA,RHO,RMIN,FEXTRA
      +          ,GEXTRA,N2)
C
C    CALCULATE THE RADIAL DENSITY FUNCTION
C
       GRAD=4.*PI*RHO
       NVAR=N/8
       DO 495 J=1,NVAR
       R=FLOAT(J-1)*DELR
       GRA=R*GRAD
495    RDF(J)=(GEXTRA(J)+GRA)*R
C
C     STORE THE RADIAL DENSITY FUNCTION ON A PERMANENT FILE
C     FILE FOR ANALYSIS BY PROGRAM GAUSS
 C
       WRITE(14,10)NVAR,DELR,(RDF(J),J=1,NVAR)
        WRITE(6,404)
404    FORMAT(1H1,19HEXTRAPOLATED R.D.F.)
        WRITE(6,71)
       WRITE(6,18)N2,DELR
       WRITE(6,20)(GEXTRA(I),I=1,N2)
       WRITE(6,405)
405    FORMAT(1H1,35HINTERFERENCE FUNCTION(EXTRAPOLATED))
       WRITE(6,71)
       WRITE(6,18)N2,DELS
       WRITE(6,20)(FEXTRA(I),I=1,N2)
C
```

```
C  CALL FILM TO PLOT THE EXTRAPOLATED R·D·F· AND THE
 C    CORRESPONDING INTERFERENCE FUNCTION
C
       CALL FILM(DELR,NPLO,GEXTRA,1,17,1,ITITLE,COORDT,
      +          Ø,INUMB,COORDN,NFRAME)
       CALL FILM(DELS,N2,FEXTRA,2,7,1,ITITLE,COORDT,Ø,INUMB,COORDN,
      +          NFRAME)
C
C    CALL THE ROUTINE WHICH ATTEMPTS TO DETERMINE THE TERMINATION
C  ERROR AND THEN MODIFY THE ORIGINAL R·D·F·
 C
       CALL ERTERM(FEXTRA,GEXTRA,GNORM,NUMS,N,SINES,FMOD,GMOD,N2,
      +          RMIN,RHO)
       WRITE(6,4Ø6)
4Ø6    FORMAT(1H1,3ØHMODIFIED INTERFERENCE FUNCTION)
        WRITE(6,71)
       WRITE(6,18)N2,DELS
       WRITE(6,2Ø)(FMOD(J),J=1,N2)
       WRITE(6,4Ø7)
4Ø7    FORMAT(1H1,15HMODIFIED R·D·F·)
       WRITE(6,71)
       WRITE(6,18)N2,DELR
       WRITE(6,2Ø)(GMOD(I),I=1,N2)
C
C    CALL FILM TO PLOT THE CORRECTED R·D·F· AND THE CORRESPONDING
C  INTERFERENCE FUNCTION
C
       CALL FILM(DELS,N2,FMOD,2,8,1,ITITLE,COORDT,Ø,INUMB,
      +          COORDN,NFRAME)
       CALL FILM(DELR,NPLO,GMOD,1,18,1,ITITLE,COORDT,Ø,INUMB,
      +          COORDN,NFRAME)
C
C    CALL FILM TO PLOT THE RADIAL DENSITY FUNCTION
 C
       CALL FILM(DELR,NVAR,RDF,1,2Ø,1,ITITLE,COORDT,Ø,INUMB,COORDN
      +          ,NFRAME)
       WRITE(6,41Ø)
41Ø    FORMAT(1H1,23HRADIAL DENSITY FUNCTION)
        WRITE(6,71)
       WRITE(6,18)NVAR,DELR
       WRITE(6,2Ø)(RDF(J),J=1,NVAR)
       CALL ENPLOT
       STOP
       END
```

```
      SUBROUTINE FASTFT(ARRAY,XIMAG,SINES,NDUM,NENTRY,INVERT,
     1                  NUM)
C
C    THIS ROUTINE ENABLES THE DISCRETE FOURIER TRANSFORM
C  TO BE COMPUTED EFFICENTLY.
C
C  ***************************************************************
C
C  INPUT:
C    ARRAY=DATA TO BE TRANSFORMED.
C    N=NUMBER OF POINTS FOR F.F.T.
C    NENTRY = 1 ON FIRST ENTRY
C             0 ON SUBSEQUENT ENTRIES
C    INVERT = 1 FOR F TO G TRANSFORM
C             0 FOR G TO F TRANSFORM
C    NUM=NUMBER OF VALUES IN ARRAY TO BE TRANSFORMED
C
C  INPUT/OUTPUT
C    SINES=ARRAY OF SINE VALUES
C      SUBROUTINE FASTFT(ARRAY,XIMAG,SINES,NDUM,NENTRY,INVERT,NUM)
C          OUTPUT ON FIRST CALL
C          INPUT ON SUBSEQUENT CALLS
C
C  OUTPUT:
C    XIMAG=TRANSFORMED ARRAY
C
C  CCCCCCCCCCCCCCCCCCCCCCCCCCCCCCCCCCCCCCCCCCCCCCCCCCCCCCCCCCCC
C
      DIMENSION XREAL(512),XIMAG(NDUM),SINES(NDUM),ARRAY(NDUM)
      DIMENSION XTWDS(3),YTWDS(3),X(3),Y(3)
      LOGICAL SKPTWD
      EQUIVALENCE(ZZ,II)
      COMMON PI,DELR,DELS
      N=NDUM
      N2=N/2
      N21=N2+1
      NUM1=NUM+1
      DO 600 J=1,NUM
600   XREAL(J)=ARRAY(J)
C
C THE INPUT ARRAY IS MADE UP TO N/2+1 POINTS WITH ZEROES.
C THIS IS THEN IMAGE INVERSED ABOUT N/2+1
C THE INPUT AND OUTPUT ARRAYS ARE SUBSEQUENTLY MODIFIED
C      TO GIVE A FOURIER PAIR
C
      DO 601 K=NUM1,N21
601   XREAL(K)=0.0
      DO 602 L=2,N2
      J=N+2-L
602   XREAL(J)=-XREAL(L)
      DO 101 K=1,N
101   XIMAG(K)=0.0
      IF(INVERT.NE.1) GO TO 100
      DEL=DELS
      DELPI=DEL/PI
      DO 103 K=1,N
103   XREAL(K)=XREAL(K)*DELPI
      GO TO 190
100   DEL=DELR
      DELLA=FLOAT(N)*DEL/2.
C
C INITIAL CHOICE OF RADICES
```

```
C
190   IFACTC=1
      IFACTB=4
      IFACTA=N/4
      IF(NENTRY.NE.1) GO TO 12
C
C CALCULATE CONSTANTS ON FIRST ENTRY
C
      MKSINE=N/4
      KSINE=MKSINE+1
      KKSINE=KSINE+1
      MSINE=KSINE+MKSINE
      MMSINE=MSINE+1
      MJSINE=MSINE-1
      LSINE=MSINE+MKSINE
      LLSINE=LSINE+1
C
C SET UP SINES AND COSINES
C
      PIE2=2.*PI
      YC=N
      DO 15 K=2,MKSINE
      XC=K-1
15    SINES(K)=SIN(XC*PIE2/YC)
      SINES(1)=0.
      SINES(KSINE)=1.
C
C START HERE ON SUBSEQUENT ENTRIES
C
12    ITIMES=0
C
C RETURN TO HERE WITH NEW FACTORS
C
16    IFACAB=IFACTA*IFACTB
      ITIMES=ITIMES+2
C
C   CALCULATION OF B-POINT TRANSFORMS
C
      INCTWD=0
      SKPTWD=.TRUE.
      DO 80 LITTLA=1,IFACTA
      DO 82 IZ=LITTLA,N,IFACAB
      IQ=IZ+IFACTA
      IY=IQ+IFACTA
      IP=IY+IFACTA
      XSUM1=XREAL(IZ)+XREAL(IY)
      XSUM2=XREAL(IZ)-XREAL(IY)
      YSUM1=XIMAG(IZ)+XIMAG(IY)
      YSUM2=XIMAG(IZ)-XIMAG(IY)
      XSUM3=XREAL(IQ)+XREAL(IP)
      XSUM4=XREAL(IQ)-XREAL(IP)
      YSUM3=XIMAG(IQ)+XIMAG(IP)
      YSUM4=XIMAG(IQ)-XIMAG(IP)
      XREAL(IZ)=XSUM1+XSUM3
      XIMAG(IZ)=YSUM1+YSUM3
      X(2)=XSUM2+YSUM4
      X(1)=XSUM1-XSUM3
      X(3)=XSUM2-YSUM4
      Y(2)=YSUM2-XSUM4
      Y(1)=YSUM1-YSUM3
```

```
      Y(3)=YSUM2+XSUM2
41    IR=IZ
      IF(SKPTWD) GO TO 83
      DO 81 IBHAT=1,3
      IR=IR+IFACTA
      XREAL(IR)=X(IBHAT)*XTWDS(IBHAT)+Y(IBHAT)*YTWDS(IBHAT)
81    XIMAG(IR)=Y(IBHAT)*XTWDS(IBHAT)-X(IBHAT)*YTWDS(IBHAT)
      GO TO 82
83    DO 84 IBHAT=1,3
      IR=IR+IFACTA
      XREAL(IR)=X(IBHAT)
84    XIMAG(IR)=Y(IBHAT)
82    CONTINUE
      IF(LITTLA.EQ.IFACTA) GO TO 80
      INCTWD=INCTWD+IFACTC
      SKPTWD=.FALSE.
      ITWID=INCTWD+1
      DO 91 IBHAT=1,3
44    IF(ITWID.LE.KSINE) GO TO 46
      IF(ITWID.GT.MSINE) GO TO45
      KTWID=MMSINE-ITWID
      YTWDS(IBHAT)=SINES(KTWID)
      KTWID=ITWID-MKSINE
      XTWDS(IBHAT)=-SINES(KTWID)
      GO TO 91
46    YTWDS(IBHAT)=SINES(ITWID)
      KTWID=KKSINE-ITWID
      XTWDS(IBHAT)=SINES(KTWID)
      GO TO 91
45    KTWID=ITWID-MJSINE
      YTWDS(IBHAT)=-SINES(KTWID)
      KTWID=LLSINE-ITWID
      XTWDS(IBHAT)=-SINES(KTWID)
91    ITWID=ITWID+INCTWD
      TEMPRE=XTWDS(2)
      XTWDS(2)=XTWDS(1)
      XTWDS(1)=TEMPRE
      TEMPRE=YTWDS(2)
      YTWDS(2)=YTWDS(1)
      YTWDS(1)=TEMPRE
80    CONTINUE
C CHOOSE NEW FACTORS        EXIT IF FINI
      IF(IFACTA.EQ.1) GO TO21
      IFACTC=IFACTC*IFACTB
      IFACTA=IFACTA/IFACTB
      IF(IFACTA.NE.0) GO TO 1
      ITIMES=ITIMES+1
      DO 40 K=1,N,2
      TEMPRE=XREAL(K)+XREAL(K+1)
      XREAL(K+1)=XREAL(K)-XREAL(K+1)
      XREAL(K)=TEMPRE
      TEMPRE=XIMAG(K)+XIMAG(K+1)
      XIMAG(K+1)=XIMAG(K)-XIMAG(K+1)
40    XIMAG(K)=TEMPRE
21    IF(INVERT.NE.1) GO TO 18
      DO 19 K=1,N
19    XIMAG(K)=-XIMAG(K)
      GO TO 166
18    XC=N
      DO 177 K=1,N
```

```
      XREAL(K)=XREAL(K)/XC
177   XIMAG(K)=XIMAG(K)/XC
166   CONTINUE
      DO 74 K=2,N
      IZ=K-1
      IY=0
      DO 51 J=1,ITIMES
      ZZ=AND(IZ,1)
      IY=IY+IY+II
51    IZ=IZ/2
      IF(IY.LT.K) GO TO 74
      IY=IY+1
      TEMPRE=XREAL(IY)
      XREAL(IY)=XREAL(K)
      XREAL(K)=TEMPRE
      TEMPIM=XIMAG(IY)
      XIMAG(IY)=XIMAG(K)
      XIMAG(K)=TEMPIM
74    CONTINUE
      IF(INVERT.EQ.1) GO TO 14
C
C  MODIFY THE OUTPUT ARRAY
C
      DO 105 K=1,N
105   XIMAG(K)=-XIMAG(K)*DELLA
14    RETURN
```

```
      SUBROUTINE DAMP(F,N,N2,NUMS,SINES,GDAMP)

C
C     THIS ROUTINE COMPUTES THE R.D.F.'S WITH VARIOUS
C  DAMPING CONSTANTS.THE DAMPING FACTOR IS GIVEN BY:
C                       EXP(-B*S*S)
C
C  ***************************************************
C
C  INPUT:
C    F=INTERFERENCE FUNCTION
C    N=NUMBER OF POINTS FOR F.F.T.
C    N2=N/2
C    NUMS=NUMBER OF F VALUES
C    SINES=ARRAY OF SINE VALUES
C
C  OUTPUT:
C    GDAMP=CALCULATED R.D.F.'S
C
C  ***************************************************************
      SUBROUTINE DAMP(F,N,N2,NUMS,SINES,GDAMP)
      COMMON PI,DELR,DELS
      DIMENSION BETAS(10),F(N2),GDAMP(N2),FDAMP(512),SSQ(512)
      DIMENSION SINES(N2)
      DIMENSION ITITLE(10),COORDT(10,2),COORDN(10,2),INUMB(10)
      READ(3,15)NUMB,(BETAS(J),J=1,NUMB)
15    FORMAT(I3/(9F7.4))
      DELSSQ=DELS**2
      WRITE(6,10)
10    FORMAT(1H1)
      DO 100 NS=1,NUMS
      SQNS=(NS-1)**2
100   SSQ(NS)=SQNS*DELSSQ
C
C   EACH SPECIFIED VALUE OF THE DAMPING CONSTANT IS TAKEN
C             IN TURN
C
      DO 110 NB=1,NUMB
      EDAMP=EXP(-BETAS(NB))
C
C THE INTERFERENCE FUNCTION IS DAMPED
C
      DO 120 NS=1,NUMS
120   FDAMP(NS)=F(NS)*(EDAMP**SSQ(NS))
C
      CALL FASTFT(FDAMP,GDAMP,SINES,N,0,1,NUMS)
      WRITE(6,20)BETAS(NB)
      WRITE(6,43)
      WRITE(6,30)N2,DELR
      WRITE(6,31)(GDAMP(I),I=1,N2)
      CALL FILM(DELR,N2,GDAMP,1,15,1,ITITLE,COORDT,0,INUMB,COORDN
     +          ,NFRAME)
110   CONTINUE
20    FORMAT(1HX,34HDAMPED RDF FOR DAMPING CONSTANT = ,F7.4)
43    FORMAT(37H     NUMBER OF POINTS    INCREMENT     )
30    FORMAT(10X,I4,7X,F10.4)
31    FORMAT(10(4X,F7.4))
      RETURN
      END
```

```
      SUBROUTINE RAHMAN(F,NUMS,RHO,N2,IFILM,NFRAME)

C     THIS ROUTINE IS A RELIABILITY CRITERION FOR THE
C  CORRECTNESS OF THE NORMALISATION.
C
C  ***************************************************************
C  INPUT:
C     F=INTERFERENCE FUNCTION
C     NUMS=NUMBER OF F VALUES
C     RHO=MATERIAL DENSITY OBTAINED FROM ERNORM
C     N2=N/2 (ADJUSTABLE DIMENSIONS)
C     IFILM=PARAMETET FOR PLOTTING
C           =1 FOR PLOTTING
C           =0 FOR NO PLOTTING
C
C  ***************************************************************
C
      COMMON PI,DELR,DELS
      DIMENSION F(N2),SUD(600),SUDEX(600)
      DIMENSION ITITLE(10),COORDT(10,2),COORDN(10,2),INUMB(10)
      D=2.0
      NUMU=100
      DELU=0.05
      SUMSQ=0.0
      CPI=1.0/PI
      NUMINT=NUMS-1
      SMAX=FLOAT(NUMINT)*DELS
      U=0.0000000001
      DO 800 NU=1,NUMU
      CONST=CPI/U
      DRHO=D*RHO
      UD=U*D
C
C  SUD IS A FUNCTION OBTAINED FROM RHO,INDEPENDANT OF THE
C   EXPERIMENTAL VALUES FOR F
C
      SUD(NU)=(SIN(UD)/UD-COS(UD))*DRHO/U**2
      ARGF1=SMAX+U
      ARGF2=SMAX-U
      TEMP1=0.5*(F(NUMS)*(SIN(ARGF1*D)/ARGF1-SIN(ARGF2*D)/ARGF2))
      TEMP2=0.0
      DO 801 NS=2,NUMINT
      S=FLOAT(NS-1)*DELS
      ARG1=S+U
      ARG2=S-U
      TEMP2=TEMP2+F(NS)*(SIN(ARG1*D)/ARG1-SIN(ARG2*D)/ARG2)
801   CONTINUE
C
C  SUDEX IS A FUNCTION OBTAINED FROM THE EXPERIMENTAL DATA
C
      SUDEX(NU)=CONST*(TEMP1+TEMP2)*DELS
      SUMSQ=SUMSQ+((SUD(NU)-SUDEX(NU))**2)
      U=U+DELU
800   CONTINUE
C
C   FOR CORRECT NORMALISATION SUD APPROACHES SUDEX
C
      STDEV=SQRT(SUMSQ)*0.01
      WRITE(6,10)
10    FORMAT(1H1,36HSTANDARD DEVIATION OF SUD FROM SUDEX)
      WRITE(6,20) STDEV
20    FORMAT(1HX,1PE16.6)
```

```
20     FORMAT(1HX,1PE16.6)
C
C WRITE OUT AND PLOT SUD AND SUDEX IF REQUIRED
C
       IF(IFILM.EQ.0) GO TO 89
       WRITE(6,87)
87     FORMAT(1H1,5H SUD )
       WRITE(6,30)NUMU,DELU,(SUD(I),I=1,NUMU)
       WRITE(6,88)
88     FORMAT(1H1,7H SUDEX )
       CALL FILM(DELU,NUMU,SUD,3,29,0,ITITLE,COORDT,0,INUMB,
      +          COORDN,NFRAME)
       CALL FILM(DELU,NUMU,SUDEX,3,30,0,ITITLE,COORDT,0,INUMB,
      +          COORDN,NFRAME)
30     FORMAT(1HX,I4,F10.4/(1HX,10F10.4))
89     CONTINUE
       RETURN
       END
×
```

```
      SUBROUTINE ERNORM(F,G,NUMDUM,N,SINES,FNORM,GNORM,EXNORM,
     +     ATOM,RHO,RMIN,N2,NMIN)
C
C THIS ROUTINE REDUCES THE OSCILLATIONS IN THE R.D.F.
C BELOW THE FIRST PEAK.THESE OSCILLATIONS ARE DUE TO
C ERRORS IN NORMALIATION AND IN THE SCATTERING FACTOR
C
C CCCCCCCCCCCCCCCCCCCCCCCCCCCCCCCCCCCCCCCCCCCCCCCCCCCCCCCC
C
C INPUT:
C   F=INITIAL INTENSITY FUNCTION
C   G=R.D.F. CORRESPONDING TO F
C   SINES=ARRAY OF SINE VALUES.
C   N=NUMBER OF POINTS FOR F.F.T.
C   N2=N/2 FOR ADJUSTABLE DIMENSIONS
C
C INPUT/OUTPUT:
C   NUMS=NUMBER OF F VALUES
C
C OUTPUT:
      SUBROUTINE ERNORM(F,G,NUMDUM,N,SINES,FNORM,GNORM,EXNORM,
     +     ATOM,RHO,RMIN,N2,NMIN)
C   GNORM=R.D.F. WITH REDUCED OSCILLATIONS BELOW THE
C              FIRST PEAK
C   FNORM=INTENSITY FUNCTION CORRESPONDING TO GNORM
C   RHO=MATERIAL DENSITY OBTAINED FROM EXPERIMENTAL DATA
C   RMIN=CALCULATED VALUE OF FIRST MINIMUM IN R.D.F.
C
C CCCCCCCCCCCCCCCCCCCCCCCCCCCCCCCCCCCCCCCCCCCCCCCCCCCCCCCC
C
      COMMON PI,DELR,DELS
      DIMENSION F(N2),G(N2),ERRG(200),ERRF(512),EXNORM(512)
      DIMENSION SUMSQ(10),GRAD(10),FNORM(N2),GNORM(N2)
      DIMENSION SINES(N2),ATOM(200)
      NUMS=NUMDUM
      N4=N2/4
      MINR=RMIN/DELR
C
C FIT STRAIGHT LINE TO R.D.F. TO OBTAIN ERROR.
C
C THIS ERROR IS TRANSFORMED.
C
      DO 97 J=1,MINR
97    ERRG(J)=G(J)+FLOAT(J-1)*DELR*4.*PI*RHO
      CALL FASTFT(ERRG,ERRF,SINES,N,0,0,MINR)
C
C   MODIFY THE ORIGINAL INTERFERENCE FUNCTION WITH THE
C   CALCULATED ERROR FUNCTION
C
      DO 103 J=1,NUMS
103   FNORM(J)=F(J)-ERRF(J)
      CALL FASTFT(FNORM,GNORM,SINES,N,0,1,NUMS)
C
C   CALCULATE THE MODIFIED NORMALISED INTENSITY
C
      DO 108 K=NMIN,NUMS
      KCOR=K+1-NMIN
      EXNORM(KCOR)=(FNORM(K)/(FLOAT(K-1)*DELS)+1.0)*ATOM(KCOR)
108   CONTINUE
      RETURN
      END
```

```
      SUBROUTINE EXTRAP(F,NUMDUM,N,SINES,INCS,BETA,RHO,
     1          RMIN,FEXTRA,GEXTRA,N2DUM)

C
C       THIS ROUTINE OBTAINS THREE R.D.F.'S FROM THREE
C  TERMINATIONS OF THE INTERFERENCE FUNCTION.BY FOLLOWING
C  ANY TRENDS A FOURTH,EXTRAPOLATED R.D.F. IS OBTAINED.
C
C  ************************************************************
C
C  INPUT:
C    F=INTERFERENCE FUNCTION
C    SINES=ARRAY OF SINE VALUES
C    NUM=NUMBER OF F VALUES
C    N=NUMBER OF POINTS FOR F.F.T.
C    N2=N/2
C    INCS=S INCREMENTS IN TERMINATION VALUES
C    BETA=DAMPING CONSTANT
C    RHO=MATERIAL DENSITY OBTAINED FROM ERNORM
        SUBROUTINE EXTRAP(F,NUMDUM,N,SINES,INCS,BETA,RHO,
       +          RMIN,FEXTRA,GEXTRA,N2DUM)
C    RMIN=FIRST MINIMUM POSITION IN R.D.F. OBTAINED FROM
C                       ERNORM
C
C  OUTPUT
C    GEXTRA=EXTRAPOLATED R.D.F.
C    FEXTRA=INTERFERENCE FUNCTION CORRESPONDING TO GEXTRA
C
C  ************************************************************
C
        COMMON PI,DELR,DELS
       +          ,FDAMP(512),NUMCAT(3),GDUMP(3,512),G(512),DEL3(512)
       +                    ,DEL2(512),FRACT(512),QUOT(512),DELG(200),B(51
       +EXNORM(512)
        DIMENSION F(N2DUM),SINES(N2DUM),FEXTRA(N2DUM),GEXTRA(N2DUM)
        N2=N2DUM
        NUM=NUMDUM
C
C    DAMP THE F VALUES
C
        DO 100 J=1,NUM
100     FDAMP(J)=F(J)*EXP(-BETA*(FLOAT(J-1)*DELS)**2)
C
C   CALCULATE THE THREE R.D.F.'S CORRESPONDING TO
C        DIFFERENT TERMINATIONS
C
        DO 101 J=1,3
        NUMCAT(J)=NUM-(J-1)*INCS
        NUMCUT=NUMCAT(J)
        CALL FASTFT(FDAMP,G,SINES,N,0,1,NUMCUT)
        DO 121 K=1,N2
121     GDUMP(J,K)=G(K)
        SUM=0.0
        DO 122 J=1,2
122     SUM=SUM+(FLOAT(NUMCAT(J)))**2
C
C  OBTAIN THE EXTRAPOLATED R.D.F.
C
        DO 762 I=1,N2
        DEL3(I)=GDUMP(3,I)-GDUMP(1,I)
        DEL2(I)=GDUMP(2,I)-GDUMP(1,I)
        IF(DEL3(I).EQ.0.0.AND.DEL2(I).EQ.0.0) GO TO 57
```

```
      FRACT(I)=DELS(I)/DEL2(I)
      IF(FRACT(I).GT.1.2) GO TO 49
      GEXTRA(I)=0.0
      DO 48 J=1,2
48    GEXTRA(I)=GEXTRA(I)+GDUMP(J,I)*(FLOAT(NUMCAT(J)))**2
      GEXTRA(I)=GEXTRA(I)/SUM
      GO TO 762
49    QUOT(I)=(DELS(I)-DEL2(I))/DEL2(I)
      IF(QUOT(I).GT.1.0) GEXTRA(I)=GDUMP(3,I)+(DELS(I)-DEL2(I)
     +          )/FRACT(I)
      IF(QUOT(I).LT.1.0) GEXTRA(I)=GDUMP(3,I)+QUOT(I)*(DELS(I)
     +          -DEL2(I))
      GO TO 762
57    GEXTRA(I)=GDUMP(1,I)
762   CONTINUE
C
C ELIMINATE OBVIOUS IRREGULARITIES BELOW THE FIRST PEAK
C
      MINR=RMIN/DELR
      DO 410 J=1,MINR
      DELG(J)=GEXTRA(J)+FLOAT(J-1)*DELR*4.*PI*RHO
410   GEXTRA(J)=GEXTRA(J)-(FLOAT(MINR-J))*DELG(J)
     +      /FLOAT(MINR)
      DO 112 K=1,N2
      B(K)=-4.*PI*RHO*FLOAT(K-1)*DELR
112   IF(GEXTRA(K).LT.B(K)) GEXTRA(K)=B(K)
C           OBTAIN FEXTRA
      CALL FASTFT(GEXTRA,FEXTRA,SINES,N,K,0,N2)
      EXNORM(1)=0.0
      DO 701 L=2,NUM
701   EXNORM(L)=FEXTRA(L)/(FLOAT(L-1)*DELS)+1.0
      RETURN
      END
```

```
      SUBROUTINE ERTERM(FEXTRA,GEXTRA,G,NUMS,N,SINES,FMOD,
     +                  GMOD,N2,RMIN,RHO)
C
C     THIS ROUTINE OBTAINS A TERMINATION ERROR AND THEN
C  MODIFIES THE ORIGINAL P.D.F.
C
C  ***************************************************************
C  INPUT:
C     GEXTRA=EXTRAPOLATED P.D.F. OBTAINED BY EXTRAP
C     FEXTRA=INTENSITY FUNCTION CORRESPONDING TO GEXTRA
C     G=ORIGINAL P.D.F.
C     N=NUMBER OF POINTS FOR F.F.T.
C     SINES=ARRAY OF SINE VALUES
C     N2=N/2
C     NUMS=NUMBER OF F VALUES
C
C  OUTPUT:
C     GMOD=G MODIFIED WITH TERMINATION ERROR
C       SUBROUTINE ERTERM(FEXTRA,GEXTRA,G,NUMS,N,SINES,FMOD,GMOD,N2
C      +           ,RMIN,RHO)
C     FMOD=INTENSITY FUNCTION CORRESPONDING TO GMOD
C
C  ***************************************************************
C
      COMMON PI,DELR,DELS
      DIMENSION FEXTRA(N2),GEXTRA(N2),GTERM(512),GERR(512)
      DIMENSION GMOD(N2),FMOD(N2),SINES(N2)
      DIMENSION G(N2),DELG(1000),B(512)
      CALL FASTFT(FEXTRA,GTERM,SINES,N,0,1,NUMS)
      DO 456 L=1,N2
456   GMOD(L)=G(L)+GEXTRA(L)-GTERM(L)
      MINR=RMIN/DELR
      DO 457 J=1,MINR
      DELG(J)=GMOD(J)+FLOAT(J-1)*DELR*4.*PI*RHO
457   GMOD(J)=GMOD(J)-(FLOAT(MINR-J))*DELG(J)/FLOAT(MINR)
      DO 458 K=1,N2
      B(K)=-4.*PI*RHO*FLOAT(K-1)*DELR
458   IF(GMOD(K).LT.B(K)) GMOD(K)=B(K)
      CALL FASTFT(GMOD,FMOD,SINES,N,0,0,N2)
```

```
      SUBROUTINE FILM(DEL,NUMDUM,YARRAY,IXLAB,IYLAB,NDUM,
     +  ITITLE,COORDT,NNUMB,INUMB,COORDN,NFRAME)
C
C
C     THIS IS A GENERAL MICROFILM ROUTINE WHICH CAN
C   PLOT ANY FUNCTION TABULATED AT EQUISPACED INTERVALS.
C   AXES ARE DRAWN,SCALED AND LABELLED AND PROVISION IS MADE FOR
C   THE INCLUSION OF ANY OTHER LABELLING INFORMATION THAT
C   MIGHT BE REQUIRED.
C
C CCCCCCCCCCCCCCCCCCCCCCCCCCCCCCCCCCCCCCCCCCCCCCCCCCCCCCCCCCCCCC
C
C   INPUT:
C         YARRAY: ARRAY CONTAINING VALUES TO BE PLOTTED
C          NUM: NUMBER OF VALUES TO BE PLOTTED
C         DEL: ABSCISSA INCREMENT
C         IXLAB: INTEGER CORRESPONDING TO REQUIRED X-AXIS LABEL
C         IYLAB: INTEGER CORRESPONDING TO REQUIRED Y-AXIS LABEL
C         NTITLE: TOTAL NUMBER OF TITLES AND CAPTIONS REQUIRED
C       IF NTITLE=0,NO TITLES APPEAR
C       IF NTITLE=1,THE TITLE CORRESPONDING TO IYLAB
C                    IS DRAWN
C       IF NTITLE>1,THE TITLE CORRESPONDING TO IYLAB
C           AND (NTITLE-1) OTHER CAPTIONS ARE DRAWN
C
C        ITITLE:ARRAY CONTAINING THE (NTITLE-1)
C          INTEGER REFERENCES TO THE REQUIRED CAPTIONS
C         COORDT: 2-D ARRAY CONTAINING THE (X,Y) COORDINATES OF THE
C               STARTING POINTS FOR THE (NTITLE-1) CAPTIONS
C               COORDT(N,1)=X-COORDINATE OF CAPTION N
C               COORDT(N,2)=Y-COORDINATE OF CAPTION N
C         MSCALE: =NUM+2; PROVIDES THE REQUIRED DIMENSION FOR THE X AND
C              Y ARRAYS WHEN USING 'SCALE'
C         NNUMB: NUMBER OF REAL NUMBERS TO BE PLOTTED
C         INUMB: ARRAY CONTAINING THE NNUMB REAL NUMBERS
C         COORDN: 2-D ARRAY CONTAINING THE (X,Y) COORDINATES OF THE
C               STARTING POINTS FOR THE NNUMB REAL NUMBERS.
      SUBROUTINE FILM(DEL,NUMDUM,YARRAY,IXLAB,IYLAB,NDUM,ITITLE,
     +          COORDT,NNUMB,INUMB,COORDN,NFRAME)
C               COORDN(M,1)=X-COORDINATE OF NUMBER M
C               COORDN(M,2)=Y-COORDINATE OF NUMBER M
C
C   INPUT/OUTPUT:
C                NFRAME: NUMBER OF FRAMES PLOTTED TO DATE
C
C   OUTPUT:
C         MICROFILM
C
C CCCCCCCCCCCCCCCCCCCCCCCCCCCCCCCCCCCCCCCCCCCCCCCCCCCCCCCCCCCCCC
C
      COMMON PI,DELR,DELS
C
C   DIMENSION ARRAYS
C
      DIMENSION XARRAY(514),YARRAY(514),COORDT(10,2),ITITLE(10)
     +         ,COORDN(10,2),INUMB(10)
      INTEGER XLAB(20),YLAB(50),NXLAB(20),NYLAB(50)
C
C   READ IN DATA FOR POSSIBLE X-AXIS LABELLING
C
      DATA XLAB(1),NXLAB(1)/4HR(A),4/
      DATA XLAB(2),NXLAB(2)/6HS(1/A),6/
```

```
      DATA XLAB(3),NXLAB(3)/6HU(1/A),6/
C
C  READ IN DATA FOR POSSIBLE Y-AXIS LABELLING
C
      DATA YLAB(1),NYLAB(1)/8HEXINT(S),8/
      DATA YLAB(2),NYLAB(2)/9HSCATTF(S),9/
      DATA YLAB(3),NYLAB(3)/9HEXNORM(S),9/
      DATA YLAB(4),NYLAB(4)/4HF(S),4/
      DATA YLAB(5),NYLAB(5)/8HFDAMP(S),8/
      DATA YLAB(6),NYLAB(6)/8HFNORM(S),8/
      DATA YLAB(7),NYLAB(7)/9HFEXTRA(S),9/
      DATA YLAB(8),NYLAB(8)/7HFMOD(S),7/
      DATA YLAB(9),NYLAB(9)/7HFFIN(S),7/
      DATA YLAB(14),NYLAB(14)/4HG(R),4/
      DATA YLAB(15),NYLAB(15)/8HGDAMP(R),8/
      DATA YLAB(16),NYLAB(16)/8HGNORM(R),8/
      DATA YLAB(17),NYLAB(17)/9HGEXTRA(R),9/
      DATA YLAB(18),NYLAB(18)/7HGMOD(R),7/
      DATA YLAB(19),NYLAB(19)/7HGFIN(R),7/
      DATA YLAB(20),NYLAB(20)/6HPDF(R),6/
C
C CALCULATE TOTAL NUMBER OF FRAMES INCLUDING THE ONE ABOUT TO BE
C PLOTTED.IF THIS NUMBER EXCEEDS 50 (THE MAX ALLOWED THROUGH ICCC)
C EXIT WITHOUT PLOTTING.
C
      NUM=NUMDUM
      NTITLE=NDUM
      NFRAME=NFRAME+1
      IF (NFRAME.GE.50) GO TO 1000
C
C CALCULATE VALUES FOR XARRAY
C
      DO 100 N=1,NUM
100   XARRAY(N)=FLOAT(N-1)*DEL
C
C SCALE AND DRAW AXES WITH APPROPRIATE LABELLING
C
      CALL SCALE(XARRAY,10.0,NUM,1)
      CALL SCALE(YARRAY,14.0,NUM,1)
      CALL AXIS(0.0,0.0,XLAB(IXLAB),-NXLAB(IXLAB),10.0,0.0,
     +          XARRAY(NUM+1),XARRAY(NUM+2))
      CALL AXIS(0.0,0.0,YLAB(IYLAB),NYLAB(IYLAB),14.0,90.0,
     +          YARRAY(NUM+1),YARRAY(NUM+2))
C
C JOIN POINTS IN YARRAY BY STRAIGHT LINE SEGMENTS
C
      CALL LINE(XARRAY,YARRAY,NUM,1,0,1)
C
C EXIT IF NO TITLES ARE REQUIRED
C
      IF(NTITLE.EQ.1) GO TO 999
C
C SELECT APPROPRIATE TITLE
C
      GO TO (1,2,3,4,5,6,7,8,9,10,11,12,13,14,15,16,
     +       17,18,19,20),IYLAB
1     CALL SYMBOL(5.65,15.1,0.35,
     +      22HEXPERIMENTAL INTENSITY ,0.1,22)
      GO TO 200
2     CALL SYMBOL(6.52,15.0,0.35,
```

```
     +       17HSCATTERING FACTOR ,0.0,17)
      GO TO 210
3     CALL SYMBOL(6.0,15.0,0.35,
     +       20HNORMALIZED INTENSITY ,0.0,20)
      GO TO 220
4     CALL SYMBOL(6.34,15.0,0.35,
     +       21HINTERFERENCE FUNCTION,0.0,21)
      GO TO 200
5     CALL SYMBOL(5.13,15.0,0.35,
     +       28HDAMPED INTERFERENCE FUNCTION,0.0,28)
      GO TO 210
6     CALL SYMBOL(1.27,15.0,0.35,
     +       49HINTERFERENCE FUNCTION WITH IMPROVED NORMALISATION,
     +                 0.0,49)
      GO TO 230
7     CALL SYMBOL(4.87,15.0,0.35,
     +       34HEXTRAPOLATED INTERFERENCE FUNCTION,0.0,34)
      GO TO 240
8     CALL SYMBOL(4.78,15.0,0.35,
     +       32HMODIFIED INTERFERENCE FUNCTION,0.0,32)
      GO TO 250
9     CALL SYMBOL(5.30,15.0,0.35,
     +       27HFINAL INTERFERENCE FUNCTION,0.0,27)
      GO TO 260
10    DUMMY
     +      =0.0
      GO TO 270
11    DUMMY
     +      =0.0
      GO TO 280
12    DUMMY
     +      =0.0
      GO TO 290
13    DUMMY
     +      =0.0
      GO TO 300
14    CALL SYMBOL(7.92,15.0,0.35,
     +      9HCRUDE PDF ,0.0,9)
      GO TO 310
15    CALL SYMBOL(3.73,15.0,0.35,
     +      30HPDF FOR DAMPED INTERFERENCE FUNCTION,0.0,30)
      GO TO 320
16    CALL SYMBOL(4.96,15.0,0.35,
     +      26HPDF CORRESPONDING TO PNORM ,0.0,26)
      GO TO 330
17    CALL SYMBOL(6.69,15.0,0.35,
     +      16HEXTRAPOLATED PDF ,0.0,16)
      GO TO 340
18    CALL SYMBOL(7.44,15.0,0.35,
     +      12HMODIFIED PDF ,0.0,12)
      GO TO 350
19    CALL SYMBOL(7.92,15.0,0.35,
     +      9HFINAL PDF ,0.0,9)
      GO TO 360
20    DUMMY
     +      =0.0
      GO TO 370
220   NTITLE=NTITLE-1
C
C EXIT TO NUMBER PLOTTING IF NO TITLES REMAIN TO BE DRAWN
```

```
C
      IF(NTITLE.LT.1) GO TO 300
      JTITLE=ITITLE(NTITLE)
C
C SELECT AND DRAW NEXT TITLE
C
      GO TO (1001,1002,1003),JTITLE
1001  CALL SYMBOL(COORDT(NTITLE,1),COORDT(NTITLE,2),0.14,
     +   12HTEMPERATURE= ,0.0,12)
      GO TO 200
1002  CALL SYMBOL(COORDT(NTITLE,1),COORDT(NTITLE,2),0.14,
     +   9HPRESSURE= ,0.0,9)
      GO TO 200
1003  CALL SYMBOL(COORDT(NTITLE,1),COORDT(NTITLE,2),0.14,
     +   12HRESISTIVITY= ,0.0,12)
      GO TO 200
C
C EXIT IF NO NUMBERS REMAIN TO BE DRAWN
C
300   IF(NNUMB.LT.1) GO TO 999
      CALL NUMBER(COORDN(NNUMB,1),COORDN(NNUMB,2),0.14,
     +          INUMB(NNUMB),0.0,3)
      NNUMB=NNUMB-1
      GO TO 300
C
C MOVE MICROFILM ONTO NEXT FRAME
C
999   CALL NEWPAGE
1000  RETURN
      END
```

```
      SUBROUTINE FRAME1
C
      COMMON PI,DELR,DELS
C
C
C SUBROUTINE TO PLOT A SINGLE FRAME OF MICROFILM
C LABELLING ****ANALYSIS OF ELECTRON DIFFRACTION DATA****
C
C
      CALL SYMBOL(5.6,10.0,0.7,11HANALYSIS OF ,0.0,11)
      CALL SYMBOL(0.7,8.3,0.7,25HELECTRO DIFFRACTION DATA.
     +          0.0,25)
      CALL NEWPAGE
      RETURN
      END
      SUBROUTINE FRAME2
C
      COMMON PI,DELR,DELS
      DIMENSION RUNCAP(7,2)
C
C
C SUBROUTINE TO PLOT A SINGLE FRAME OF MICROFILM CONTAINING ALL
C DETAILS NECESSARY FOR DOCUMENTING A SINGLE DEPOSITION
C
C
      CALL SYMBOL(0.5,13.0,0.7,12HDATE OF RUN:,0.0,12)
      CALL SYMBOL(0.5,11.3,0.7,9HMATERIAL:,0.0,9)
      CALL SYMBOL(0.5,9.6,0.7,10HSUBSTRATE:,0.0,10)
      CALL SYMBOL(0.5,7.9,0.7,15HFILM THICKNESS:,0.0,15)
      CALL SYMBOL(0.5,6.2,0.7,23HDEPOSITION TEMPERATURE:,0.0,23)
      CALL SYMBOL(0.5,4.5,0.7,16HDEPOSITION RATE:,0.0,16)
      CALL SYMBOL(0.5,2.8,0.7,22HDEPOSITION PRESSURE:,0.0,22)
      READ(4,20)((RUNCAP(I,J),J=1,2),I=1,7)
20    FORMAT(I2,A10)
      CALL SYMBOL(9.6,13.8,0.7,RUNCAP(1,2),0.0,RUNCAP(1,1))
      CALL SYMBOL(7.5,11.3,0.7,RUNCAP(2,2),0.0,RUNCAP(2,1))
      CALL SYMBOL(8.2,9.6,0.7,RUNCAP(3,2),0.0,RUNCAP(3,1))
      CALL SYMBOL(11.7,7.9,0.7,RUNCAP(4,2),0.0,RUNCAP(4,1))
      CALL SYMBOL(17.3,6.2,0.7,RUNCAP(5,2),0.0,RUNCAP(5,1))
      CALL SYMBOL(12.4,4.5,0.7,RUNCAP(6,2),0.0,RUNCAP(6,1))
      CALL SYMBOL(15.2,2.8,0.7,RUNCAP(7,2),0.0,RUNCAP(7,1))
      CALL NEWPAGE
      RETURN
      END
```

```
      PROGRAM NORMAL(INPUT,OUTPUT,TAPE1,TAPE2,TAPE3,TAPE4)

C
C     THIS PROGRAM NORMALISES THE EXPERIMENTAL DATA AND
C    CALCULATES THE INTERFERENCE FUNCTION.
C
C     TWO METHODS OF NORMALISATION ARE AVAILABLE:
C
C           (1) HIGH ANGLE FITTING
C           (2) KROGH-MOE METHOD
C
C CCCCCCCCCCCCCCCCCCCCCCCCCCCCCCCCCCCCCCCCCCCCCCCCCCCCCCCCCCCCCCCC
C
C       INPUT:
C           NUMS=NUMBER OF EXPERIMENTAL POINTS
C           NMIN=MINIMUM NUMBER FROM WHICH DATA WAS READ
C           DELS=INCREMENT IN S(=4*PI*SIN(THETA)/WAVELENGTH)
C           EXINT=EXPERIMENTAL INTENSITY
      PROGRAM NORMAL(INPUT,OUTPUT,TAPE1,TAPE2,TAPE3,TAPE4)
C           SFAC=ATOMIC SCATTERING FACTOR SQUARED
C       OUTPUT:
C           ENORM=NORMALISED INTENSITY
C           F=INTERFERENCE FUNCTION
C
C CCCCCCCCCCCCCCCCCCCCCCCCCCCCCCCCCCCCCCCCCCCCCCCCCCCCCCCCCCCCCCCC
C
      DIMENSION EXINT(500),SFAC(500),ENORM(500),F(500),SSQ(500)
      READ(1,11)NUMS,NMIN,DELS,(EXINT(K),K=NMIN,NUMS)
      READ(2,10)NUMS,DELS,(SFAC(K),K=1,NUMS)
10    FORMAT(I4,F10.4/(6(2X,F8.4)))
11    FORMAT(2I4,F10.4/(6(2X,F8.4)))
      NUMINT=NUMS-1
C
C   CHOOSE WHETHER TO USE HIGH-ANGLE FITTING
C
      PRINT,/,/,*IF HIGH ANGLE FITTING IS REQUIRED,ENTER ZERO*
      READ,ITEST1
      IF(ITEST1)101,100,101
C
C   SELECT THE MINIMUM S VALUE FROM WHICH TO NORMALISE
C
100   PRINT,/,*EXPERIMENTAL DATA CUTS-OFF AT ARRAY NO.*,NUMS
102   PRINT,*READ IN MIN. ARRAY NO. FOR FITTING*
      READ,MINS
      MIN=MINS+1
      SMIN=FLOAT(MINS-1)*DELS
      SMAX=FLOAT(NUMS-1)*DELS
      SUM1=(SFAC(MINS)*SMIN+SFAC(NUMS)*SMAX)*0.5
      SUM2=(EXINT(MINS)*SMIN+EXINT(NUMS)*SMAX)*0.5
      DO 800 NS=MIN,NUMINT
      S=FLOAT(NS-1)*DELS
      SUM1=SUM1+SFAC(NS)*S
800   SUM2=SUM2+EXINT(NS)*S
      A1=SUM1/SUM2
C
C           A1 IS NORMALISATION FACTOR
C
      PRINT,/,*NORMALIZATION CONSTANT = *,A1
C
C   CHOOSE WHETHER TO SELECT DIFFERENT MINIMUM S VALUE
C
      PRINT,/,*IF DIFFERENT MIN. ARRAY NO. REQUIRED,ENTER ZERO*
S
```

```
      READ,JTEST1
      IF(JTEST1)101,102,101
C
C    CHOOSE WHETHER TO USE KROGH-MOE METHOD
C
101   PRINT,/,/,*IF KROGH-MOE METHOD REQUIRED,ENTER ZERO*
      READ,ITEST2
      IF(ITEST2)106,105,106
105   DELSQ=DELS**2
      DO 803 NS=NMIN,NUMS
803   SSQ(NS)=FLOAT(NS)**2*DELSQ
      SUM1=(SSQ(NMIN)+SSQ(NUMS))*0.5
      SUM2=((SSQ(NMIN)*EXINT(NMIN)/SFAC(NMIN))+(SSQ
     +          (NUMS)*EXINT(NUMS)/SFAC(NUMS)))*0.5
      NMIN1=NMIN+1
      DO 804 NS=NMIN1,NUMINT
      SUM1=SUM1+SSQ(NS)
      SUM2=SUM2+(SSQ(NS)*EXINT(NS)/SFAC(NS))
804   CONTINUE
C
C    READ IN BULK DENSITY
C
997   PRINT,/,*READ IN BULK DENSITY*
      READ,RHO0
      SUM1=SUM1-2.0*(3.141593**2)*RHO0
C
C          A2 IS NORMALISATION FACTOR
C
      A2=SUM1/SUM2
      PRINT,/,*NORMALIZATION CONSTANT =*,A2
C
C  CHOOSE WHETHER TO SELECT A DIFFERENT DENSITY
C
      PRINT,/,*IF DIFFERENT DENSITY REQUIRED,ENTER ZERO*
      READ,JTEST2
      IF(JTEST2)106,997,106
106   CONTINUE
C
C    CHOOSE WITH WHICH METHOD TO NORMALISE
C
      PRINT,/,*TO NORMALISE WITH METHDO 1,ENTER-1,WITH *
      PRINT,*METHOD2,ENTER ZERO,AND TO AVERAGE ENTER +1*
      READ,ITEST3
      IF(ITEST3)400,401,402
400   AFIN=A1
      GO TO 57
401   AFIN=A2
      GO TO 57
402   AFIN=(A1+A2)/2.0
C
C      NORMALISE THE EXPERIMENTAL DATA AND CALCULATE THE
C         INTERFERENCE FUNCTION
C
57    DO 701 J=NMIN,NUMS
      ENORM(J)=AFIN*EXINT(J)
      F(J)=FLOAT(J-1)*DELS*(ENORM(J)/SFAC(J)-1.0)
701   CONTINUE
C
C    EXTRAPOLATE THE INTERFERENCE FUNCTION FROM THE MINIMUM
C         S VALUE TO THE ORIGIN
```

```
C
      FCALC=-FLOAT(NMIN-1)*DELS
      FRACT=(FCALC-F(NMIN))/FCALC
      N1MIN=NMIN-1
      DO 914 J=1,N1MIN
      F(J)=-FLOAT(J-1)*DELS*(1.0-FRACT)
914   CONTINUE
      WRITE(3,11)NUMS,NMIN,DELS,(ENORM(J),J=NMIN,NUMS)
      WRITE(4,10)NUMS,DELS,(F(J),J=1,NUMS)
      PRINT,/,*NORMALIZED INTENSITY STORED ON TAPE 3*
      PRINT,*INTERFERENCE FUNCTION STORED ON TAPE 4*
      STOP
      END
```

```
      PROGRAM INTEG(INPUT,OUTPUT,TAPE1,TAPE2,TAPE3,
     1      TAPE6=OUTPUT)
C
C     THIS PROGRAM INTEGRATES THE STRUCTURE FACTOR,CALCULATED
C  BY PARTF,OVER A SERIES OF SPECIFIED SPHERES
C
C
C  CCCCCCCCCCCCCCCCCCCCCCCCCCCCCCCCCCCCCCCCCCCCCCCCCCCC
C
C       INPUT:
C            NCOORD=NUMBER OF ATOMS IN THE UNIT CELL
C            COORD =CO-ORDINATES OF THE ATOMS
C            S     =4*PI*SIN(THETA)/WAVELENGTH
C          DELS=SPECIFIED INCREMENT IN S
C          NUMS=NUMBER OF POINTS AT WHICH THE INTEGRATED
C                 STRUCTURE FACTOR IS REQUIRED
C          DEL =ANGULAR INCREMENT IN BOTH THETA AND THI
      PROGRAM INTEG(INPUT,OUTPUT,TAPE1,TAPE2,TAPE3,TAPE6=OUTPUT)
C       OUTPUT:
C            SUMFAC=SPHERICALLY INTEGRATED STRUCTURE FACTOR
C
C  CCCCCCCCCCCCCCCCCCCCCCCCCCCCCCCCCCCCCCCCCCCCCCCCCCCC
C
      DIMENSION SUMFAC(300)
      COMMON COORD(25,3),NCOORD
      READ(3,313)DEL,DELS,NUMS
313   FORMAT(2F7.4,I4)
      NUMMER=NUMS+1
      PI=3.142
      PI2=2.*PI
      READ(1,93)NCOORD,((COORD(I,J),J=1,3),I=1,NCOORD)
93    FORMAT(I2/(3F10.4))
      DO 91 J=1,NUMS
      S=FLOAT(J)*DELS
      DELSIG=DEL
C
C     THE INTEGRATION IS CARRIED OUT USING SPHERICAL
C       CO-ORDINATES OF INCREMENT DEL
C
161   SUMFAC(J)=0.0
      PHI=-DELSIG
19    PHI=PHI+DELSIG
      THETA=-DELSIG
17    THETA=THETA+DELSIG
      IF(THETA.GT.PI) GO TO 999
      X=S*SIN(THETA)*COS(PHI)
      Y=S*SIN(THETA)*SIN(PHI)
      Z=S*COS(THETA)
C
C     THE CORRESPONDING CARTESIAN CO-ORDINATES ARE CALCULATED
C
      SUMFAC(J)=SUMFAC(J)+PARTF(X,Y,Z)*SIN(THETA)
C
C     THE STRUCTURE FACTOR AT THE POINT (X,Y,Z) IS CALCULATED
C           BY PARTF
C
      GO TO 17
999   IF(PHI.LT.PI2) GO TO 19
      SUMFAC(J)=SUMFAC(J)*DELSIG**2
      ANS=SUMFAC(J)
      WRITE(6,703)S,ANS
703   FORMAT(4X,F10.4,10X,F10.4)
```

```
91      CONTINUE
        WRITE(2,61)NUMS,DELS,(SUMFAC(K),K=1,NUMS)
61      FORMAT(I4,F10.4/(6(2X,F8.4)))
        STOP
        END
        FUNCTION PARTF(X,Y,Z)
C
C    PARTF CALCULATES THE STRUCTURE FACTOR PARTF(X,Y,Z) AT THE
C    POINT (X,Y,Z).X,Y,Z ARE SPECIFIED IN THE MAIN PROGRAM
C
        COMMON COORD(25,3),NCOORD
        PI=3.142
        SUMR=0.0
        SUMI=0.0
        DO 96 I=1,NCOORD
        FUN=(COORD(I,1)*X+COORD(I,2)*Y+COORD(I,3)*Z)*2.*PI
        SUMR=SUMR+COS(FUN)
96      SUMI=SUMI+SIN(FUN)
        PARTF=(SUMR**2+SUMI**2)**0.5
        RETURN
        END
```

```
      PROGRAM GAUSS(INPUT,OUTPUT,TAPE1,TAPE2,TAPE3)


C
C     THIS PROGRAM EVALUATES THE FIRST CO-ORDINATION NUMBER
C  USING THE RADIAL DENSITY FUNCTION. TWO METHODS OF SUMMING
C  THE AREA UNDER THE PEAK ARE USED:
C        (1) SETTING THE SURROUNDING MINIMA AS THE SUMMATION
C                  LIMITS
C        (2) THE SYMMETRICAL METHOD
C   IT THEN FITS A GAUSSIAN TO THE FIRST PEAK FROM WHICH ANOTHER
C  VALUE OF THE CO-ORDINATION NUMBER CAN BE OBTAINED.
C
C
CCCCCCCCCCCCCCCCCCCCCCCCCCCCCCCCCCCCCCCCCCCCCCCCCCCCCCCCCCCCCCCCCC
C
C        INPUT:
         PROGRAM GAUSS(INPUT,OUTPUT,TAPE1,TAPE2,TAPE3)
C              U=RDF=RADIAL DENSITY FUNCTION
C
C        OUTPUT:
C             RDF=RADIAL DENSITY FUNCTION(FIRST PEAK ONLY)
C             GAUS=GAUSSIAN FIT TO RDF
C
CCCCCCCCCCCCCCCCCCCCCCCCCCCCCCCCCCCCCCCCCCCCCCCCCCCCCCCCCCCCCCCCCC
C
C
         DIMENSION RDF(500),U(500),MAXIMA(50),MINIMA(50)
        +         ,COORD(3),GAUS(500)
         EQUIVALENCE (U,RDF)
         READ(1,10)NRMAX,DELR,(U(J),J=1,NRMAX)
10       FORMAT(I4,F10.4/(6(2X,F8.4)))
         N=0
         M=0
C
C   FIND THE ARRAY NUMBERS OF THE MAXIMA AND THE MINIMA IN
C   THE RADIAL DENSITY FUNCTION
C
         KMAX=NRMAX-1
         DO 1000 K=2,KMAX
         IF(U(K).LE.U(K-1).OR.U(K).LE.U(K+1)) GO TO 1001
         N=N+1
         MAXIMA(N)=K
1001     IF(U(K).GE.U(K-1).OR.U(K).GE.U(K+1)) GO TO 1000
          M=M+1
         MINIMA(M)=K
1000     CONTINUE
         PRINT,*ARRAY NOS OF MAXIMA ARE*,/
         PRINT 100,(MAXIMA(I),I=1,N)
100      FORMAT(10I6)
         PRINT,/,*ARRAY NOS OF MINIMA ARE*,/
         PRINT 100,(MINIMA(I),I=1,M)
         PI=3.141593
C
C    READ IN THE ARRAY NUMBERS OF THE FIRST REAL PEAK AND
C   THE SURROUNDING MINIMA,IGNORING THE SMALL,SPURIOUS PEAKS
C    AT SMALL R VALUES.IN PRACTICE IT IS USUALLY ONLY THE FIRST
C   PEAK WHICH HAS MINIMA AROUND IT.
C
         PRINT,/,*READ IN ARRAY NOS OF MAXIMUM AND SURROUNDING MINIMA.
         READ,MAXR,MINR1,MINR2
         MR=MAXR+1
C
```

```
C    SUM THE AREAS BELOW THE FIRST PEAK USING THE METHODS
C   (1) AND (2) INDICATED ABOVE.
C
       COORO(1)=0.0
       DO 802 J=MINR1,MAXR
802    COORD(1)=COORO(1)+ROF(J)*DELR
       COORO(2)=2.0*COORO(1)-ROF(MAXR)*DELR
       DO 803 J=MR,MINR2
803    COORD(1)=COORO(1)+RDF(J)*DELR
       PRINT,/,*APPROXIMATE COORDINATION NUMBERS*
        PRINT,*    METHOD 1        METHOD 2  *
        PRINT 101,COORO(1),COORO(2)
101    FORMAT(2X,F10.4,6X,F10.4)
C
C    FIT A GAUSSIAN FUNCTION TO THE FIRST PEAK
C
C    COMMENCE BY FINOING AN APPROXIMATE VALUE OF SIGMA
C
       HALF=ROF(MAXR)/2.0
       DIFF =RDF(MAXR)
       DO 804 KR=MINR1,MAXR
       IF(ABS(RDF(KR)-HALF).GE.DIFF) GO TO 804
        DIFF=ABS(ROF(KR)-HALF)
       HALFR1=KR
804    CONTINUE
       DIFF=ROF(MAXR)
       DO 805 KR=MAXR,MINR2
       IF(ABS(RDF(KR)-HALF).GE.DIFF) GO TO 805
        HALFR2=KR
805    CONTINUE
       SIGAPP=(HALFR2-HALFR1)*DELR*0.5
       PRINT,/,*APPROXIMATE VALUE OF SIGMA*
       PRINT,/,SIGAPP
       FNORM=RDF(MAXR)
       PI2=2.*PI
       PIS=SQRT(PI2)
       APROXN=FNORM*SIGAPP*PIS
       PRINT,/,*APPROXIMATE COORDINATION NUMBER*
        PRINT,/,APROXN
C
C  COMPUTE THE GAUSSIAN FUNCTIONS,FOR A RANGE OF SIGMA,
C  AND SELECT THE VALUE OF SIGMA WHICH GIVES THE BEST FIT
C   TO THE RADIAL DENSITY FUNCTION
C
       PRINT,/,*READ IN MIN AND MAX VALUES FOR SIGMA*
       READ,SIGMIN,SIGMAX
       MINSIG=100.0*SIGMIN
       MAXSIG=100.0*SIGMAX
       DO 806 NSIG=MINSIG,MAXSIG
       SIGMA=FLOAT(NSIG)*0.01
       SUMSQ=0.0
       DO 807 KR=MINR1,MAXR
       FIT=FNORM*EXP(-((FLOAT(KR-1-MAXR)*DELR)**2)/((SIGMA**2)*2.0))
       SUMSQ=(FIT-RDF(KR))**2+SUMSQ
807    CONTINUE
       IF(NSIG.EQ.MINSIG)SUMMIN=SUMSQ
       IF(SUMSQ.GT.SUMMIN) GO TO 806
       SUMMIN=SUMSQ
       STORE=SIGMA
806    CONTINUE
```

```
      STDEV=SQRT(SUMMIN/FLOAT(MINR2-MINR1+1))
       PRINT,/,*BEST VALUE OF SIGMA*
      PRINT,STORE
      PRINT,/,*STANDARD DEVIATION*
      PRINT,STDEV
      COORDN=FNORM*STORE*SQRT(2.Ø*PI)
      PRINT,/,*COORDINATION NUMBER*
      PRINT,COORDN
C
C   GENERATE THE GAUSSIAN FUNCTION OVER THE RANGE OF THE
C    FIRST PEAK
C
      MC=MINR2+1Ø
      DO 8Ø8 KR=1,MC
      GAUS(KR)=FNORM*EXP(-((FLOAT(KR-1-MAXR)*DELR)**2)/((STORE**2)
     +          *2.Ø))
8Ø8   CONTINUE
      WRITE(2,1Ø)MC,DELR,(RDF(J),J=1,MC)
      WRITE(3,1Ø)MC,DELR,(GAUS(J),J=1,MC)
      PRINT,/,*GAUSSIAN FIT TO FIRST PEAK STORED ON TAPE 3*
      PRINT,*RDF STORED ON TAPE2*
      STOP
      END
```

```
      PROGRAM SCATTER(INPUT,OUTPUT,TAPE1,TAPE2,TAPE3,
     +    TAPE5=OUTPUT,TAPE6,TAPE62)
C
C   THIS PROGRAM CALCULATES THE TOTAL DIFFRACTED
C  INTENSITY FROM THE SUPPLIED ATOMIC SCATTERING
C  FACTOR,THE STRUCTURE FACTOR AND THE INTENSITY
C FUNCTION CALCULATED BY FERENC
C
C CCCCCCCCCCCCCCCCCCCCCCCCCCCCCCCCCCCCCCCCCCCCCCCC
C     INPUT:
C           ATOM=ATOMIC SCATTERING FACTOR
C           SFAC=SPHERICALLY INTEGRATED STRUCTURE FACTOR
C           NX,NY,NZ=NUMBER OF ATOMS ALONG CRYSTAL SIDES
C             NUMS=NUMBER OF DATA POINTS
C             DELS=INCREMENT IN S
C      PROGRAM SCATTER(INPUT,OUTPUT,TAPE1,TAPE2,TAPE3,TAPE5=OUTPUT
C     +          ,TAPE6,TAPE62)
C              A  =CELL EDGE OF ELEMENT
C
C     OUTPUT:
C           S=4*PI*SIN(THETA)/WAVELENGTH
C           CALINT=CALCULATED TOTAL INTENSITY FUNCTION
C
C CCCCCCCCCCCCCCCCCCCCCCCCCCCCCCCCCCCCCCCCCCCCCCCC
C
      DIMENSION ATOM(300),SFAC(300),CALINT(300),S(300)
      DIMENSION TOTINT(300),SNEW(300)
      READ(2,61)NUMS,DELS,(SFAC(K),K=1,NUMS)
      READ(1,61)NUMS,DELS,(ATOM(J),J=1,NUMS)
C   SET MINIMUM DATA VALUE FOR PLOTTING
C
      MIN=13
      NMIN=MIN+1
      NEW=NUMS-MIN
      NUM1=NUMS-1
C
C      SELECT PLOTTING MODE
C            INDEX=0   LARGE PLOT OF CALINT
C                  =1   4 SMALL PLOTS
C
      INDEX=1
61    FORMAT(I4,F10.4/(6(2X,F8.4)))
      READ(3,63)NX,NY,NZ,A
63    FORMAT(3I4,F7.4)
      FNX=FLOAT(NX)
      FNY=FLOAT(NY)
      FNZ=FLOAT(NZ)
      DO 109 I=1,NUMS
      S(I)=FLOAT(I)*DELS
C
C     CALL ROUTINE TO CALCULATE THE INTENSITY FUNCTION
C
      CALL FERENC(NX,NY,NZ,A,TOTI,S(I))
      IF(I.NE.1) GO TO 79
      AFACT=1.0/TOTI
79    TOTT=AFACT*TOTI
      TOTINT(I)=TOTT
109   CALINT(I)=TOTI*ATOM(I)*SFAC(I)
      WRITE(6,62)NUMS,NMIN,DELS,(CALINT(L),L=MIN,NUM1)
62    FORMAT(2I4,F10.4/(6(2X,F8.4)))
C
C     CALL KINEMATIC ROUTINES TO PLOT THE CALCULATED
```

```
C                RESULTS
C
      CALL START(2)
      IF(INDEX.EQ.1) GO TO 17
      CALL SCALE(S,17.0,NUMS,1)
      DO 110 J=1,NEW
      CALINT(J)=CALINT(J+MIN)
110   S(J)=S(J+MIN)
      S(NEW+1)=S(NUMS+1)
      S(NEW+2)=S(NUMS+2)
      CALL SCALE(CALINT,10.0,NEW,1)
      CALL AXIS(0.0,0.0,7HS-VALUE,-7,17.0,0.0,S(NUMS+1),S(
     +         NUMS+2))
      CALL AXIS(0.0,0.0,20HCALCULATED INTENSITY,20,10.0,90.0,
     +          CALINT(NEW+1),CALINT(NEW+2))
      CALL SYMBOL(6.0,9.0,0.14,
     +          36HNUMBER OF ATOMS ALONG CRYSTAL SIDES:,0.0,36)
      CALL NUMBER(7.0,8.0,0.14,FNX,0.0,-1)
      CALL NUMBER(8.0,8.0,0.14,FNY,0.0,-1)
      CALL NUMBER(9.0,8.0,0.14,FNZ,0.0,-1)
      CALL LINE(S,CALINT,NEW,1,1,3)
      GO TO 16
17    DO 99 K=1,NEW
      TOTINT(K)=TOTINT(K+MIN)
      CALINT(K)=CALINT(K+MIN)
      SFAC(K)=SFAC(K+MIN)
99    SNEW(K)=S(K+MIN)
      CALL SCALE(TOTINT,5.0,NEW,1)
      CALL SCALE(S,9.0,NUMS,1)
      SNEW(NEW+1)=S(NUMS+1)
      SNEW(NEW+2)=S(NUMS+2)
      CALL PLOT(-1.0,0.0,-3)
      CALL AXIS(0.0,0.0,7HS VALUE,-7,9.0,0.0,S(NUMS+1),
     +          S(NUMS+2))
      CALL AXIS(0.0,0.0,18HINTENSITY FUNCTION,18,
     +          5.0,90.0,TOTINT(NEW+1),TOTINT(NEW+2))
      CALL SYMBOL(1.5,5.25,0.14,
     +          36HNUMBER OF ATOMS ALONG CRYSTAL SIDES:,0.0,36)
      CALL NUMBER(3.0,5.0,0.14,FNX,0.0,-1)
      CALL NUMBER(4.0,5.0,0.14,FNY,0.0,-1)
      CALL NUMBER(5.0,5.0,0.14,FNZ,0.0,-1)
      CALL LINE(SNEW,TOTINT,NEW,1,0,INTEQ)
      CALL PLOT(0.0,6.0,-3)
      CALL SCALE(ATOM,6.0,NUMS,1)
      CALL AXIS(0.0,0.0,7HS VALUE,-7,9.0,0.0,S(NUMS+1),
     +          S(NUMS+2))
      CALL AXIS(0.0,0.0,24HATOMIC SCATTERING FACTOR,24,6.0,90.0,
     +          ATOM(NUMS+1),ATOM(NUMS+2))
      CALL LINE(S,ATOM,NUMS,1,0,INTEQ)
      CALL PLOT(10.0,0.0,-3)
      CALL SCALE(SFAC,6.0,NEW,1)
      CALL AXIS(0.0,0.0,7HS VALUE,-7,9.0,0.0,S(NUMS+1),S(NUMS+2))
      CALL AXIS(0.0,0.0,16HSTRUCTURE FACTOR,16,6.0,90.0,
     +          SFAC(NEW+1),SFAC(NEW+2))
      CALL LINE(SNEW,SFAC,NEW,1,0,INTEQ)
      CALL PLOT(0.0,-6.0,-3)
      CALL SCALE(CALINT,5.0,NEW,1)
      CALL AXIS(0.0,0.0,7HS VALUE,-7,9.0,0.0,S(NUMS+1),S(NUMS+2))
      CALL AXIS(0.0,0.0,15HTOTAL INTENSITY,15,5.0,90.0,
     +          CALINT(NEW+1),CALINT(NEW+2))
```

```
      CALL LINE(SNEW,CALINT,NEW,1,0,INTEQ)
16    CALL ENPLOT
      STOP
      END
      SUBROUTINE FERENC(NAMX,NBMX,NCMX,A,TOTI,R)
C
C   THIS ROUTINE CALCULATES THE INTENSITY FUNCTION,TOTI,
C FOR A GIVEN CRYSTAL SIZE
C
      TOTI=FLOAT(NAMX)*FLOAT(NBMX)*FLOAT(NCMX)
      NAL=NAMX*2-1
      NBL=NBMX*2-1
      NCL=NCMX*2-1
      DO 1000 NA=1,NAL
      NAA=-NAMX+NA
      DO 1000 NB=1,NBL
      NBB=-NBMX+NB
      DO 1000 NC=1,NCL
      NCC=-NCMX+NC
      AM=FLOAT(NAMX)
      BM=FLOAT(NBMX)
      CM=FLOAT(NCMX)
      AA=FLOAT(NAA)
      BB=FLOAT(NBB)
      CC=FLOAT(NCC)
      PQSL=(((ABS(AA)**2)+(ABS(BB)**2)+(ABS(CC)**2))**0.5)*A
      IF(PQSL.EQ.0.0) GO TO 1000
      F=PQSL/A
      G=(AM-ABS(AA))*(BM-ABS(BB))*(CM-ABS(CC))
      FI=(SIN(R*PQSL)/(R*PQSL))*G
      TOTI=FI+TOTI
1000  CONTINUE
      RETURN
      END
```

APPENDIX B

The Fast Fourier Transform (F.F.T)

The most efficient method of evaluating a Fourier transform is by means of the F.F.T which utilizes the Discrete Fourier Transform. This is defined as

$$Y = 1/N \sum_{k=0}^{N-1} X_k \exp(-j2\pi kn/N) \quad n=0,1,....N-1 \text{ ——— (1)}$$

$$X = \sum_{n=0}^{N-1} Y_n \exp(j2\pi kn/N) \quad k=0,1,... .N-1 \text{ ——— (2)}$$

It is necessary then to manipulate the Fourier Integral expressions(equations(10) and (11) of chapter 3) into their discrete form.We have

$$F(s)= \int_0^{\infty} G(r)\sin(rs)ds \text{ ——— (3)}$$

Sample F(s) at intervals of Δs, and define $S' = 2\pi/\Delta s$

Then:

$$F(n\Delta s) = \int_0^{\infty} G(r)\sin(nr2\pi/S')dr \text{ ———(4)}$$

which can be rewritten as:

$$F(n\Delta s) = \sum_{k=0}^{\infty} \int_{kS'}^{(k+1)S'} G(r)\sin(2\pi nr/S')dr \text{ ——— (5)}$$

Let $r' = r-ks$

$$F(n\Delta s) = \sum_{k=0}^{\infty} \int_0^{S'} G(r'+ks)\sin(2\ n(r'+ks)/S')dr$$

$$F(n\Delta s) = \int_0^{S'} \left(\sum_{k=0}^{\infty} G(r'+ks) \right) \sin(2\pi nr'/S')dr$$

since $\sin(2\pi nk)=0$, $\cos(2\pi nk) =1$

$$F(n\Delta s) = \int_0^{S'} G_\beta(r)\sin(2\pi nr/S)dr \text{ ——— (6)}$$

where

$$G_\beta(r) = \sum_{k=0}^{\infty} G(r+ks) \text{ ——— (7)}$$

Equation (6) can be inverted to give an expression of the form:

$$G_\beta(r) = C \sum_{n=0}^{\infty} F(n\Delta s)\sin(2\pi nr/s')$$

To evaluate the constant C, multiply both sides by $\sin(2\pi mr/S')$ and integrate with respect to r between the limits 0 and S'.

$$\int_0^{S'} G_\beta(r)\sin(2\pi mr/S')dr$$

$$= C\sum_{n=0}^{\infty} F(n\Delta s)\int_0^{S'}\sin(2\pi mr/S')\sin(2\pi nr/S')dr$$

$$= C\sum_{n=0}^{\infty} F(n\Delta s)\int_0^{S'} 1/2(\cos(2\pi(n-m)r/S') - \cos(2\pi(n+m)r/S'))dr$$

$$= C/2\left(F(m\Delta s)\int_0^{S'}(1+\cos(2\pi .2mr/S'))dr + \sum_{\substack{n=0 \\ n\neq m}}^{\infty} F(n\Delta s)\int_0^{S'}(\cos(2\pi(n-m)r/S') - \cos(2\pi(n+m)r/S'))dr\right)$$

Now use the fact that $\int_0^{S'}\cos(2\pi pr/S') = 0$

$$\int_0^{S'} G_\beta(r)\sin(2\pi mr/S')dr = C/2F(m\Delta s)\ S' = F(m\Delta s)$$

from equation (6)

Hence $C = 2/S'$ and we have

$$G_\beta(r) = 2/S'\sum_{n=0}^{\infty} F(n\Delta s)\sin(2\pi nr/S') \qquad (8)$$

If $G_\beta(r)$ is sampled at N equispaced points in the interval $(0,S')$ then the interval between samples is

$$\Delta r = S'/N = 2\pi/N.\Delta s$$

i.e. $N = 2\pi/\Delta s.\Delta r$ ——— (9)

Then

$$G_\beta(p\Delta r) = 2/S'\sum_{n=0}^{\infty} F(n\Delta s)\sin(2\pi np/N) \qquad p=0,1,\ldots..N-1$$

$$= 2/S'\sum_{n=0}^{N-1}(F(n\Delta s)\sin(2\pi np/N) + F(n\Delta s+N\Delta s)\sin(2\pi(n+N)p/N) + F(n\Delta s+2N\Delta s)\sin(2\pi(n+2N)p/N) + \ldots\ldots\ldots)$$

$$= 2/S'\sum_{n=0}^{N-1}\left(\sum_{l=0}^{\infty} F(n\Delta s+lN\Delta s)\right)\sin(2\pi np/N)$$

$$= 2/S'\sum_{n=0}^{N-1} F_\beta(n\Delta s)\sin(2\pi np/N)$$

$$G_\beta(p\Delta r) = 2/S'\sum_{n=0}^{N-1} F_\beta(n\Delta s)\sin(2\pi np/N) \qquad (10)$$

Similarly one could put

$$F_\beta(n\Delta s) = C' \sum_{p=0}^{N-1} G_\beta(p\Delta r)\sin(2\pi np/N)$$

and evaluate C' by multiplying both sides by $\sin(2\pi nm/N)$ and summing from m=0 to N-1. Alternatively one can use the fact that $G(p\Delta r)$ and $F(n\Delta s)$ are a discrete Fourier pair and by comparison with equations (1) and (2)

$$1/N = C'.2/S'$$

$$\text{so } C' = S'/2N$$

Since $N = 2\pi/\Delta r.\Delta s$, we have for the Discrete Fourier pair:

$$\underline{F(n\Delta s) = \Delta r/2 \sum_{p=0}^{N-1} G(p\Delta r)\sin(2\pi np/N)} \quad \text{———} \quad (11)$$

$$\underline{G(p\Delta r) = \Delta s/\pi \sum_{n=0}^{N-1} F(n\Delta s)\sin(2\pi np/N)} \quad \text{———} \quad (12)$$

where $N = 2\pi/\Delta r.\Delta s$

and $$G_\beta(p\Delta r) = \sum_{k=0}^{\infty} G(p\Delta r + ks) = G(p\Delta r + kN\Delta r)$$

$$F_\beta(n\Delta s) = \sum_{l=0}^{\infty} F(n\Delta s + lN\Delta s)$$

On comparing the Diiscrete Fourier transform we wish to evaluate with equations (1) and (2) it is evident that $\Delta s.F_\beta(n\Delta s)/\pi$ and $G_\beta(p\Delta r)$ form a Discrete Fourier pair. It is, then, necessary to modify the data accordingly. On transforming the function $F_\beta(n\Delta s)$ it should first be multiplied by $\Delta s/\pi$, while if $G_\beta(p\Delta r)$ has been transformed the answer should be divided by $\Delta s/\pi$ to give $F_\beta(n\Delta s)$. It was mentioned in Chapter (3) that F(s) and G(r) will be periodic in form with a half period of $\pi/\Delta r$ and $\pi/\Delta s$ respectively. This means that $N\Delta s$ and $N\Delta r$ represent one complete period in F and G respectively. Consequently if Δs and Δr a re chosen with care then

$$F(s+N\Delta s) = 0 \quad \text{and}$$

$$G(r+N\Delta r) = 0$$

and $F_\beta(n\Delta s)$ and $G_\beta(p\Delta r)$ can be replaced with $F(n\Delta s)$ and $G(p\Delta r)$(i.e. the experimental data).It should be noted however that the calculated Discrete Fourier Pair will consist of one complete period.This necessitated modifying the experimental data F(s) to be periodic.If n values of F(s) have been determined then the n+1 to (N/2 +1) terms are set to zero and the (N/2 +2) to N terms are set to be the inverse of those in the first half period.Similarly only the first N/2 terms are considered out of the N terms in the output.

Finally it should be noted that the equations(1) and (2) refer to the complex quantities Y_n and X_K .In this particular application then the modified data F(s) is read into the real input while the imaginary input is set to zero.The required result will then be in the imaginary part of the transform since the sine terms refer to the imaginary part of the exponential.

In using equation (1) it can be seen that the entire sequence X_K is used to calculate every Y_n.This results,due to the periodicity in $\exp(-j2\pi kn/N)$,the same value of $X_K\exp(-j2\pi kn/N)$ being calculated for many different combinations of n and k.The F.F.T. reduces this redundancy by factoring the number of data values such that intermediate results,which are themselves transforms of shorter sequences ,are stored.

Suppose N = A.B.C then the entire data sequence can be specified by $n = \hat{c}+\hat{b}.C+\hat{a}.B.C$

where $\hat{c} = 0,1,2,.....C-1$

$\hat{b} = 0,1,2,.....B-1$

$\hat{a} = 0,1,2,.....A-1$

Treating X_k in a similar way equation (1) can be expressed as

$$Y_{\hat{c}+\hat{b}C+\hat{a}BC} = \sum_{a=0}^{A-1}\sum_{b=0}^{B-1}\sum_{c=0}^{C-1} X_{a+bA+cAB}\exp(-2\pi j(\hat{c}+\hat{b}C+\hat{a}BC)(a+bA+cAB)/N)$$

Simplifying this expression, and putting $\exp(-2\pi jp)=e(p)$, gives the Cooley version of the F.F.T.

$$Y_{\hat{c}+\hat{b}C+\hat{a}BC} = \sum_{a=0}^{A-1} e(\hat{a}a/A)\,e(a(\hat{c}+\hat{b}C)/ABC)\sum_{b=0}^{B-1} e(\hat{b}b/B)\,(\,e(b\hat{c}/BC)\sum_{c=0}^{C-1} e(\hat{c}c/C)X_{a+bA+cAB}\,) \quad \text{——————} \quad (13)$$

This indicates how the F.F.T. is calculated for, by inspection, the bracketed operation can only be specified in A.B.C. ways, one for each value of a,b,c. These N values are calculated and stored rather than evaluating the actual sum $(A.B)^2.C$ times (once for all choices of a,b,c,a and b). For further details see Cooley and Tukey(1965), or Gentleman and Sande(1966).

In fact various ways of calculating equation(13) have been put forward and generally it is required that N be a power of 2. This condition leads to the value chosen in this particular application.

We have $N = 2\pi/\Delta r.\Delta s$ and in Chapter (3) Δr and Δs were chosen such that they had maximum values of 0.125Å^{o} and 0.125Å^{o-1} respectively. Then N is defined by

$$N = 2^n > 2\pi/(0.125)^2$$

and the smallest value of N which is consistent with this condition is N = 512.

REFERENCES

Adamsky,Behrndt and Brogan 9 (1969), 542

Alder,Frankel and Lewinson:J.Chem.Phys. 23 (1955), 417

Behrndt: J.Appl. Phys. 37 (1966) , 3841

Behrndt: J.Vac.Sci.Technol. 6 (1969), 439

Behrndt: J.Vac.Sci.Technol. 7 (1970), 385

Belevtsev a nd Kommik: Soviet Physics(solid state)
14 (1973), 2759

Bennet and Wright: Phys.Stat.Sol.(a) 13 (1972), 135

Bernal: Proc. Royal Soc. 280A (1964),229

Bienenstock and Bagley:J. Appl. Phys. 37 (1960) , 4840

Breitling:J. Vac. Sci. Technol. 6 (1969) , 628

Buckel:

Budo and Caswel: J.Appl.Phys. 35 (1964), 644

Bulow and Buckel: Z.Physik 145 (1956), 141

Debye: Ann Physik 46 (1915), 809

Debye and Scherrer: Nachder Gott.Ges 1 16 (1916)

Denbigh and Grigson:J.Sci.Instrum. 42 (1965), 305

Duwez and Willens:Trans.Metal. Soc.A.I.M.E.
227 (1963), 362

Frost: Prog.Metal.Phys. 5 (1954), 96

Fujime: Jap.J.Appl.Phys. 5 (1966) ,778

Fujime: Jap.J.Appl.Phys. 5 (1966) , 1029

Glove r: Prog.Low Temp.Phys. 6 (1969)

Gokulara thnam: J.Mater.Sci. 9 (1974), 673

Grigson and Barton:Brit.J.Appl.Phys. 17 (1966), 1019

Grigs on,Dove and Stilwell:Nature 204 (1964), 173

Hilsch:Proc.Int.Conf.Low Temp.Phys. Oxford (1951),119

Ichikawa:Jap.J.Appl.Phys. 7 (1970), 748

James:The Optical Principles of The Diffraction of X-Rays (1948)

Jonscher and Walley:J.Vac.Sci.and Technol. 6 (1969),622

Kaplow,Strong and Averbach:Phys.Rev. 138A (1964),1336

Karle and Karle:J.Chem. Phys. 18 (1950), 957

Kato and Horokoshi:Jap.J. Appl.Phys. 4 (1965), 326

Krikorian and Sneed:Trans. 10th Nat. Vac.Symp. (1963), 368

Krogh-Moe: Acta Crysta 9 (1956) 951

Leonhardt,Richter and Rosstteutscher Physik 165 (1962)121

Longini and Pansino:J.Appl.Phys. 40 (1969), 2653

Mader,Norwick and Widmer:Acta Met. 15 (1967), 203

Mader:J. Vac. Sci. Technol. 2 (1965), 35

Maitrepierre:J.Appl.Phys. 40 (1969), 4826

Morozumi and Ritter:Acta Crysta 6 (1953), 588

Moss and Thomas: Brit.J.Appl.Phys. 15 (1964), 673

Mrafko and Duhai:Phys.Stat.Sol.(a) 22 (1974), 151

Oshima and Nakamura: Jap.J.Appl.Phys. 8 (1969), 844

Palatnik,Gladkik and Naboka:Soviet Phys. 4 (1962),143

Paulson and Friedberg:Thin Solid Films 5 (1970), 47

Preece and Wilman:Phil. Mag. 16 (1967), 447

Rahman:J.Chem.Phys. 42 (1965), 3540

Richter and Breitling: Z.Naturforsch 16a (1961), 187

Robertson and Unvala:Phil.Mag. 24 (1971), 1253

Rudee and Howie:Phil.Mag. 25 (1972), 1001

Scott:Nature 194 (1962) , 956

Suits: Phys.Rev. 131 (1963), 588

Wagner:J.Vac.Sci. Technol. 6 (1969), 650

Wagner:

Warren: J.Appl. Phys. 8 (1939), 645

ACKNOWLEDGMENTS

I should like to record the great debt I owe to Dr. B Gunnell and Dr. P Jarvis for all the help they provided at various times during this research. In addition I am sure that Dr. Unvala will accept the thanks that he deserves. Finally I would add that none of this could have been possible without the encouragement and willingness of Carolyn Richards.